
2807711958

ROYAL FREE THESIS 1996

IN VIVO STUDIES OF ISCHAEMIA-REPERFUSION INJURY IN HYPOTHERMICALLY-STORED RABBIT RENAL AUTOGRAFTS

NICHOLAS JAMES LANE

A THESIS SUBMITTED FOR THE DEGREE OF
DOCTOR OF PHILOSOPHY
IN THE UNIVERSITY OF LONDON
1996

UNIVERSITY DEPARTMENT OF SURGERY
ROYAL FREE HOSPITAL MEDICAL SCHOOL
UNIVERSITY OF LONDON

ProQuest Number: U092479

All rights reserved

INFORMATION TO ALL USERS
The quality of this reproduction is dependent upon the quality of the copy submitted.

In the unlikely event that the author did not send a complete manuscript
and there are missing pages, these will be noted. Also, if material had to be removed,
a note will indicate the deletion.

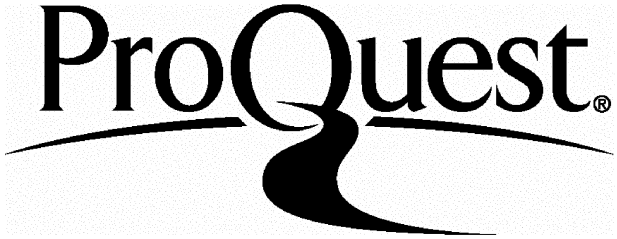

ProQuest U092479

Published by ProQuest LLC(2016). Copyright of the Dissertation is held by the Author.

All rights reserved.
This work is protected against unauthorized copying under Title 17, United States Code.
Microform Edition © ProQuest LLC.

ProQuest LLC
789 East Eisenhower Parkway
P.O. Box 1346
Ann Arbor, MI 48106-1346

08904.

I dedicate this thesis to my parents, my brother
and my supervisors Colin Green and Barry Fuller
in gratitude for all their support,
for having faith in me when I needed it
and never losing it.

ACKNOWLEDGEMENTS

I would like to thank the Dunhill Medical Trust for financial support. I owe a great debt of gratitude to many current and former members of the Department of Surgical Research at the Northwick Park Institute for Medical Research: to Maureen Thomiley for introducing me to *in vivo* spectroscopy and for endless hours of passionate debate about what it all meant; to Sanjiv Manek for teaching me the rudiments of pathology and keeping a trained eye on my histological interpretations; to Sandra Simpkin for instructing me in the techniques of microsurgery, anaesthesia and animal husbandry; to Colin Shurey for the support and freedom of the Theatres; to Padmini Sarathchandra and Pat Fryer for processing all my electron microscopy samples and telling me what to do with them; to Sam Toffa for shared thoughts on renal preservation; to Graham Goddard for re-awakening a love of research and for bearing patiently with many flights of scientific fancy; to Ian Ambrose for stiff draughts of reality and other beverages; and to Ana Hidalgo for perpetual inspiration.

ABSTRACT

Ischaemia-reperfusion injury is a major cause of graft failure following renal transplantation. These studies were undertaken to elucidate the pathogenesis of ischaemia-reperfusion injury and the effects of specific therapeutic interventions, with the aim of extending the 'safe' preservation period of kidneys stored prior to transplantation.

An *in vivo* renal autograft model was used throughout. Mitochondrial function was assessed non-invasively using surface fluorometry and near infrared spectroscopy of respiratory chain components NADH and cytochrome oxidase. Changes in renal haemoglobin oxygenation and concentration were measured using near infrared spectroscopy. Pathological markers were measured in assays of susceptibility to lipid peroxidation and enzyme immunoassays of plasma eicosanoid levels. Intra-renal perfusion was evaluated using barium sulphate angiography, micro-angiography and colloidal carbon vascular labelling. Morphological changes were evaluated using light and electron microscopy.

Revascularization of stored kidneys led to the development of severe vascular congestion in the medulla and acute tubular necrosis in the cortex. Congestion was a consequence of ischaemic swelling of the medullary thick ascending tubules, developing within 10 min of reperfusion and beginning to clear within 1 h. Respiratory chain dysfunction occurred rapidly upon reperfusion, persisted for at least 3 h and was independent of vascular congestion. Iron chelation attenuated susceptibility to lipid peroxidation and limited cortical necrosis but did not effect respiratory chain function, medullary congestion or long-term renal viability. Inhibition of inflammation using anti-inflammatory or antioxidant drugs also limited cortical necrosis but had no effect on medullary congestion or long-term viability. Medullary tubular dysfunction was shown to be responsive to but not prevented by substitution of impermeant solutes, as judged by changes in tissue oxygenation following infusions of the diuretic frusemide.

It is concluded that renal ischaemia-reperfusion injury is a consequence of several concurrent pathological changes and that effective therapy must be targeted to several specific cell types.

TABLE OF CONTENTS

LIST OF FIGURES

CHAPTER 1

CHAPTER 3

CHAPTER 4

CHAPTER 5

CHAPTER 6

CHAPTER 7

CHAPTER 8

CHAPTER 9

LIST OF PLATES

CHAPTER 1

CHAPTER 2

Plate 2.1 Anastamoses of the renal artery (right) and vein (left).

Plate 2.2 Autografted kidney during reperfusion.

CHAPTER 3

Plate 3.1 Electron micrograph of renal proximal tubule cells after 72 h of storage and no reperfusion (magnification x 5000).

Plate 3.2 Electron micrograph mTAT cells after 72 h of storage and no reperfusion (magnification x 5000).

Plate 3.3 Electron micrograph of renal proximal tubule cells after 72 h of storage and 1 h of reperfusion (magnification x 5000).

Plate 3.4 Electron micrograph of mTAT cells after 72 h of storage and 1 h of reperfusion (magnification x 5 000).

Plate 3.5 Light micrograph of the cortico-medullary junction of a kidney stored for 72 h but not reperfused (magnification x 40) showing mild intracellular and interstitial medullary oedema.

Plate 3.6 Light micrograph of the cortico-medullary junction of a kidney stored for 72 h and reperfused for 1 h (magnification x 40) showing severe medullary congestion and moderate oedema of the cortico-medullary junction but negligible cortical congestion.

Plate 3.7 Light micrograph of the renal cortex of a Group 10 infarcted kidney at autopsy 3 days after revascularization (magnification x 40).

Plate 3.8 Light micrograph of the renal cortex of a Group 10 kidney which had undergone gradual severe necrosis of the entire kidney at autopsy 6 days after revascularization (magnification x 40), showing necrotic infarcted area inflammatory infiltrate, calcification and fibrosis.

CHAPTER 4

Plates 4.1, 4.2 and 4.3 Representative barium sulphate angiograms of halved kidneys (top) and 2 mm thick renal sections (bottom) in (1) an unstored untransplanted kidney (Group 3); (2) a transplanted 72 h stored, 1 h reperfused kidney (Group 4); (3) a transplanted 72 h stored 3 h reperfused kidney (Group 4).

Plate 4.4 Dispersal of barium sulphate (viewed under polarized light) in the cortex of an unstored, 5 min reperfused kidney (Group 3), after staining with sodium rhodozinate. (magnification x 60).

Plate 4.5 Dispersal of barium sulphate in the cortex of a 72 h stored, 5 min reperfused kidney (Group 4) after staining with sodium rhodozinate and viewed under polarized light (magnification x 60).

CHAPTER 5

Plate 5.1 Light micrograph of the renal cortex showing minimal intracellular oedema in a Group 1 (unstored transplanted) kidney (magnification x 100).

Plate 5.2 Light micrograph of the renal cotex showing severe cortical intracellular oedema in a Group 2 (72 h stored transplanted) kidney (magnification x 40).

CHAPTER 6

Plate 6.1 Light micrograph of the renal cortex showing minimal to mild intracellular oedema in a Group 1 (unstored transplanted) kidney (magnification x 40).

Plate 6.2 Electron micrograph showing slightly swollen cortical proximal tubular mitochondria in a Group 2 (72 h stored transplanted) kidney (magnification x 25,000).

Plate 6.3 Light micrograph of the renal cotex showing mild to moderate cortical intracellular oedema in a Group 2 (72 h stored transplanted) kidney (magnification x 40).

Plate 6.4 Light micrograph of the renal cotex showing significant reduction in cortical intracellular oedema in a Group 3 (72 h stored + CP 130) transplanted kidney (magnification x 40).

Plate 6.5 Light micrograph of the renal cortex of a Group 2 infarcted kidney at autopsy 3 days after revascularization (magnification x 40), showing tubular outlines and massive inflammatory infiltrate at the top right.

Plate 6.6 Light micrograph of the renal cortex of a Group 2 kidney which had undergone gradual severe necrosis of the entire kidney at autopsy 6 days after revascularization, showing mild inflammatory infiltrate at the left and calcified necrotic tissue in the centre.

CHAPTER 7

Plate 7.1 Light micrograph of peri-vascular colloidal carbon penetration in the cortico-medullary junction of a Group 1 (untreated) kidney after 30 min of reperfusion (magnification x 40).

Plate 7.2 Light micrograph of the renal cortex of a Group 1 (untreated) kidney 3 days after revascularization showing widespread cortical calcification (C) (magnification x 60).

Plate 7.3 Light micrograph of the renal cortex of a Group 2 (BW B70C treated) kidney 3 days after revascularization showing well preserved tubular structure (magnification x 40).

Plate 7.4 Electron micrograph of cortical proximal tubules in a Group 1 (untreated) kidney 3 days after revascularization (magnification x 5,000), showing loss of nuclear material, swollen mitochondria and loss of brush border.

Plate 7.5 Electron micrograph of cortical proximal tubules in a Group 2 (BW B70C treated) kidney 3 days after revascularization (magnification x 5000), showing intact brush border, normal nuclear appearance and unswollen mitochondria.

LIST OF TABLES

ABBREVIATIONS

$\%SaO_2$	percentage mixed haemoglobin saturation
µl	microlitre
µmol	micromoles
6-k-$PGF_{1\alpha}$	6-keto-prostaglandin $F_{1\alpha}$
ACE	angiotensin converting enzyme
ADP	adenosine diphosphate
AMP	adenosine monophosphate
ATN	acute tubular necrosis
ATP	adenosine 5′ triphosphate
ATPase	adenosine 5' triphosphatase
BP	blood pressure
BW B70C	E-N-(3-(3-(4-fluorophenoxy) phenyl)-1 (R,S)-methylprop-2-enyl)-N-hydroxyurea
Ca^{2+}	calcium ion
cAMP	cyclic adenosine monophosphate
CAPD	continuous ambulatory peritoneal dialysis

cGMP	cyclic guanosine monophosphate
Cl^-	chloride ion
CO_2	carbon dioxide
CP102	1-hydroxyethyl-3-hydroxypyridin-4-one
cyt aa_3	cytochrome oxidase
DFX	desferrioxamine
DMSO	dimethylsulphoxide
DNA	deoxyribonucleic acid
EDRF	endothelial-derived relaxation factor
EDTA	ethylene diaminetetra-acetic acid
ELISA	enzyme immunoassay
EM	electron microscopy
ESRF	end-stage renal failure
Fe^{2+}	ferrous ion
Fe^{3+}	ferric ion
FMN	flavin mononucleotide
g	gram
GFR	glomerular filtration rate
h	hours
H_2O_2	hydrogen peroxide
Hb	deoxyhaemoglobin
HbD	haemoglobin oxygenation index
HbO_2	oxyhaemoglobin
HbT	total haemoglobin
HCA	hypertonic citrate solution
HCA-Peg	hypertonic citrate solution containing polyethylene glycol in place of mannitol
HETE	hydroxyeicosatetraenoic acid
HPETE	hydroperoxyeicosatetraenoic acid
HSP-70	heat shock protein (molecular weight 70 KD group
i.m.	intramuscular
i.v.	intravenous
K^+	potassium ion
KD	kilo Dalton
kPa	kilo Pascals
l	litre
LTB_4	leukotriene b_4
M	molar
MDA	malondialdehyde
min	minutes
ml	millilitre
mmol	millimole
mol	moles
M_r	relative molecular weight
mTAT	medullary thick ascending tubule
MW	molecular weight
n	number in a single group
Na^+	sodium ion
NAD^+	oxidized nicotineamide adenine dinucleotide
NADH	reduced nicotineamide adenine dinucleotide
NADP	oxidized nicotinamide adenine dinucleotide phosphate
NADPH	reduced nicotineamide adenine dinucleotide phosphate

NIRS	near infrared spectroscopy
nm	nanomoles
NMHH	N-methyl hexanoylhydroxamic acid
NO	nitric oxide
NZW	New Zealand White
O_2	oxygen
$O_2^{\bullet-}$	superoxide radical
$^{\bullet}OH$	hydroxyl radical
OD	optical density
p	probability
PEG	polyethylene glycol
PGE_2	prostaglandin E_2
PGF_2	prostaglandin F_2
PGI_2	prostacyclin
pH	potential of hydrogen (acidity)
pO_2	oxygen partial pressure
PZ51	ebselen (2-phenyl-1,2-benzisoselenazol-3-(2H) one)
rpm	revolutions per minute
s.c.	subcutaneous
S1, S2	convoluted sections of the proximal tubule
S3	straight descending (*pars recta*) section of the proximal tubule
SD	standard deviation
sec	seconds
SEM	standard error mean
TBA	thiobarbituric acid
TBA-RM	thiobarbituric acid-reactive material
TNF	tumour necrosis factor
TxA_2	thromboxane A_2
TxB_2	thromboxane B_2
UW	University of Wisconsin
v/v	volume/volume
VLDL	very low density lipoprotein
vs	versus
w/v	weight/volume
x g	times gravity

INTRODUCTION

1.1 The Clinical Problem

In the United Kingdom, over 4000 patients suffer end-stage renal failure (ESRF) each year. Since the introduction of cyclosporin in 1978 (Calne *et al.*, 1978), renal transplantation has become the treatment of choice for all but a few of these patients, and is superior to dialysis in terms of survival, quality of life and cost to the community (Green, 1995). However, full exploitation of renal transplantation is limited by the number of suitable donor organs. Fewer than half the ESRF patients in the UK get the opportunity of a renal graft (Green, 1995). Unless the hyperacute rejection processes associated with xenotransplantation are overcome, this problem is unlikely to be resolved. It is therefore crucial to make full use of organs harvested from heart-beating cadavers. The key to this is effective preservation, thereby allowing time for tissue antigen matching and transport of organs over sometimes continental distances to suitable recipients, while guaranteeing immediate function after transplantation. This thesis is devoted to the improvement of current techniques of renal preservation.

1.2 The Role of the Kidney

The kidneys function to excrete waste products and to maintain fluid, electrolyte and acid-base homeostasis. These functions are achieved in the first instance by the continuous filtration of blood plasma through the glomeruli and into the renal tubules). The hydrostatic pressure required for this is generated by a combination of circulatory pressure (increased by the narrowing of the arterioles on entry to the glomeruli), and osmotic pressure gradients across the glomerular membranes. Some solutes and water are reabsorbed in various parts of the renal tubules, and other solutes are secreted by the tubular epithelial cells into the urinary spaces. When the normal composition of blood is disturbed by a surfeit of water or dissolved substances, the excess is excreted in the form of urine.

The extracellular fluids are continually reprocessed by the kidneys. A volume equal to the total extracellular fluid of the body is filtered and modified by the tubular cells every two hours. Although the kidneys normally exist in pairs, there is a great deal of reserve function, and it is quite possible for individuals to live in good health with a single functional organ. In their

regulatory function, the kidneys are relatively independent of direct nervous control. Salt and water balance is controlled predominantly via the hormones of the adrenal cortex, the parathyroid, the pituitary glands and the kidneys themselves.

1.3 The Kidney: Anatomy and Physiology

1.3.1 The Anatomy of the Kidney

The kidneys lie in the dorsal area of the abdominal cavity of vertebrates. Their combined weight in man is about 300 g. Each kidney comprises 8 to 10 lobules, consisting of pyramidal tissue known as the renal papillae. The apices of the papillae project into the cup-shaped minor calyces, which in turn feed into the two major calyces, the principal branches of the renal pelvis (Fig 1.1). The papillae consist of parallel bundles of nephrons, which are the basic functional units of the kidney, each one consisting of a glomerulus and attached tubule. In man, each kidney comprises about 1.2 million nephrons (Deetjen, Boylan and Kramer, 1975). Many nephrons discharge into a single collecting duct; and many collecting ducts join as they converge in the papillae. In transverse section, the disposition of the glomeruli, the tubules and the collecting ducts delineate the characteristic subdivisions of the mammalian kidney into the cortical, and the outer and inner medullary zones (Fig 1.1). The structure and function of the nephron is discussed in the next section.

Each kidney is normally supplied by a single renal artery, arising directly from the aorta, and dividing into two or more branches on entry into the kidney. The branches (segmental arteries) pass dorsally and ventrally across the renal pelvis before subdividing to form the interlobular arteries. From these, the arcuate arteries arise and course roughly parallel to the surface of the kidney at the cortico-medullary junction. A second set of interlobular arteries arise from the arcuate arteries, pass outward towards the surface of the organ, and branch into the afferent arterioles. Each nephron receives a single afferent arteriole, which enters the glomerulus and forms a knot of capillary loops. These capillary knots generate the necessary surface area and hydrostatic pressure to enable ultrafiltration of plasma across the basement membranes, forming tubular fluid.

Outflow from the glomerular capillaries passes into the efferent arterioles, which exit the glomerulus alongside the afferent arterioles at the vascular pole (Fig 1.2). The efferent arteriole is smaller in diameter than the afferent arteriole, increasing the resistance to the outflow of blood from the glomerulus, and therefore the hydrostatic pressure for ultrafiltration within the glomerulus.

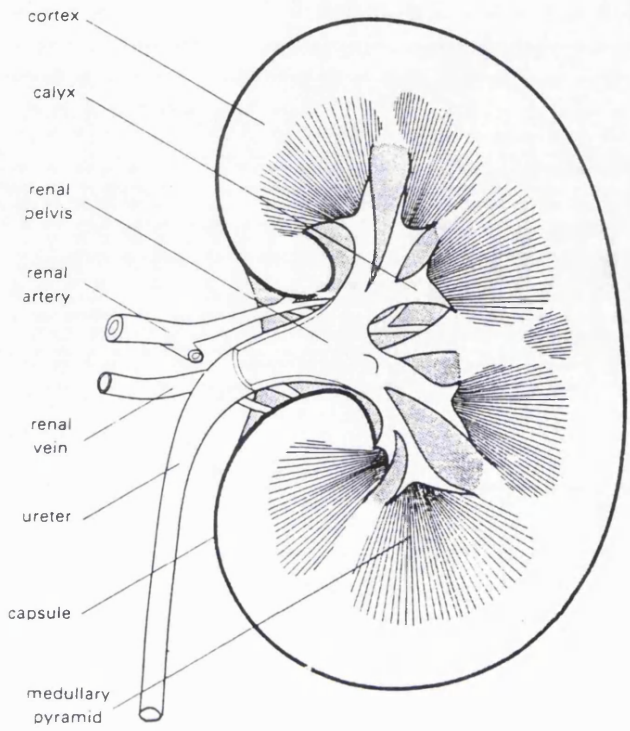

Fig 1.1 Structure of the mammalian kidney

The fate of the efferent arterioles depends on the intra-renal location of the glomerulus served. From superficial cortical glomeruli, the efferent arterioles divide profusely to form a network of cortical peritubular capillaries. From glomeruli positioned deeper in the cortex (juxta-medullary glomeruli), the emerging efferent arterioles are relatively thick, and divide to form characteristic looped bundles of vessels known as the *vasa recta*, which run longitudinally through the medulla, in parallel with the nephrons. The arterial *vasa recta* divide within the medulla to form a network of fine capillaries, from which the outflow passes into parallel bundles of venous *vasa recta*. The great length of the *vasa recta*, which traverse much of the medulla, introduces considerable resistance, whereby blood flow is reduced sufficiently to allow movement of solutes and water from the medullary tubules, during the process of *countercurrent multiplication* (see Section 1.3.3).

Venous drainage is arranged in a manner similar to the arterial inflow; there are no arterio-venous anastomoses, hence no direct pathway by which blood from the renal arteries can circumvent the glomerular and peritubular capillary networks. The peritubular capillaries eventually unite to form peritubular venules, and then interlobular veins, which also receive drainage from the *vasa recta*. From these, blood drains through the arcuate veins to the

interlobular veins (running between the renal pyramids), the segmental veins, and ultimately to a single renal vein, which exits at the renal hilus (Fig 1.2).

The nerve supply of the kidneys is derived from the renal plexus of the sympathetic autonomic nervous system. Vasomotor nerves from this plexus accompany the renal arteries, and contribute to the control of blood flow through the kidney by regulating the diameters of the afferent and efferent arterioles.

1.3.2 Structure and Function of the Nephron

The nephron is the smallest functional unit of the kidney. It consists of a glomerulus, a proximal convoluted tubule, a loop of Henle, and a distal convoluted tubule, which opens into a collecting duct (Fig 1.3). The glomeruli, proximal and distal convoluted tubules are found only in the renal cortex, the loop of Henle mostly in the medulla.

The Glomerulus

The capillary knot of the glomerulus is caged within a double-walled epithelial cup known as Bowman's capsule. Ultrafiltration of plasma in the glomerulus takes place across a filtration membrane which consists of three components (Plate 1.1):

- a layer of capillary endothelium
- basement membrane
- specialized epithelial cells of Bowman's capsule.

Filtration occurs passively, the net driving force depending on the combination of hydrostatic pressure and osmotic pressure. Pore size is therefore the most important factor in determining the molecular size of substances that can be filtered. The single layer of endothelium has large pores (fenestrations) of 50 to 100 nm that prevent filtration of blood cells but allow all components of plasma to pass through. The basement membrane, which lies between the endothelium and the visceral layer of the glomerular capsule, consists of collagen fibrils in a glycoprotein matrix, and prevents the filtration of larger proteins. The epithelial cells of the capsule (podocytes) do not form a continuous barrier, but branch freely and interdigitate with each other. The digits are known as pedicels, and cover the basement membrane, except for filtration slits of 20 to 50 nm. A thin membrane (the slit membrane) extends across the filtration slits and prevents filtration of medium sized proteins.

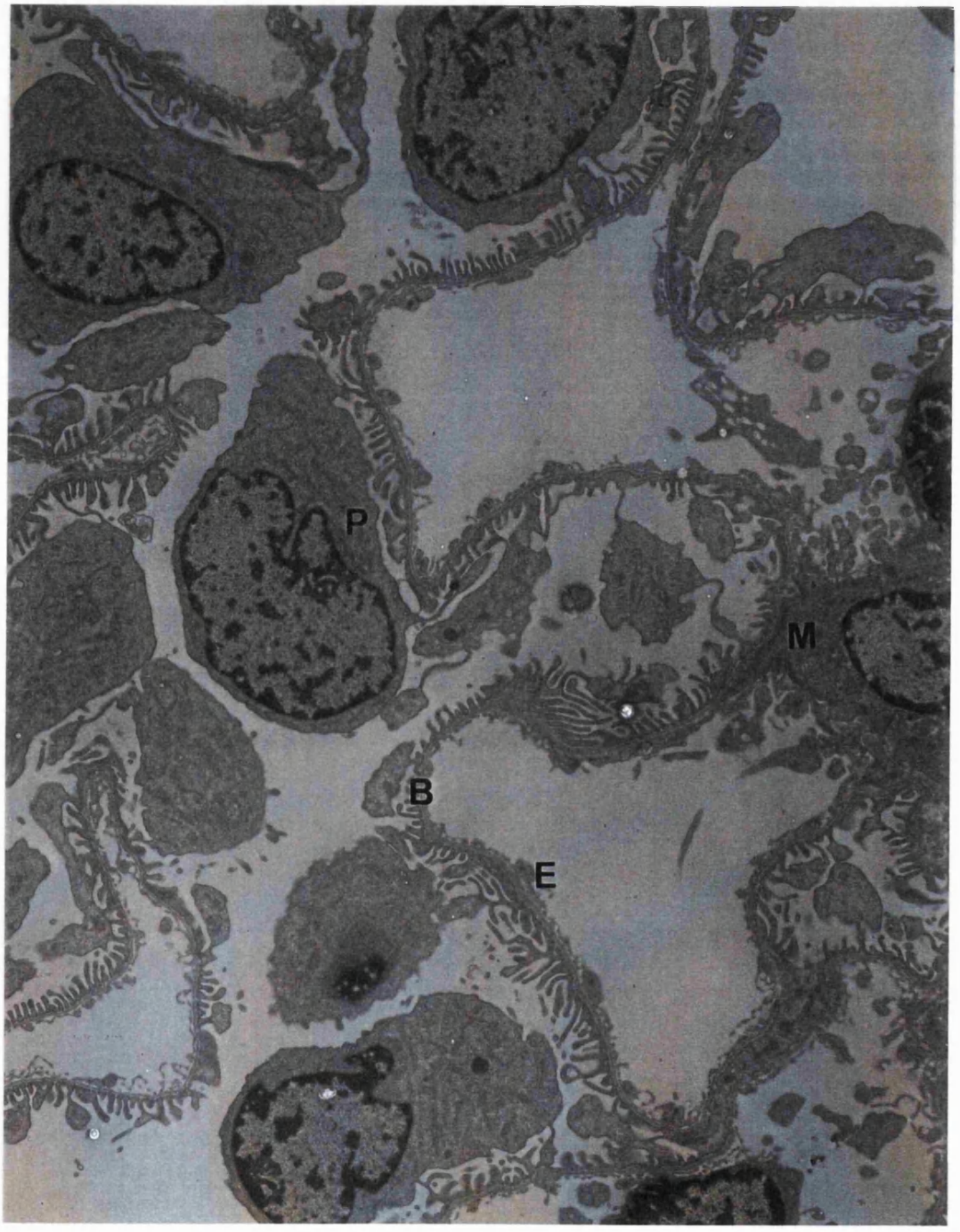

Plate 1.1 **Transmission electron micrograph of a glomerulus (magnification x 5000) showing structure of the ultrafiltration membranes, comprising fenestrated endothelium (E), podocytes (P) and basement membranes (B) of the glomerular capillaries and urinary space, as well as mesangial cells (M) (see text).**

The first application of micropuncture by Wearn and Richards (1924) proved that the composition of glomerular filtrate is that of an ultrafiltrate of plasma; it is virtually free of protein, and the concentrations in it of dissolved low molecular weight substances differ only slightly from their concentrations in plasma. Three factors are responsible for these small but definite concentration differences: (i) the volume occupied by plasma proteins; (ii) the binding of some eletrolytes to plasma proteins; and (iii) the existance of a Gibbs-Donnan equilibrium. This last is due to the excess of negative charges on plasma proteins at pH 7.4. The thermodynamic equilibrium therefore comprises not only concentration differences, but also electrical differences across the filtration membranes.

The amount of filtrate formed in all the glomeruli of both kidneys per minute is called the glomerular filtration rate (GFR). In a normal adult, the GFR is about 125 ml/min, which amounts to 180 l/day.

The Proximal Convoluted Tubule

The normal rate of glomerular filtration is so high that the volume of fluid entering the proximal tubule in half an hour is greater than the total plasma volume. Therefore, returning most of the filtered water and many of the filtered solutes to the bloodstream is a critical renal function. As the filtrate passes through the renal tubules and collecting ducts, about 99% of it is reabsorbed, and only about 1% leaves the body as urine (about 1 to 2 l/day) (Tortora and Grabowski, 1996). The proximal convoluted tubule is responsible for the greatest part of tubular reabsorption, normally accounting for 100% of the filtered glucose and amino acids, 80-90% of HCO_3^-, 65% of water, Na^+ and K^+, and 50% of Cl^- and urea (Tortora and Grabowski, 1996).

In conformity with their large energy turnover, the cuboidal epithelial cells of the proximal convoluted tubule exibit a high degree of morphological differentiation. They are densely packed with elongated mitochondria, and lined on the lumenal (apical) side with a profuse *brush border* of microvilli, which increase the surface area for reabsorption some 60-fold (Deetjen, Boylan and Kramer, 1979) (Plate 1.2). The basolateral membrane is convoluted into a labyrinth of canaliculi which penetrate deeply into the cell, and presumably serve a similar purpose. In their variety and quantity of enzymes, the cells of the proximal tubule surpass those in all other parts of the nephron.

About 80% of the total dissolved material in the glomerular filtrate consists of sodium salts. The active transport of sodium is therefore the primary event in the reabsorption of filtrate. Transport

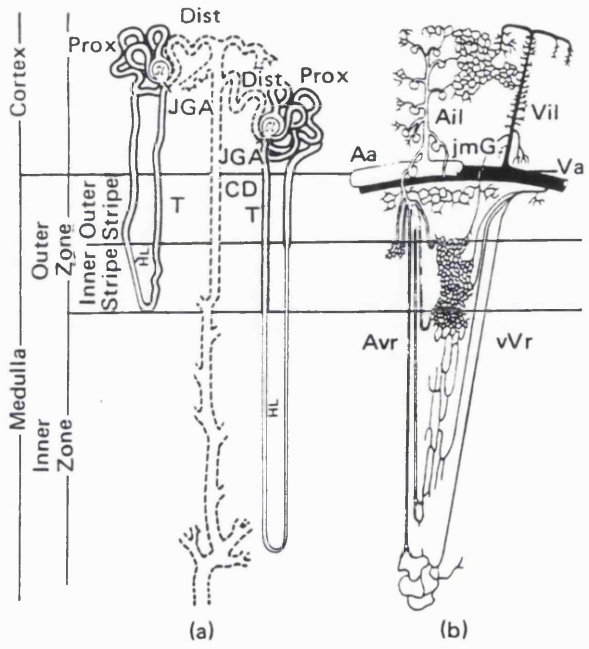

Fig 1.2 Structure of the nephron (a) and its vascular supply (b). Gl, glomerulus; Prox, proximal convoluted tubule; HL, Henle's loop; JGA, juxtaglomerular apparatus; Dist, distal convoluted tubule; CD, collecting duct; T, medullary thick ascending tubule; Aa arcuate artery; Ail, interlobular artery; Vil, interlobular vein; Va, arcuate vein; jGm, juxtaglomerular glomerulus; aVr arterial *vasa recta*; vVr, venous *vasa recta*. From Deetjen, Boylan and Kramer, 1975.

of sodium against an electrochemical gradient requires energy that must be made available by the oxidative phosphorylation of glucose in the mitochondria (see Section 1.7), thereby generating the energy transduction molecule adenosine 5′ triphosphate (ATP). Thus, above the basal level of oxygen consumption, which is similar to other epithelial structures in the resting state, oxygen consumption in the kidney increases in proportion to the rate of sodium reabsorption.

The principle of sodium reabsorption is similar throughout the renal tubules, and depends on conserving a low intracellular Na^+ concentration in the tubule cells, and a negative charge with respect to the exterior. As a result of these differences, Na^+ can diffuse passively down a concentration gradient from the tubular lumen, through leakage channels in the brush border or apical membranes. The low intracellular Na^+ levels upon which this process depends are maintained by sodium pumps on the basolateral membranes (most particularly, the Na^+-K^+-ATPase), which actively expel Na^+ into the interstitial fluid. Na^+ then diffuses through the interstitial fluid and into the peritubular capillaries. Although the Na^+-K^+-ATPase imports K^+ at the same time as it extrudes Na^+, the basolateral membranes contain numerous K^+ leakage channels. Thus, the net effect of the Na^+-K^+-ATPase is the reabsorption of Na^+.

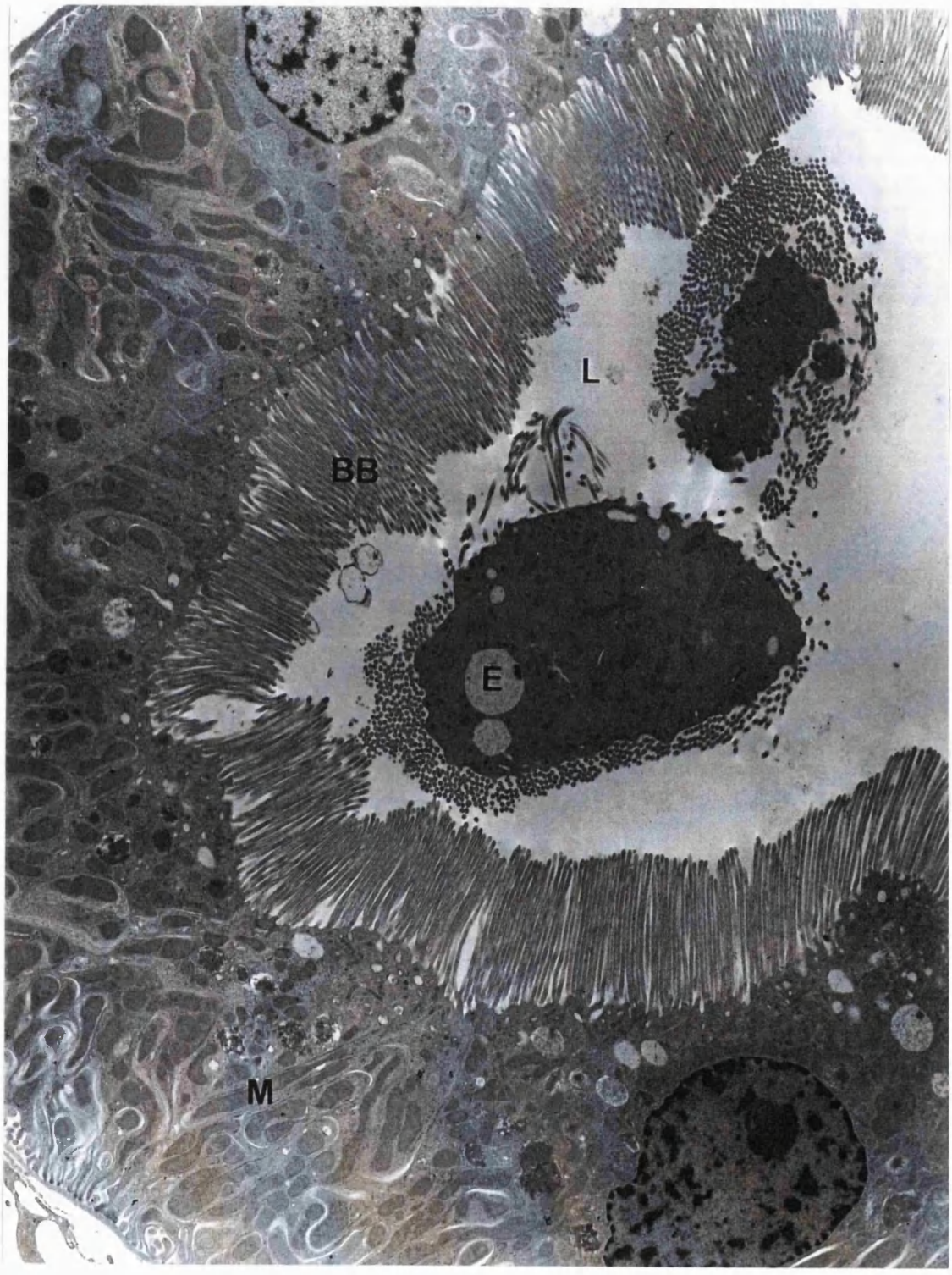

Plate 1.2 **Transmission electron micrograph of a proximal tubule, S1 segment (magnification x 7500) showing densely packed elongated mitochondria (M), endocytotic vesicles (E), dense brush-border (BB) and clear lumen (L). The cellular material in the lumen is convoluted tubule in cross section.**

Because the energy derived from ATP directly fuels the extrusion of Na^+ from the cell, the Na^+-K^+-ATPase is an example of a *primary* active transport mechanism.

Reabsorption of Na^+ promotes the *secondary* reabsorption of water and solutes, by osmosis and diffusion respectively. The movement of water shadows that of Na^+ from the filtrate to the peritubular capillaries, thereby restoring the osmotic balance, and depends partly on the raised osmotic pressure of the plasma proteins in the peritubular capillaries (a consequence of haemoconcentration following glomerular filtration). As water leaves the glomerular filtrate, the concentration of the remaining filtered solutes increases, leading to the reabsorption of some, including K^+, Cl^-, HCO_3^- and urea, by simple diffusion down a concentration gradient. This process is enhanced by the movement of anions down electrical gradients towards the higher Na^+ concentration in the peritubular capillaries. The osmotically driven flux of water may also carry Na^+ Cl^- and other solutes mechanically out of the tubular lumen - a passive process known as *solvent drag* (Deetjen, Boylan and Kramer, 1975).

The reabsorption of glucose is also affected by means of a sodium-oriented mechanism. In this case, glucose-Na^+-symporters on the apical membrane use the Na^+ concentration gradient to drive the simultaneous reabsortion of glucose. Substances brought into proximal tubule cells by symporters (membrane pumps that transport two substances in the same direction across a membrane), generally leave the cell by facilitated diffusion (via a membrane carrier), and enter the peritubular capillaries by simple diffusion. Several different Na^+ symporters reabsorb filtered glucose, various amino acids, lactic acid, and other nutrients. Reabsorption of these nutrients also stimulates reabsorption of water by osmosis. Thus, as the ultrafiltrate passes down the proximal tubule, some 70% of it is reabsorbed, with no change in its sodium or osmotic concentration (Tortora and Grabowski, 1996).

Each symporter has a limiting rate constant, known as its *transport maximum* (T_m), measured in mg/min. If the blood concentration of a solute, and therefore its concentration in the glomerular filtrate, rises above a level which exceeds the capacity of tubular reabsorption, it surpasses the *renal threshold*, and is found at elevated levels in the urine. For example, when glucose is found in the urine, as in patients suffering diabetes mellitus, the condition is known as *glucosuria*, and is associated with an increased volume of urine, since the osmotic reabsorbtion of water is correspondingly decreased.

Most tubular secretion (leading to elimination of substances via the urine) occurs in the proximal convoluted tubule. Secreted substances include H^+, K^+, NH_4^+, creatinine, and some drugs, such as penicillin. Secretion of H^+ via Na^+-H^+ antiporters (membrane pumps that transport two substances in opposite directions across a membrane) on the apical membrane helps to control blood pH, by stimulating the simultaneous reabsorption of HCO_3^-. Extruded H^+ combines with HCO_3^- in the tubular lumen, in a reaction catalysed by carbonic anhydrase (located in the brush border membrane). H_2CO_3 dissociates to form water and CO_2, which diffuses into the cell, where the reaction is reversed. Thus, extrusion of H^+ stimulates the simultaneous reabsorption of both HCO_3^- and Na^+.

The Loop of Henle

The loop of Henle connects the proximal convoluted tubule with the distal convoluted tubule by way of a hairpin loop extending into the medulla. About 80 to 85% of nephrons have short loops of Henle that penetrate only as far as the outer medulla. The descending limb of the loop is lined with cuboidal epithelial cells, similar to those of the proximal convoluted tubule (but without a brush border), and is known as the *pars recta*, or straight descending limb of the proximal tubule. The ascending limb is lined with cuboidal epithelial cells of similar morphology to the cells of the distal convoluted tubule (see below), and is known as the medullary thick ascending tubule (mTAT) (Plate 1.3). Nephrons with short loops of Henle are usually derived from glomeruli in the superficial cortex, and are known as *cortical nephrons*. They receive their blood supply from peritubular capillaries arising from the efferent arterioles.

The remaining 15 to 20% are *juxtamedullary nephrons*, with glomeruli situated deep in the cortex, and long loops of Henle that stretch through the medulla almost as far as the renal papilla. In addition to the *pars recta* and mTAT sections of the loop of Henle, these tubules extend in a fine loop, lined with flat epithelial cells - the thin descending and thin ascending limbs. They receive their blood supply from the peritubular capillaries and the *vasa recta*. However, the environment in the inner medulla is predominantly hypoxic, and the epithelial cells are adapted to glycolysis and the anaerobic production of ATP, possessing few small mitochondria and very little recognizable ultrastructure; they are in fact scarcely distinguishable from the endothelial cells of the neighbouring *vasa recta* (Plate 1.4). In agreement with the morphological picture, there is a striking poverty of enzymes, especially those involved in oxidative metabolism.

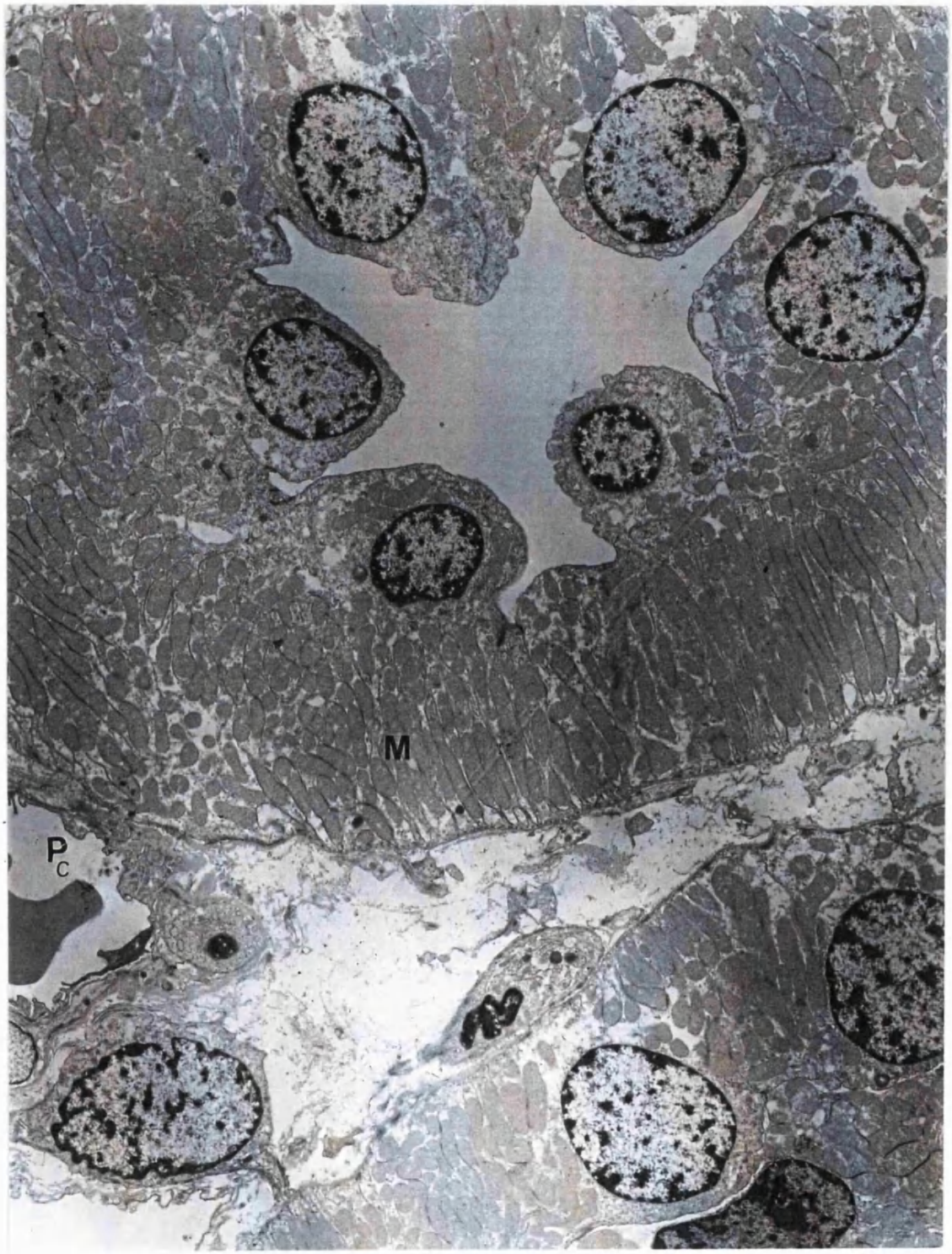

Plate 1.3 **Transmission electron micrograph of medullary thick ascending tubules (mTAT) in the cortico-medullary junction area of the kidney (magnification x 5000) showing densely packed mitochondria (M) and a peritubular capillary (Pc).**

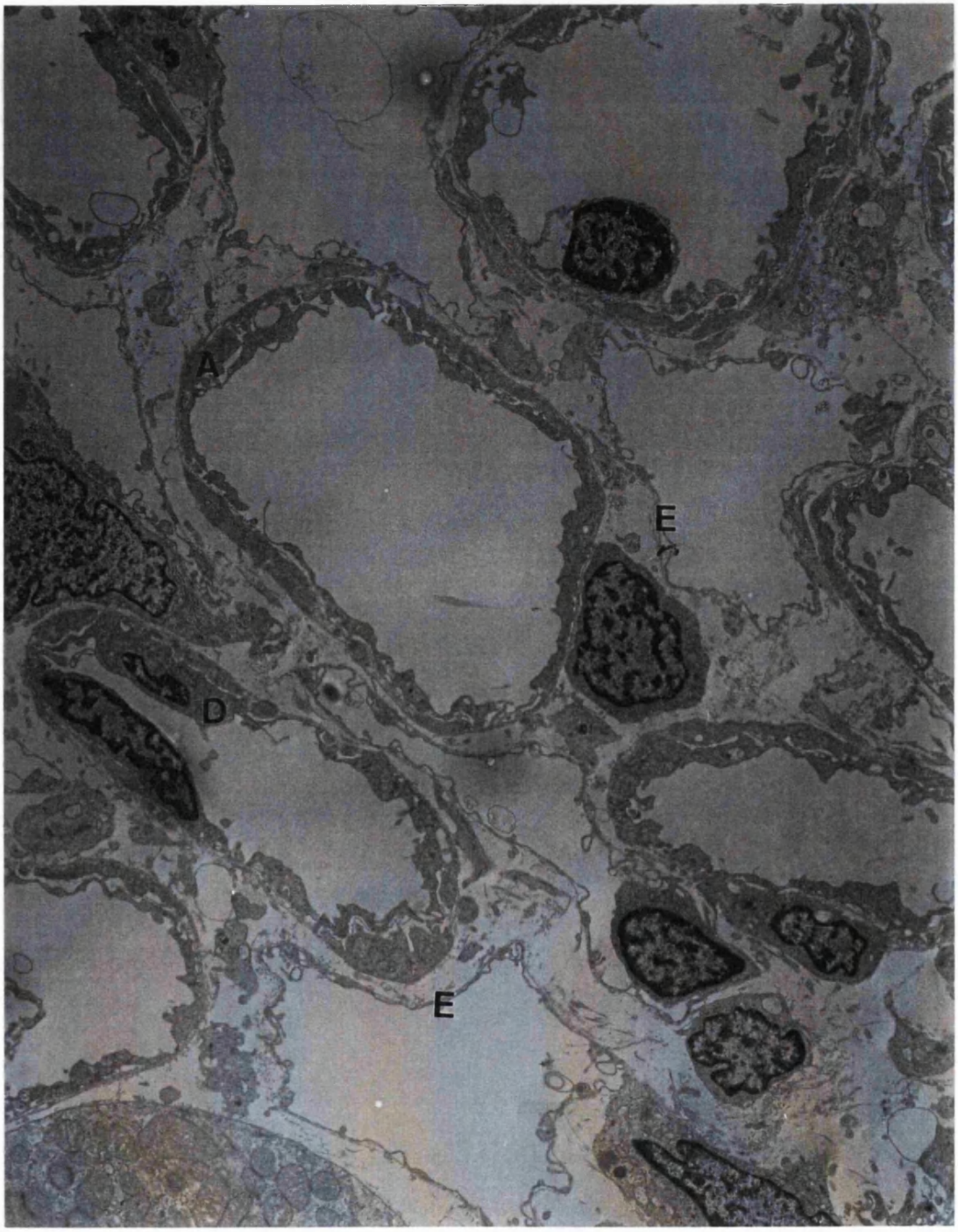

Plate 1.4 **Transmission electron micrograph of the thin segment of the loop of Henle, (magnification x 5000) showing epithelial cells of the descending (D) and ascending (A) limbs and endothelial cells (E) of the vasa recta.**

The loop of Henle is responsible for the reabsorption of about 30% of the filtered K^+, 35% of the Cl^-, and 15% of the water. The cells of the mTAT are also specifically responsible for the reabsorption of Mg^{2+} and Ca^{2+}. However, reabsorption of water by osmosis is not automatically coupled with the reabsorption of solutes. While some water is reabsorbed in the descending limb, little or none is absorbed in the ascending limb; the apical surfaces of these cells are normally completely impermeable.

The major activity of the mTAT is the reabsorption of Na^+, K^+ and Cl^- by means of Na^+-K^+-$2Cl^-$ symporters on the apical membrane. As in the proximal tubules, the mechanism is dependent on the active extrusion of Na^+ ions from the mTAT cells by Na^+-K^+-ATPase antiporters on the basolateral membranes, into the interstitial fluid, whence they diffuse into the *vasa recta*. K^+ diffuses down its concentration gradient into the blood, while Cl^- follows down an electrical gradient. As the mTAT cells are impermeable to water, reabsorption of Na^+ Cl^- establishes an ionic osmotic gradient in the renal medulla. As the ions pass into the interstitial fluid of the outer medulla, they become concentrated, and are carried deep into the inner medulla by the blood flowing in the *vasa recta*. The physiological significance of this in the production of hypertonic urine is discussed in Section 1.3.3.

The Na^+-K^+-$2Cl^-$ symporter is also clinically significant in that it is inhibited by loop diuretics (which derive their name from their specificity for the loop of Henle) such as frusemide. By completely inhibiting the reabsorption of sodium chloride in the mTAT, loop diuretics induce intense diuresis (increased urine volume). The consequences of inhibiting the Na^+-K^+-$2Cl^-$ symporter following renal transplantation are the subject of Chapter 9 of this thesis.

The Distal Convoluted Tubule

Each ascending limb comes into close apposition with the vascular pole of its glomerulus of origin. At this point of contact is found the *macula densa*, which marks the beginning of the distal convoluted tubule. The cells of the macula densa are of characteristic columnar morphology, and the apical membrane contains receptors sensitive to the sodium concentration in the tubular lumen. The adjacent cells of the medial layer of the afferent arteriole have an epithelioid appearance, with granular cytoplasm. These epithelioid cells are known as *juxtaglomerular cells*, and are thought to be responsible for renin production (an enzyme involved in the control of renal blood flow). Together with the macula densa, they constitute the *juxtaglomerular apparatus*, which is responsible for the autoregulation of renal blood flow, and consequently the rate of glomerular filtration (see Section 1.3.4).

The cells of the distal tubule are cuboidal but, unlike the proximal tubule, do not have a brush border. The mitochondria are less densely packed and the basal labyrinth is less copiously convoluted. Enzymes are present in equal variety but in lower concentration than in the proximal cells. Fluid enters the distal convoluted tubules at a much slower rate of about 25 ml/min, as 80% of the filtered water has by now been absorbed (Tortora and Grabowski, 1996). As fluid flows down the tubule, Na^+-Cl^- symporters in the apical membranes reabsorb Na^+ and Cl^-. By the time the fluid reaches the end of the distal tubule, about 90% of the filtered solutes and water have been returned to the blood-stream.

The Collecting Ducts

Two different cell types are present in the collecting ducts. The majority are large cuboidal cells, known as *principal cells*, which possess numerous basal invaginations, but are otherwise as poorly differentiated in their morphology and histochemistry as the cells of the thin portion of Henle's loop. They are nevertheless responsible for the reabsorption of the final 9% of water and Na^+, in a process controlled by two regulatory hormones, antidiuretic hormone (ADH) and aldosterone (see Section 1.3.4).

A few cells in the collecting tubules are better differentiated, with more numerous mitochondria and apical microvilli, and are known as *intercalated cells.* They play a role in secretion of H^+, thereby contributing to acid-base homeostasis.

In the collecting ducts, as in all other segments of the nephron, the enzymes concerned with anaerobic energy production are found in relatively high concentration.

1.3.3 Countercurrent Multiplication

As long ago as 1927, Crane noted that animals such as the frog, whose nephrons possess no loop of Henle, were not capable of producing concentrated urine. In fact, there is a very close correlation between the maximum concentrating ability of a kidney, and the relative thickness of the medulla (i.e. the length of the loop of Henle)(O'Dell and Schmidt-Nielsen, 1960).

In 1942, Kuhn and Ryffel proposed that the hairpin loops of Henle could mediate the urinary concentrating process by means of a countercurrent mechanism similar to that used to conserve heat in a furnace. However, unlike a furnace (where a simple exchange of heat between opposed pipes takes place), Kuhn argued that the active transport of Na^+ Cl^- from the ascending loop of

Henle into the hypertonic interstitium could build up and maintain a small osmotic gradient between the ascending and descending limbs - a gradient that could be established at every level of the loop. Because tubular fluid moves in opposite directions in the two limbs of the loop, a small 'single' effect at each level would lead to a large overall effect on the concentration gradient between the base and the apex of the loop (that is, the 'single' effect is multiplied; Fig 1.3). This gradient would be directly proportional to the length of the hairpin loop and to the concentration gradient between the two limbs, and inversely proportional to the (square of) the flow rate. While various minutiae have yet to be elucidated, the basic principles of Kuhn and Ryffel have been subsequently confirmed (Wirz, Hargitay and Kuhn, 1951; Gottschalk, 1964; Jamison, Bennett and Berliner, 1967).

As currently understood, sodium is pumped out of the medullary thick ascending tubule (mTAT) and into the surrounding interstitium (see Section 1.3.2); but because the apical membranes of the mTAT are impermeable to water, there is no accompanying osmotic movement of water. The increasing osmolarity of the surrounding interstitium therefore draws water from more permeable structures, including the descending limbs, the collecting ducts and the *vasa recta*. As a consequence, the osmolarity of fluid in all of these increases progressively as they approach the renal papilla in the manner proposed by Kuhn and progressively decreases as it moves back up the ascending limb. To maintain a gradient of 300 to 1200 mOsm/l across the renal medulla from the outer medulla to the papilla, requires that the sodium pump sustain at each level only a limited concentration gradient of 100 mmol/litre of Na^+ Cl^-. This is thermodynamically a very economical arrangement, and enables the production of hypertonic urine to proceed at the expense of only a fraction of the energy that would be required to achieve the same effect in a single step.

When it emerges from the ascending limb of the loop of Henle into the distal tubule, the tubular fluid is slightly hypotonic with respect to plasma. As the wall of the distal tubule is permeable to water, osmotic equilibrium is re-established in the cortex by loss of water from the tubular fluid to its isotonic surroundings. This efflux of water, with some further reabsorption of Na^+ Cl^-, reduces the volume of tubular fluid, so that only about 50% of fluid leaving the loop of Henle eventually reaches the collecting ducts, in which it once again traverses the medulla.

In its passage towards the papilla, this residual fluid loses more water (and Na^+ Cl^-), leading to the progressive concentration of urea and other solutes. Because duct cells deep in the renal

medulla are freely permeable to urea (whereas the mTAT, distal tubule and cortical collecting ducts are quite impermeable to it, leading to a build-up in its concentration), some urea diffuses into the interstitial fluid of the inner medulla (where it helps maintain a high osmolarity), while the rest is excreted. Thus, reabsorption of water from the tubular fluid of the collecting ducts promotes the recycling of urea through the interstitial fluid of the medulla, which in turn promotes water reabsorption. As a consequence, the final urine produced amounts to only about 1% of the glomerular filtrate, and its osmolarity is very nearly as high as that of the interstitial fluid at the papillary tip.

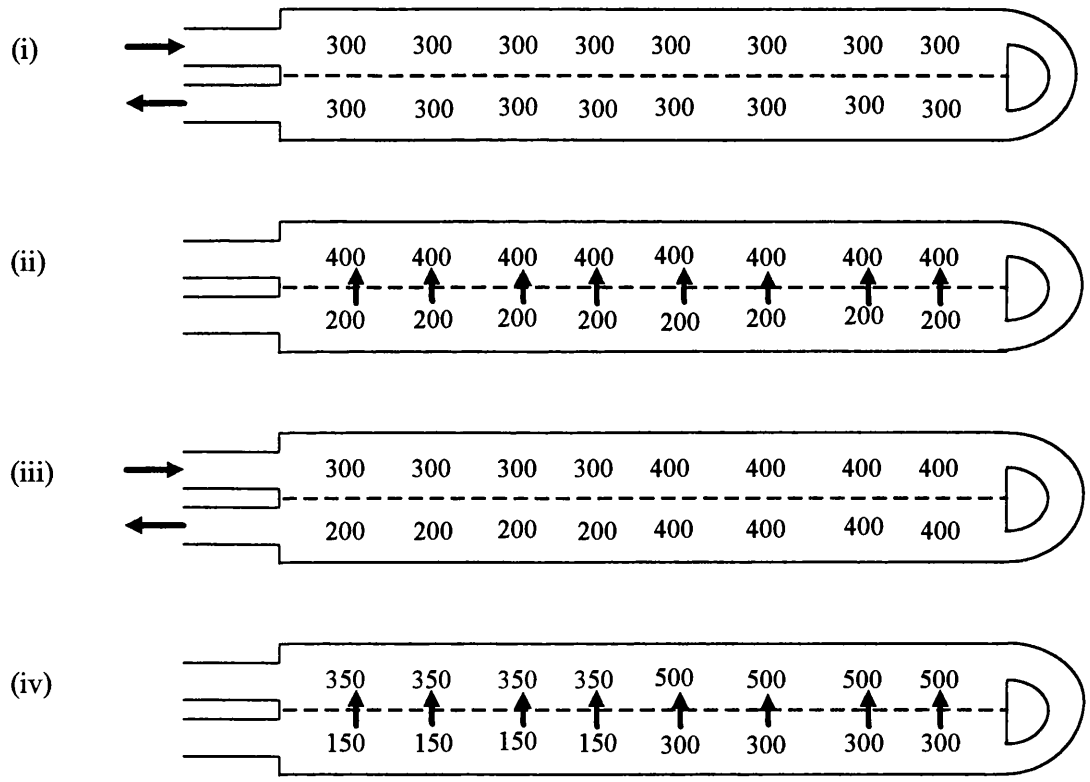

Fig 1.3 Modus operandi of countercurrent multiplication. Note that the process is depicted in stages rather than as a continuous process. (i) and (iii) represent fluid movement through a hairpin loop divided by a membrane impermeable to water; the numbers indicate the osmolarity of the fluid in mOsm/l. (ii) and (iv) represent the effect of an energy-dependent Na^+ extrusion across the dividing membrane, leading to the generation of a concentration gradient down the loop.

1.3.4 Physiological Control

Control of the GFR, Na^+ and water reabsorption is predominantly hormonal, but autoregulation and neural regulation also play a role. Renal autoregulation operates via a negative feedback system, in which secretion of an unidentified vasoconstrictor (a prostaglandin? see below) by the cells of the juxtaglomerular apparatus is modulated by Na^+ levels in the tubular fluid (Tortora and Grabowski, 1996).

Neural regulation is achieved via the sympathetic stimulation of renal vasoconstriction. With moderate sympathetic stimulation, both afferent and efferent arterioles constrict to a similar degree, thereby decreasing the GFR only slightly. In contrast, strong sympathetic stimulation (which occurs, for example, during exercise) causes mainly afferent vasoconstriction, thereby dramatically reducing the GFR and enhancing blood flow to extra-renal tissues. In addition, strong sympathetic stimulation potentiates adrenal secretion of the hormone adrenalin, which also stimulates vasoconstriction of the afferent arterioles.

Hormonal Control of Glomerular Filtration

Two hormones - angiotensin II and atrial natriuretic peptide (ANP) - contribute to the regulation of blood pressure, and therefore GFR. When the GFR decreases, the Na^+ content of the tubular fluid at the macula densa drops, stimulating the juxtamedullary cells to secrete an enzyme called renin into the blood (see Section 1.3.2). Renin cleaves the circulating plasma protein angiotensinogen (produced by the liver), forming an inert decapeptide hormone precursor called angiotensin I. As angiotensin I passes through the lungs, it is converted into the vasoactive peptide hormone angiotensin II, by the angiotensin converting enzyme (ACE). Angiotensin II has several important renal and systemic actions, including:

- Stimulation of vasoconstriction in the efferent arterioles, thereby increasing the hydrostatic pressure within the glomerulus, and raising the GFR back to normal. It also constricts arterioles elsewhere in the body, thereby increasing systemic vascular resistance and blood pressure
- Stimulation of aldosterone secretion by the adrenal cortex, thereby increasing reabsorption of Na^+ Cl^- and water in the renal collecting ducts (see below). In turn, this increases blood volume, restoring blood pressure and GFR to normal
- Stimulation of antidiuretic hormone secretion from the posterior pituitary gland, thereby promoting reabsorption of water in the renal collecting ducts (see below)

- Stimulation of the thirst centre in the hypothalamus, prompting fluid intake, and restitution of normal blood volume.

Normalization of systemic and renal blood pressure and GFR leads to an increase in Na^+ concentration at the macula densa, and inhibition of renin release.

The second hormone that influences glomerular filtration is atrial natriuretic factor (ANF). As its name suggests, it is secreted by cells in the atria (superior chambers) of the heart, in response to mechanical stretching of the atrial walls (which occurs when blood volume is raised). ANF has many direct effects on the cardiovascular system, on other hormones, and on the central nervous sytem. In the kidney, it dilates the afferent arterioles, increasing the GFR, stimulating natriuresis (excretion of Na^+), and consequently diuresis. It also suppresses the actions of anti-diuretic hormone, aldosterone and renin (see below).

Hormonal Control of Sodium and Water Reabsorption

The hormones aldosterone and antidiuretic hormone (ADH) maintain homeostasis of blood volume, composition and pressure, by regulating Na^+ and water reabsorption in the *principal* cells of the collecting ducts (see Section 1.3.2). Aldosterone (secreted by the adrenal cortex) stimulates increased synthesis and incorporation of Na^+-K^+ antiporters into the apical membranes of the principal cells, leading to enhanced K^+ secretion, Na^+ absorption, and Na^+-K^+-ATPase activity. When blood levels of aldosterone are low, the principal cells reabsorb little sodium, leading to a state of natriuresis, and consequently diuresis. ADH is produced by the hypothalamus and released into the bloodstream by the posterior pituitary gland. In the absence of ADH (a condition known as *diabetes insipidus*), the principal cells have a very low permeability to water, and up to 20 l per day of very dilute urine may be passed. ADH acts to stimulate incorporation of water-channel proteins into the apical membranes of the principal cells (Tortora and Grabowski, 1996), leading to increased water reabsorption.

The Eicosanoids: Prostaglandins and Leukotrienes

Eicosanoids act as local hormones (mediators) in most tissues of the body, and are formed from a ubiquitous 20-carbon fatty acid called *arachidonic acid* (formerly known as eicosatetraenoic acid, from the Greek *eikosi*, meaning twenty), which is incorporated into membrane phospholipids by the action of acyltansferase enzymes. The release of arachidonic acid in response to a stimulus occurs primarily through activation of the enzymes phospholipase A_2 and C. Three distinct enzymatic pathways exist to produce a plethora of eicosanoid mediators, with

diverse biological activities: the cyclooxygenase pathway; the lipoxygenase pathway and the cytochrome P-450 pathway (Fig 1.4). All three involve the incorporation of one or more oxygen atoms into arachidonic acid. In the kidney, the eicosanoids are involved physiologically in the regulation of blood pressure and of ion transport in the tubules. They are also potent mediators of the inflammatory response and are therefore of great importance in many pathological conditions as well as in the course of renal transplantation (see Section 1.7 and Chapters 7-10).

Prostaglandins and thromboxanes are produced by the action of cyclooxygenase. The primary prostaglandins and thromboxanes produced in the renal cortex (by the epithelial cells and mesangial cells of the glomerulus) are PGI_2 (also known as prostacyclin), PGE_2, and thromboxane A_2. Prostacyclin and PGE_2 counter the physiological effects of angiotensin II, stimulating vasodilation, and reducing endothelial cell permeability (via a cyclic adenosine monophosphate (cAMP) dependent mechanism). Thromboxane A_2 is a potent vasoconstrictor, neutrophil chemoattractant and stimulator of vascular permeability, but plays a limited role in the normal physiological function of the kidney. In the renal medulla, the cells of the collecting ducts, the thin descending limbs and the interstitium produce abundant PGE_2, as well as some $PGF_{2\alpha}$, PGD_2 and thromboxane A_2.

The leukotrienes are formed by a family of lipoxygenase enzymes, of which the most important enzymes endogenous to the kidney are 12- and 15-lipoxygenase (the numbers indicating the point of insertion of a single hydroperoxy group into the 20-carbon fatty acid chain). The principal end-products of these enzymes are the 12- and 15- hydroxyeicosatetraenoic acids (12- and 15-HETE), which are formed in glomerular mesangial cells, and may play a role in regulating the activity of renal epithelial cell ion channels (Frazier and Yorio, 1992). In addition, various products of 5-lipoxygenase (which is found in circulating neutrophils and in platelets) are important pro-inflammatory mediators, among them leukotrienes (LT) B_4, C_4, D_4 and E_4.

The cytochrome P-450-dependent mono-oxygenases are the third major pathway of arachidonic acid metabolism. This family of mixed function oxidases includes haemoprotein, cytochrome P-450, NADPH cytochrome reductase and phosphatidylcholine (Conney, 1982). Cytochrome P-450 metabolism of arachidonic acid requires molecular oxygen and reduced nicotinamide adenine dinucleotide phosphate (NADPH) in a 1 : 1 stoichiometry, but the enzyme is not particularly substrate-specific, and can also catalyse the oxidation of other polyunsaturated fatty acids. The products of cytochrome P-450 and their sites of action have only recently been identified (Frazier and Yorio, 1992). The principal products (19- and 20-HETE, and 20-COOH-

arachidonic acid) are produced in the proximal convoluted tubule and the mTAT, and have been shown variously to inhibit the Na^+-K^+-ATPase, and to stimulate vasodilation (Schwartzman *et al.*, 1986).

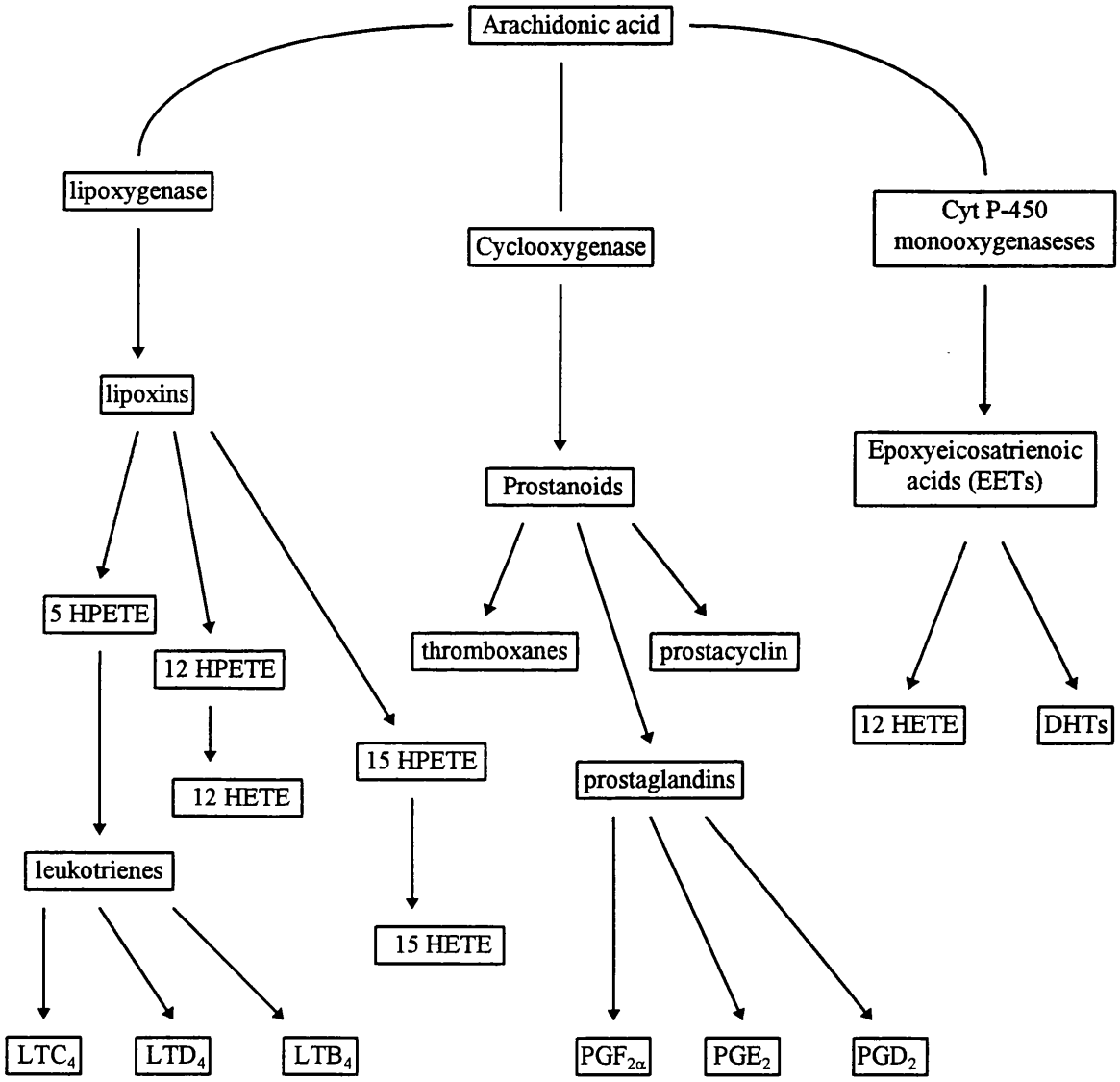

Fig 1.4 Eicosanoid cascade (see text).

Nitric Oxide and Endothelin

In addition to the gamut of hormones and eicosanoids discussed above, two endothelial-derived factors are involved in the modulation of vascular tone in the kidney: *endothelial-derived relaxation factor* (EDRF), and *endothelin*.

In 1987, EDRF was shown to be identical to nitric oxide (NO), and to be formed from the amino acid L-arginine by the enzyme NO synthase, which exists in both constitutive and inducible forms (Moncada, Palmer and Higgs, 1989). The constitutive form is Ca^{2+}-dependent, and releases NO for short periods in response to receptor or physical stimulation; induction of the other form is stimulated by activated macrophages or cytokines and once expressed, synthesizes NO for long periods (up to 3 hours). NO has a very short half-life (less than 5 seconds), and acts locally by activating the enzyme guanylate cyclase in the adjacent vascular smooth muscle cells, leading to elevated levels of the secondary messenger cyclic guanosine monophosphate (cGMP). In the cardiovascular system, release of NO serves as a general adaptive mechanism, whereby the endothelium reacts to changes in its environment, regulating blood flow and pressure through its action on vascular smooth muscle. In addition, NO regulates the interaction between the endothelium and platelets and probably blood-borne cells, and may play a role in the control of smooth muscle proliferation (Moncada, Palmer and Higgs, 1991).

The term *endothelin* refers to a family of 21-amino acid peptides, found in at least four distinct isoforms: ET-1, ET-2, ET-3 and endothelin β, which share sequence homology, a hairpin loop configuration and a hydrophobic C-terminus. It is formed by proteolysis of a pro-hormone by the *endothelin converting enzyme*, and possibly stored in secretory granules before secretion (Simonson and Dunn, 1991). Endothelin has a surprisingly wide range of biological actions in diverse tissues and species, and is among the most potent vasoconstrictors yet discovered (Yanagisawa *et al.*, 1988; Gunning, *et al.*, 1996). In the kidney, it causes potent efferent arteriolar vasoconstriction, and contraction of the interlobular and arcuate arteries. The actions of endothelin on Na^+ handling are complex, and include reductions in the filtered Na^+ load to tubular reabsorptive sites, as well as attenuation of Na^+-K^+-ATPase activity in the mTAT, via a PGE_2-dependent mechanism (Zeidel *et al.*, 1989). There have also been reports that endothelin inhibits renin secretion *in vitro*, possibly by increasing intracellular Ca^{2+} levels (Moe *et al.*, 1991). Its duration of action *in vivo* is very long, and 1 to 3 hours are typically required for mean arterial pressure to return to baseline levels (Simonson and Dunn, 1991).

1.4 Renal Diseases

Fifty to eighty people per million of the population develop end-stage renal failure (ESRF) each year (Gabriel, 1990). The pathophysiological manifestations of renal disease are dictated by the site of injury within the kidney, and are frequently secondary to other disorders, such as hypertension, acute hypotension, diabetes or infection. The major diseases leading to ESRF are: glomerulonephritis; diabetic nephropathy; toxic nephropathy; malignant hypertension; polycystic

renal disease; and chronic pyelonephritis. In addition, obstructions to urine flow caused by prostate enlargement, kidney stones, abnormal development of urethral valves, or reflux of urine can result in persistent back pressure, causing tubular damage and ultimately ESRF.

Glomerulonephritis

Primary glomerular diseases constitute a heterogeneous collection of disorders in which the glomeruli are the sole or predominant tissue involved. Environmental factors such as microbial infections (most notably streptococci) or drugs are frequently associated with the pathogenesis of glomerulonephritis, but many primary glomerular diseases also have an underlying genetic basis. Post-streptococcal glomerulonephritis (PSGN) is a typical example; this is an immune complex disease, in which antibodies to constituents of the native glomerular capillary wall develop. The capillary lumens become occluded by proliferating cells, and the glomeruli swell and become bloodless. The major clinical manifestations are: proteinuria; haematuria; reduced GFR; oliguria (diminished urine production); and alterations in Na^+ excretion, leading to oedema, circulatory congestion and hypertension. Disorders of glomerular structure and function constitute some 40% of the total incidence of ESRF.

Diabetic Nephropathy

Persistent albuminuria (>30 mg/day), associated with nodular glomerular intercapillary lesions and accompanied by arterial hypertension are the hallmarks of diabetic nephropathy, which may occur in both insulin dependent and independent diabetes. The pathogenesis is not fully understood, but appears to derive from the effects of sustained hyperglycaemia on the glomeruli, the consequences of which are changes in endothelial cell shape, generalised basement membrane thickening, vasoconstriction, over-synthesis of extracellular matrix (by mesangial cells), and loss of responsiveness to vasoconstrictors such as angiotensin II. Diabetic nephropathy is the single most common cause of ESRF in the United States, accounting for 33% of all patients enrolled in the Medicare ESRF program (Parving, Osterby, Anderson and Hsueh, 1996).

Toxic Nephropathy

As the kidney concentrates and excretes metabolic waste, chemicals and many drugs, it may become exposed to toxic concentrations of these substances. Nephrotoxic substances such as analgesics, aminoglycoside antibiotics, penicillins, cyclosporin, or heavy metals such as lead may cause injury at a number of sites in the kidney, and produce characteristic clinical syndromes.

Malignant Hypertension

The process of malignant hypertension begins with a critical degree of renal vascular damage, generally associated with severe essential hypertension. The deficit in renal perfusion triggers a massive release of renin, leading to vasoconstriction and sodium retention. In turn, this causes a massive increase in systemic blood pressure. However, the compromised kidney, unable to participate in systemic hypertension, continues to behave as though the local hypotension were systemic. A vicious circle develops which terminates in systemic arteriolar necrosis.

Polycystic Renal Diseases

Renal cysts are abnormal, fluid-filled sacs that arise in the renal parenchyma. They occur in a multitude of unrelated conditions, and may be hereditary, developmental or acquired. Polycystic renal diseases are a subset of hereditary renal disorders in which the cysts are distributed throughout both kidneys. Many patients report pain that may be associated with gross or microscopic haematuria (mainly due to cyst rupture), but proteinuria is seldom severe. Hypertension is common, as are symptoms of renal infection and lithiasis (development of kidney stones). The most common form of the disease is autosomal dominant polycystic renal disease, which affects about 1 person in 1000 (Welling and Grantham, 1996).

Chronic Pyelonephritis

A single species of bacteria - *E. coli* - accounts for the overwhelming majority of urinary tract infections, which are themselves the most common of all bacterial infections. The usual course of uncomplicated acute pyelonephritis is one of healing rather than progressive damage. Tissue destruction is largely the result of bacterial multiplication and inflammation. However, a variety of bacterial and host factors (such as unusual infecting organisms, urinary tract obstructions, pregnancy or diabetes mellitus) can modify this sequence of events and lead to progressive tissue damage. The most common morphological changes observed in chronic pyelonephritis are coarse or focal scarring and tubular dilatation. The clinical manifestations of these changes include hypertension, an inability to conserve sodium, decreased urine concentrating ability, and a tendency towards acidosis. Data from the European Dialysis and Transplant Association show that 22% of adults with ESRF suffer from chronic pyelonephritis (Rubin, Cotran and Tolkoff-Rubin, 1996).

1.5 Treatment Possibilities: Dialysis or Transplantation?

Unlike patients dying from terminal failure of other vital organs, patients with ESRF can be kept alive by haemodialysis or continuous ambulatory peritoneal dialysis (CAPD). Haemodialysis is

the diffusion of substances between the blood and dialysis fluid (dialysate) across a semi-permeable membrane. Access to blood is achieved via an external arteriovenous shunt or, more commonly, an arteriovenous fistula introduced surgically. The electrolyte composition of the dialysate, whether for haemodialysis or peritoneal dialysis, is very similar to that of normal plasma. Solutes move down their concentration gradients from blood to dialysate at speeds dependent on their molecular size and shape. The rate of removal of a solute increases as the volumes of blood and dialysate exposed to each other increase.

CAPD is a form of dialysis in which the dialysate remains continuously within the peritoneal cavity. Unfortunately, dialysate must be exchanged through a catheter every four to eight hours without respite. The principle of CAPD is essentially similar to haemodialysis, except that blood flow through the peritoneal capillary bed is relatively constant, and the volume of dialysate is small compared with that used during haemodialysis. Peritoneal dialysis is therefore much less efficient than haemodialysis over a short period of time but, in compensation, CAPD is a continuous process.

Apart from the medical or surgical complications which accompany ESRF, there are various problems associated with dialysis itself. Access to the circulation becomes increasingly difficult in the course of chronic haemodialysis. The life-time of a shunt, placed at the wrist or the ankle, is limited; and the probability of thrombotic obstruction or infection in the surrounding tissues is high. Anaemia and hypotension, caused by the depressed erythropoesis common to most forms of ESRF, is magnified by any blood lost in the course of dialysis. Rapid changes in solute balance can create large concentration gradients between various body compartments, culminating in disequilibrium syndrome comprising headaches, vomiting and occasional fits (as a result of cerebral oedema). Renal osteodystrophy (bone disease) - common, but usually silent, in patients dying of ESRF - often becomes symptomatic in the course of dialysis, and is associated with the calcification of soft tissues. Persistent hypertriglyceridaemia, possibly resulting from a defect in very low density lipoprotein (VLDL)-triglyceride removal, is also common in ESRF patients, and may be exacerbated by the dextrose in the peritoneal fluid during CAPD, accelerating the progression of atherosclerosis (Gabriel, 1985). Not surprisingly, severe stresses and psychological problems frequently develop, and dialysis patients have a substantial psychiatric morbidity (Gabriel, 1985). Mortality is typically 10-15% over the first year, with a gradual and sustained loss of patients thereafter, mortality at six years being about 30-50% (Gabriel, 1985).

Renal transplantation has evolved to be a superior treatment to dialysis in terms of survival, quality of life and cost-effectiveness, and can now be claimed as the treatment of choice for ESRF. Patients liberated from dialysis can eat a normal diet, will probably feel more healthy, are more mobile and are of more value to the community both socially and economically. However, full exploitation of renal transplantation is limited by the number of suitable donor organs. Fewer than half the ESRF patients in the United Kingdom get the opportunity of a renal graft (Green, 1995), and the rest are by necessity treated with dialysis. Transplantation and dialysis should therefore be regarded as complementary treatments for ESRF. In fact, because dialysis is available as a back-up, patient survival rates following transplantation do not accurately reflect renal graft survival. While more than 90% of patients receiving grafts from living related donors survive for two years, only about 84% of the grafts themselves are still functional at this time (United States Renal Data System, 1993, cited in Ramos and Ravenscraft, 1993). Similarly, more than 80% of patients receiving cadaver kidneys are alive after 2 years, but only about 65% of the original grafts are functional. Many patients whose primary grafts fail return to dialysis before going on to receive a second graft (secondary transplantation). Graft failure may be a result of many factors, including acute rejection, chronic rejection, ischaemic acute renal failure, drug toxicity, infection, steroid related disorders and hypertension.

Many of these drawbacks have been at least partially overcome in the last forty years, since the first successful renal transplant. Indeed, the history of renal transplantation is a remarkable catalogue of scientific and clinical innovations, and comprises one of the 20th centuries' most outstanding medical endeavours.

1.6 Renal Transplantation

1.6.1 History of Renal Transplantation

The Russian surgeon Voronoy performed the first human kidney allograft in 1933 (Voronoy, 1936), but the patient died within two days. He performed six similar operations in the next sixteen years with no success. Later, in the 1950s, several series of human kidney transplants were performed in Paris (Michon *et al.*, 1953) and Boston (Hume *et al.*, 1955) but no immunosuppressive drugs were used to prevent rejection and all but one of the patients died early. That one man, however, survived nearly 6 months, and Murray and his colleagues in Boston were sufficiently encouraged to start up a renal transplantation programme between identical twins (Murray *et al.*, 1955). This proved remarkably successful.

The work of Simonsen and colleagues (1953) and Dempster (1953) during the late 1940s and early 1950s with allografted dog kidneys (kidneys transplanted between genetically different animals of the same species), had shown that the rejection phenomena encountered by Carrel and Guthrie early in the century (1905), and later by Medawar (1944), applied in equal measure to transplanted kidneys. They drew attention to the massive renal infiltrations of lymphoid cells, which accompanied progressive renal failure. Their observations and ideas were developed further by Mitchison (1953) and later by Gowens *et. al.* (1962), and led to the realization that, although cell-mediated immunity was mainly responsible for acute rejection in the first few days after transplantation, humoral mechanisms and cytotoxic antibodies were also involved in the host response to allografts.

The development of a new antimitotic drug, 6-mercaptopurine, and the finding that it had potent immunosuppressive effects (Schwartz and Dameschek, 1959), inspired Calne in 1960 to experiment with its use in renal allografts in dogs. Rejection was at least postponed by the drug, and many of the dogs survived for weeks while being treated (Calne, 1960). Soon afterwards, a derivative of 6-mercaptopurine called azathioprine was used clinically in Boston (Hume *et al.*, 1960) with encouraging results, and marked the beginning of the modern era of transplantation. With the addition of steroids to azathioprine in 1963 (Starzl, Marchioro and Waddell, 1963), a standard immunosuppressive regimen, that remained relatively unchanged for nearly two decades, was established. During this time, improvements in patient survival resulted from:

- Better surgical techniques
- Realization that low doses of steroid are as effective and safer than high doses
- The discovery that blood transfusion before transplantation lowers the chances of rejection
- Realization that patients well matched at the DR site of the human leukocyte antigen (HLA) locus of the major histocompatibility complex (MHC) fare better than those mismatched.

By 1978, renal transplantation had become a valuable treatment for ESRF, but one which - owing to the typical graft survival of 1-2 years - effectively provided periods of relief for chronic dialysis patients (Gabriel, 1985). Then, in 1978, the clinical advent of a novel immunosuppressive agent, cyclosporin A, in a pilot clinical trial undertaken by Calne and his team in Cambridge (Calne *et al.*, 1978), changed the face of renal transplantation, and indeed revolutionized the transplantation of other solid organs, such as liver, heart and lung (which had hitherto had little success). Cyclosporin (a fungal metabolite that inhibits both the humoral and

cell-mediated immune responses, but does not affect the maturation of stem cells) was shown to be as potent an immunosuppressive agent in man as had been revealed earlier in animals (Borel *et al.*, 1976). While its use did not significantly improve renal graft survival in the few centres which already had acceptable 1-year survival rates (above 75%), it made a significant positive impact in those centres which were previously achieving survival rates of only 50-65% (Green, 1988). As a result, two-year patient survival rates are now typically in excess of 80% (United States Renal Data System, 1993, cited in Ramos and Ravenscraft, 1993). These consistently high success rates have brought about a revolution in the public perception of renal transplantation from one of scepticism or even antipathy to one of reluctant approbation.

1.6.2 Current Status of Renal Transplantation

The major obstacle facing renal transplantation today is no longer the prevention of rejection. Although several novel immunosuppressive drugs have been introduced in the last few years, including FK506, rapamycin, and the immunophilins, the incentive to develop them stemmed more from the unwanted side-effects of cyclosporin, such as its chronic nephrotoxicity, than from any inherent shortcomings in its immunosuppressive potency. It seems that a ceiling may now have been reached in terms of conventional approaches to immunosuppression.

Instead, the overriding issue in modern transplantation is the acute shortage of suitable donor organs. More than 4000 patients in the United Kingdom are diagnosed with ESRF each year, yet only 1500 to 1600 renal transplants are performed annually (Green, 1995). Until the problems associated with xenotransplantation (transplantation of organs between different species, for example from pig to man), or cryopreservation (freezing of organs) are overcome, it is vital to make the best use of existing sources of organs - predominantly heart-beating cadavers. The scope for improvement in this respect was illustrated by Ramos and Ravenscraft in 1993, who reported that delayed graft function (DGF) occurs in up to 70% of renal transplant recipients, who are typically maintained on dialysis for periods of up to several weeks until renal function is restored. Not only does this necessity approximately double the economic costs of transplantation (Rosenthal *et al.*, 1991), but long-term graft survival is also significantly impaired in patients with DGF. For example, Rosenthal and colleagues (1991) found the 1- and 2-year graft survival rates in patients with early function to be 93% and 86% respectively, compared with only 65% and 55% respectively in patients with DGF. The majority of patients suffering from DGF had sustained acute tubular necrosis (ATN), as a result of damage incurred during the period of extra-corporeal preservation.

Effective renal preservation could therefore increase the availability of organs for transplantation in several ways. Firstly, prevention of DGF would improve long-term graft survival, thereby releasing organs otherwise committed to patients requiring secondary transplants. Secondly, extended preservation, allowing routine tissue typing and transport of organs over sometimes continental distances to suitably DR-matched recipients, would reduce the likelihood of rejection, again reducing the necessity for secondary transplants. Thirdly, better preservation techniques could salvage organs that would otherwise become too damaged to warrant transplantation, or make available organs from donors over 50 years of age, which are currently not considered suitable because of their low ischaemic tolerance (Segoloni *et al.*, 1991). Currently, kidneys stored for periods of up to 24 hours are likely to regain function soon after transplantation (Green, 1995), whereas kidneys stored for longer than 24 hours (up to a maximum of about 50 hours), are likely to sustain reversible ATN, clinically manifest as DGF. The principal cause of ATN, and the major barrier to extended preservation, is a pathological syndrome known as *ischaemia-reperfusion injury*.

1.7 Ischaemia-Reperfusion Injury

The passage of blood or any other fluid through an organ such as the kidney is termed *perfusion*. Interruption of this flow for any length of time is known as *ischaemia*; and the restoration of flow is termed *reperfusion*. Damaging periods of ischaemia, followed by reperfusion with fully oxygenated blood, may occur in many clinical conditions, such as acute myocardial infarction, stroke and rheumatoid arthritis. Ischaemia and reperfusion are also inevitable consequences of some surgical procedures, including the resection of tumours, vascular reconstruction, and the harvesting and transplantation of tissues and solid organs. A series of degenerative biochemical and pathophysiological changes ensue, which may lead ultimately to tissue death, and which are termed collectively *ischaemia-reperfusion injury*. Although many of these changes only become visible during reperfusion, the severity of ischaemia-reperfusion injury depends in large part on the progression and magnitude of changes occurring during the ischaemic period.

The degree of ischaemic damage depends on the tissue sensitivity, which varies with different tissues or organs and different species, and storage factors, such as the duration of ischaemia and the storage temperature. The relationship between reduced temperature and decreased rates of many biological reactions became evident in studies of isolated tissues in the early years of this century (Avramovic, 1924); and the demonstration that deliberate hypothermia could ameliorate ischaemic damage led to an important advance in transplantation surgery (Levy *et al.*, 1959; Calne *et al.*, 1963). However, it soon became clear that the overall depression of cell function

caused by hypothermia itself could only delay, not prevent, the changes resulting from ischaemia, and might introduce additional damaging factors, such as molecular reorganization of cell membranes or cytoskeletal elements (Karow and Pegg, 1981; Fuller, 1987; Green, 1995). Nevertheless, in the course of clinical renal transplantation, kidneys are cooled to 0-10°C, either after they have been removed from the donor, or whilst the donor is cooled by whole body cooling. Thus, a transplanted kidney is likely to have been subject to warm (37°C), hypothermic (5-30°C), and cold (0-5°C) ischaemia between the donor's death and the restoration of blood flow.

1.7.1 Changes Occurring During Ischaemia

The primary change occurring at the onset of ischaemia is the suppression of mitochondrial electron transport (responsible for energy transduction during oxidative phosphorylation; see Section 1.7.2). This causes depletion of ATP, a net breakdown of adenine nucleotides through ADP and AMP to non-phosphorylated metabolites including hypoxanthine, and the accumulation of reduced pyridine nucleotides, such as reduced nicotinamide adenine dinucleotide (NADH), which can no longer be oxidized by mitochondrial electron transfer (see Section 1.7.2). As a result, membrane pumps, such as the Na^+-K^+-ATPase and the Ca^{2+}-ATPase, are inactivated, and internal homeostasis between intracellular compartments is lost. Ions diffuse down electrical and chemical gradients, thereby dissipating the physiological transmembrane ionic gradients. K^+ is lost to the extracellular spaces, while Ca^{2+}, Na^+ and Cl^- (accompanied by the osmotic movement of water) enter the cell freely after failure of the energy-dependent pumps that normally exclude them. The influx of water leads to cellular swelling and hydropic degeneration (intracellular oedema). Ca^{2+} infusion may activate Ca^{2+}-dependent degradative enzymes, such as proteases and phospolipases, and Ca^{2+}-dependent second-messengers, such as diacylglycerol (DAG) and inositol triphosphate (IP_3) (see Section 1.7.2), leading to changes in the phospholipid content of cell membranes, altered membrane permeability, and further loss of homeostasis (Cotterill *et al.*, 1990). The reductive intracellular conditions promote release of sequestered Fe^{2+} from ferritin (Healing *et al.*, 1990; Goddard *et al.*, 1992) and from endogenous cytochromes, such as cytochrome P-450 (Paller and Jacob, 1994), and this iron may catalyse free radical formation upon re-oxygenation (see Section 1.7.2). Toxic metabolites, such as lactic acid, H^+, and denatured proteins accumulate, leading to a fall in intracellular pH. These changes in the intracellular environment disrupt lysosomes, releasing autolytic enzymes into the cytoplasm.

While the activation of phospholipases, proteases and lysosomal enzymes, and the accumulation of glycolytic metabolites may be suppressed by hypothermia, inactivation of membrane pumps

and loss of cellular ionic homeostasis is not affected by the cold. Thus, cold ischaemia primes the activation of degradative enzymes, which are fully activated upon restitution of normothermia during reperfusion. Similarly, the consequences of altered mitochondrial structure and function are not expressed until restitution of normothermia and normoxia. As a consequence, the major patho-physiological manifestations of ischaemia-reperfusion injury do not become apparent until reperfusion with fully oxygenated blood.

1.7.2 Changes Occurring Upon Reperfusion

At a macroscopic level, two characteristic pathological changes become manifest during reperfusion of ischaemically damaged kidneys (Summers and Jamison, 1971; Ratych and Bulkley, 1986; Mason, 1988; Green, 1995). The most obvious is a deficit in vascular outflow from the renal medulla, known as the *no-reflow phenomenon*, or more appropriately *medullary congestion*; the second is the development of ATN, particularly in the renal cortex and the cortico-medullary junction. While medullary congestion typically clears over a period of hours or days (Mason, 1988), its cause and effect in terms of the aetiology of renal ischaemia-reperfusion injury (expressed clinically as reversible or irreversible acute renal failure) are not fully established. Whether a relationship exists between medullary congestion (which could cause tubular necrosis via normothermic secondary ischaemia), and cortical ATN (which may have a much more complex aetiology; see below), is a central theme of this thesis, and could have fundamental implications for the management of renal preservation.

That renal ischaemia-reperfusion injury has a multifaceted aetiology is suggested by the very limited success of previous attempts at pharmacological and therapeutic manipulation (see Section 1.7.3). During the past two decades, strenuous efforts have been made to identify the principal causes of ischaemia-reperfusion injury. Particular attention has been paid to:

- Cellular swelling and secondary ischaemia
- Oxidative stress and oxygen-derived free radicals
- Ca^{2+} redistribution, necrosis and apoptosis
- Eicosanoids and other vasoactive mediators.

Cellular Swelling and Secondary Ischaemia

Although hypothermia cannot prevent the loss of cellular ionic homeostasis brought about by the suppression of active transport, most clinical preservation solutions incorporate hyperosmolar

impermeant solutes to attenuate cellular swelling (see Section 1.7.3). Despite this, numerous reports have shown that medullary congestion during reperfusion is not the result of vascular coagulation, but is instead caused by cellular swelling (Summers and Jamison, 1971; Ratych and Bulkley, 1986; Mason, 1988; Jacobson *et al.*, 1988; Heyman *et al.*, 1994; Kumada *et al.*, 1994; Lane *et al.*, 1996). Both endothelial cells and parenchymal cells have been implicated in this process, but the mechanism, surprisingly, is contentious. McCord (1985), and Ratych and Bulkley (1986) have argued that xanthine oxidase (see below), which is specifically localized in the endothelial cells of the outer medulla, catalyses free radical generation upon reperfusion, leading to inactivation of endothelial Na^+-K^+-ATPase during reperfusion, disruption of intercellular tight junctions and physical blockade of the vascular lumens with swollen endothelial cells. In contrast, Mason and colleagues (1989) could find no evidence of endothelial cell swelling, and argued that lumenal compression of the *vasa recta* occurred as a result of passive tubular swelling in the outer medulla during the ischaemic period itself. The observation that xanthine oxidase expression differs between species may partly explain these experimental inconsistencies (Halliwell and Gutteridge, 1985).

The unusual vascular anatomy of the kidney, whereby the glomerular and peritubular capillary beds are arranged in sequence, combined with the absence of arterio-venous anastomoses in the kidney (see Section 1.3), may exaggerate the pathophysiological significance of medullary congestion. As the vascular supply of the medulla is derived from juxta-medullary glomeruli, it seems likely that medullary haemostasis would disrupt perfusion of the deeper cortex, thereby enlarging the volume at risk of secondary ischaemia. Indeed, Brezis and colleagues (1984), and Heyman and co-workers (1994) have shown that proximal tubule cells located in the cortico-medullary junction of kidneys rendered warm ischaemic are particularly susceptible to ischaemia-reperfusion injury. However, the significance of medullary congestion in the aetiology of cold ischaemic damage following renal storage and transplantation is unknown.

Oxidative Stress and Oxygen-Derived Free Radicals

Restitution of normothermia during reperfusion of ischaemically damaged kidneys, leading to the activation of primed degradative enzymes, is not the only potentially damaging consequence of reperfusion. The reintroduction of oxygen may also be detrimental, through the uncontrolled formation of *oxygen-derived free radicals* in a phenomenon known as the *oxygen paradox*. However, while much evidence has now accumulated demonstrating the formation of these reactive species in transplanted organs (Green *et al.*, 1986; Fuller *et al.*,1988; Connor *et al.*,

1992; Pincemail *et al.*, 1993) little is known of their true significance in the aetiology of ischaemia-reperfusion injury following renal transplantation.

Free radicals are atoms or molecules with one or more unpaired electrons (•). The thermodynamic instability of such an electronic configuration renders them typically highly chemically reactive. By losing or gaining a single electron, free radicals attain the thermodynamic stability of a shared electronic orbital. However, abstraction or donation of a single electron from or to a non-radical species produces another radical, thereby initiating a chain reaction, which is terminated only by the collision of two radical species.

Free radicals are generated continuously under normal physiological conditions via the splitting of water into hydroxyl radicals ($^{\bullet}OH$) and hydrogen atoms ($H^{\bullet}$) by electromagnetic radiation, and by the "leakage" of electrons from the respiratory chain to molecular oxygen, in the course of oxidative phosphorlyation (see below), forming superoxide radicals ($O_2^{\bullet-}$) (Fridovich, 1989). The ubiquitous formation of free radicals has necessitated the evolution of complex antioxidant systems in almost all organisms comprising: enzymes such as *superoxide dismutase* (*SOD*) (which catalyses the dismutation of $O_2^{\bullet-}$), *catalase* (which catalyses the reduction of hydrogen peroxide to water) and *glutathione peroxidase* (which catalyses the reduction of organic hydroperoxides); and co-factors such as *vitamin C, vitamin E, glutathione and* β *carotine*. These antioxidant systems restrain the propagation of destructive free radical chain reactions. The aggressive reactivity of free radical species has even been harnessed to physiological benefit by activated neutrophils during the "respiratory burst", whereby ejaculation of reactive oxygen species onto invading bacteria brings about their prompt destruction and phagocytosis.

The intracellular changes that occur during ischaemia are thought to both increase the formation of free radical species upon reperfusion, and to deplete antioxidant enzymes and cofactors (Farrari *et al.*, 1986). One mechanism by which superoxide radicals may be formed during reperfusion involves the enzyme xanthine dehydrogenase (referred to above), which catalyses the catabolism of hypoxanthine (an adenine nucleotide metabolite formed during ischaemia; see Section 1.7.1) through xanthine to uric acid. During ischaemia, the increase in intracellular Ca^{2+} concentration stimulates the Ca^{2+}-dependent proteolytic conversion of xanthine dehydrogenase to xanthine oxidase, which catalyses the same reactions using molecular oxygen as an electron acceptor, thereby generating $O_2^{\bullet-}$ radicals. However, as discussed above, this mechanism is of questionable relevance to clinical renal transplantation (Halliwell and Gutteridge, 1985).

Endothelial cells may also be damaged by aggressive oxygen radicals produced within the vascular lumens by activated neutrophils during their respiratory burst (Granger *et al.*, 1989). The role of chemotactic eicosanoids in attracting and activating neutrophils is discussed below; however, neutrophil-mediated damage tends to occur hours to days after reperfusion and is unlikely to account for damage occurring *upon* reperfusion.

The major and universal source of $O_2^{\bullet-}$ radicals in transplanted organs is therefore likely to be electrons "leaked" from electron transport chains, particularly the mitochondrial respiratory chains (Fridovich, 1989), and those associated with cytochrome P-450 (Paller and Jacob, 1994). Reduction of respiratory chain components (Fig 1.5), loss of mitochondrial ultrastructure and mitochondrial swelling during ischaemia, could combine to promote excessive formation of $O_2^{\bullet-}$ radicals during reperfusion, overwhelming the native mitochondrial antioxidant capacity.

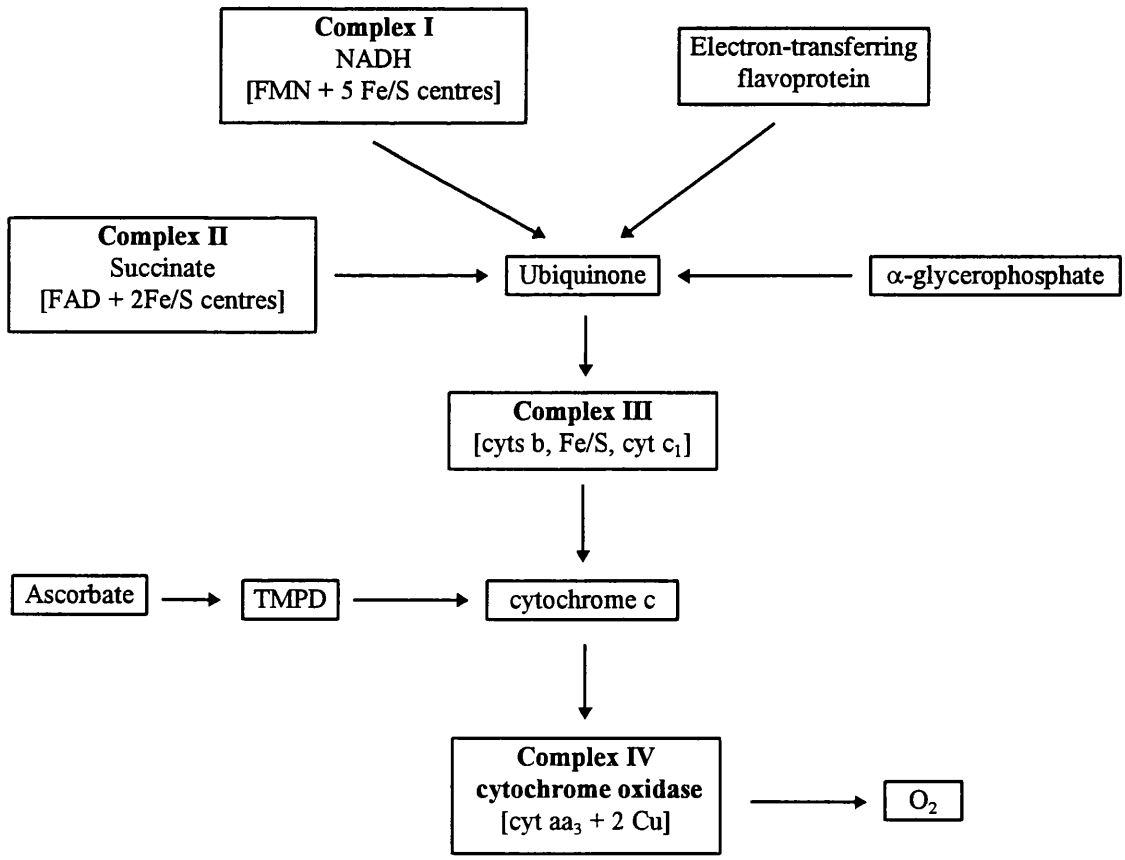

Fig 1.5 Mitochondrial respiratory chain (see text)

Such a scenario has been described extensively *in vitro* (Malis and Bonventre, 1986; Baker and Kalyanaraman, 1989; Hardy *et al.*, 1991; Ambrosio *et al.*, 1993; Reinheckel *et al.*, 1995; Sammut *et al.*, 1995), but its applicability to transplanted, ischaemically damaged kidneys, has not been established. *In vivo* mitochondrial function therefore forms a major element of this thesis. In fact, formation of $O_2^{\bullet-}$ alone may not be sufficient to cause significant mitochondrial or cellular damage. Free radicals vary substantially in their reactivity, and $O_2^{\bullet-}$, in comparison with $^{\bullet}OH$, is relatively unreactive. The potentially damaging consequences of $O_2^{\bullet-}$ production, however, are realized in the presence of transition metals, such as iron or copper, which exist in thermodynamic equilibrium in several different oxidation states. For this reason iron, which is biologically abundant, is normally tightly sequestered, either within the prosthetic group of haemoproteins, such as haemoglobin and the cytochromes, or within "storage" proteins, such as ferritin and transferrin, or as aconitase. "Free" iron, in the form of low molecular weight chelates with citrate, ADP or NADH, normally exists in minute quantities, its concentration controlled by the *iron regulatory element* (*IRE*) (Goddard *et al.*, 1992; Lash and Saleem, 1995). Low molecular weight iron that is not required for the synthesis of haemoproteins is sequestered in the Fe^{3+} form within ferritin, and its entry or release from ferritin is achieved by reduction to the Fe^{2+} form (Lash and Saleem, 1995).

Reduction of Fe^{3+} to Fe^{2+} may be promoted by the reductive intracellular conditions imposed by ischaemia, and this may stimulate release of iron from ferritin (Goddard *et al.*, 1992). That there is a significant increase in the concentration of intracellular low molecular weight iron (chelatable by clinical iron chelators such as desferrioxamine) during renal ischaemia, has been demonstrated by Gower and colleagues (1989), and by Paller and Jacob (1994). "Free" low molecular weight iron is able to catalyse the generation of $^{\bullet}OH$ radicals from $O_2^{\bullet-}$ or hydrogen peroxide (which itself can degrade haem proteins, thereby releasing more iron; Gutteridge, 1984) via a mechanism known as the Fenton reaction:

$$Fe^{2+} + H_2O_2 \rightarrow Fe^{3+} + OH^- + {}^{\bullet}OH$$

$$Fe^{3+} + O_2^{\bullet-} \rightarrow Fe^{2+} + O_2$$

$$Fe^{2+} + H_2O_2 \rightarrow Fe^{3+} + OH^- + {}^{\bullet}OH$$

Thus, Fe^{2+} is continuously regenerated, and the net product is $^{\bullet}OH$. The $^{\bullet}OH$ radical (or $^{\bullet}OH$-like species; Wink *et al.*, 1994) is extremely reactive, and will attack any adjacent biological molecule. However, diffuse membrane damage may be sustained via the formation of less

reactive radical species, such as peroxy radicals (lipid-OO$^{\bullet}$), which propagate free radical chain reactions amongst polyunsaturated fatty acids in the cellular membranes - a process known as lipid peroxidation (Halliwell and Gutteridge, 1986):

$$\text{lipid-H} + {}^{\bullet}\text{OH} \rightarrow \text{H}_2\text{O} + \text{lipid}^{\bullet}$$
$$\text{lipid}^{\bullet} + \text{O}_2 \rightarrow \text{lipid-OO}^{\bullet}$$
$$\text{lipid-OO}^{\bullet} + \text{lipid-H} \rightarrow \text{lipid}^{\bullet} + \text{lipid-OOH}$$

Lipid hydroperoxides (lipid-OOH) may also break down via an iron catalysed mechanism to form peroxy and alkoxy radicals (LO$^{\bullet}$):

$$2\ \text{lipid-OOH} \xrightarrow{\text{I-R-O-N}} \text{LOO}^{\bullet} + \text{LO}^{\bullet} + \text{H}_2\text{O}$$

If lipid peroxidation is allowed to propagate, it can destroy the phospholipid balance and permeability characteristics of cellular membranes, and could even lead to their collapse. Lipid peroxides themselves may also fragment to produce a number of cytotoxic derivatives, such as aldehydes, and this has been the basis of a number of assays of free radical damage to biological systems (Yagi, 1982).

Specific damage to proteins or to DNA may also be sustained by free radical generation. Certain groups within proteins, such as thiol groups and disulphide bridges, are particularly sensitive to free radical damage (Davies *et al.*, 1987a-d), and this may lead to the specific inactivation and subsequent proteolysis of crucial thiol-containing membrane pumps, such as the Na^{+}-K^{+}-ATPase (Maridonneau *et al.*, 1982; Thomas and Reed, 1990) and the Ca^{2+}-ATPase (Bellomo *et al.*, 1983; Vile and Winterbourn, 1990; Holmberg *et al.*, 1991). Specific protein damage may also be related to spatial factors. For example, proteins bound to reactive iron- or copper-containing prosthetic groups are highly susceptible to auto-inactivation (Davies *et al.*, 1987a-d). Similarly, within the mitochondrial respiratory chains, electron leakage occurs principally at two sites (complexes I and III; Fig 1.5), and it is thought that this spatial restriction may lead to the auto-inactivation of these sites upon reoxygenation (Trümper *et al.*, 1988; Veitch *et al.*, 1992; Sled and Vinogradov, 1993; Ambrosio *et al.*, 1993; Reinheckel *et al.*, 1995). In the nucleus, iron derived from ferritin particles within or surrounding the nucleus has been shown catalyse $^{\bullet}$OH generation (Kukielka and Cederbaum, 1994), leading to denaturation of DNA, alterations in the

structural integrity of the nucleus and mutagenesis. Such changes have been implicated in the pathogenesis of certain cancers (Sun, 1990).

There is also evidence that free radical injury to the endothelium can cause loss of endothelium-dependent vasorelaxation during reperfusion (Lefer and Ma, 1991). Nitric oxide (which is itself a free radical: $NO^{\bullet}$) reacts with $O_2^{\bullet -}$ to form peroxynitrite (Saran *et al.*, 1989), and this may cause vasospasm (Laurindo *et al.*, 1991).

Calcium Redistribution, Necrosis and Apoptosis

Massive calcium deposits are a commonly found in necrotic kidneys after ischaemia-reperfusion injury, and much evidence suggests that Ca^{2+} redistribution could play a key role in early reperfusion damage (Chien *et al.*, 1977; Watts *et.al.*, 1980; Opie, 1989; Cotterill *et al.*, 1990; Green, 1995). Inactivation of Ca^{2+}-ATPases in the cell membranes, endoplasmic reticulum and mitochondria occurs during ischaemia, and their thiol groups are susceptible to specific free radical-mediated denaturation upon reperfusion (Bellomo *et al.*, 1983; Holmberg *et al.*, 1991). Loss of calcium homeostasis has manifold implications to cellular function during reperfusion, including:

- Activation of phospholipases, such as phospholipases A_2 and C, which degrade membrane phospholipids, releasing free arachidonic acid, the substrate for cyclo-oxygenase, lipoxygenase and cytochrome P-450, and stimulating $O_2^{\bullet -}$ generation (see Section 1.3.4 and below)
- Potentiation of oxygen-derived free radical damage to mitochondrial membranes and complexes (especially complex I), possibly via a phospholipase A_2-mediated mechanism (Malis and Bonventre, 1986)
- Activation of Ca^{2+}-dependent proteolysis of xanthine dehydrogenase to xanthine oxidase (see above)
- Activation of cytoplasmic Ca^{2+}-dependent proteases, which affect several cytoskeletal proteins (leading to cytoskeletal disruption), the Ca^{2+}ATPase and protein kinase C (Paller and Greene, 1994)
- Stimulation of apoptosis (programmed cell death), via activation of Ca^{2+}-dependent endonucleases in the nucleus (Richter, 1993). Apoptosis has been implicated in ATN by the demonstration of apoptotic bodies in biopsies from renal allografts, and the appearance of characteristic DNA fragmentation (Matsuno *et al.*, 1994).

Eicosanoids and Other Vasoactive Mediators

The normal physiological actions of the eicosanoids were outlined in Section 1.3.4. In addition to their vaso-activity and their involvement in the regulation of active tubular transport, the eicosanoids play an important role in the mediation of inflammation. It is thought that ischaemia and reperfusion may induce a shift in eicosanoid production from physiological vasodilators, such as prostacyclin and PGE_2, to pro-inflammatory vasoconstrictors, such as thromboxane A_2 and leukotriene B_4, possibly as a consequence of the suppression of prostacyclin generation by lipid hydroperoxides formed during lipid peroxidation (Lelcuk *et al.*, 1985; Lands, 1985; Fuller *et al.*, 1988).

As well as stimulating the influx and activation of inflammatory cells (leading to chronic endothelial and parenchymal damage, and tissue remodelling), induction of eicosanoid synthesis could exacerbate early medullary vascular congestion, by promoting vasoconstriction (thereby reducing blood flow and increasing blood pressure), enhancing microvascular permeability (favouring the extravasation of plasma and blood cells and promoting tubular swelling) and stimulating platelet activation and the coagulation cascade. Furthermore, all three mechanisms of eicosanoid production involve the transient formation of $O_2^{\bullet -}$ via prosthetic iron at the catalytic centre of the respective enzymes. Cyclooxygenase and lipoxygenase are activated by trace quantities of hydroperoxide or superoxide (the levels of which are normally suppressed by glutathione peroxidase and superoxide dismutase); once activated, they both have the capacity to produce huge quantities of eicosanoids before excessive free radical formation at the catalytic centre of the enzymes causes their autodestruction (Lands, 1986). Stimulation of hydroperoxide generation and inflammation may therefore amplify both eicosanoid production and lipid peroxidation by a positive feedback mechanism, whereby lipid peroxidation stimulates eicosanoid production, which in turn stimulates inflammatory activation and production of lipid hydroperoxides, thence stimulating further propagation of lipid peroxidation (Lands, 1986).

Eicosanoid production may also affect other vascular mediators. For example, prostaglandins modulate renin release, and therefore indirectly affect cortical vasoconstriction and glomerular filtration (Lefer, 1985); while production of superoxide by activated neutrophils may neutralize nitric oxide (see above), possibly causing vasospasm (Laurindo *et al.*, 1991).

1.7.3 Amelioration of Ischaemia-Reperfusion Injury: Current Status of Renal Preservation

The single most important principle in preservation is the use of hypothermia (see Section 1.7). In almost all transplantation centres, donor kidneys are initially flushed free of blood by infusing a cold electrolyte solution via the renal artery, and allowing the effluent to escape via the renal vein, thereby preventing intra-renal degradation of haemoglobin (and release of toxic breakdown products), clearing extracellular spaces (Pegg, 1978) and achieving rapid cooling. The kidney is then immersed in the same cold solution and either stored (packed in ice at 0-4°C, to inhibit metabolism as completely as possible), or continuously perfused at 5-10°C (to provide for some limited metabolism and the removal of waste products). The continuous perfusion method, while possibly permitting extended safe preservation times (up to 4 days), and scope for organ procurement from non-heart-beating cadavers or high risk donors (Tesi *et al.*, 1993; Matsuno *et al.*, 1994), suffers the disadvantages of technical difficulties in maintaining sterility, expense and complexity, making it dependent on the availability of very skilled staff. Consequently, it is currently used routinely in very few centres. Because of its wide-spread applicability, the cold storage method has therefore been used in this thesis.

The formulation of asanguinous solutions for cold storage is based on several principles designed to attenuate the likely causes of ischaemia-reperfusion injury discussed above:

- Prevention of cell swelling
- Maintainance of physiological pH
- Maintainance of physiological ionic gradients
- Prevention of free radical-mediated reperfusion injury.

A range of impermeant solutes have been included in clinically-tested preservation solutions to increase the osmolarity and oppose the net movement of water into cells, thereby preventing cell swelling. These include glucose, sucrose, mannitol, raffinose and lactobionate (Collins *et al.*, 1969; Ross *et al.*, 1976; Belzer and Southard, 1988). Their efficacy depends on molecular size and charge, and varies according to the particular organ and the duration of ischaemia (Marsh *et al.*, 1989; Kumano *et al.*, 1994). Maintainance of pH is achieved by inclusion of simple buffering systems, of which the most common and apparently effective is the phosphate buffering system (Belzer and Southard, 1988).

The most effective means of maintaining physiological ionic gradients is contentious. In early experimental work, high potassium concentration (mimicing intracellular conditions) was thought essential (Collins *et al.*, 1969; Acquatella *et al.*, 1972). However, Fuller and Pegg (1976) reported that potassium concentrations much higher than normal plasma levels led to poor renal function. A number of more recent studies have claimed that solutions containing high concentrations of sodium ions were equally or even more effective than those with high potassium (Moen *et al.*, 1989; Sumimoto *et al.*, 1989; Marshall *et al.*, 1991). Prevention of calcium influx into cells is also important, but Marsh and co-workers (1990) have shown that removal of calcium (or magnesium) from the preservation solution leads to cellular swelling even in the presence of impermeants. However, inclusion of calcium chelators or antagonists such as citrate or chlorpromazine in the preservation solution does appear to be beneficial (Green *et al.*, 1993; Schilling *et al.*, 1993; McAnulty *et al*, 1993).

Many components have been added to preservation solutions in various attempts to ameliorate free radical-mediated reperfusion injury but with mixed success. Mannitol, included in hypertonic citrate solution, has been shown to directly scavenge hydroxyl radicals (Hansson *et al.*, 1983), but the extreme reactivity of these radicals means that direct scavengers are unlikely to be effective, except at extremely high intracellular concentrations and the value of mannitol is more likely to be related to its osmotic activity. Allopurinol (an inhibitor of xanthine oxidase - see Section 1.7.2) and reduced glutathione (the co-factor for glutathione peroxidase - see Section 1.7.2) are incorporated into the University of Wisconsin (UW) solution, but can apparently be omitted without detrimental effect (Wahlberg *et al.*, 1989). Similarly, additive components such as superoxide dismutase, vitamin E, membrane stabilizers (such as glycine or methylprednisolone), inhibitors of phospholipase and lipid peroxidation, and various iron chelators have been evaluated in many model systems, but none have proved consistently beneficial. Indeed, it is worthy of note that some of the best functional results in kidneys stored for 72 h before transplantation were achieved with a simple phosphate-buffered sucrose solution (Lam *et al.*, 1989).

Hypertonic citrate solution (see Chapter 2) has been used in all the studies described in this thesis, as it is cheap, effective, widely used in clinical practice and relatively simple, allowing additions to be made without fear of duplication.

1.8 Hypothesis and Aims of Thesis

Free radical-mediated events, and the consequent imbalance in eicosanoid metabolism, may play an important role in the aetiology of ATN following renal storage and transplantation. However, susceptibility to free radical damage varies morphologically, and little is known of either the spatial or temporal sequence of events leading to ATN. Medullary vascular congestion is common after prolonged ischaemia, and this may disturb cortical reperfusion, resulting in secondary ischaemia, which can alone cause ATN. The relative importance *in vivo* of oxidative reperfusion injury, as opposed to secondary ischaemia, is unknown. The studies presented in this thesis were designed to investigate the relationship between intra-renal oxygenation and cellular/mitochondrial function, and the corresponding therapeutic implications, using an *in vivo* New Zealand White (NZW) rabbit renal autograft model. It is hypothesized that:

Acute renal failure following prolonged hypothermic storage and transplantation is a consequence of both oxidative reperfusion injury and secondary ischaemia. Therefore, pharmacological strategies aimed at prolonging the safe storage time of transplanted kidneys cannot be successful unless they effectively combat both causes.

The aims of the thesis are therefore to:

(i) Establish patterns of damage to the renal parenchyma and vascular system resulting from storage and transplantation in the NZW rabbit renal autograft model

(ii) Develop non-invasive methods of measuring renal haemoglobin and tissue oxygenation *in vivo*

(iii) Define the relationship between tissue oxygenation and cellular/mitochondrial function *in vivo*

(iv) Investigate specific therapeautic approaches to mitigating renal ischaemia-reperfusion injury *in vivo*.

CHAPTER 2

MATERIALS AND METHODS

2.1 Materials

All renal autografts were carried out using female New Zealand White rabbits (2.5-3 kg) supplied by Interfauna. Rat livers were taken from male Sprague Dawley rats, raised in the SPF Unit at Northwick Park Hospital. Microsurgical instruments were from John Weiss Ltd and the operating microscope was a Zeiss OPMI6-DF. Surgical sutures were from Ethicon, Edinburgh, UK.

Anaesthetics used were: Hypnorm® (Janssen Pharmaceuticals Ltd, Oxford, UK); diazepam (Phoenix Pharmaceuticals Ltd, Gloucester, UK); Vetalar® (ketamine hydrochloride; Parke-Davies Veterinary, Pontypool,UK); Rompun® (xylazine; Bayer, Bury St Edmunds, UK).

Frusemide (Lasix) and procaine were from Phoenix Pharmaceuticals; Heparin (Multiparin) was from CP Pharmaceuticals, Wrexham, UK; Haemaccel was from Behringwerke AG, Marberg, Germany); hypertonic citrate solution, saline for i.v. infusion and mannitol were from Baxter Health Care, Thetford, UK. Micropaque® standard (100% w/v barium sulphate) for angiography was from Nicholas Laboratories Ltd, Slough, UK. Electron microscopy reagents were from Agar Scientific, Stanstead, UK. Sterile phosphate buffered saline (PBS), ethylenediaminetetra-acetic acid (EDTA) and Tris buffer were prepared at Northwick Park Hospital.

The near infra-red spectrometer was a Hamamatsu NIRO-500; the spectrofluorimeter was a Perkin Elmer LS 50 and the spectrophotometer was a Uvicon 810P. Continucath 1000 arterial oxygen electrodes were from Biomedical Sensors Ltd, High Wycombe, UK. The pressure transducer and electrocardiogram was from Roche/Kontron Medical. The electron microscope was a JEOL 1200EX STEM and the light microscope was a Leitz Laborlux S.

All chemicals used in purification procedures were Spectral grade (marked with S) from BDH. All other chemicals were Analar grade from Sigma. The chemicals used were:

adenosine diphosphate

bovine serum albumin

S butan-1-ol

carboxymethylcellulose

S chloroform

copper sulphate

S ethanol (99.7%)

ferric sulphate

ferrous sulphate

Folin and Ciocalteu's phenol reagent (2M)

S hexane

hydrochloric acid

malondialdehyde tetraethylacetal

S methanol

S methyl formate

nicotinamide adenine dinucleotide (NADH)

nicotinamide adenine dinucleotide phosphate (NADPH)

phosphotungstic acid

polyethylene glycol (Average M_r 600)

potassium sodium tartrate

potassium chloride

sodium carbonate

sodium chloride

sodium dodecyl sulphate

S sulphuric acid (1M)

thiobarbituric acid

xylene

Serum leukotriene and prostaglandin levels were assayed using commercially available immunoassay systems from Amersham International. C2 reverse phase chromotography columns were also from Amersham International. Serum urea and creatine levels were measured using commercially available kits from Boehringer Mannheim.

Desferrioxamine was from Ciba Geigy. BWB 70C was a gift from the Wellcome Research Laboratories, Guildford, UK; NMHH was a gift from the Free Radical Research Group, UMDS Guys Hospital, London; CP102 was a gift from the Department of Pharmacy, Kings College,

London. Ebselen (PZ51) and its metabolites I (2-glucuronylselenobenzanilide) and II (4-hydroxy-2-methylselenobenzanilide) were a gift from A. Nattermann & Co. GmbH (Cologne, Germany).

2.2 Surgical Procedures

2.2.1 Surgical Anaesthesia

All animal procedures were carried out according to Home Office regulations, Animals (Scientific Procedures) Act, 1986. General anaesthesia in rabbits was induced by two different methods depending on the duration of anaesthesia required:

(i) For short-term anaesthesia (1-2 h), rabbits were deeply sedated with an intra-muscular (i.m.) injection of 0.2 ml/kg fentanyl citrate (0.315 mg/ml) + fluanisone (10 mg/ml) (Hypnorm®) followed by slow injection of 1.0 mg/kg diazepam (5 mg/ml) and hypnorm by slow intravenous (i.v.) infusion as required. Animals were supplied with 100% oxygen (2 l/min) via an open face mask throughout the surgical procedure. 1 ml heparin (1000 IU) and 1 ml frusemide (10 mg/ml) were administered i.v. prior to laparotomy.

(ii) For long-term (terminal) anaesthesia (3-6 h), rabbits were deeply sedated with an i.m. injection of 50 mg/kg ketamine hydrochloride (100 mg/ml) and 8 mg/kg xylazine (20 mg/ml), tracheotomized and artificially ventilated (ventilation volume 21 ml) with a 50 : 50 oxygen : nitrous oxide mixture. This method allowed maintainance of normal blood pressure, and plasma partial pressures of oxygen and carbon dioxide throughout the surgical procedures. Heparin and frusemide were administered i.v. prior to laparotomy as described above. Surgical anaesthesia was maintained by continuous i.v. infusion of ketamine and xylazine (50mg : 8mg/kg/h).

2.2.2 Physiological Monitoring (During Long-Term Anaesthesia)

The left femoral artery was carefully dissected and cannulated with an 18-gauge plastic cannula, which was inserted for a distance of 5 cm until the tip reached the base of the aorta. The cannula provided protective housing for a Continucath 1000 oxygen electrode coupled via a 3-way tap to a pressure transducer. Blood pressure (BP) and oxygen partial pressure (pO_2) were continuously monitored throughout the study period. To ensure satisfactory renal perfusion, mean arterial systolic/diastolic blood pressure must be maintained above 50 mmHg and preferably above 80 mmHg. The quality of renal cortical perfusion is visible to the eye at low perfusion pressures, and is also detectable by near infra-red spectroscopy (see Section 2.2). BP was therefore

maintained within the range 80-120 mmHg during reperfusion by continuous i.v. infusion of 30 ml/h Haemaccel (3.5% colloidal infusion), or as required. Intermittent blood samples were taken (from the 3-way tap) for determination of arterial carbon dioxide partial pressure (pCO_2), pH, electrolyte levels and conductivity (Hct). Core temperature was monitored using an oesophageal probe and was maintained between 37 and 39^{0}C with a heated pad (37^{0}C). In addition, the electrocardiogram (ECG), percentage inspired oxygen (FiO_2, maintained at 50%) and percentage expired carbon dioxide ($EtCO_2$, maintained at 5%) were continuously monitored.

2.2.3 Nephrectomy and Autografting Procedures

All microsurgical instruments were sterilized by boiling followed by spraying with 0.5% chlorhexidine in ethanol prior to nephrectomy or autografting. The anaesthetized rabbit was shaved abdominally and dressed in previously autoclaved drapes. The right kidney was exposed through a mid-line abdominal incision. The intestines were gently displaced, externalized, swathed in warmed damp sterile swabs and supported on a sandbag raised slightly above the level of the peritoneum. In the course of long operations, the intestines were additionally wrapped in clingfilm to reduce heat and moisture loss. The connective tissue surrounding the kidney was carefully separated and the renal vessels divided and ligated as close to the aorta as possible using 2/0 silk thread. The renal artery was then cannulated with the rounded glass tip of a pipette inserted into a 21-gauge butterfly cannula after removal of the needle, and flushed with 40 ml ice-cold hypertonic citrate solution (HCA; 0-2^{0}C) from an ice-cooled bag suspended at a height of 1.5m. The maximum perfusion pressure (measured using a pressure-gauge) was therefore 90 mmHg.

The perfused kidney was plunged into a sterile glass beaker containing HCA (0-2^{0}C) and the beaker was surrounded by ice. The total warm ischaemic time was less than 2 min. Perfused kidneys were then either autografted immediately into the donor rabbit or stored for 24, 48 or 72 h within a closed polystyrene container packed with ice and held in a refrigerator prior to autografting. The storage temperature was thus maintained at a steady 0-2°C. The composition of HCA solution is shown in Table 2.1.

After the storage period, kidneys were autografted into the donor rabbit. The rabbits were anaesthetized as described above, and the body cavity opened along the same mid-line incision. The left kidney was carefully dissected out from the connective tissue and removed after clamping the renal artery and vein proximal to the kidney using weighted bulldog clamps with protective rubber housing. The ureter was severed close to the kidney. The experimental graft

(stored or unstored) was then autografted into the left renal bursa. The severed ends of the renal vein were carefully cleaned using isotonic saline to remove blood clots and procaine to prevent nervous or muscular spasm, and placed within the jaws of a double clamp. The ends were clipped with microsurgical scissors to ensure removal of tissue damaged during handling, and immobilized with stay sutures using 8/0 surgical silk suture under an operating microscope. The vein was then anastomosed using approximately 15 interrupted sutures to ensure strength, and the procedure repeated for the renal artery (with the same number of sutures). Upon reperfusion of autografted kidneys (by removal of the clamps), recipient rabbits received a 1 ml i.v. bolus of frusemide and a 60 ml slow i.v. infusion of sodium chloride solution (0.9%). The hypothermic ischaemic time during the autografting operation prior to reperfusion was approximately 20 min.

Table 2.1: Composition of Hypertonic Citrate Solution

Solute	**(mmol/l)**
Sodium	80
Potassium	80
Magnesium	40
Citrate	55
Sulphate	40
Mannitol	100
Osmolarity (mOsmol/l)	485
pH	7.1

For animal recovery in survival studies, the ureter was also anastomosed. A sterile plastic stent of 1 cm length and 1 mm lumenal diameter was inserted into the two severed ends of the ureter to prevent blockage of the lumen, and the ureter wall anastomosed around this using interrupted 8/0 surgical silk sutures. The surrounding fatty and connective tissue were then anastomosed to prevent leakage of urine from the ureter, and the kidney immobilized by drawing over the surrounding connective tissue and secured with interrupted sutures using 6/0 gut suture. The intestines were carefully replaced within the abdomen, and the peritoneal and muscle wall sutured using interrupted 0/0 gut sutures. Finally, the overlying skin was joined using interrupted 2/0 silk sutures.

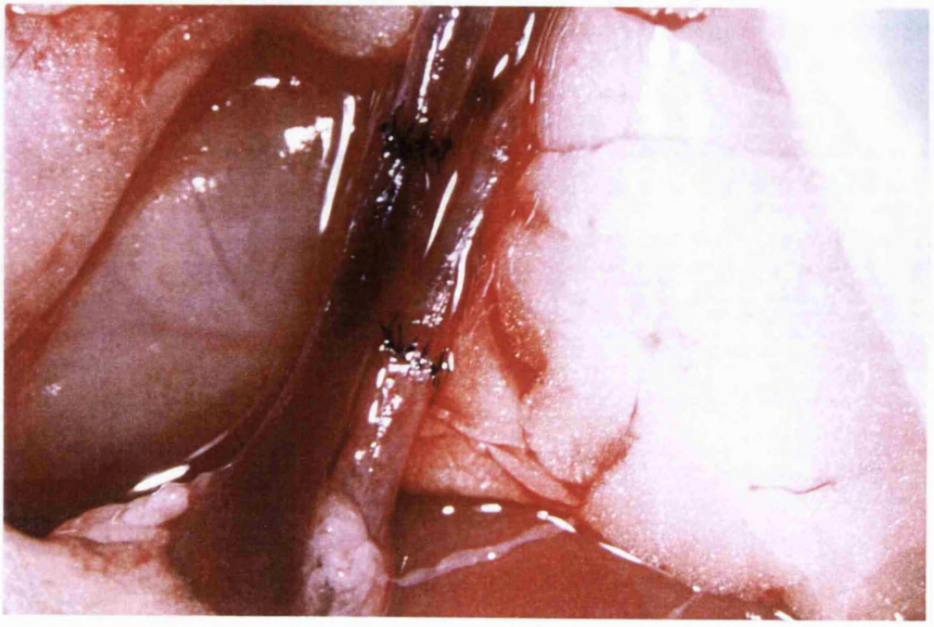

Plate 2.1 **Anastamoses of the renal artery (right) and vein (left).**

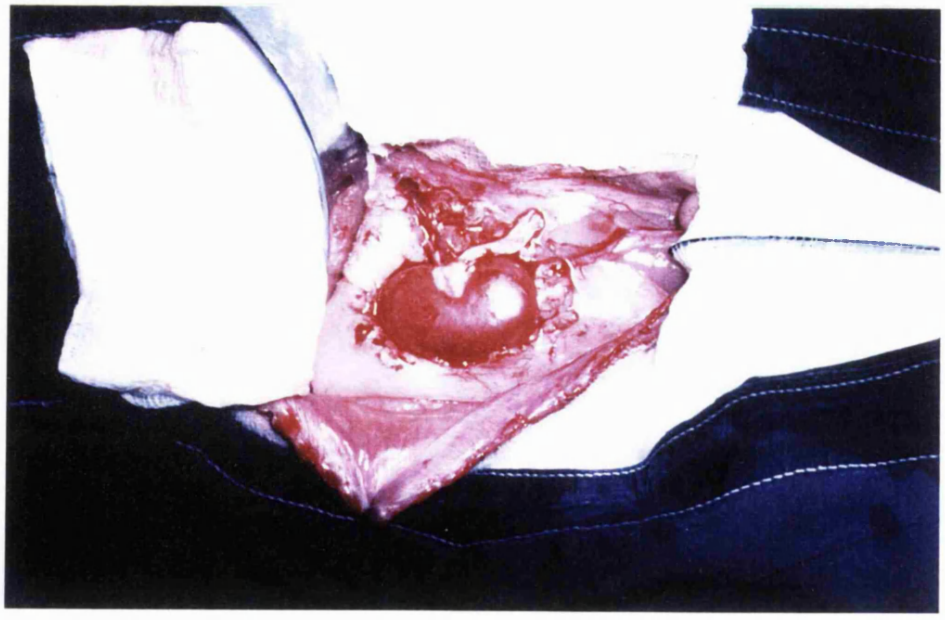

Plate 2.2 **Autografted kidney during reperfusion.**

2.2.4 Determination of Survival

Rabbits allowed to recover after autografting were treated with: 10 ml i.v. mannitol; 1 ml i.m. frusemide; and 60 ml sub-cutaneous (s.c.) isotonic saline immediately after recovery and on the subsequent four days. Serum samples (2 ml) were taken from the marginal ear vein for analysis of serum urea and creatinine (see Section 2.4.4), on days 1 to 4, 6 and 10 after transplantation. Rabbits developing uraemia were killed and autopsied as soon as clinical symptoms were observed. Renal function was assessed by:

- Observation of kidney colour and urine production immediately after revascularization
- Measurement of serum urea and creatinine
- The clinical appearance of each animal
- Evidence of urine production
- The macroscopic and microscopic appearance of each kidney at autopsy.

2.3 *In Vivo* Spectroscopic Analysis

2.3.1 Near InfraRed Spectroscopic Measurements of Oxyhaemoglobin, Deoxyhaemoglobin and Cytochrome Oxidase.

NIRS measurements were made using a NIRO-500 monitor (Hamamatsu). This technique has been used for measurements of cerebral oxygenation for many years (Jobsis, 1977; Wyatt *et al.*, 1986; Wyatt *et al.*, 1990; Brazy, 1991) However, its use in renal physiology has been limited. NIR transmission spectroscopy through tissues up to 10 cm is possible because of the relative transparency of biological tissues to NIR light (700 to 1000 nm). Absorption due to oxyhaemoglobin (HbO_2), deoxyhaemoglobin (Hb) and cytochrome oxidase (cyt aa_3, the terminal member of the respiratory chain; see Section 1.7.2) can be quantified using a modified form of the Beer-Lambert Law, which is applicable to a homogenous scattering medium in which absorption changes are linearly related to concentration, and which may be expressed as:

$$\text{absorption (OD)} = (\Sigma cLB) + G$$

where OD is the optical density, Σ is the extinction coefficient of the chromophore (mmol/l/cm), c is concentration (mmol/l), L is the difference between the points where light enters and leaves the tissue (cm), B is a pathlength factor that takes account of the scattering of light in the tissue (which causes the optical pathlength to be greater than L) and G is a factor related to the

geometry of the tissue. If L, B and G remain constant, then changes in chromophore concentration can be obtained from the expression:

$$\Delta c = \Delta OD/\Sigma LB$$

Concentration changes in HbO_2, Hb and cyt aa_3 across the kidney were calculated by linear summation of absorption changes (measured in absorbance units) at 772 nm, 830 nm, 842 nm and 909 nm. The multiplication factors for HbO_2 and Hb were obtained from spectroscopic and biochemical measurements of a wide range of haemoglobin concentrations in a scattering medium (Cope and Delpy, 1988; Cope *et al.*, 1988; Hazeki and Tamura, 1989). The multiplyer coefficients used in the estimation of concentration changes of cyt aa_3 were obtained from experimental procedures involving fluorocarbon transfusion studies in anaesthetized animals (Wray *et al.*, 1988). The NIRO-500 multiplication factors are shown in Table 2.2. One indication of the reliability of these algorithms is the independence of the cyt aa_3 response compared with HbO_2. For example, cyt aa_3 can become oxidized in damaged tissues in which the mitochondria are uncoupled, or in response to respiatory chain inhibitors, despite no measurable change in HbO_2 levels.

Table 2.2: Near infra-red spectroscopic multiplication factors

Wavelength (nm)	**772**	**830**	**842**	**909**
Hb	1.2209	−0.8437	−0.7215	0.6859
HbO_2	−0.6945	−0.4851	−0.1382	1.9579
cyt aa_3	−0.0871	0.7550	0.5309	−1.1466

The optical pathlength (B) has been determined for the cerebellum by time of flight measurements of an ultra-short pulse of light across the head (Delpy *et al.*, 1988). However, there have been no previous estimates of B in kidneys and an estimate was not made in the present studies. Nevertheless, as all the studies presented in this thesis subjected 2 or more groups of kidneys to identical protocols (with the exception of storage time); and, as the optical pathlength and differential pathlength factor have been shown to be constant within the NIR region despite gross changes in oxygenation and perfusion before and after death (Cope *et al.*,

1988; Delpy *et al.*, 1988; Hazeki and Tamura, 1989) the relative changes in chromophore concentration determined in this study are directly comparable between groups.

Transmission NIRS was used in all studies, in which the NIR probes were placed on either side of the kidney at a distance (L) of 1 cm and immobilized using a retort stand, to give an indication of haemoglobin oxygenation across both the cortex and medulla. NIRS in reflectance mode was not used as the probes, when placed adjacent to each other, were physically too large to give an indication of cortical parameters only. Baseline measurements of HbO_2, Hb and cyt aa_3 were made every 5 sec *in situ* for approximately 5 min prior to reperfusion (i.e. before removal of the clamps but after completion of the anastamoses) and changes in these parameters were then measured every 5 sec for the duration of reperfusion (for up to 6 h). Concentration changes in HbO_2 and Hb during reperfusion were used to calculate the following parameters:

(i) Total haemoglobin concentration ([HbT] = [HbO_2] + [Hb])

(ii) Haemoglobin oxygenation index ([HbD] = [HbO_2] – [Hb])

(iii) Percentage mixed haemoglobin saturation (renal SaO_2 = [HbO_2]/[HbT] x 100).

The use of this final parameter is dependent on changes from time 0, at which point the organ is essentially blood-free. Thus, changes in [HbT] are relative to a known baseline and may be considered absolute.

2.3.2 Surface Fluorometric (SF) Measurements of Mitochondrial NADH

Mitochondrial pyridine nucleotide fluorescence is an indicator of intracellular hypoxia or mitochondrial respiratory chain redox state. Cytosolic NADH fluorescence does not appear to significantly contribute to the relative fluorescence intensity measured owing to quenching of fluorescence by cytosolic glyceraldehyde 3-phosphate dehydrogenase. Similarly, although the fluorescence maximum of NADPH is very similar to that of NADH, NADPH fluorescence is not sensitive to changes in oxygenation (Chance and Williams, 1955). Thus, changes in pyridine nucleotide fluorescence during reperfusion predominantly reflect oxidation or reduction of mitochondrial NADH.

SF measurements were made using a Perkin Elmer LS 50 with a fibre-optic attachment. The SF probe was placed gently touching the surface of the *ex vivo* or *in situ* kidney and fixed in position by attachment to a retort stand. Emission spectra of NADH from 366 to 600 nm were obtained by excitation at a fixed wavelength of 340 or 366 nm (slit widths 10/10 nm). These

wavelengths were chosen to make: (i) comparisons with published data; and (ii) compensatory changes for the effect of scattering, which is dependent upon changes in blood volume and haemoglobin deoxygenation (Kobayashi *et al.*, 1971; Eke *et al.*, 1979). In agreement with Kobayashi and colleagues (1971) and Franke, Barlow and Chance (1976), it was observed that changes in reflectance in the perfused organ were small; hence, fluorescence readings were corrected only by baseline variations at 420 nm. To assess the effect of movement and normal cyclical variations in haemoglobin oxygenation levels on NADH fluorescence, each spectrum was performed at least in duplicate, within 1 min, and in some studies repeatedly scanned up to 10 times. The values obtained in this manner differed by 5 to 10% at most.

2.4 Biochemical Analysis

2.4.1 Enzyme Immunoassay of Serum Leukotrienes and Prostaglandins

Oxidation of arachidonic acid via cyclooxygenase or lipoxygenase results in the production of vasoactive eicosanoids such as the thromboxanes, prostacyclin, prostaglandins and leukotrienes. Cyclooxygenase and lipoxygenase activity occurs in a wide variety of cells, which in the kidney include mesangial cells, endothelial cells, mTAT cells, collecting duct cells and inflammatory cells. Assays of serum leukotriene b_4 (LTB_4, a potent vasoconstrictor and chemoattractant), thromboxane b_2 (TxB_2, a breakdown product of TxA_2, a potent vasoconstrictor) and 6-keto-prostaglandin $F_{1\alpha}$ (6-k-$PGF_{1\alpha}$, a breakdown product of prostacyclin, a potent vasodilator) were made by enzyme immunoassay (ELISA) using commercially available enzyme immunoassay systems.

The principle of enzyme immuoassay depends on competition between unlabelled eicosanoid in the serum sample and a fixed quantity of peroxidase-labelled ligand for a limited number of binding sites on a specific antibody. The amount of peroxidase-labelled ligand bound by the antibody is therefore inversely proportional to the concentration of added unlabelled ligand. The peroxidase ligand bound to the antibody is immobilized on polystyrene microtitre wells precoated with a second antibody. Unbound ligand can therefore be removed from the well by means of simple washing procedures. The amount of peroxidase labelled eicosanoid bound to the antibody is determined by the addition of a substrate such as tetramethylbenzidine/hydrogen peroxide. The reaction is stopped by acidification (1 M sulphuric acid), and the resultant colour read at 450 nm in a microtitre plate photometer. The concentration of unlabelled eicosanoid in the sample is determined by interpolation from a standard curve.

Serum samples (0.35 ml) were taken from the renal vein of anaesthetized rabbits after 10, 30, 60, 120, 240 and 360 min of reperfusion, snap frozen in liquid nitrogen and stored at -20^0C until required. On thawing, samples were purified by a triple phase wash (with 5 ml redistilled water, 5 ml ethanol (10% v/v) and 5 ml hexane) on C2 reverse phase chromatography columns, eluted with methyl formate, evaporated to dryness and reconstituted in 0.35 ml phosphate buffered saline (assay buffer). ELISA assays were then carried out as described by Amersham. The average optical density (OD) was calculated for each set of duplicate wells. The percentage of bound ligand for each standard and sample was then calculated according to the following relationship:

$$\%B/B_0 = \frac{\text{(standard or sample OD - non specific binding OD)}}{\text{(B_0 OD - non specific binding OD)}} \times 100$$

where B_0 is the OD in the zero standard wells. The standard curve was constructed by plotting B/B_0 as a function of the log eicosanoid concentration (in pg) per well. The pg/well value of each sample was read directly from the standard curve and multiplied by 20 to give pg/ml of serum.

2.4.2 Determination of Lipid Peroxidation in Rabbit Kidneys

Oxygen derived free radical attack can lead to the propagation of membrane lipid peroxidation of polyunsaturated fatty acids (Halliwell and Gutteridge, 1984). Lipid radicals are formed which can break down via further interaction with molecular oxygen to form lipid hydroperoxides and eventually a plethora of low molecular weight products. The susceptibility of renal homogenates to lipid peroxidation was determined after incubation of homogenates at 37^0C in open vessels with mechanical shaking for 60 min by fluorescent measurement of two such low molecular weight markers of lipid peroxidation.

Nephrectomies were performed as described in Section 2.2.3. Kidneys were flushed with 40 ml HCA, and stored as described above at $0\text{-}2^0$C for the required time (0-72 h). After the storage period, kidneys were dissected into cortex and medulla, suspended (5% w/v) in phosphate-buffered saline (40 mM KH_2PO_4 : K_2HPO_4; pH 7.4) and homogenized using a Potter-Elvehjem homogenizer. The protein content of homogenates (stored at -70^0C) was determined later by the method of Lowry *et al.*, (1951) using bovine serum albumin as the standard (see Section 2.4.3). The two markers of lipid peroxidation determined were:

(i) *Lipid-soluble Schiff's base formation* (Bidlack and Tappel, 1973). Duplicate aliquots (1 ml) were removed after 0 and 60 min of incubation at 37^0C, the lipids extracted into 4 ml chloroform : methanol (2 : 1) in tubes pre-washed with chloroform/methanol to remove possible contamination, vortexed and centrifuged in a bench-top centrifuge for 10 min at 3000 rpm. The lower chloroform layer was monitored for a fluorescence maximum between 400 and 450 nm (usually 417 nm) when excited at 360 nm on a Perkin-Elmer LS 50 spectrofluorimeter standardized against a fluorescent polymer block. Readings were corrected by those obtained from PBS buffer alone. The change in fluorescence intensity following the incubation period was taken to indicate tissue susceptibility to lipid peroxidation.

(ii) *Thiobarbituric acid reactive material (TBA-RM) formation* (Suematsu and Abe, 1982). Duplicate aliquots (1 ml) were removed after 0 and 60 min of incubation at 37^0C. These aliquots were then incubated at 95^0C with 100 µl sodium dodecyl sulphate (SDS), 150 µl phosphotungstic acid (PTA), 0.5 ml thiobarbituric acid (TBA) and 1 ml hydrochloric acid (1 M). The SDS was added to the homogenate to solubilize the fat in the renal tissue. Lipids were isolated by precipitation with serum protein using the phosphotungstic acid-hydrochloric acid system. After the incubation period, samples were allowed to cool before addition of 2.5 ml butan-1-ol, then vortexed and centrifuged in a bench-top centrifuge for 10 min at 3000 rpm. TBA reactivity was determined in the upper butanol phase by monitoring fluorescence at 553 nm when excitated at 515 nm. The change in fluorescence intensity following the incubation period was taken to indicate tissue susceptibility to lipid peroxidation. A standard curve was constructed using a series of different concentrations of malondialdehyde (MDA) tetraethylacetal and results were expressed as nmol MDA equivalents/mg protein/h.

2.4.3 Protein Determination

Lipid peroxidation results were corrected for variability in the protein content of homogenates (Lowry *et al.*,, 1951). Stored homogenates were re-homogenized and diluted 20-fold in PBS buffer. Duplicate aliquots (200 µl) were then added to 3 ml of a reaction mixture containing potassium sodium-tartrate (0.02%), $CuSO_4$ (0.01%) and Na_2CO_3 (2%) in 0.1 M NaOH. After incubating at room temperature for 30 min, 300 µl of Folin and Ciocalteu's phenol reagent (2 M) was added, and the tubes were vortexed and incubated at room temperature for exactly 30 min before reading at 650 nm on a Uvicon 810P spectrophotometer. The protein concentration was

interpolated from a standard curve constructed from a series of concentrations of bovine serum albumin (0-200 mg protein) subjected to the same procedure.

2.4.4 Measurements of Serum Urea and Creatinine

Blood samples (2 ml) were taken from the marginal ear vein (swabbed with xylene to dilate the vein) of rabbits which had been allowed to recover after autografting, using a heparinized syringe and a 23-gauge needle immediately after completion of the autograft operation and subsequently on days 1 to 4, 6 and 10. Samples were immediately centrifuged in a bench-top centrifuge at 1000 x g and stored at -20^0C until required for assay of urea and creatinine.

(i) Serum urea concentrations were measured by the enzymatic colorimetric method described by Fawcett and Scott (1960), using a commercially available kit (Boehringer Mannheim). The principle depends on cleavage of urea with urease (Berthelot's reaction):

$$\text{urea-}2H_2O \xrightarrow{\text{urease}} 2NH_4^+ + CO_3^{2-}$$

Ammonium ions (NH_4^+) react with phenol and hypochlorite to give a coloured complex.

Serum samples were first diluted 20-fold in isotonic saline and mixed thoroughly. Duplicate aliquots (200 µl) were incubated for 10 min at 37^0C with 100 µl urease (10 U ml) in 50 mM phosphate buffer, prior to addition of 5 ml phenol (0.106 M) and 5 ml sodium hypochlorite (11 mM) and incubated for a further 15 min at 37^0C. The absorbance at 550 nm was read in a Uvicon 810P spectrophotometer against a distilled water blank, and the concentration of urea calculated from the equation:

$$c\ (\text{mmol/L}) = 10 \times \frac{\text{Abs sample}}{\text{Abs standard}}$$

in which the standard was urea (0.5 mM).

(ii) Serum creatinine concentrations were measured by the colorimetric method described by Bartels (1971), using a commercially available kit (Boehringer Mannheim). Creatinine forms a coloured complex with picrate in alkaline medium (Jaffe's reaction). The assay principle depends on measurement of the rate of formation of the complex.

Serum samples (250 µl) were first deproteinized by addition of 250 µl sodium chloride (0.9%) and 500 µl trichloroacetic acid (1.2 M). After vortexing and centrifuging at 10,000 G for 2 min, duplicate samples (500 µl) of the pure supernatant were added to an equal volume of a 1:1 v/v mixture of picric acid (35 nM) and sodium hydroxide (1.6 mM). The samples were mixed and incubated at 25^{0}C in an Eppendorf 5320 thermostat for 20 min, and the absorbance at 520 nm measured in a Uvicon 810P spectrophotometer against a distilled water blank. The creatinine concentration was calculated from the formula:

$$c\ (\text{mmol/l}) = 177 \times \frac{\text{Abs sample}}{\text{Abs standard}}$$

in which the standard was creatinine (177 µmol/l).

2.5 Histological Analysis

2.5.1 Transmission Electron Microscopy

Small blocks of renal tissue (2mm^3) were cut from: (i) the superficial cortex; (ii) the cortico-medullary junction; and (iii) the medulla, and fixed in 3% phosphate buffered glutaraldehyde. The blocks were post-fixed in 1% osmium tetroxide, dehydrated in a graded acetone series and embedded in Spurr resin. Ultra-thin sections were cut and mounted on copper grids, stained with uranyl acetate and lead citrate, and carbon coated. Specimens were examined blindly in a JEOL microscope and scored by cell-type on a scale of 0 to 4 (Table 2.3).

Table 2.3: Scoring system for histological analysis

Score	Severity of Lesion
0	None
1	minimal
2	mild
3	moderate
4	severe

The cell types or structures examined were:

(i) **In the cortex:** proximal tubule, distal tubule, cortical collecting duct, glomerular mesangial cells, glomerular endothelial cells, glomerular basement membrane, basal laminae, peritubular capillary endothelial cells

(ii) **In the medulla:** mTAT, thin segment, medullary collecting duct, arterial *vasa recta*, venous *vasa recta*, peritubular capillary endothelial cells, basal laminae, connective tissue.

2.5.2 Light Microscopy

Slices were taken from all kidneys soon after termination of reperfusion and fixed in 10% formal saline for processing to paraffin wax. Sections were stained with haematoxylin and eosin (H&E) for light microscopical analysis. Ischaemia-reperfusion damage was assessed in (i) the cortex; (ii) the cortico-medullary junction; and (iii) the medulla, by the following histological parameters:

- Intracellular oedema
- Interstitial oedema
- Congestion
- Haemorrhage
- Inflammatory cell infiltrate
- Necrosis.

These parameters were scored blind by the investigator, and subsequently corroborated by an independent pathologist on a scale of 0 to 4 as shown in Table 2.3.

For kidneys perfused with barium sulphate, sections were fixed in 10% formal saline for processing to paraffin wax, stained with sodium rhodozinate to highlight barium sulphate in the vasculature and viewed under polarized light.

2.5.3 Colloidal Carbon Vascular Labelling

Peri-vascular penetration of infused colloidal carbon was evaluated as an indication of endothelial cell retraction and increased vascular permeability. Colloidal carbon (50:50 w/v Indian ink/saline) was twice filtered through a 0.45 μm Millipore filter and injected in a bolus (0.4 ml) directly into the renal artery of anaesthetised rabbits 30 min after reperfusion and allowed to clear from the vascular bed (5 min). Kidneys were then harvested, fixed in formal

saline, sectioned and stained with H&E. Penetration of colloidal carbon was estimated blind on a scale of 0 to 4, as described by Table 2.3 in (i) the renal cortex; (ii) cortico-medullary junction and (iii) the medulla.

2.5.4 Barium Sulphate Angiography

Nephrectomized kidneys were perfused via the renal artery with 1 ml of barium sulphate (50 : 50 w/v barium sulphate : isotonic saline) from a bag suspended at a height of 1.5 m. The maximum (measured) perfusion pressure was therefore 90 mmHg. Barium sulphate was infused immediately after nephrectomy in unstored kidneys, or following transplantation after 5, 60 and 180 min of reperfusion in kidneys stored for 24, 48 or 72 h. Kidneys were then sectioned and angiograms were taken at 22 mV with 30 sec exposure. The angiograms were scored blind on a scale of 0 (no perfusion); 1 (minimal perfusion); 2 (patchy perfusion); 3 (wide-spread perfusion) and 4 (normal perfusion) in both the cortex and medulla.

2.6 *In Vitro* Techniques

2.6.1 Rat Liver Microsome Preparation

Male S.D. rats (wt. 200-250g) were sacrificed by cervical dislocation and the livers perfused via the portal vein with 50-80 ml ice cold 0.9% NaCl, blotted dry and chopped. A 25% (w/v) suspension was made in Tris/KCl/EDTA buffer (50/125/1 mM, pH 7.4), and the samples were homogenized in 10 strokes using a Potter-Elvehjem type homogenizer. Homogenates were centrifuged at 20,000 x g for 20 min, the supernatant collected and subjected to further centrifugation at 100,000 x g for 60 min. The microsomal pellet was washed with 2-3ml Tris/KCl buffer (50/125 mM), resuspended to the original volume in Tris/KCl, and centrifuged at 100,000 x g for 60 min. The pellet was again washed and resuspended in Tris/KCl to a final concentration equivalent to 1.5 g liver/ml buffer, and kept frozen under liquid nitrogen until use.

2.6.2 Determination of Microsomal Lipid Peroxidation

Peroxidation of rat liver microsomes (final microsomal protein concentration 0.5 mg/ml) was stimulated with NADPH/$Fe_2(SO_4)_3$-ADP (final concentrations 1 mM, 50 μM, and 4 mM respectively). Ferric sulphate and ADP were premixed 30 min prior to initiation of peroxidation, and samples were incubated at 37°C in a shaking water bath. Aliquots (0.2 ml) of the incubation mixture were taken prior to initiation, and at various time points up to 60 min. Lipid peroxidation was determined by measurement of TBA-reactive material as described in Section 2.4.2.

2.7 Statistical Analysis

The results of spectroscopic and biochemical studies were analysed using unpaired Student's t tests with two way analysis of variance. Statistical differences in assessments of histopathology and barium sulphate angiography between groups have been tested by a Kruskal-Wallis oneway anova to test the medians of all groups for equality, followed by the Mann-Whitney U test to compare each group against controls. Results were considered statistically significant when the p value was less than 0.05, and highly significant when less than 0.005.

CHAPTER 3

HISTOLOGICAL AND BIOCHEMICAL PARAMETERS OF RENAL FUNCTION FOLLOWING HYPOTHERMIC STORAGE

3.1 Introduction

The majority of studies concerning renal ischaemia-reperfusion injury have used warm ischaemic models, in which the renal vessels were clamped for varying periods of time (Mason *et. al.*, 1983; Yamamoto *et. al.*, 1984; Shanley *et. al.*, 1986; Andersson and Jennische, 1987; Bayati *et. al.*, 1990; Hellberg *et. al.*, 1991; Vetterlein *et. al.*, 1994). Many of the changes associated with warm ischaemia, such as inhibition of mitochondrial electron transport, inactivation of membrane pumps, loss of cellular homeostasis and cellular swelling also occur during cold ischaemia at a slower rate: hypothermia alone delays, rather than prevents, the onset of irreversible damage (Green 1995). However, when the renal vessels are simply clamped, erythrocytes and other blood cells remain trapped within the vasculature. Degradation of haemoglobin, release of haem iron and activation of neutrophils may therefore occur during the ischaemic period itself.

These factors are limited by flushing the organ with ice-chilled preservation solution prior to ischaemia. However, this procedure itself introduces other variables. Endothelial cells, for example, are sensitive to hypothermia alone and the standard flushing procedures adopted during hypothermic preservation for transplantation may damage the endothelium and jeopardize subsequent organ viability (McKeown *et. al.*, 1993; Hidalgo *et. al.*, 1995). In this context, the selection of preservation medium used may greatly affect the post-ischaemic function of a transplanted organ (Hidalgo *et. al.*, 1995).

Not only the type of ischaemia but also the choice of experimental model may play a role in post ischaemic renal function. The organs of different species differ in their tolerance of warm ischaemia. At normothermic temperatures, the organs of pigs and dogs have a higher ischaemic tolerance than those of rats or rabbits, while hibernating animals have an ability to "store" their organs at low temperatures during hibernation (Green *et. al.*, 1984). Even when a single model system is used, it is important to gauge the handling skills of a single investigator. Warm ischaemia induced by clamping

the renal vessels is a relatively simple, reproducible procedure, hence its wide-spread usage. In contrast, the outcome of an autograft or transplant operation, requiring microsurgical expertise in small animal models, depends in large part on the manipulative skills of the surgeon.

In recognition of these factors, it was considered important to begin this thesis with an analysis of some of the basic histopathological and biochemical changes occurring before and after autografting in the New Zealand White rabbit renal autograft model in the hands of this investigator, and to compare them with changes reported in other models of renal ischaemia-reperfusion injury.

3.2 Objective

The studies presented in this chapter were designed to establish patterns of parenchymal and vascular damage in NZW rabbit kidneys subjected to various periods of cold ischaemia, or to cold ischaemia followed by autografting.

3.3 Methods

3.3.2 Methodology

A total of 48 NZW rabbits were anaesthetized by an i.m. injection of fentanyl fluanisone and diazepam; oxygen was supplied via an open face mask (see Chapter 2 for full details). Kidneys were flushed with ice-cold (0-2^{0}C) HCA and stored for 0, 24, 48 or 72 h prior to analysis of susceptibility to lipid peroxidation and histopathological change, or to autografting. Autografted kidneys were either removed under terminal anaesthesia after 1 h of reperfusion in 2 groups for histopathological analysis, or the rabbits were allowed to recover for determination of long-term viability.

Histopathological changes were assessed by light and electron microscopy. Susceptibility to lipid peroxidation was determined by analysis of TBA-reactive material and Schiff's bases in renal homogenates incubated for 1 h at 37^{0}C. Long term viability was assessed by measurement of serum urea and creatinine levels, evidence of urine production and clinical symptoms of uraemia.

3.3.2 Experimental Groups

Group 1: Freshly nephrectomized left and right kidneys (n=6) drawn at random from a pool of 24 kidneys from bi-laterally nephrectomized rabbits were flushed with ice-cold hypertonic citrate solution and halved. Half the kidney was homogenized for analysis of susceptibility to lipid peroxidation, while the other half was sectioned for light and electron microscopical analysis.

Group 2: Freshly nephrectomized left and right kidneys (n=6, as above) were flushed as in Group 1 and stored for 24 h before being subjected to the same protocol used in Group 1.

Group 3: Freshly nephrectomized left and right kidneys (n=6) were flushed as in Group 1 and stored for 48 h before being subjected to to the same protocol used in Group 1.

Group 4: Freshly nephrectomized left and right kidneys (n=6) were flushed as in Group 1 and stored for 72 h before being subjected to to the same protocol used in Group 1.

Group 5: Freshly nephrectomized right kidneys (n=6) were flushed as in Group 1 and stored for 48 h prior to autografting. Reperfusion was terminated after 1 h by lethal infusion of sodium pentobarbitone (200 mg/kg), and kidneys were analysed by light and electron microscopy.

Group 6: Freshly nephrectomized right kidneys (n=6) were flushed as in Group 1 and stored for 72 h prior to autografting. Reperfusion was terminated after 1 h by lethal infusion of sodium pentobarbitone (200 mg/kg), and kidneys were analysed by light and electron microscopy.

Group 7: Freshly nephrectomized right kidneys (n=6) were flushed as in Group 1 and autografted immediately into the left renal bursa. Rabbits were allowed to recover for analysis of long term viability.

Group 8: Freshly nephrectomized right kidneys (n=6) were flushed as in Group 1 and stored for 24 h prior to autografting into the left renal bursa. Rabbits were allowed to recover for analysis of long term viability.

Group 9: Freshly nephrectomized right kidneys (n=6) were flushed as in Group 1 and stored for 48 h prior to autografting into the left renal bursa. Rabbits were allowed to recover for analysis of long term viability.

Group 10: Freshly nephrectomized right kidneys (n=6) were flushed as in Group 1 and stored for 72 h prior to autografting into the left renal bursa. Rabbits were allowed to recover for analysis of long term viability.

3.4 Results

3.4.1 Histology

In Figs 3.1 and 3.2 are shown mean oedematous changes occurring in different cell types within the kidney after different periods of ischaemia alone or ischaemia followed by 1 h of reperfusion, as judged by electron microscopical analysis. Individual cells were scored in 10 grid squares per specimen (n=6), and the mean values obtained are displayed in Figs 3.1 and 3.2. Different cell types within the kidney were found to be differentially susceptible to ischaemia or reperfusion. Glomerular cells, with the exception of endothelial cells, were relatively unaffected by ischaemia and reperfusion. Indeed, the only cell type in the cortex affected by ischaemia alone was the proximal tubule (Fig 3.1), which had become slightly oedematous (grade 1) after 72 h of storage without reperfusion. However, this change did not achieve significance. There was no mitochondrial swelling, and little brush border blebbing (Plate 3.1).

In the medulla (Fig 3.2) the thick ascending tubules (mTAT) were significantly affected by ischaemia alone ($p<0.05$, Mann-Whitney U-test; n=6). After 48 h of ischaemia, mTAT cells were minimally swollen (grade 1, range 0.5-1.5) and after 72 h this had developed to minimal-mild swelling (grade 1.5, range 1-2) with slight mitochondrial swelling (Plate 3.2). Other medullary cell types were not significantly affected by ischaemia alone but the interstitial spaces (connective tissue) were also becoming oedematous after 72 h of ischaemia.

After 48 or 72 h of storage and 1 h of reperfusion, almost all cell types were affected, but to different degrees (Figs 3.1 and 3.2). In the cortex, proximal tubule cells were moderately oedematous (grade 3, range 2-3.5, n=6) after 48 h of storage, and moderately to severely swollen (grade 3.5, range 3-4, n=6) after 72 h of storage. Both of these changes were highly significant ($p<0.005$, Mann Whitney U-test) compared with unreperfused tissue. Brush border membranes were severely disrupted and mitochondria were swollen with loss of cristae structure (Plate 3.3). Distal tubules and peritubular endothelial cells were less severely affected, with mild to moderate (grade 2-3) changes after 72 h of storage and 1 h of reperfusion. In the medulla, the mTAT cells were moderately oedematous after 48 h of storage and 1 h of reperfusion (grade 3, range 2-3.5, $p<0.05$ compared with unreperfused tissue), and severely oedematous after 72 h of storage and 1 h of reperfusion (grade 4, range 3.5-4, $p<0.005$ compared with unreperfused tissue). Mitochondria were swollen but cristae were mostly intact (Plate 3.4). Other cell types were significantly affected by reperfusion, but none were severely damaged (Fig 3.2). The basal laminae of both tubules and capillaries were barely affected by reperfusion, as judged by EM.

Changes in particular cell types were not easily detectable by light microscopy, but gross histopathological changes occurring across the cortex and medulla could be analysed in a single specimen, and were therefore representative of the kidney as a whole. The changes scored by light microscopy reflected the changes scored at EM level, confirming that the EM specimens were representative and not marred by processing or sampling artefacts. The only changes noted before reperfusion by light microscopy were minimal interstitial and mild intracellular medullary oedema (Fig 3.3, Plate 3.5) after 72 h storage. After reperfusion, there was moderate to severe cortical intracellular oedema (grade 3.5, range 2.5-4), severe interstitial and intracellular medullary oedema (grade 4, range 3-4) and severe medullary vascular erythrocyte congestion (grade 4, range 3-4; Plate 3.6). All these changes were highly significant ($p<0.005$, Mann-Whitney U-test) compared with unreperfused tissue. There was minimal cortical congestion (Plate 3.6), very little haemorrhage and no frank necrosis or inflammatory infiltrate.

3.4.2 Determination of Lipid Peroxidation

Susceptibility to lipid peroxidation, as determined by measurement of TBA-reactive material and Schiff's bases in homogenates of the renal cortex and medulla, increased with the duration of storage (Figs 3.6 and 3.7). In unstored kidneys, there was negligible formation of TBA-reactive material or Schiff's bases in the renal cortex after 1 h of *in vitro* incubation at 37^0C. In contrast, both TBA-reactive material and Schiff's base formation were significantly higher ($p<0.05$) in the medulla of unstored kidneys compared with the cortex. With the exception of TBA-reactive material in the medulla, there were significant ($p<0.05$) increases in both markers of lipid peroxidation after 24 h of storage in both the cortex and medulla. After 48 or 72 h of storage, the increases in susceptibility to lipid peroxidation had become highly significant ($p<0.005$) in both the cortex and medulla. Increases in susceptibility to lipid peroxidation correlated well with the histopathological changes noted in Section 3.41.

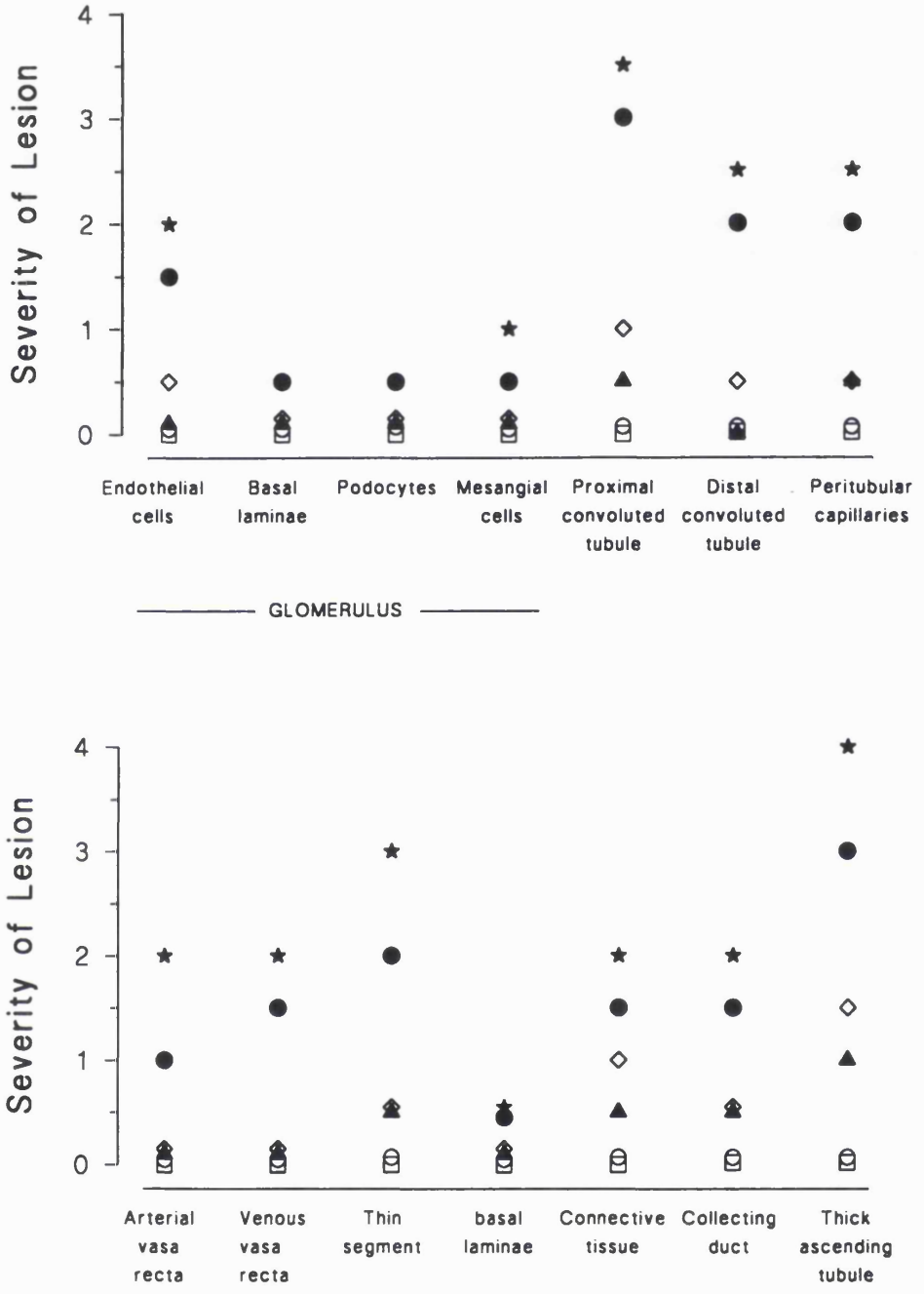

Figs 3.1 and 3.2
Severity of intracellular oedema in different cell types of the renal cortex (top) and medulla (bottom), as judged by electron microscopy. All points are mean determinations of 10 grid squares per specimen in 6 different kidneys. Cell types were scored as described in Methods Section 2.5.2. □ = unstored, no reperfusion; ○ = 24 h stored, no reperfusion; ▲ = 48 h stored, no reperfusion; ◇ = 72 h stored, no reperfusion; ● = 48 h stored, 1 h reperfusion; ★ = 72 h stored, 1 h reperfusion. The figures show that different renal cell types are differentially susceptible to increasing durations of cold ischaemia and to reperfusion.

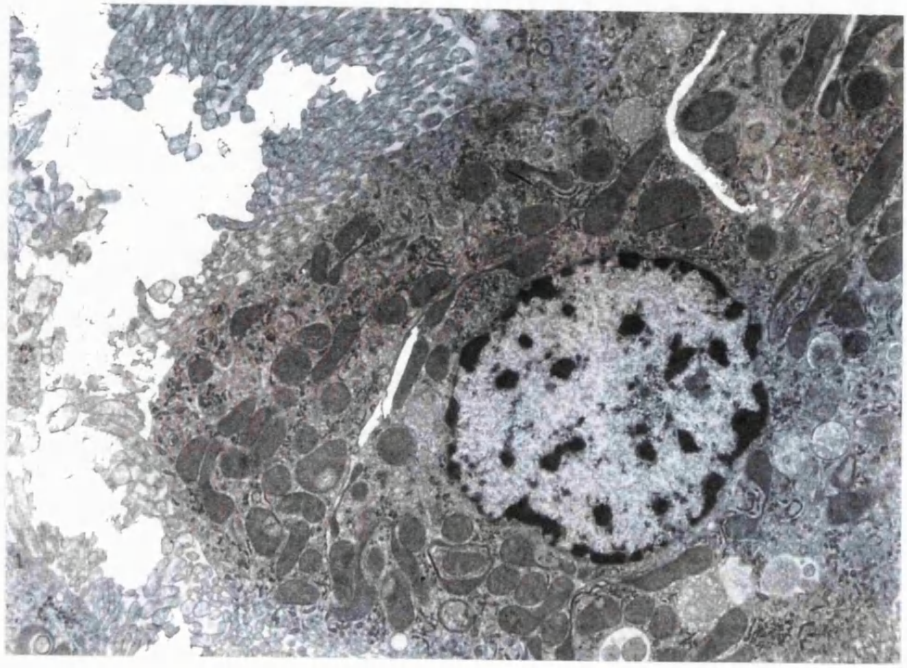

Plate 3.1 **Electron micrograph of renal proximal tubule cells after 72 h of storage and no reperfusion (magnification x 5000). The cells are slightly oedematous but the brush border membranes are intact and mitochondrial swelling is negligible. Cristae are just visible and well spaced.**

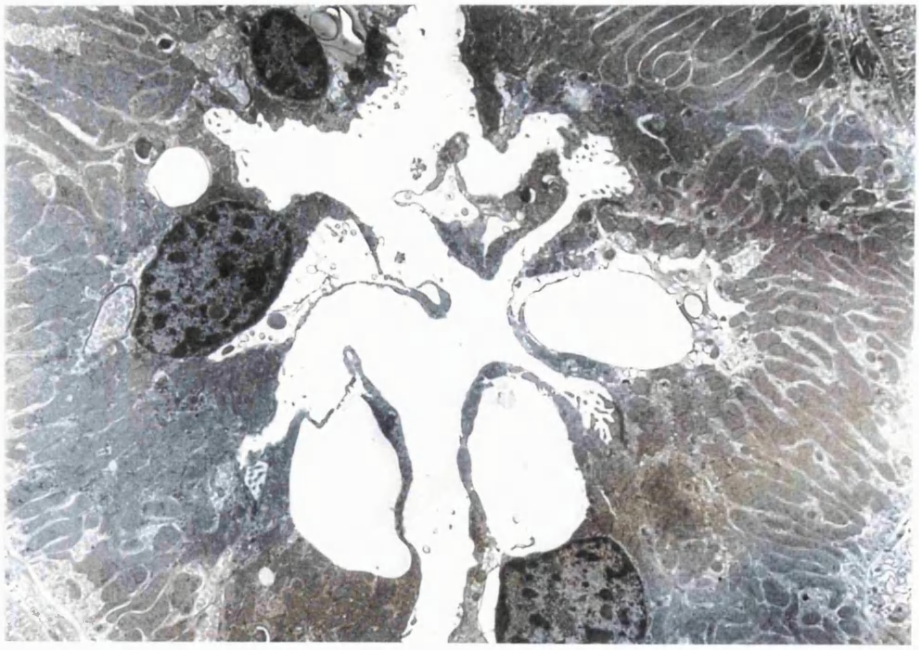

Plate 3.2 **Electron micrograph mTAT cells after 72 h of storage and no reperfusion (magnification x 5000). The cells are mildly oedematous with slightly swollen mitochondria.**

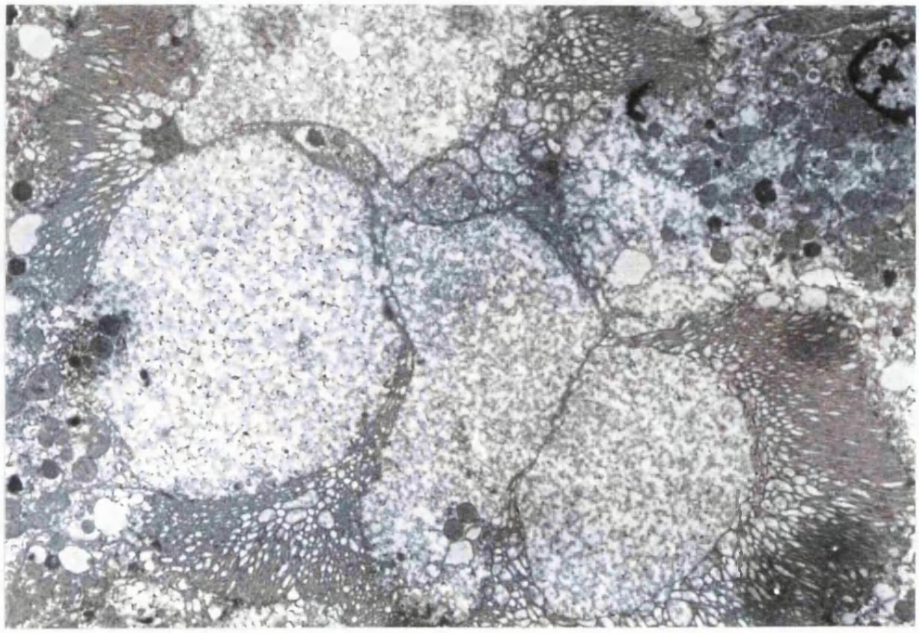

Plate 3.3 **Electron micrograph of renal proximal tubule cells after 72 h of storage and 1 h of reperfusion (magnification x 5000). The cells are severely oedematous with severe brush border membrane blebbing, intralumenal cast formation, mitochondrial swelling and disintegrating cristae structure.**

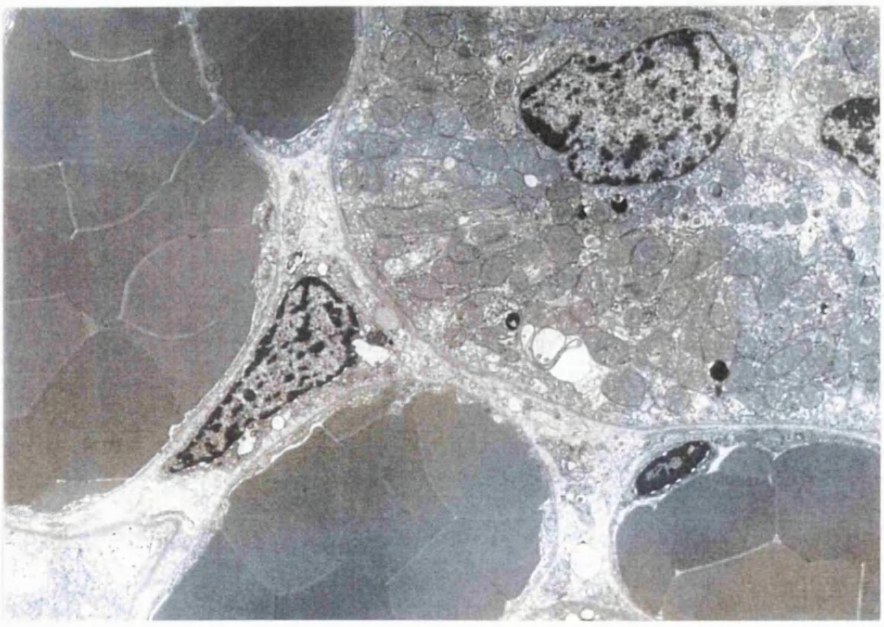

Plate 3.4 **Electron micrograph of mTAT cells after 72 h of storage and 1 h of reperfusion (magnification x 5 000). The cells are severely oedematous with swollen mitochondria and disintegrating cristae. Peritubular capillaries are compressed showing rouleaux formation.**

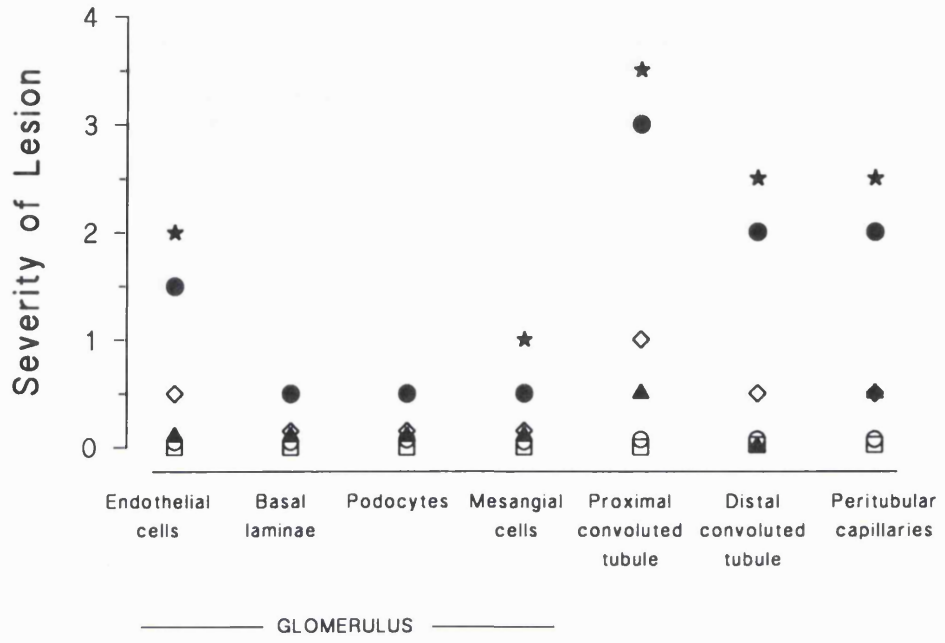

Fig 3.3 Severity of histopathological lesions in the renal cortex and medulla, as judged by light microscopy. All points are mean determinations in 6 kidneys (see Methods). □ = unstored, no reperfusion; ○ = 24 h stored, no reperfusion; ▲ = 48 h stored, no reperfusion; ◇ = 72 h stored, no reperfusion; ● = 48 h stored, 1 h reperfusion; ★ = 72 h stored, 1 h reperfusion. An analogous pattern can be discerned to that observed using electron microscopy.

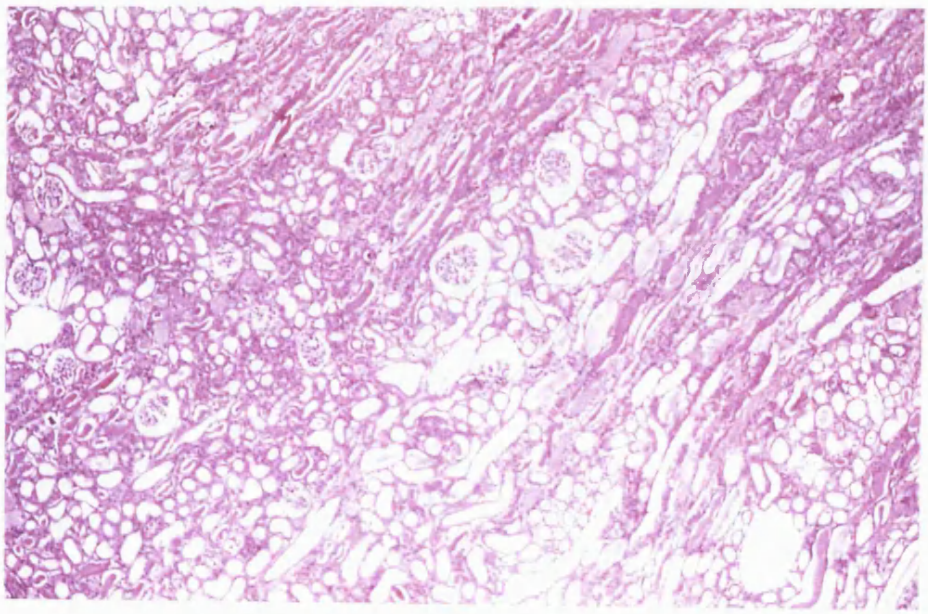

Plate 3.5 **Light micrograph of the cortico-medullary junction of a kidney stored for 72 h but not reperfused (magnification x 40) showing mild intracellular and interstitial medullary oedema.**

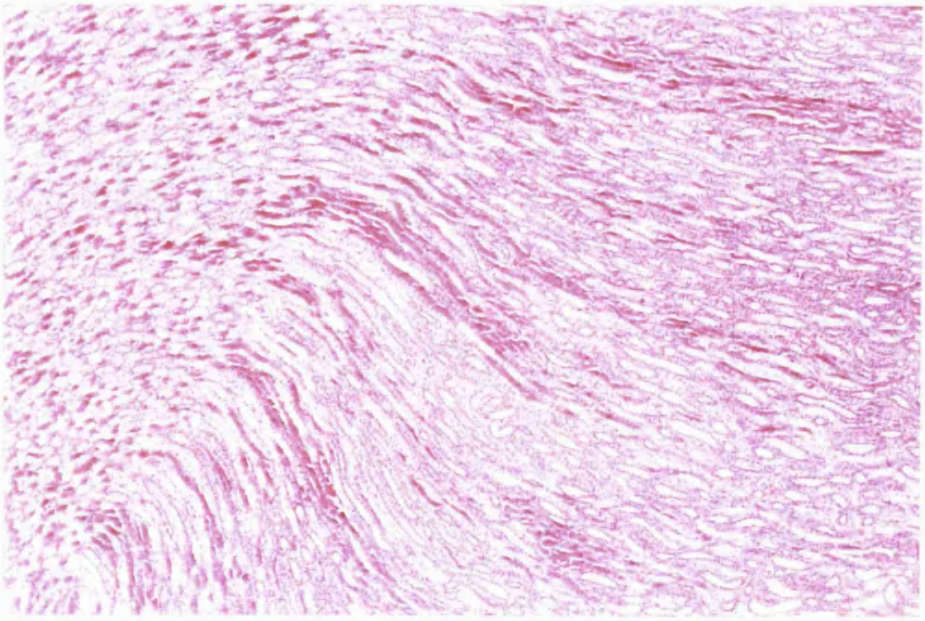

Plate 3.6 **Light micrograph of the cortico-medullary junction of a kidney stored for 72 h and reperfused for 1 h (magnification x 40) showing severe medullary congestion and moderate oedema of the cortico-medullary junction but negligible cortical congestion.**

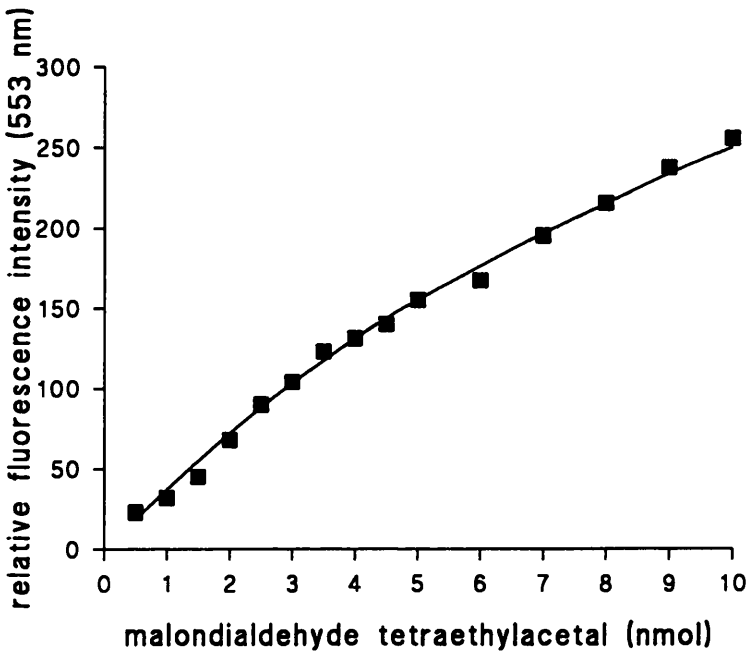

Fig 3.4 Standard curve for malondialdehyde tetraethylacetal (nmol) vs relative fluorescence intensity at 553 nm when excited at 513 nm (values are mean of duplicate determinations).

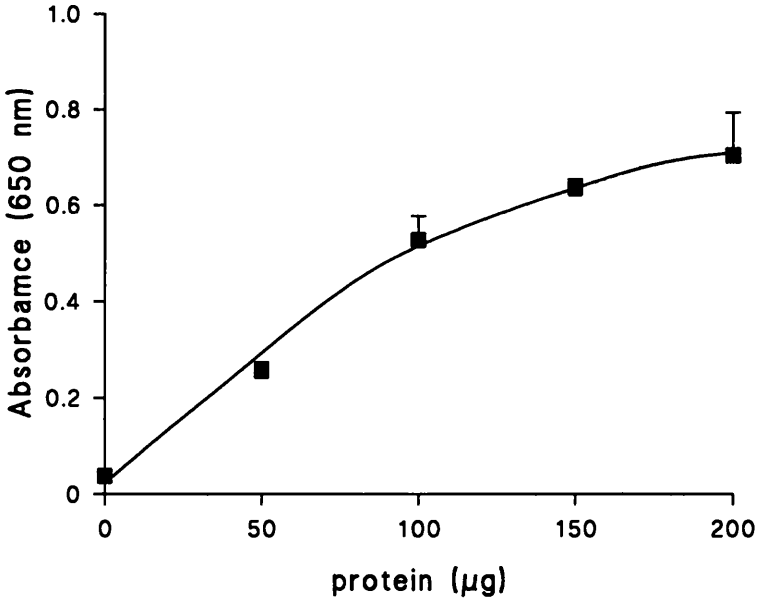

Fig 3.5 Standard curve for bovine serum albumin (µg) vs absorbance at 650 nm. Results are presented as mean ± SEM of triplicate determinations.

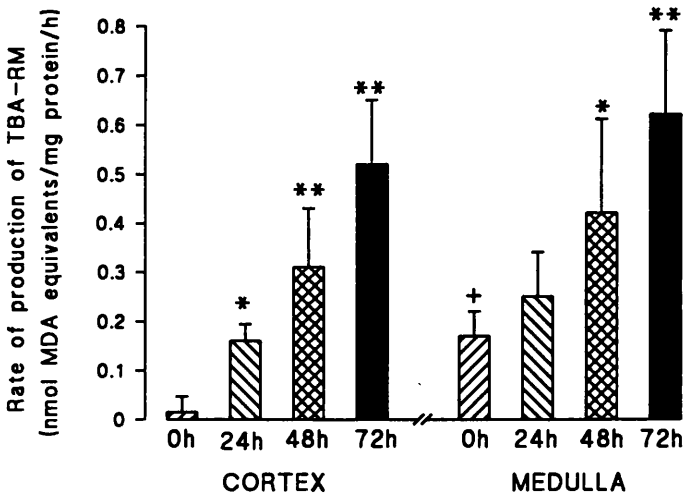

Fig 3.6 Rate of formation of TBA-reactive material in homogenates of renal cortex and medulla. Results are presented as mean and SD (n=6) for Groups: 1 (unstored); 2 (24 h stored); 3 (48 h stored; 4 (72 h stored). $*p<0.05$, $**p<0.005$ compared with Group 1; $^{+}p<0.05$ cortex compared with medulla. The figure shows that increases in susceptibility to lipid peroxidation are both highly significant and proportional to the duration of ischaemia in both the renal cortex and medulla but that early changes are greatest in the medulla.

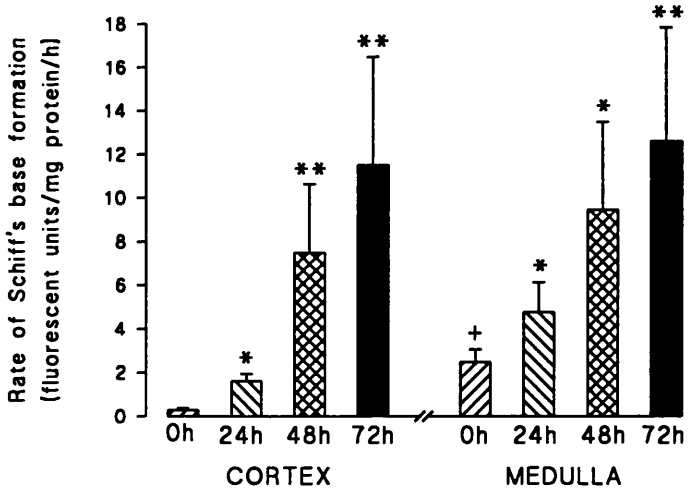

Fig 3.7 Rate of formation of Schiff's bases in homogenates of renal cortex and medulla. Results are presented as mean and SD (n=6) for Groups: 1 (unstored); 2 (24 h stored); 3 (48 h stored); and 4 (72 h stored). $*p<0.05$, $**p<0.005$ compared with Group 1; $^{+}p<0.05$ cortex compared with medulla. The figure shows that increases in susceptibility to lipid peroxidation are both highly significant, and proportional to the duration of ischaemia in both the renal cortex and medulla, but that early changes are greatest in the medulla.

3.4.3 Survival Determination

Renal function in kidneys stored for 0, 24, 48 or 72 h before autografting was monitored by analysis of serum urea and creatinine levels (Figs 3.8 and 3.9). All animals displaying clinical symptoms of uraemia were immediately killed. All animals suffering renal failure as a result of technical problems such as ureter blockage or venous thrombosis at the anastomosis were not included in the experimental groups (a total of 4 animals). Unstored transplanted kidneys were able to support life in all cases (n=6) although serum urea and creatinine levels were elevated for several days after the autograft operation. Similarly, recipients of kidneys stored for 24 h were all healthy 4 weeks after autografting (n=6). After 48 h of storage, only 3/6 recipients were still alive after 4 weeks. The three animals that did not survive were sacrificed after several days, showing advanced symptoms of uraemia and highly elevated serum levels of creatinine and urea (Figs 3.8 and 3.9). After 72 h of storage, only 1/6 recipients survived. All other rabbits had died or were sacrificed by day 6 with highly elevated serum urea and creatinine levels and advanced symptoms of uraemia. Histological analysis (using light microscopy) of kidneys taken at autopsy showed either complete infarction (Plate 3.7) or gradual severe necrosis of the whole kidney (Plate 3.8). That necrosis was gradual in these instances was illustrated by the demarcation of successive necrotic zones by acute inflammatory infiltrate and casts (necrotic debris); large calcific deposits were also prominent. These changes were most prominent in the renal cortex and the cortico-medullary junction.

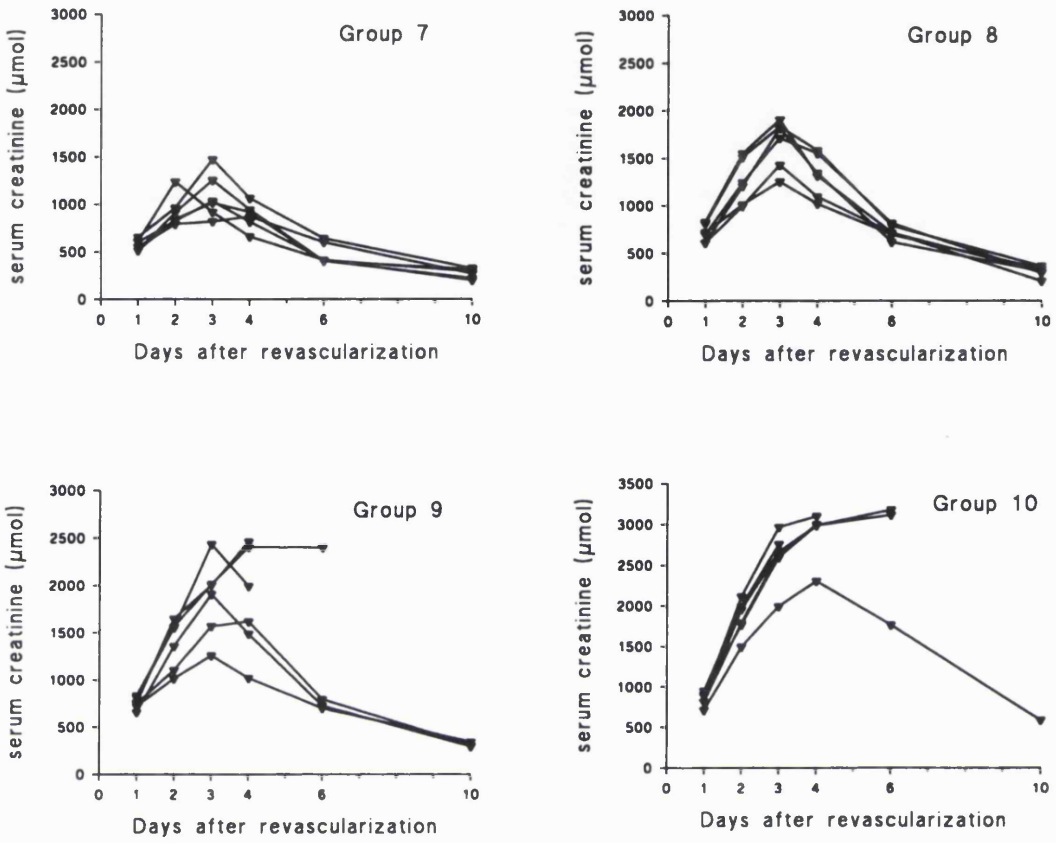

Fig 3.8 Concentration of serum creatinine (µmol) in Groups 7 (unstored), 8 (24 h stored), 9 (48 h stored) and 10 (72 h stored) for up to 10 days post transplant (▼ denotes individual rabbits). Peak serum creatinine level (days 2 to 4) increases with the duration of storage and correlates well with survival. Discontinuation of a line denotes death or sacrifice of an animal.

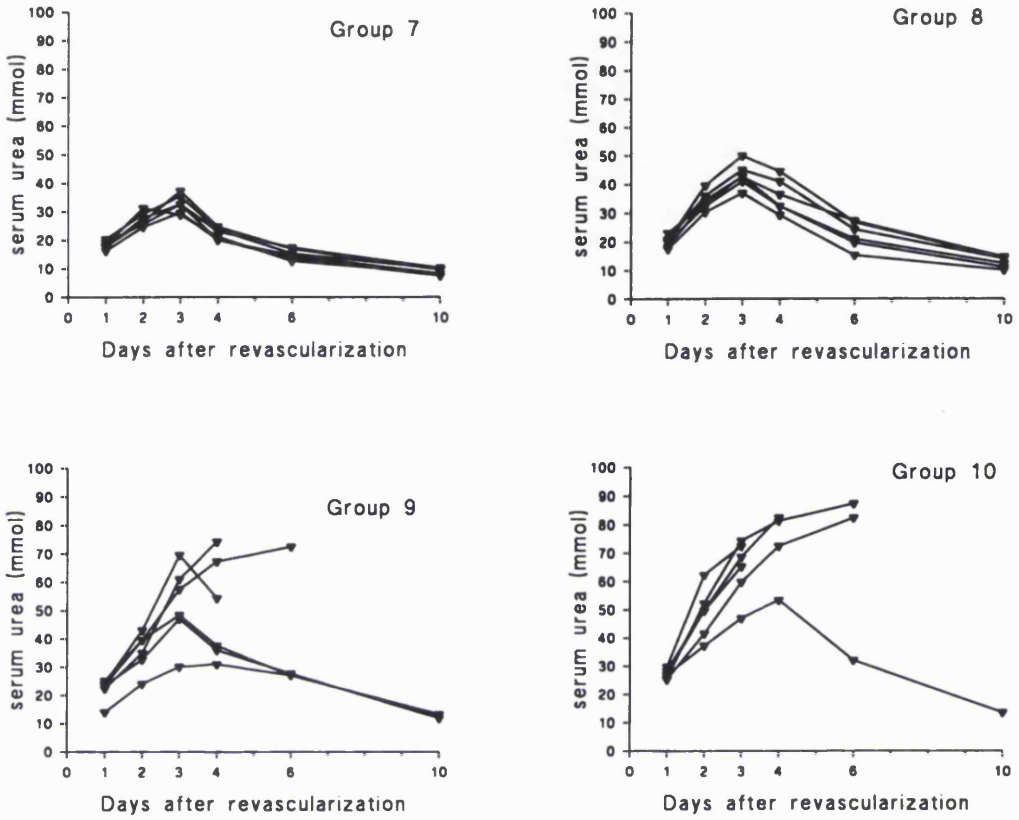

Fig 3.9 Concentration of serum urea (mmol) in Groups 7 (unstored), 8 (24 h stored), 9 (48 h stored) and 10 (72 h stored) for up to 10 days post transplant (▼ denotes individual rabbits). As with serum creatinine levels, peak urea (days 2 to 4) increases with the duration of storage and correlates well with survival. Discontinuation of a line denotes death or sacrifice of an animal.

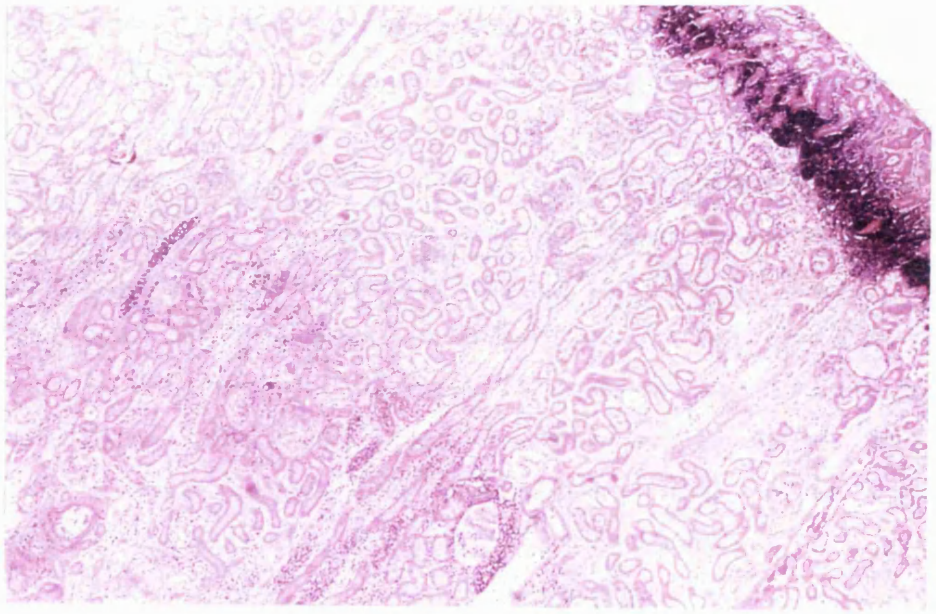

Plate 3.7 Light micrograph of the renal cortex of a Group 10 infarcted kidney at autopsy 3 days after revascularization (magnification x 40). Tubular outlines can be distinguished; the dark band at the top right is an inflammatory infiltrate of neutrophils.

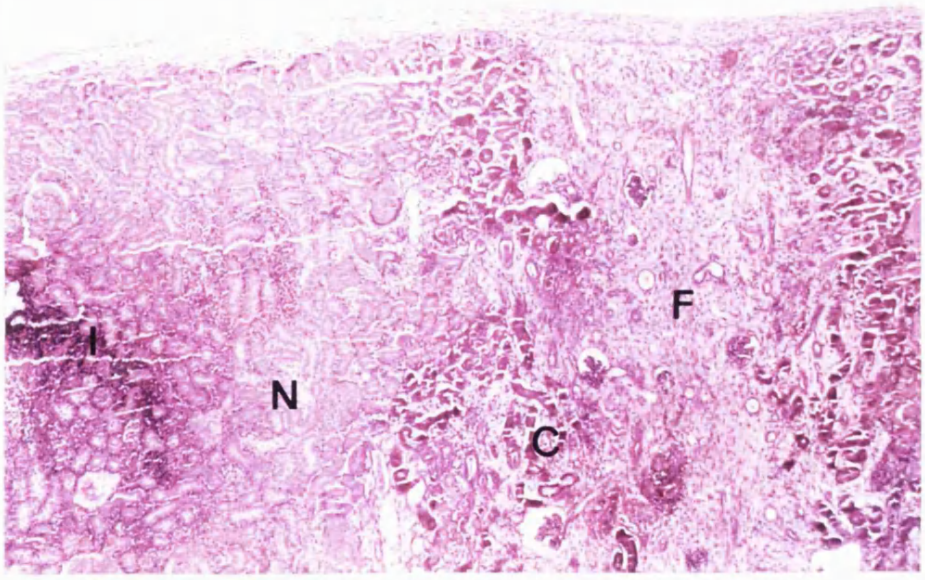

Plate 3.8 Light micrograph of the renal cortex of a Group 10 kidney which had undergone gradual severe necrosis of the entire kidney at autopsy 6 days after revascularization (magnification x 40), showing necrotic infarcted area (N) inflammatory infiltrate (I), calcification (C) and fibrosis (F).

3.5 Discussion

The results presented in this chapter show that a continuum of pathological changes had occurred in the NZW rabbit kidneys during both the storage period and after autografting. The earliest change detectable by electron microscopy was oedematous swelling of the mTAT after about 48 h of cold ischaemia. Swelling of these cells during warm ischaemia has been reported by others (Mason *et. al.*, 1983; Yamamoto *et. al.*, 1984; Mason 1988; and Bayati *et. al.*, 1990). Using image analysis of tubular diameters, Mason and co-workers (1983) showed that following 90 min of warm ischaemia, the average tubular diameter of the mTAT had increased by 40%, and that the peritubular capillaries and *vasa recta* were correspondingly compressed. The authors suggested that medullary erythrocyte congestion during reflow was caused by such vascular compression, leading to the characteristic formation of rouleaux, or densely packed, polygonally shaped erythrocytes. These could also be seen following 72 h of cold ischaemia and 1 h of reflow in the NZW rabbit renal autograft model (Plate 3.4). However, swelling of the mTAT in warm ischaemic models appears to be a consequence of plasma extravasation from the peritubular capillaries during ischaemia, resulting in haemoconcentration and an increase in vascular resistance and capillary hydrostatic pressure (Bayati *et. al.*, 1990). In the cold ischaemic model, the absence of plasma and the presence of hyperosmolar concentrations of impermeant solutes such as mannitol during the storage period may be expected to significantly alter patterns of cell swelling, haemoconcentration and rouleaux formation. Nevertheless, the development of medullary congestion in the cold ischaemic model after revascularization appeared to be analogous to that seen in warm ischaemic models.

Mason (1988) also noted that vascular erythrocyte congestion correlated with poor nephron function, particularly those situated in the cortico-medullary junction. However, although erythrocyte congestion can be ameliorated by haemodilution, this does not prevent the development of mTAT necrosis, possibly because reduction of the haematocrit also reduces the oxygen carrying capacity of blood (Andersson and Jennische, 1987; Hellberg *et. al.*, 1991). Mason (1988) and others (Hanley and Davidson, 1981; Cronin, 1986) reported that congestion could also be prevented by intravenous infusion of hyperosmolar mannitol prior to ischaemia and that parameters of renal function such as GFR improved as a result. The hypertonic citrate solution used in the experiments presented in this chapter contained hyperosmolar mannitol (Table 2.1) yet this did not prevent the development of medullary congestion following cold ischaemia. The reason for this is not clear but it is possible that mannitol, which is a relatively small impermeant solute, could have gained access to intracellular locations following prolonged cold storage, and therefore failed to prevent or even exacerbated cell swelling. Interestingly, it has been shown that infusion of hyperosmolar mannitol after, rather than before, warm ischaemia actually exacerbates medullary congestion (Hellberg *et. al.*, 1991). These

authors hypothesized that post-ischaemic mannitol infusion could have increased tubular work by washing out lumenal casts, thereby increasing the GFR. However, this hypothesis could not be applied to the cold ischaemic model used here as a hyperosmolar mannitol reflush was not administered either before or after reperfusion.

While medullary congestion was the most prominent histopathological change observed in all autografted stored kidneys the cortex was seldom congested despite the development of severe intracellular oedema, particularly of the proximal convoluted tubules. The reasons for this are likely to be differences in the vascular architecture of the cortex compared with the medulla, and differences in the timing of oedematous change (which occurred prior to reperfusion in the outer medulla). Cortical bloodflow is normally very rapid - on a per-gram basis, the renal cortex is the most highly perfused tissue in the body (Brenner *et. al.*, 1986) - whereas medullary blood pressure and flow rates are very low, allowing efficient countercurrent multiplication, solute reabsorption and urine concentration (Zimmerhackl *et. al.*, 1987). Cortical vascular congestion has occasionally been observed in warm ischaemic models following release of the clamps (Gower *et. al.*, 1993). However, this may have been a consequence of haemoglobin degradation or neutrophil entrapment during the ischaemic period, neither of which were factors in the cold ischaemic model reported here. Most studies of regional blood flow in the kidney following warm ischaemia have shown that cortical blood flow is not significantly affected by haemodilution (Andersson and Jennische, 1987; Hellberg *et. al.*, 1991; Vetterlein *et. al.*, 1994) and is relatively unaffected by acute ischaemia (Vetterlein *et. al.*, 1986; Mason, 1988; Hellberg *et. al.*, 1991). Here again, the warm ischaemic and cold ischaemic models appear to be comparable, at least in so far as there were no signs of cortical erythrocyte congestion in the NZW rabbit renal autograft model. The haemodynamics and vascular resistance of autografted stored NZW rabbit kidneys is the subject of the next chapter.

Proximal tubular morphological integrity was well maintained throughout the ischaemic period compared with the mTAT but became severely oedematous following reflow. These changes correlated well with susceptibility to lipid peroxidation, which was negligible in the cortex of unstored kidneys and highly elevated after prolonged ischaemia. In contrast, the medulla, which became oedematous during the ischaemic period itself, was significantly more susceptible to lipid peroxidation after short periods of ischaemia than the cortex ($p<0.05$; Figs 3.6 and 3.7). The reasons for this are not clear, but it may be inferred that the cortex is more susceptible to direct oxidative injury upon reperfusion after prolonged ischaemia, whereas the medulla tends to produce TBA-reactive material more continuously, possibly as a result of continuous prostaglandin biosynthesis. Gower and co-workers (1987) have shown that approximately 50% of TBA-reactive material formed

in the renal medulla is produced by this mechanism. This possibility is also compatible with the idea that medullary damage is more directly a result of ischaemia alone, whether this be primary (during the storage period) or secondary (as a consequence of poor medullary reperfusion after revascularization).

The severity of the histopathological and biochemical changes discussed above correlated well with compromises in long term renal viability. As the storage time was increased, post ischaemic renal function (assessed by serum levels of urea and creatinine, evidence of urine production and clinical symptoms of uraemia) deteriorated. Serum levels of urea and creatinine remained quite low in rabbits transplanted with unstored and 24 h stored kidneys and renal viability was 100%. After 48 or 72 h storage, there was moderate to severe intracellular oedema in both the cortex and medulla, severe medullary congestion, highly significantly increased susceptibility to lipid peroxidation, highly elevated serum urea and creatinine levels and poor long term viability. It is not clear from these findings alone whether any of these factors were causes, rather than symptoms, of acute renal failure. However, it is clear that the pathological developments observed in this cold ischaemic model were comparable with changes described in warm ischaemic models of acute renal failure. The following chapters are devoted to elucidating the importance of these factors in the aetiology of acute renal failure following storage and transplantation and the value of pharmacological intervention.

3.6 Conclusions

(i) The medullary thick ascending tubules (mTAT) were susceptible to ischaemia alone, and had become mildly swollen after 72 h of cold ischaemia.

(ii) Swelling of the mTAT appeared to be responsible for compression of the medullary microvasculature upon reperfusion, resulting in medullary erythrocyte congestion.

(iii) Medullary erythrocye congestion was the most prominent pathological change observed upon reperfusion of stored autografted kidneys. Prolonged cold storage (48 or 72 h) followed by reperfusion also caused moderate to severe oedema in most sections of the nephron particularly those with a high energy requirement such as the mTAT and the proximal tubules.

(iv) Increases in intracellular oedema, medullary erythrocyte congestion and susceptibility to lipid peroxidation were directly proportional to the ischaemic storage time and inversely proportional to renal viability.

CHAPTER 4

HAEMOGLOBIN OXYGENATION KINETICS AND SECONDARY ISCHAEMIA IN THE NZW RABBIT RENAL AUTOGRAFT MODEL

The studies presented in this chapter are based on a paper published in:
*Transplantation 1996; **61:** 689-696.*

4.1 Introduction

In Chapter 3, some basic parameters of histopathological and functional damage to autografted stored kidneys were defined. Renal function was assessed by serum urea and creatinine levels, and these were shown to correlate with long term viability. In kidneys subjected to ischaemia but not reperfusion, histopathological damage was restricted mainly to swelling of the medullary thick ascending tubule (mTAT) and the *pars recta* (S3 segment) of the proximal tubule in the outer medulla. After reperfusion of autografted kidneys subjected to 48 or 72 h of hypothermic storage, the most prominent histopathological feature was erythrocyte congestion, especially in the outer but also the inner medulla. These findings correspond to those reported in warm ischaemic models, in which the renal vessels were clamped for varying periods (Brezis *et al.*, 1984; Yamamoto *et al.*, 1984; Mason, 1988). In both models, medullary congestion appeared to derive from the ischaemic swelling of the outer medullary tubules, leading to compression of the *vasa recta* and peritubular capillaries.

That early medullary congestion is a consequence of mechanical constriction of the medullary vasculature rather than thrombosis has been demonstrated in several models. Heparinization does not affect congestion (and all rabbits in the present studies have been treated with heparin); nor does inhibition of platelet activating factor (PAF) (Ratych and Bulkley, 1986). In contrast, haemodilution has been shown to ameliorate the severity of medullary congestion without preventing necrosis of the mTAT or the *pars recta* (Andersson and Jennische, 1987). Thus, while it is true that severe congestion correlates with renal dysfunction and poor viability, it is nevertheless possible that medullary congestion and tubular necrosis are not directly related. Necrosis of the outer medullary tubules may indeed be a result of secondary ischaemia during reperfusion caused by erythrocyte congestion

(Mason, 1988). However, after prolonged ischaemic insult ATN becomes more widespread and involves other sections of the tubule, particularly the proximal S1 segment in the superficial cortex (Shanley *et al.*, 1986). Since superficial cortical bloodflow has been shown to be relatively unaffected even after prolonged ischaemia (Mason *et al.*, 1983; Hellberg *et al.*, 1991) widespread cortical necrosis does not appear to be solely dependent upon secondary ischaemia.

Medullary congestion is associated with the acute phase of renal ischaemic injury, and tends to clear within 24 h in warm ischaemic models, suggesting that tubular swelling abates over time. The precise timing of medullary congestion, and its consequences in terms of secondary ischaemic necrosis in the NZW rabbit renal autograft model are unknown. Tubular necrosis in the superficial cortex or even the deeper cortex may derive instead from free radical-mediated oxidative injury upon re-oxygenation. Cultured proximal tubule cells subjected to hypoxia have been shown to be susceptible to free radical-mediated injury upon re-oxygenation (Paller and Neumann, 1991) while direct detection of free radicals by electron paramagnetic spin resonance studies have confirmed that free radicals are generated *in vivo* upon reperfusion of ischaemic livers (Togashi *et al.*, 1994). That free radical-mediated injury may play a role in tubular necosis after renal transplantation is supported by much circumstantial evidence of improvements in tubular function or morphology as a result of antioxidant therapies (Ratych and Bulkley, 1986; Gower *et al.*, 1992; Schilling *et al.*, 1993).

4.2 Objective

The studies in this chapter were designed to determine the kinetics of haemoglobin oxygenation and the intra-renal distribution of blood flow during *in situ* reperfusion of autografted single stored kidneys, to provide an indication of the severity, extent and duration of medullary congestion in this model after 72 h hypothermic storage. The findings of this chapter will serve as a framework against which the timing of renal functional injury can be considered in subsequent chapters.

4.3 Methods

4.3.1 Methodology

A total of 44 adult female NZW rabbits in 2 groups of 6 animals and 2 groups of 16 animals were deeply sedated with an i.m. injection of ketamine and xylazine, tracheotomized and artificially ventilated with a 50 : 50 oxygen : nitrous oxide mixture for periods of up to 4 h (see Chapter 2 for full details). Direct non-invasive measurements of concentration changes in renal HbO_2 and Hb were made using NIRS in transmission mode (see Chapter 2). In addition, the distribution of infused barium sulphate within the kidney was analysed at discrete time-points by angiography and phase contrast microscopy. Renal morphology was evaluated by light microscopy.

4.3.2 Experimental Groups

Group 1: Freshly nephrectomized left kidneys were flushed with 40 ml cold (0-2^{0}C) HCA via the renal artery and autografted immediately into the left renal bursa using standard microsurgical techniques. The autografted kidneys (n=6) were monitored continuously *in situ* during reperfusion by NIRS as described in Chapter 2

Group 2: Kidneys were flushed as in Group 1 and then stored in HCA surrounded by ice to maintain a temperature of 0-2^{0}C for 72 h before autografting (n=6). Kidneys were then subjected to the same protocol as Group 1.

Group 3: 16 kidneys in 4 subgroups of 4 animals were perfused with barium sulphate either immediately after nephrectomy and perfusion with HCA, or following autografting without storage after 5, 60 or 180 min of reperfusion, as described in Chapter 2.

Group 4: 16 kidneys in 4 subgroups of 4 animals were perfused with barium sulphate either after 72 h hypothermic storage and no reperfusion, or following 72 h storage and autografting after 5, 60 or 180 min of reperfusion.

4.4 Results

4.4.1 Near Infrared Spectroscopic Measurements of Renal Haemodynamics

In Figs 4.1 and 4.2 are shown representative time course plots of changes in concentration of HbO_2, Hb, HbT and HbD in a Group 1 (unstored transplanted) kidney and a Group 2 (72 h stored transplanted) kidney during 3 h of reperfusion. Baseline measurements of [HbO_2] and [Hb] were made for 5 min before reperfusion. Changes in [HbO_2] and [Hb] were then monitored for 3 h of reperfusion in 6 Group 1 and 6 Group 2 kidneys.

In Fig 4.3 the mean and SEM values for [HbO_2] at discrete time points in Group 1 and Group 2 kidneys are displayed. Reperfusion resulted in rapid increases in [HbO_2] within 1 min in both groups, the rate of increase in Group 1 kidneys being significantly greater ($p<0.05$). After 1 min there was a sharp decrease in [HbO_2] in Group 1 kidneys from 1494 ± 138 μM at 1 min to 1077 ± 224 μM at 3 min (p=0.053). Thereafter, [HbO_2] increased to 1482 ± 285 μM at 20 min and did not change significantly during the remaining 140 min of reperfusion. In Group 2 kidneys, [HbO_2] peaked at 1016 ± 287 μM after 2 min of reperfusion and then decreased sharply to 590 ± 86 μM at 5 min (p=0.059). The rate and magnitude of changes in [HbO_2] in the first 5 min of reperfusion of Group 2

kidneys were smaller than Group 1 kidneys but the only significant difference occurred at 1 min and the haemodynamic changes were similar to those in Group 1 kidneys. However, there was no significant recovery in [HbO_2] after 5 min of reperfusion in Group 2 kidneys and [HbO_2] was significantly lower compared with Group 1 kidneys after 10 min of reperfusion ($p<0.05$). Thereafter, there was no significant change in Group 2 [HbO_2], and the levels remained significantly lower than Group 1 kidneys for the remainder of the reperfusion period tested.

In Fig 4.4 the mean and SEM changes in [Hb] at discrete time points in Group 1 and Group 2 kidneys are shown. There were no significant differences in the rates of increase of [Hb] in the first 2 min of reperfusion between the two groups. However, in Group 1 kidneys the [Hb] had plateaued by 3 min at 763 ± 101 μM and dropped slowly thereafter to 473 ± 138 μM after 3 h of reperfusion. In Group 2 kidneys, [Hb] continued to increase after 2 min to reach a maximum of 1756 ± 322 μM after 10 min, a significantly greater concentration than Group 1 kidneys ($p<0.05$). Furthermore, unlike Group 1 kidneys the [Hb] in Group 2 increased to levels significantly in excess of the [HbO_2] in the same kidneys by 10 min ($p<0.05$). Group 2 [Hb] remained higher than the [HbO_2] and the [Hb] in Group 1 for the remainder of reperfusion. However, after 1 h of reperfusion, Group 2 [Hb] had fallen to 1123 ± 243 μM and the differences were no longer significant. After 1 h of reperfusion there were no further significant changes in [Hb] in either group.

Changes in [HbT] at discrete time points in Group 1 and Group 2 kidneys are shown in Fig. 4.5. The rates of increase in [HbT] were significantly greater in Group 1 compared with Group 2 kidneys in the first 1 min of reperfusion. However, after 2 min and during the remainder of reperfusion there were no significant differences in HbT between the two groups. Nevertheless, there was a fall in [HbT] in Group 2 kidneys from a peak at 10 min of 2465 ± 317 μM to 1647 ± 293 μM after 1 h which parallelled the decrease in [Hb] over the same period.

Fig 4.6 shows the percentage renal haemoglobin saturation in Group 1 and Group 2 kidneys ([HbO_2]/[HbT] x 100; see Chapter 2). In both groups, saturation reached 69% (± 2% and 1% respectively) after 1 min of reperfusion. In Group 1 kidneys there was a transient decrease in saturation to 57% ± 9% after 3 min of reperfusion before recovery to 78% ± 6% at 1 h. In Group 2 kidneys there was a profound haemoglobin desaturation to 25% ± 9% at 10 min ($p<0.005$ compared with Group 1) and no significant recovery in the remaining 170 min. Changes in percent haemoglobin saturation in Group 2 kidneys did not correlate with changes in [HbT].

4.4.2 Intra-Renal Distribution of Blood Flow

In Plates 4.1 to 4.3 are shown characteristic contrast angiograms, depicting barium sulphate distribution after infusion of a 1 ml bolus (50 : 50 w/v barium sulphate : isotonic saline) via the renal artery in: (i) an unstored untransplanted kidney; (ii) a transplanted 72 h stored, 1 h reperfused kidney; and (iii) a transplanted 72 h stored, 3 h reperfused kidney. In Plate 4.1, the cortical and medullary vasculature are discernable. The mottled appearance of the cortex results from barium sulphate particles trapped in the glomeruli. The striations in the medulla are a consequence of barium sulphate in the *vasa recta*, which delineate the urinary tract. Phase contrast microscopy revealed that the barium sulphate particles remained within the vasculature rather than the urinary tract even in severely damaged kidneys (Plates 4.4 and 4.5). Barium sulphate perfusion was scored as 4 (well perfused) in both cortex and medulla. In Plate 4.2, cortical barium sulphate perfusion was scored at 3-4 and was not apparently different from unstored unreperfused controls. However, barium sulphate particles did not penetrate the medullary vasculature at a maximum perfusion pressure of 90 mm Hg (scored at 0-1). After 3 h of reperfusion (Plate 4.3), cortical perfusion was good (scored at 3-4) and medullary perfusion was returning to normal (scored at 3).

The mean and range of barium sulphate scores for kidneys subjected to varying lengths of reperfusion are shown in Fig 4.7 (n=4 at each time point). There were no sigificant differences in either cortical or medullary barium sulphate perfusion in Group 3 (unstored) kidneys. Nor were there any significant disturbances in cortical barium sulphate perfusion at any time point in 72 h stored transplanted kidneys (Group 4). In contrast, medullary barium sulphate perfusion was very poor even before reperfusion: scores were significantly ($p<0.05$) lower than Group 3 kidneys at all time points up to and including 1 h reperfusion. However, after 3 h of reperfusion medullary perfusion had improved and was not significantly different from Group 3 controls.

4.4.3 Histology

In Group 1 kidneys there was very little oedema; in isolated instances there was mild to moderate focal intracellular oedema, especially of the proximal tubule. There was minimal congestion, no haemorrhage and no inflammatory infiltrate (Fig 4.8). In Group 2 there was widespread severe cortical intracellular oedema in almost every instance (Fig 4.8). In the medulla, there was moderate interstitial oedema and moderate to severe congestion (Fig 4.8) but the cortex was not usually congested. There was no inflammatory infiltrate in any specimen.

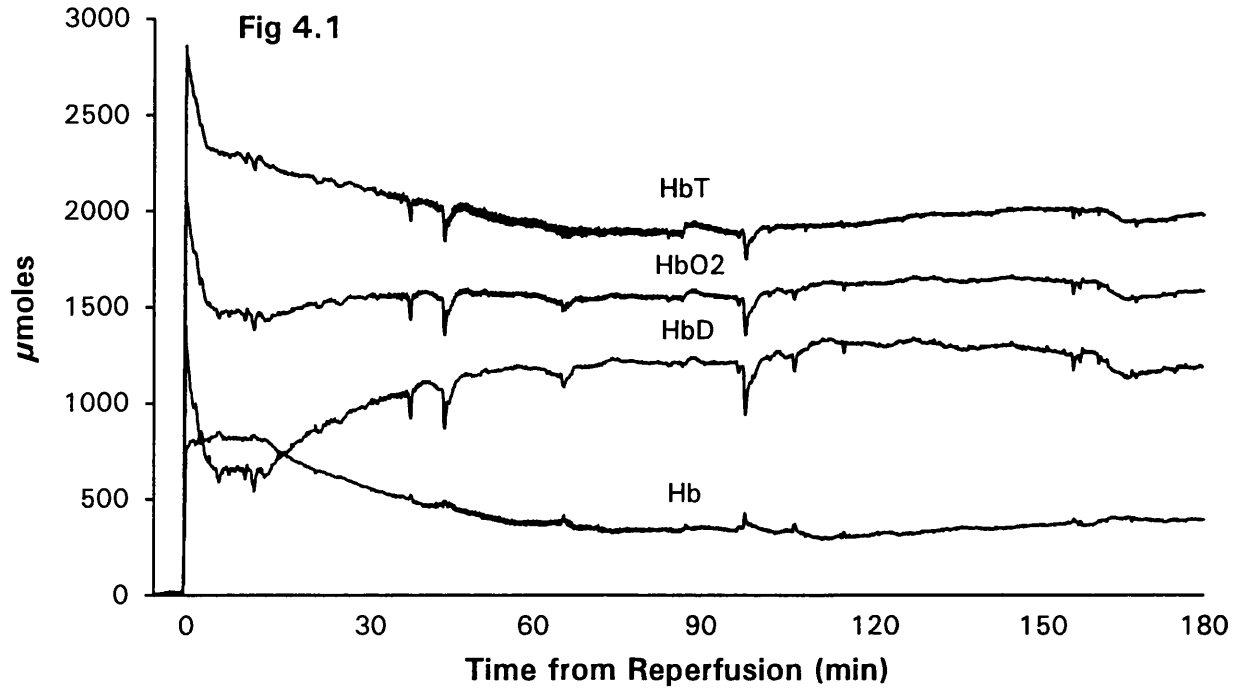

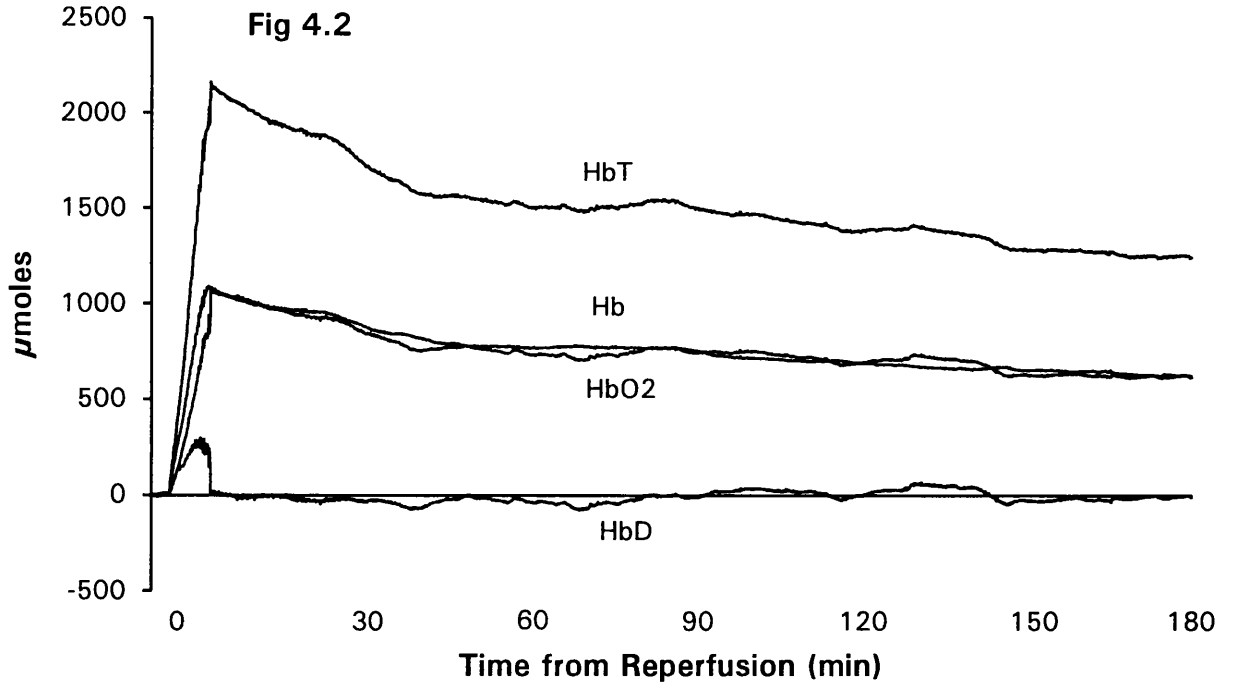

Figs 4.1 and 4.2
Representative time-course plots of changes in concentration (µM) of HbO_2, Hb, HbT and HbD (µM) in single Group 1 (unstored transplanted, top) and Group 2 (72 h stored transplanted, bottom) kidneys. The unstored kidney is more rapidly perfused upon revascularization and shows markedly better haemoglobin oxygenation throughout the duration of reperfusion.

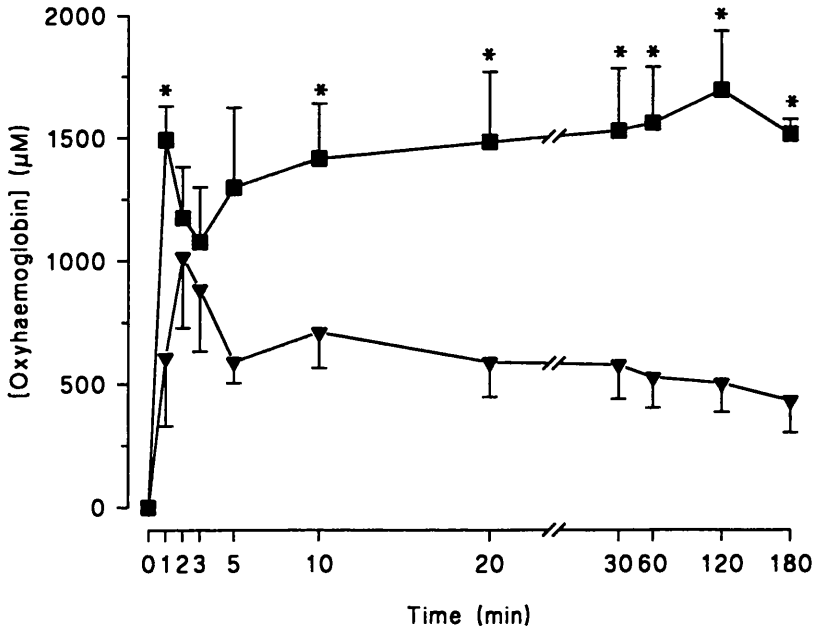

Fig 4.3 Time course of mean and SEM changes in concentration of HbO_2 (μM) in Group 1 (unstored) and Group 2 (72 h stored) kidneys. ■ = Group 1 (n=6); ▼ = Group 2 (n=6). *p<0.05. Stored kidneys were comparably perfused for the first 5 min of reperfusion but thereafter haemoglobin oxygenation was significantly worse than that in unstored kidneys.

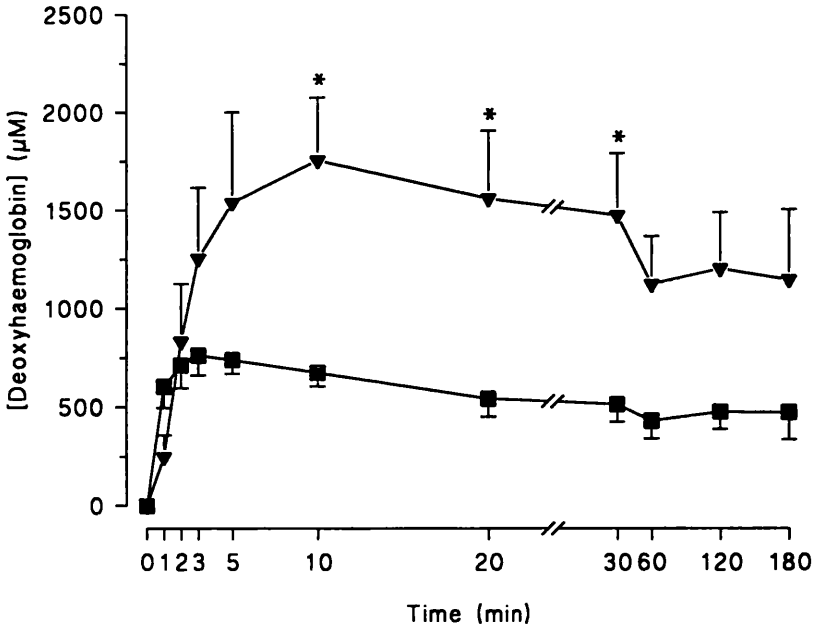

Fig 4.4 Time course of mean and SEM changes in concentration of Hb (μM) in Group 1 (unstored) and Group 2 (72 h stored) kidneys. ■ = Group 1 (n=6); ▼ = Group 2 (n=6). *p<0.05. The low HbO_2 levels in stored kidneys (Fig 4.3) are reflected in the very high Hb levels seen here - after 10 min of reperfusion, they were significantly higher than in unstored kidneys.

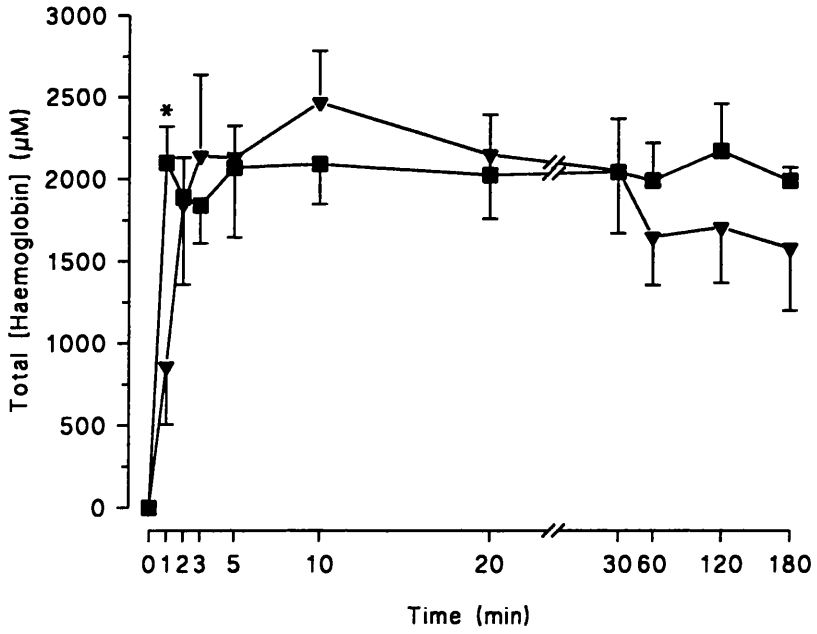

Fig 4.5 Time course of mean and SEM changes in concentration of HbT (μM) in Group 1 (unstored) and Group 2 (72 h stored) kidneys. ■ = Group 1 (n=6); ▼ = Group 2 (n=6). *$p<0.05$. It is evident that the sharp distinction in haemoglobin oxygenation seen in Figs 4.3 and 4.4 are not reflected in the HbT concentration as shown here.

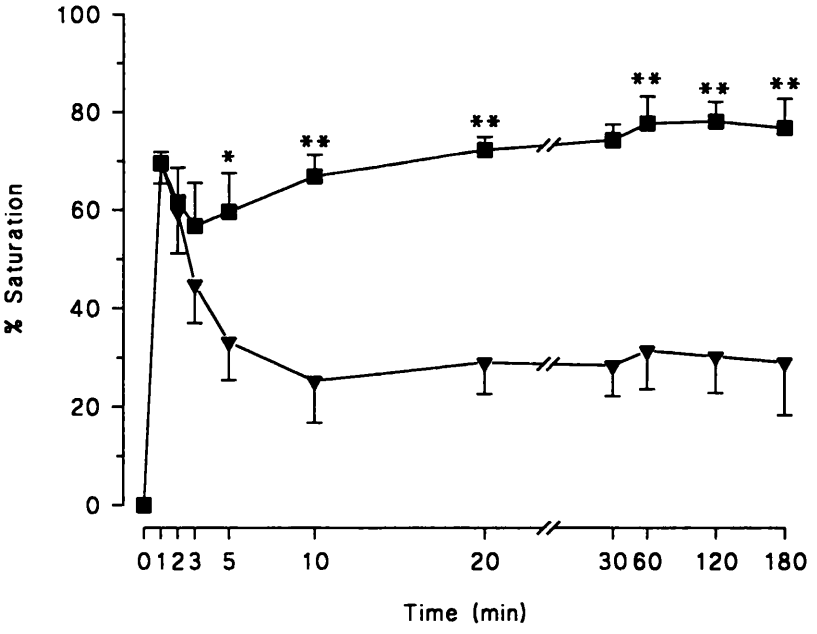

Fig 4.6 Time course of mean and SEM changes in renal haemoglobin saturation (%) in Group 1 (unstored) and Group 2 (72 h stored) kidneys. ■ = Group 1 (n=6); ▼ = Group 2 (n=6). *$p<0.05$; **$p<0.005$. The trans-renal SaO_2 demonstrates graphically that stored and unstored kidneys have equivalent haemoglobin saturation during the first few min of reperfusion, but that significant differences develop after 5 min of reperfusion.

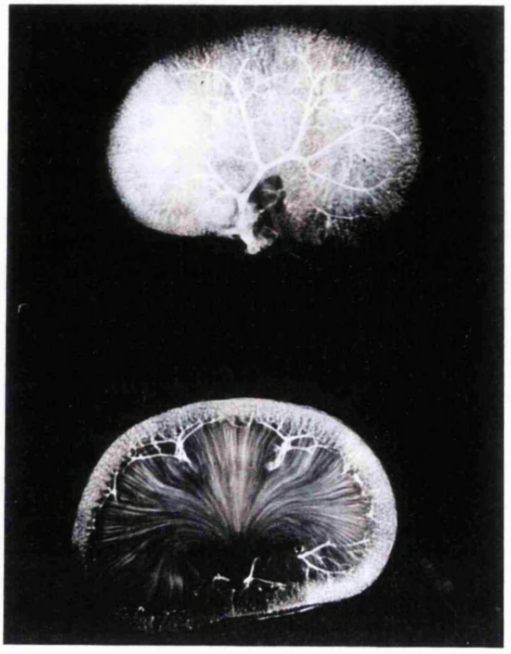

4.1

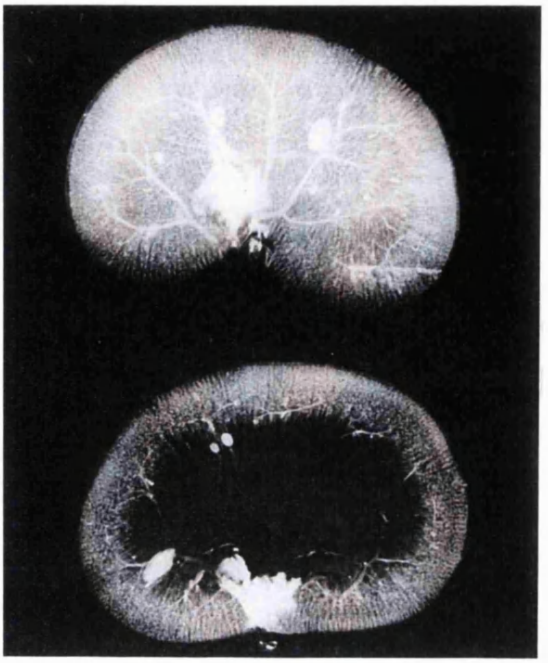

4.2

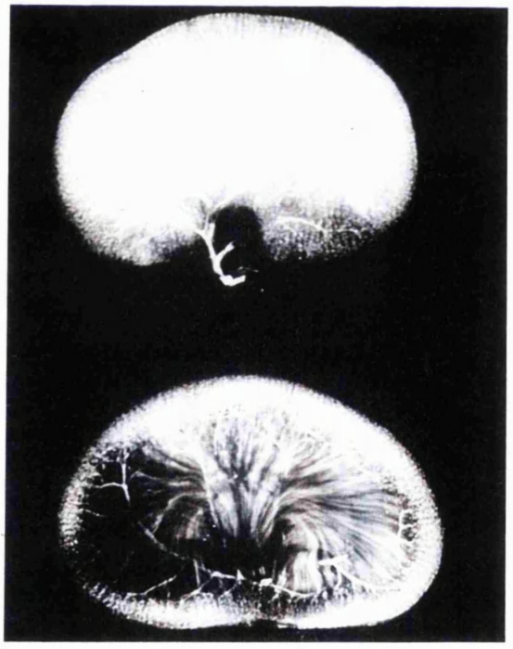

4.3

Plates 4.1, 4.2 and 4.3:
Representative barium sulphate angiograms of halved kidneys (top) and 2 mm thick renal sections (bottom) in (1) an unstored untransplanted kidney (Group 3); (2) a transplanted 72 h stored, 1 h reperfused kidney (Group 4); (3) a transplanted 72 h stored 3 h reperfused kidney (Group 4).

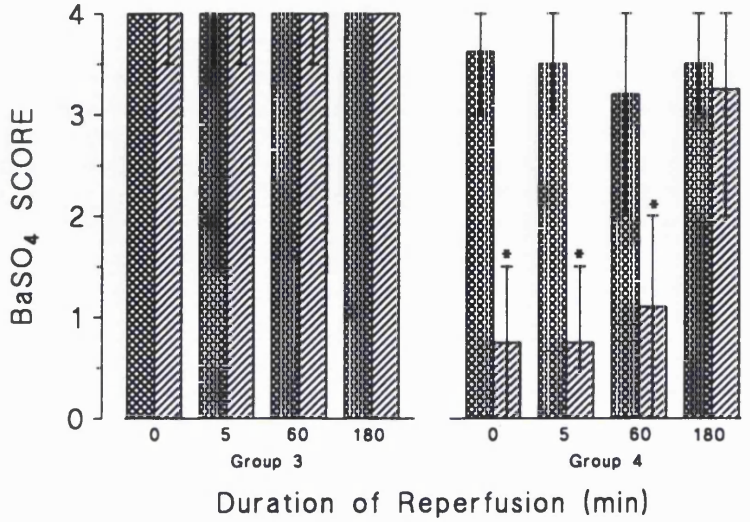

Fig 4.7 Mean and range barium sulphate scores in Group 3 (unstored) and Group 4 (72 h stored) kidneys. The angiograms (n=4 for each time point) were scored blind on a scale of: 0 (no perfusion); 1 (minimal perfusion); 2 (patchy perfusion); 3 (wide-spread perfusion); and 4 (normal perfusion) in both the cortex (checked bars) and medulla (hatched bars); *$p<0.05$, Mann-Whitney U-test. Unstored kidneys are well perfused throughout the duration of reperfusion, whereas stored kidneys are poorly perfused in the medulla for the first 1-3 h but well perfused in the cortex throughout the procedure.

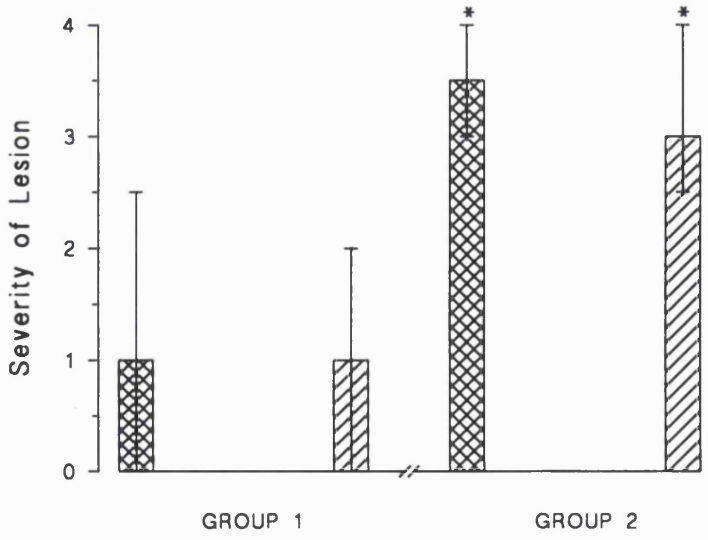

Fig 4.8 Mean and range scores (n=6) for cortical intracellular oedema (checked bars) and medullary congestion (hatched bars) in Groups 1 (unstored) and 2 (72 h stored). Renal sections were scored blind on a scale of: 0 (no damage); 1 (minimal damage); 2 (mild damage); 3 (moderate damage); and 4 (severe damage). *$p<0.05$, Mann Whitney U-test. Both oedema and congestion are significantly worse in stored kidneys

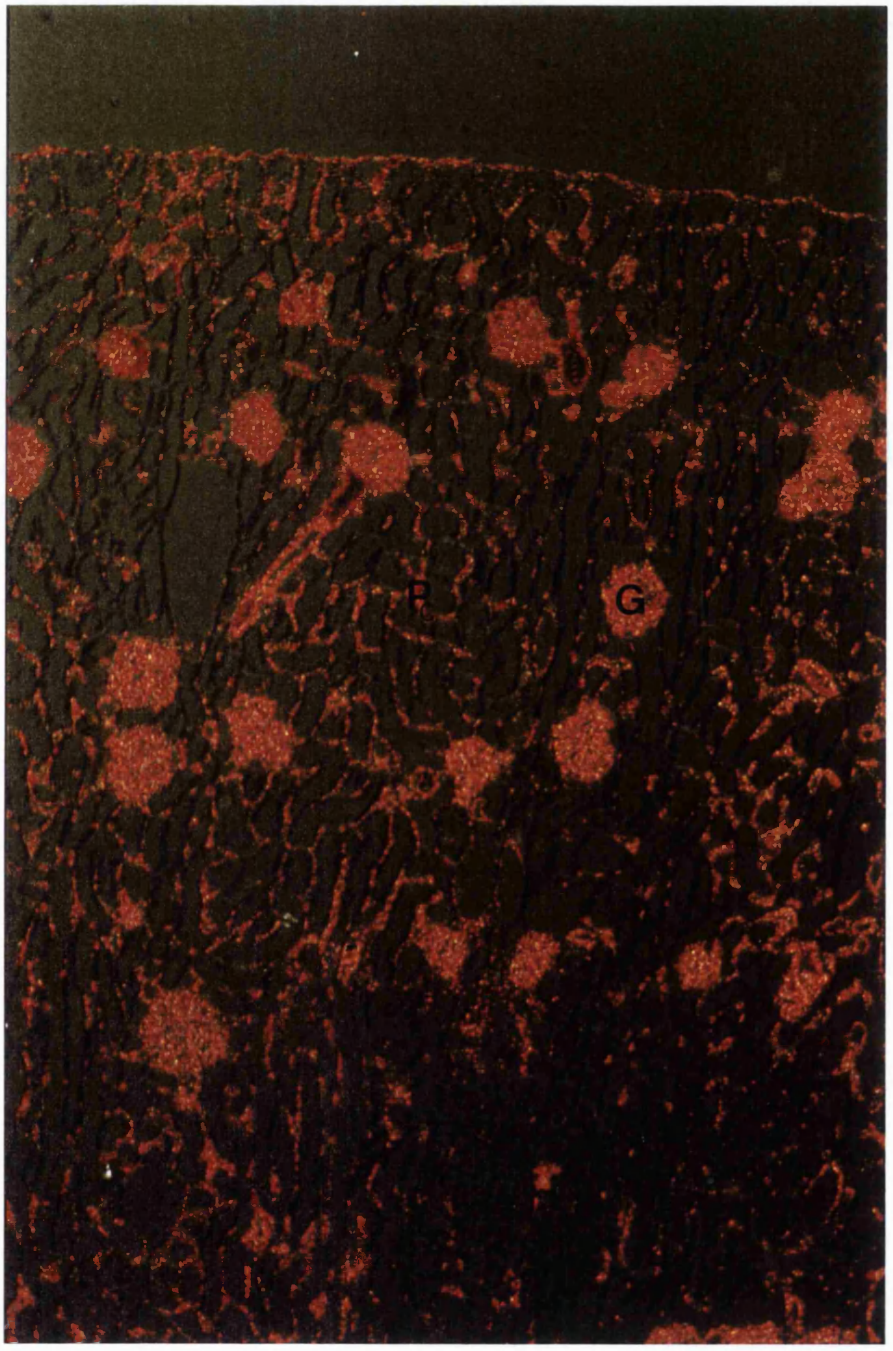

Plate 4.4: Dispersal of barium sulphate (viewed under polarized light) in the cortex of an unstored, 5 min reperfused kidney (Group 3), after staining with sodium rhodozinate. (magnification x 60). The stain picks out the glomeruli (G) and peritubular capillaries (Pc) of a well-perfused renal cortex with great clarity.

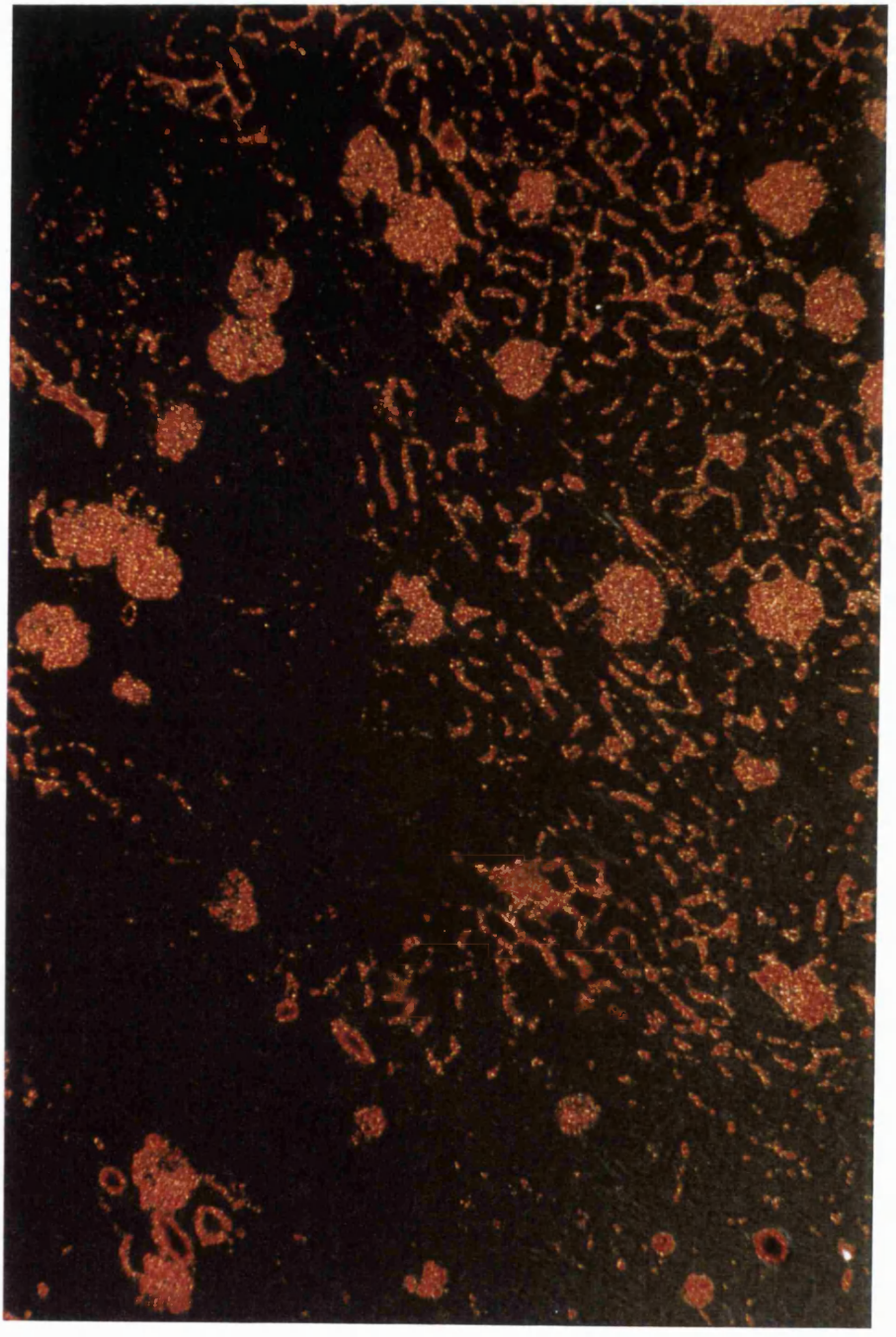

Plate 4.5: Dispersal of barium sulphate in the cortex of a 72 h stored, 5 min reperfused kidney (Group 4) after staining with sodium rhodozinate and viewed under polarized light. (magnification x 60). Areas of unreperfused tissue are visible in the deeper cortex.

4.5 Discussion

The results demonstrate that NIRS can be used to monitor changes in renal haemoglobin oxygenation kinetics following hypothermic storage and transplantation. When used in transmission mode, NIRS measures changes in haemoglobin concentration across both the cortex and medulla. Since the optical pathlength factor due to scatter in renal tissue has not been established, changes in haemoglobin concentration measured in this chapter are relative. However, as the two groups of kidneys were of similar size and dimensions and were subjected to the same treatments (with the exception of storage time) and as it has previously been shown that the optical pathlength is not significantly affected by gross differences in haemoglobin oxygenation (Cope *et al.*, 1988), comparison between the two groups of kidneys is justified. This premise is supported by the fact that the mean [HbT] and the range of SEM values for [HbT] were similar in both groups (Fig 4.5) despite large differences in haemoglobin oxygenation.

Reperfusion of Group 1 kidneys resulted in rapid increases in [HbO_2] within 1 min (Fig 4.3) followed by a sharp decrease from 1494 ± 138 μM at 1 min to 1077 ± 224 μM at 3 min. However, [HbO_2] had recovered by 20 min and did not change significantly thereafter. Group 1 [Hb] increased at a slower rate and had plateaued by 3 min (Fig 4.4). The abrupt fall in [HbO_2] during the second and third minutes of reperfusion was accompanied by a less dramatic reduction in [HbT] (Fig 4.5) and a small increase in [Hb] (Fig 4.4), implying that an initial reactive hyperaemia (signified by the fall in [HbT]) was associated with low tissue pO_2 in the renal parenchyma (signified by the larger fall in [HbO_2]). These changes are expected as a normal consequence of warm ischaemia and oxygen debt during the transplant procedure.

The rates and the magnitude of changes in [HbO_2] in the first 5 min of reperfusion of Group 2 kidneys were less than Group 1 but the only significant difference ($p<0.05$) occurred at 1 min and the changes in NIRS parameters were essentially similar in the two groups (Fig 4.3). The slower rate of increase of [HbO_2] (and [HbT]; Fig 4.5) in the first 1 min of reperfusion is suggestive of greater vasoconstriction or vasospasm in the stored kidneys. Afferent and efferent arteriolar vasoconstriction has been reported in several models of renal ischaemia and reperfusion (Klausner *et al.*, 1989; Chan *et al.*, 1994) and may account for the modest decreases previously reported in cortical bloodflow after ischaemia; cortical, unlike medullary bloodflow is not affected by haemodilution (Hellberg *et al.*, 1991).

In this study, vasoconstriction appeared to be a transient response to reperfusion (or a delayed recovery from extended hypothermia) since Group 2 [HbO_2] levels were not significantly different from Group 1 between 2 and 10 min of reperfusion and [HbT] remained similar in both groups

throughout the 3 h of reperfusion. The sharp drop in Group 2 [HbO_2] after 2 min of reperfusion is therefore likely to have been a response to parenchymal ischaemia, as seen in Group 1 kidneys, rather than a result of vasoconstriction. Unlike Group 1 kidneys however, there was no decrease in [HbT] corresponding to the drop in [HbO_2] (Fig 4.5). It is possible that early vasoconstriction precluded a reactive hyperaemia in Group 2 or that the sustained rise in [Hb] after 3 min of reperfusion (Fig 4.4) masked any cortical hyperaemia. This sustained increase in [Hb] may have been partly a result of prolonged ischaemia in Group 2 (with greater oxygen extraction in the more ischaemic group) but is also likely to be a function of developing vascular congestion in the medulla. This phenomenon is sometimes referred to as medullary hyperaemia (Brezis *et al.*, 1984; Yamamoto *et al.*, 1984; Mason, 1988). However, trapping of erythrocytes in the outer zone of the medulla is a pathological development rather than genuine reactive hyperaemia.

That the sustained rise in [Hb] during the first 10 min of reperfusion does indeed correlate with the development of vascular congestion in the medulla is confirmed by barium sulphate angiographical analysis of intra-renal perfusion (Fig 4.7). *Ex vivo* barium sulphate angiography does not necessarily completely reflect distribution of blood flow within the kidney. Rather, it gives an indication of vascular resistance (Hollenberg *et al.*, 1968) as the barium sulphate suspension was infused at a maximum perfusion pressure of 90 mm Hg and in a non-pulsatile manner. Moreover, barium sulphate particles, although of similar size to erythrocytes, lack their plasticity and are more likely to become lodged in the glomeruli or the peritubular capillaries. Nevertheless, areas of tissue well perfused with barium sulphate are likely to have been well perfused with blood during reperfusion. Thus, cortical perfusion appears to have been normal in Group 4 kidneys throughout the period of reperfusion (Fig 4.7). On the other hand, it is likely that medullary perfusion was under-estimated by angiography. After 72 h of storage and before reperfusion, medullary vascular resistance was sufficiently high to prevent perfusion with barium sulphate (Fig 4.7, t=0). During reperfusion, this situation persisted for at least the first 60 min. Nevertheless, both histological analysis and NIRS demonstrated that blood was able to penetrate (if not drain from) the medulla during the first 10 min of reperfusion.

After 30 min of reperfusion of Group 2 kidneys there were decreases in both [Hb] ($p<0.005$) and [HbT], but no significant change in [HbO_2]. A similar reduction in [Hb] after 45 min of reperfusion has been reported using NIRS in a renal model of warm ischaemia and reperfusion (Vaughan *et al.*, 1995). As there was no fall in [HbO_2] (Fig 4.3) it is likely that the decrease in [Hb] was a result of clearance of desaturated blood from the renal medulla. Despite this, there was no significant increase in medullary barium sulphate perfusion even after 1 h of reperfusion. Here again, it is likely that the angiographical studies under-estimated medullary perfusion at this time point for the reasons

discussed above. After 3 h of reperfusion, vascular resistance in the medulla had dropped sufficiently to allow nearly normal barium sulphate perfusion (Plate 4.3 and Fig 4.7). Thus, it seems likely that tubular swelling in the outer medulla diminished over the course of reperfusion, resulting in a fall in vascular resistance and recovery from medullary congestion. The fact that clearance of congestion was not accompanied by an increase in trans-renal SaO_2 presumably reflects the severity of parenchymal ischaemia in the medulla, and this is underlined by the poor histopathological appearance of the medulla even after 3 h of reperfusion. The stability of renal SaO_2 and of cortical barium sulphate perfusion over this time suggests that cortical reperfusion was not greatly affected by shifts in medullary perfusion. This inference is in agreement with Hellberg and co-workers (1991), who demonstrated the independence of bloodflow through the renal cortex and medulla following warm ischaemia.

4.6 Conclusions

(i) Vascular resistance was high in the medulla even before reperfusion, probably as a result of ischaemic swelling of the mTAT and the *pars recta* of the proximal tubules

(ii) Medullary vascular congestion developed during the first 10 min of reperfusion. That haemoglobin in the trapped erythrocytes became severely desaturated over this time was confirmed by NIRS

(iii) Medullary congestion began to clear after 30 min of reperfusion but this was not accompanied by an increase in renal haemoglobin saturation, suggesting that tissue pO_2 in the medulla remained very low

(iv) Cortical vascular resistance was not significantly different from controls, nor were the haemoglobin oxygenation kinetics in Group 2 significantly different from Group 1 during the first 5 min of reperfusion even across the entire kidney and despite the development of medullary congestion. Thus, it seems likely that cortical bloodflow and haemoglobin oxygenation were very similar in the first 5 to 10 min of reperfusion and probably thereafter.

CHAPTER 5

IN VIVO MEASUREMENTS OF MITOCHONDRIAL NADH FLUORESCENCE AND CHANGES IN CYTOCHROME OXIDASE OXIDATION DURING REPERFUSION

The studies presented in this chapter are based on a paper published in:
Kidney International 1994; 45: 1489-1496.

5.1 Introduction

In Chapter 4, the haemodynamic changes occurring during 3 h of reperfusion in unstored and 72 h stored autografted kidneys were defined. It was shown using NIRS that medullary erythrocyte congestion, as reflected by profound haemoglobin desaturation, developed during the first 10 min of reperfusion of 72 h stored kidneys and began to clear after only 30-60 min. However, the haemoglobin oxygenation kinetics during reperfusion of stored kidneys were not significantly different from unstored controls during the first 5 min of reperfusion even across the entire kidney and despite the development of medullary congestion. Furthermore, barium sulphate angiographical studies demonstrated that cortical vascular resistance remained low throughout the period evaluated. The severity of medullary congestion has been shown to correlate with renal dysfunction (Mason, 1988) but it is not known how profoundly changes in haemoglobin oxygenation affect mitochondrial function *in vivo*.

During organ storage, mitochondrial electron transfer is rapidly inhibited, resulting in depletion of ATP, a net breakdown of adenine nucleotides to non-phosphorylated metabolites and the accumulation of reduced pyridine nucleotides (Calman *et al.*, 1973). These changes result in a loss of cellular homeostasis involving a fall in intracellular pH (Sehr *et al.*, 1979; Fuller *et al.*, 1988) mitochondrial calcium loading and cellular swelling (Hardy *et al.*, 1991). Post-ischaemic mitochondrial function depends on a combination of factors:

(i) Preservation of inner mitochondrial membrane integrity and the structure and activities of the respiratory chain complexes I to IV during the ischaemic period (Taegtmeyer *et al.*, 1985; Hardy *et al.*, 1991)

(ii) Free radical mediated auto-inactivation of respiratory chain complexes as a result of electron leakage during reperfusion (Ambrosio *et al.*, 1993)

(iii) Preservation of cellular integrity and homeostasis, particularly calcium homeostasis, during both ischaemia and reperfusion (Hardy *et al.*, 1991)

(iv) Sufficient levels of NADH, ADP and oxygen to allow efficient mitochondrial phosphorylation upon and during reperfusion (Belzer and Southard, 1988).

In recent studies, the activities of respiratory chain complexes I to IV in mitochondria isolated from perfused rat hearts subjected to global ischaemia or anoxic perfusion prior to ischaemia were investigated (Veitch *et al.*, 1992). The results indicated that differences in the sensitivity of these complexes to ischaemic damage were dependent upon the duration of the ischaemic episode and the presence of oxygen. The most sensitive site was complex I (Veitch *et al.*, 1992). Similar findings have been reported by others (Malis and Bonventre, 1986; Hardy *et al.*, 1991; Sammut *et al.*, 1995) in isolated mitochondria and by Ambrosio and colleagues (1993) in Langendorff perfused hearts. However, the extent to which these results may be extrapolated to the *in vivo* setting or from one organ to another is uncertain.

For a respiratory component to be used as an early indicator of ischaemia-reperfusion damage *in vivo* it must be:

- Of mitochondrial origin
- Responsive to decreasing or low pO_2
- Measurable by non-invasive means.

There are two components of the respiratory chain that satisfy these requirements: mitochondrial NADH and cytochrome oxidase (cyt aa_3), the terminal member of the respiratory chain (see Fig 1.5). Chance and Williams (1955) showed that direct *in vivo* measurements of fluorescence could be made from intracellular pyridine nucleotides in brain and kidney, and the possible importance of these measurements as indicators of intracellular hypoxia has been emphasised (Franke *et al.*, 1976; Mayevesky *et al.*, 1983; Mayevesky 1984; Mayevesky *et al.*, 1990). It has been shown that fluorescent signals from cytosolic NADH are negligible compared with those from the mitochondrial pool as a result of quenching of fluorescence by cytosolic glyceraldehyde 3-phosphate dehydrogenase

(O'Connor 1977). More recently, the use of pyridine nucleotide fluorescence measurement to determine changes in mitochondrial and cytosolic redox status in perfused rat livers has been reported (Okamura *et al.*, 1992) and was found to correlate closely with energy charge and mitochondrial phosphorylative activity (Okamura *et al.*, 1992; Tokunaga *et al.*, 1987).

These *in vivo* measurements may be extended by measurements of changes in cyt aa_3 oxidation using NIRS (see Chapters 2 and 4). Cytochrome oxidase is composed of 13 protein subunits, 2 haem units and 2 copper atoms (Cu_A and Cu_B)(Malmstrom 1990). Absorption of near infrared light by cyt aa_3 occurs almost entirely at the Cu_A centre. The oxidised form of Cu_A has a characteristic spectrum, whereas the reduced form has no distinguishable absorption (Beinert *et al.*, 1980). Recent studies have shown that spectra measured *in vivo* and *in vitro* are identical (McCormick *et al.*, 1993). The concentration of oxidised Cu_A depends on the supply of oxygen, the availability of respiratory electrons and the level of the mitochondrial proton-motive force, which is a function of the rate of cellular ATP utilization (Rich *et al.*, 1988; McCormick *et al.*, 1993). All three factors are likely to be affected by ischaemia and reperfusion. Thus, measurement of changes in both mitochondrial NADH fluorescence and cyt aa_3 oxidation during *in vivo* reperfusion of autografted kidneys should give an indication of mitochondrial respiratory chain function.

5.2 Objective

The studies presented in this chapter were designed to determine the characteristic changes in mitochondrial NADH fluorescence (using surface fluorescence spectroscopy) and cyt aa_3 oxidation (using NIRS) occurring upon and during 3 h of *in situ* reperfusion of unstored and 72 h stored autografted kidneys.

5.3 Methods

5.3.1 Methodology

A total of 16 female NZW rabbits (2.5 kg) in 2 groups (see below) were anaesthetised with an i.m. injection of ketamine (50 mg/kg) and xylazine (8 mg/kg), trachaeotomized and artificially ventilated with a 50 : 50 oxygen : nitrous oxide mixture for periods of up to 5 h (see Chapter 2 for full details). Direct non-invasive measurements of changes in mitochondrial NADH fluorescence and cyt aa_3 oxidation were made in both groups using surface fluorescence spectroscopy and NIRS over 3 h of reperfusion. Renal morphology was evaluated by light microscopy.

5.3.2 Experimental Groups

Group 1: Freshly nephrectomized right kidneys were flushed with 40 ml of ice cold (0-2^{0}C) HCA via the renal artery and autografted immediately into the left renal bursa using standard microsurgical techniques. The contra-lateral kidneys were removed during the autograft operation and flushed with ice cold HCA (0-2^{0}C) for measurements of *ex vivo* NADH fluorescence (see below).

Group 2: Kidneys were flushed as in Group 1 and then stored in HCA surrounded by ice to maintain a temperature of 0-2^{0}C for 72 h before autografting. The contra-lateral kidneys were removed during the autograft operation and flushed with ice cold HCA (0-2^{0}C) for measurements of *ex vivo* NADH fluorescence (see below).

5.3.3 Experimental Protocol for Surface Fluorescence Measurements

The intensity of NADH fluorescent emission, and spectral properties, were measured in:

(i) *Ex-vivo* control freshly harvested flushed contra-lateral kidneys, stored in HCA at 0-2^{0}C on ice for up to 90 min (Group 1 control) and after 72 h of storage (Group 2 control)

(ii) *In situ* Group 1 kidneys, prior to transplantation and reperfusion with blood

(iii) *In situ* Group 2, 72 h stored kidneys prior to transplantation and reperfusion with blood.

The change in the intensity of the NADH emission was measured in both experimental Groups in response to:

(i) Reperfusion measured in both Groups up to 3 hours post-transplant at 5, 15, 45, 60 min and at 2 and 3 h

(ii) Reperfusion in which continuous measurements of NADH fluorescence intensity were made by scanning up to 90 min at 1000 nm/min between 366 and 600 nm in an additional 3 unstored and stored transplants to ensure that any variation in fluorescence intensity was not due to movement artefact (positional) or heterogeneity of NADH due to mitochondrial clustering (Franke, Barlow and Chance, 1976)

(iiii) Alterations in the inspired FiO_2

(iv) Rapid intravenous infusion of sodium pentobarbitone (200 mg/kg in less than 5 sec) which inhibits the respiratory chain at complex I NADH dehydrogenase (Renault, 1987). NADH fluorescence was monitored for a further 20 minutes.

Percentage changes in NADH fluorescence from baseline were calculated. The relative fluorescence intensity of NADH at 480 nm after subtraction of baseline fluorescence at 420 nm prior to reperfusion was taken to represent 100% of NADH fluorescence, and percentage changes during and after reperfusion were calculated relative to this value.

5.3.4 Experimental Protocol for NIRS Measurements of Cyt aa_3

Concentration changes in HbO_2, Hb and oxidized cyt aa_3 were continuously measured in *in situ* kidneys during reperfusion in both groups for 3 h (see Chapters 2 and 4). Baseline measurements were made for 5 min prior to reperfusion.

5.4 Results

5.4.1 Surface Fluorescence Measurements of Mitochondrial NADH

The relative fluorescence emission of control kidneys which had been removed and flushed with HCA and stored on ice for up to 90 min did not significantly change after storage (2.97 ± 0.013 immediately after flushing compared with 3.03 ± 0.09 after 90 min on ice (mean ± SEM, n=9 estimates) and there were no significant differences between the relative fluorescence intensity of the 2 groups *in situ* before reperfusion; 2.85 ± 0.196 (Group 1, n=9 kidneys) and 2.94 ± 0.26 (Group 2, n=9 kidneys) (Fig 5.1). During reperfusion, an increase in fluorescence emission of NADH at 470 nm from the surface of the perfused rabbit kidney when excited at 366 nm was obtained in response to decreasing the systemic pO_2 from 21 to 5 Kpa (Fig 5.2).

In Table 5.1 is shown the percentage change in fluorescence from the pre-reperfusion values during the initial phase (0-20 min) after reperfusion of Group 1 and Group 2 kidneys. There were no significant differences between the percent oxidation observed in the 2 Groups; 82.85% ± 11.29% (Group 1) compared with 89.85% ± 11.92% (Group 2). In Fig 5.3 are shown emission spectra obtained by continuous scanning of NADH fluorescence pre- and post-reperfusion in a Group 1 kidney. Immediate oxidation of between 70% and 100% of the total NADH occurred within 1 min (Table 1) and values thereafter oscillated within this range. In comparison, the magnitude and rate of oxidation of NADH was slightly slower in some Group 2 kidneys (Fig 5.4) but despite this nearly 100% of the NADH became oxidised over the first few minutes of reperfusion. The slower rate of oxidation may have been related to the slower rate of reperfusion observed in some Group 2 kidneys (see also Chapter 4).

5.4.2 Effect of Sodium Pentobarbitone Infusion

A broad fluorescence emission maximum of NADH (excitation wavelength 340 nm) was measured in both *ex vivo* and *in situ* kidneys, which shifted to lower wavelengths upon sodium pentobarbitone infusion, the shift being consistent with an altered NADH fluorophore (Figs 5.3 and 5.4). In Group 1 kidneys, infusion of sodium pentobarbitone 200 mg/kg (< 5 sec) resulted in rapid regeneration of NADH in all 9 kidneys within 1 min, as would be expected upon inhibition of complex I NADH dehydrogenase (Renault *et al.*, 1987) (Table 1). In Group 2 kidneys, sodium pentobarbitone infusion caused a decreased rate and magnitude or no NADH regeneration in 5 of 7 kidneys within the monitoring period of 20 min (Table 1). In a single kidney, sodium pentobarbitone infusion stimulated an increase in NADH fluorescence to a maximum of 37% of the pre-reperfusion value after 5 min, whereafter fluorescence remained relatively constant. In the final kidney NADH fluorescence increased to a relative intensity comparable with those observed in Group 1 kidneys. It is notable that this kidney was minimally oedematous and and displayed normal cyt aa_3 responses (see below).

5.4.3 NIRS Measurements of Cyt aa_3 Oxidation

In Fig 5.5 is shown a representative plot of change in concentration of HbO_2, Hb and cyt aa_3 following reperfusion of a Group 1 kidney. The initial stages of reperfusion resulted in a large increase in [HbO_2] and in [Hb], a net increase in the oxygenation index and a small oxidation of cyt aa_3. However, as [HbO_2] fell at the end of the reactive hyperaemia phase cyt aa_3 became reduced. In all the unstored transplanted renal grafts cyt aa_3 became steadily oxidised over 3 h of reperfusion to approximately 50% of the change observed in the initial stages of reperfusion (Table 5.1). The reduction of cyt aa_3 in all 6 kidneys in Group 1 correlated with minimal oedema and with the expected response to sodium pentobarbitone, NAD^+ reduction. In Group 2, there were no significant changes in cyt aa_3 oxidation compared with baseline in 4 of 5 kidneys and this was associated with suppressed NADH regeneration upon inhibition of NADH dehydrogenase by sodium pentobarbitone. In a single Group 2 kidney, oxidation of cyt aa_3 occurred slowly over 2 to 3 h. Regeneration of NADH was more pronounced upon infusion of sodium pentobarbitone and histological analysis confirmed that the histopathological changes were relatively mild (Table 5.1).

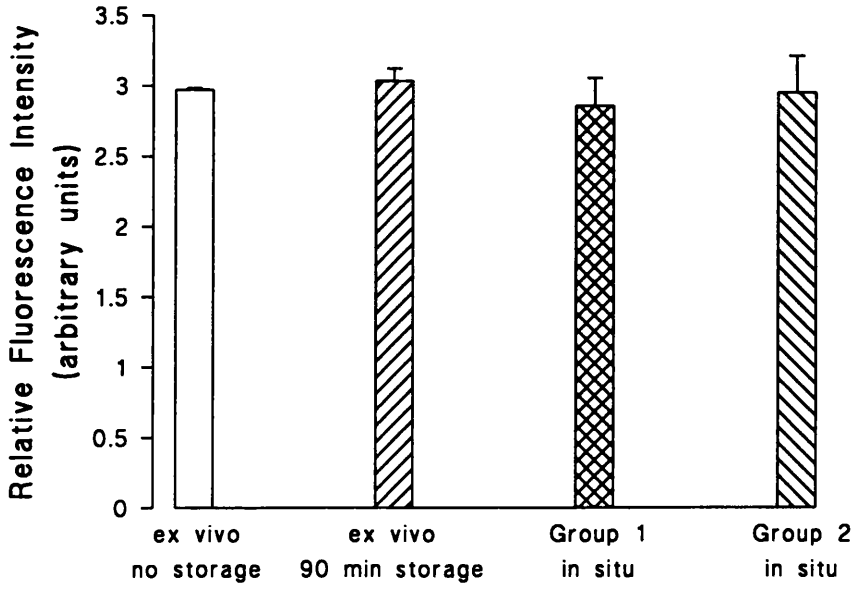

Fig 5.1 Mean and SEM changes in relative fluorescence intensity of mitochondrial NADH from flushed kidneys prior to reperfusion (n=6). Storage of organs for up to 72 h did not affect the intensity of NADH fluorescence.

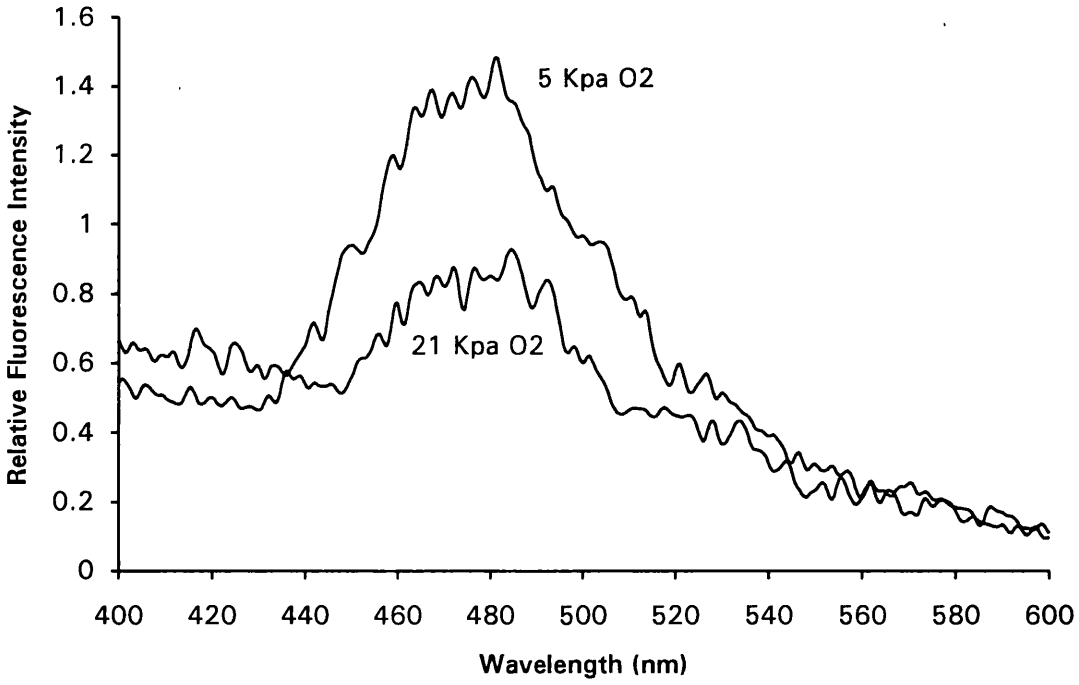

Fig 5.2 Change in relative fluorescence intensity of mitochondrial NADH in an unstored transplanted kidney reperfusing *in situ* in response to a change in arterial pO_2 from 21 Kpa to 5 Kpa. The decrease in pO_2 resulted in an approximate doubling of NADH fluorecence intensity.

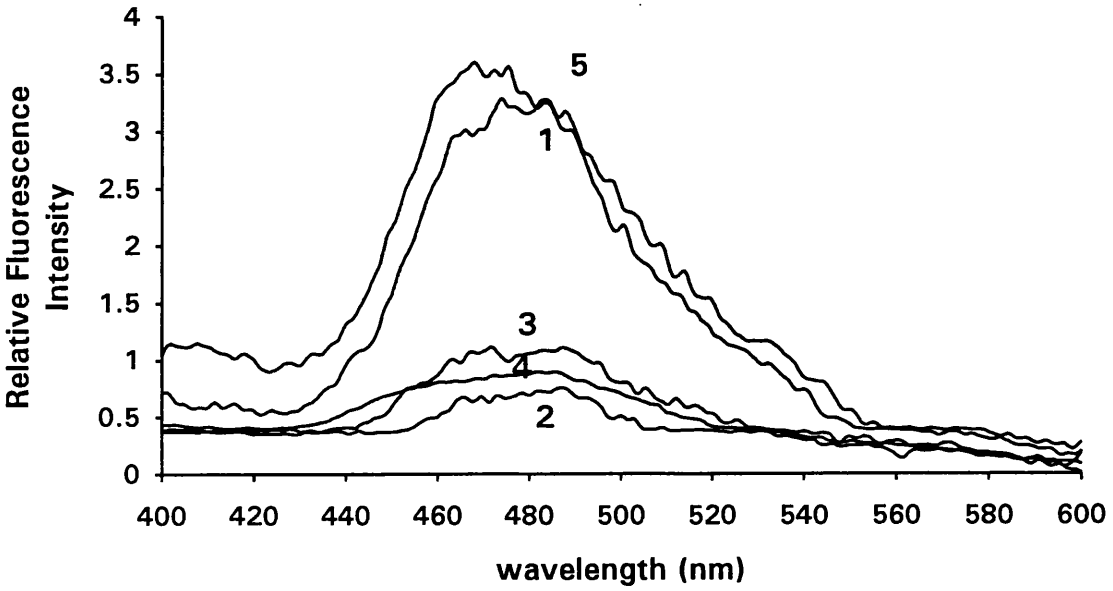

Fig 5.3 *In vivo* surface fluorescence measurements of NADH in a Group 1 (unstored transplanted kidney) showing rapid oxidation of NADH upon reperfusion and complete regeneration of NADH after inhibition of the respiratory chain with sodium pentobarbitone. 1: Pre-reperfusion; 2: 1 min after reperfusion; 3: 12 min after reperfusion; 4: 60 min after reperfusion; 5: 5 min after sodium pentobarbitone infusion (200 mg/kg).

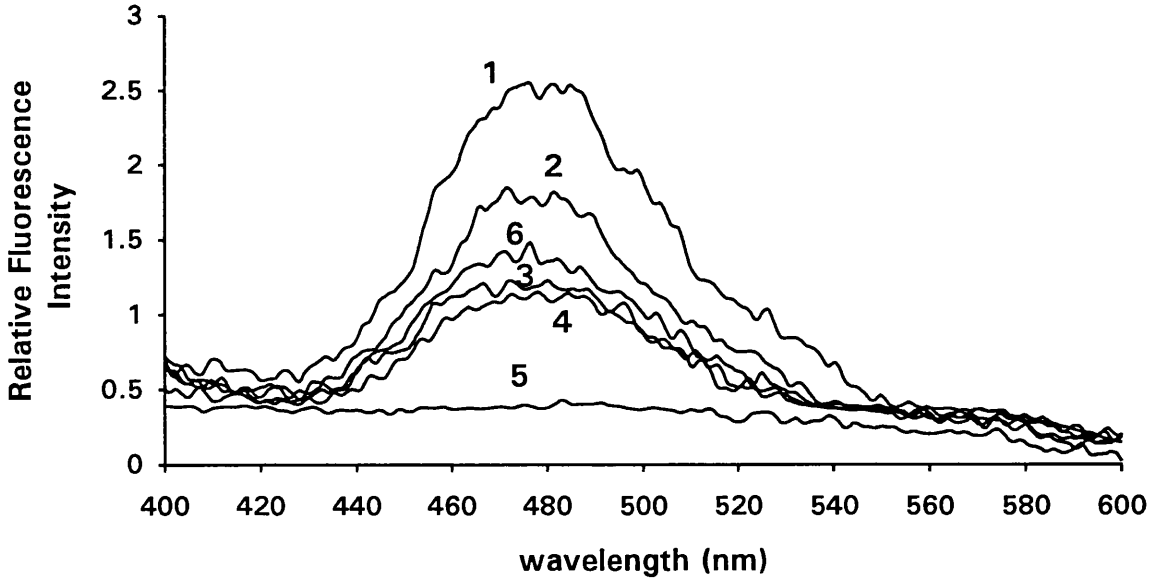

Fig 5.4 *In vivo* surface fluorescence measurements of NADH in a Group 2 (72 h stored transplanted kidney), showing slower but ultimately complete oxidation of NADH upon reperfusion and incomplete regeneration of NADH after inhibition of complex I. 1: Pre-reperfusion; 2: 1 min after reperfusion; 3: 2 min after reperfusion; 4: 4 min after reperfusion; 5: 6 min after reperfusion: and 6. 5 min after sodium pentobarbitone infusion.

Table 5.1 **Correlation between cyt aa_3 oxidation, NADH fluorescence and morphology**

Group	Maximal redox change in cyt aa_3 upon reperfusion (μmol)	% NADH oxidized upon reperfusion	% of pre-reperfusion NADH formed upon sodium pentobarbitone infusion	Severity of cortical oedema
1	−58.3	90	95	mild-moderate
	−60.0	72	76	mild
	−49.7	96	69	absent
	−62.0	70	70	absent
	−103.1	87	70	mild
	−65.3	NIRS only	NIRS only	NIRS only
	SF only	72	70	SF only
	SF only	88	100	SF only
	SF only	95	80	SF only
2	nsd	96	0	severe
	−16.5 ± 0.238	67	82	moderate
	nsd	96	0	severe
	nsd	84	8	severe
	nsd	86	0	moderate
	SF only	100	0	SF only
	SF only	100	37.5	SF only

nsd: no significant difference.

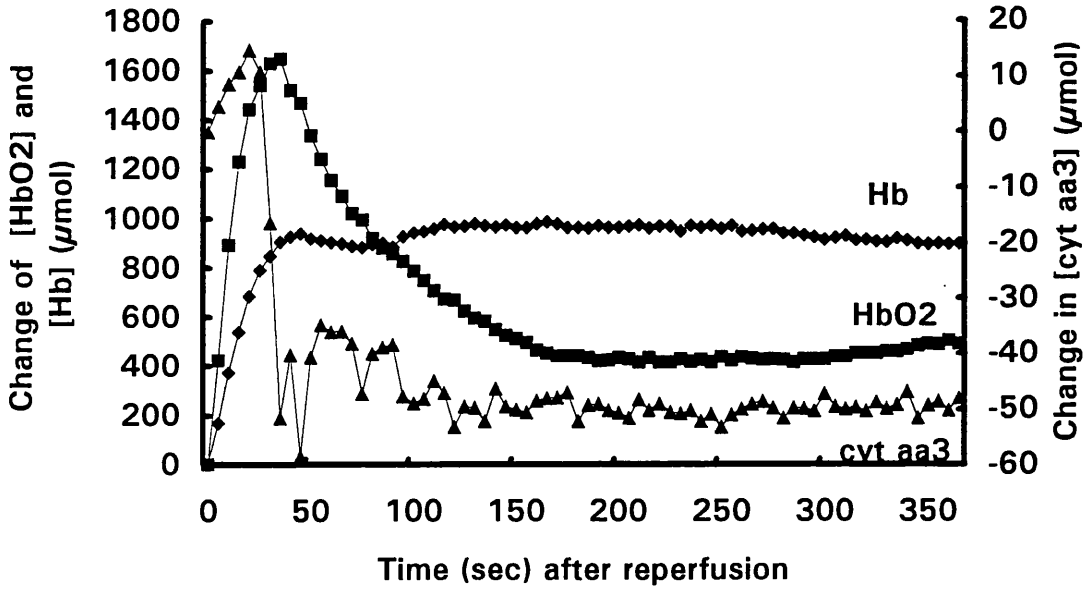

Fig 5.5 Changes in concentration of HbO_2, Hb and cyt aa_3 upon reperfusion of a Group 1 (unstored) autografted kidney. The haemodynamic changes upon reperfusion were rapid and the sudden reduction in cyt aa_3 after 0.5 min of reperfusion, corresponding to the end of the initial hyperaemic period was characteristic.

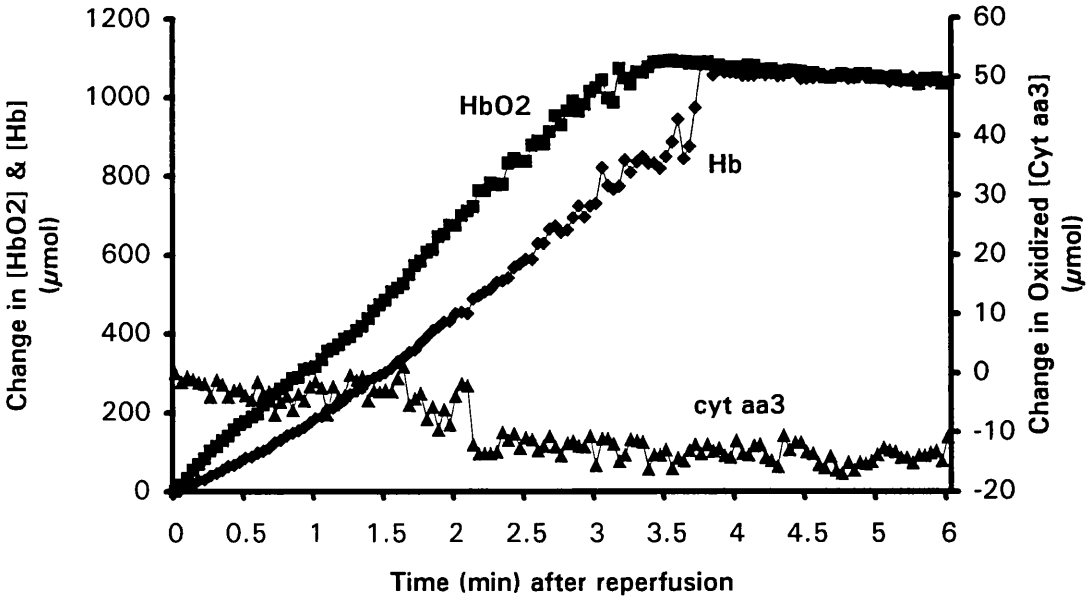

Fig 5.6 Change in concentration of HbO_2, Hb and cyt aa_3 upon reperfusion of a Group 2 (72 h stored) autografted kidney. The haemodynamic changes upon reperfusion were much slower and there was no apparent change in cyt aa_3 oxidation (note the difference in scale between Figs 5.5 and 5.6).

5.4.4 Histological and Functional Examination of Kidneys

In Group 1 kidneys there was very little oedema. In isolated instances there was focal mild to moderate intracellular oedema, especially of the proximal tubular cells. There was no congestion, haemorrhage or inflammatory infiltrate (neutrophils) in any specimen (Plate 5.1). In Group 2 kidneys, there was severe cortical intracellular oedema in almost every instance but no cortical congestion (Plate 5.2). In the medulla, there was moderate interstitial oedema and congestion. Estimations of renal function following 72 h storage and transplantation were obscured by purely mechanical factors. While it is true that the glomerular filtration rate correlates with functional viability, severe medullary congestion can entirely abolish urine production even if tubular or glomerular function is unimpaired. Thus after 72 h storage and transplantation, urine production was negligible for the first 1-2 h of reperfusion and so estimations of GFR were not possible and must be assumed to be zero. Urine production tended to increase after this period despite no apparent change in respiratory chain function. These changes correlated with the clearance of medullary congestion as measured using NIRS and evaluated by barium sulphate angiography (see Chapter 4).

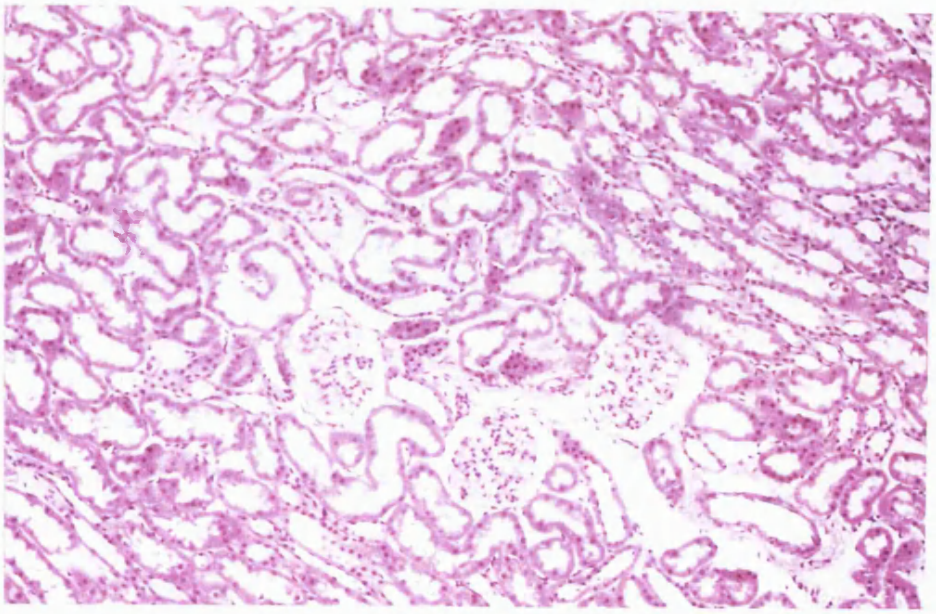

Plate 5.1 **Light micrograph of the renal cortex showing minimal intracellular oedema in a Group 1 (unstored transplanted) kidney (magnification x 100).**

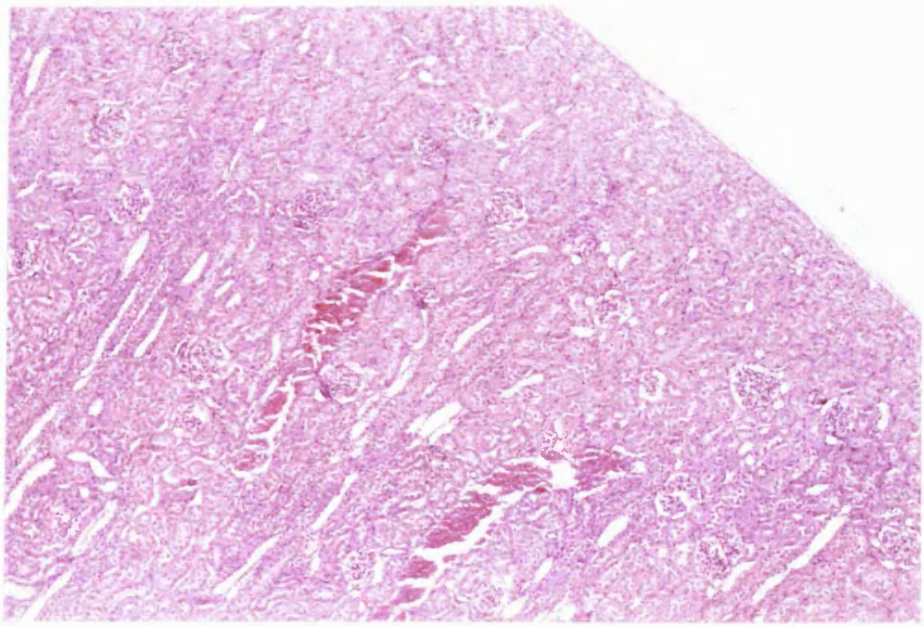

Plate 5.2 **Light micrograph of the renal cotex showing severe cortical intracellular oedema in a Group 2 (72 h stored transplanted) kidney (magnification x 40).**

5.5 Discussion

The NADH emission spectra measured in these studies in the rabbit renal cortex were similar to characteristic NADH fluorescence emission spectra reported by others *in vitro* and *in vivo* in rat brain and kidney when excited at 340 nm and at 366 nm (Franke, Barlow and Chance, 1976; Mayevesky *et al.*, 1983; Mayevesky, 1984; Mayevesky *et al.*, 1990). *In situ* NADH measurements made before reperfusion were not significantly different between the two groups. It is therefore unlikely that fluorescence of NADH was altered as a result of enhancement or quenching during storage or loss of pyridine nucleotides. Although nucleotide levels in tissue homogenates were not measured in this study, there are several factors which support the view that the fluorescent emission can be attributed to NADH. Most importantly, there are few other fluorophores whose emission characteristics are identical to those of NADH, which have oxygen-dependent emission spectra and which are responsive to sodium pentobarbitone, which inhibits NADH dehydrogenase at complex I, thereby stimulating a selective increase in NADH fluorescence (Renault, 1987). The maximum NADH emission measured in revascularised unstored transplanted kidneys after either low $p0_2$ or sodium pentobarbitone infusion was not significantly different from the NADH emission measured during storage in the absence of haemoglobin. This suggests that the presence of blood did not affect the maximum measured NADH signal in these experiments. Similar findings have been reported by others (Kobayashi *et al.*, 1971; Franke, Barlow and Chance, 1976).

The results presented in this chapter demonstrate that it is possible to make both discrete and continuous measurements of NADH fluorescence in the *in situ* transplanted kidney. In all kidneys there were large NADH peaks before reperfusion which disappeared in each case within a few minutes of reperfusion. In Group 1 kidneys, the oxidation of NADH occurred within 1 min of reperfusion, and thereafter surface fluorescence measurements of NADH were responsive to fluctuations in systemic pO_2 (Fig 5.2). Similar responses were noted by Franke and colleagues (1976) who correlated surface fluorescence monitoring of reduced pyridine nucleotides with the physiological function of *ex vivo* perfused rat kidneys during and following various hypoxic insults. The rate of oxidation of NADH upon reperfusion appeared to be slightly slower in Group 2 kidneys (in the 5 kidneys monitored continuously) and NADH oxidation appeared to be complete (Fig 5.4; Table 5.1). Moreover, in Group 2 kidneys there were few oscillations in NADH fluorescence intensity in response to minor alterations in pO_2 or vascular changes. These findings are suggestive but not definitive evidence of respiratory chain dysfunction *in vivo*.

The effect of sodium pentobarbitone administration was also quite distinct in the two groups. In Group 1 kidneys, rapid increases in the relative fluorescence intensity of NADH to pre-reperfusion

levels were observed within 1 min but there was typically little or no response to sodium pentobarbitone infusion in Group 2 kidneys. It is possible that this failure of most Group 2 kidneys to respond to infusion of sodium pentabarbitone was a result of circulatory defects preventing distribution of sodium pentobarbitone to the renal tubules of these kidneys. However, it has been shown that superficial glomerular blood flow is relatively unaffected by even severe ischaemic episodes (Mason, 1988) and the haemodynamic and angiographical data presented in Chapter 4, showing good cortical perfusion throughout the procedures, are consistent with this finding. Taken together therefore, these data strongly suggest that 72 h storage resulted in mitochondrial dysfunction.

In Group 1 kidneys, rapid oxidation of NADH upon reperfusion and oscillation of fluorescence intensity in response to fluctuations in pO_2 correlated with minimal histological change and consistent reductions in cyt aa_3 (which appeared to be associated with the end of an immediate hyperaemic phase; Fig 5.5). These reductions in cyt aa_3 imply that cyt aa_3 must have become hyperoxidised either during ischaemia or transiently upon reperfusion. Such hyperoxidation is in fact consistent with the known kinetics of oxidation of cyt aa_3 and similar patterns have been measured in anaesthetised rats in response to release of carotid occlusion (Wiemsperger *et al.*, 1981) and in cat skeletal muscle (Hampson and Piantadosi, 1986). In both cases, return to normal baseline conditions after hyperaemia was associated with a reduction of cyt aa_3

While the affinity of oxygen for cyt aa_3 is greater than that for Hb in the *in vitro* situation and cyt aa_3 is almost completely oxidised in the steady state *in vitro* (Chance and Williams, 1955; Piantadosi, 1989) it has been reported that cyt aa_3 is not normally fully oxidized *in vivo*, and values between 20% to 50% reduced have been reported in kidneys and other organs (Mills and Jobsis; 1972; Balaban and Sylvia, 1981; Atkins and Lankford 1991). In fact, oxygen concentration gradients occur normally in the kidney and substantial portions, particularly in the cortico-medullary junction, operate on the brink of hypoxia despite high arterial and venous pO_2 values (Leichtweiss *et al.*, 1969). Furthermore, the oxygen supply to mitochondria may be partly determined by mitochondrial clustering in renal tissue (Leichtweiss *et al.*, 1969). Such clustering could also contribute to a steady state reduction of mitochondrial cytochromes during normoxia.

In contrast, 4 of 5 Group 2 kidneys displayed no change in cyt aa_3 oxidation upon reperfusion. The single Group 2 kidney which did exhibit a similar cyt aa_3 response to Group 1 kidneys was also able to regenerate NADH upon sodium pentobarbitone infusion and was only moderately oedematous. Severe cortical oedema combined with medullary congestion in the early hours of reperfusion were shown in Chapter 3 to be associated with developing renal failure. In this chapter, a consistent

correlation was found between the NADH and cyt aa_3 responses and histological appearance. The fact that NADH regeneration did not generally occur in 72 h stored kidneys following pentobarbitone inhibition of NADH dehydrogenase at complex I suggests that mitochondrial dysfunction could be localized to complex I or result from substrate deficiency leading to complex I. Similarly, it has been observed that mitochondria isolated from perfused rat hearts subjected to global ischaemia and reperfusion were unable to metabolise NAD^+ linked substrates and the site of damage was shown to be complex I (Hardy *et al.*, 1991; Veitch *et al.*, 1992). It is probably not coincidental that the two main sites of mitochondrial damage during ischaemia, complexes I and III, are also the major sources of oxygen-derived free radical production during normal electron transfer in mitochondria *in vitro* (Cadenas *et al.*, 1977). The possibility that low molecular weight iron may play a role in catalysing the auto-inactivation of susceptible respiratory chain complexes via the Fenton reaction (see Chapter 1) forms the subject of the next chapter.

5.6 Conclusions

(i) Both surface fluorescence spectroscopy and near infrared spectroscopy were capable of detecting changes in concentration or redox state of respiratory chain components during *in vivo* reperfusion of autografted kidneys.

(ii) There was a good correlation between changes in NADH fluorescence and cyt aa_3 oxidation in unstored autografted kidneys in response to both reperfusion and sodium pentobarbitone infusion.

(iii) The responses of both NADH fluorescence and cyt aa_3 oxidation to reperfusion and pentobarbitone infusion in 72 h stored autografted kidneys were abnormal compared to controls, suggesting damage to the respiratory chain, or substrate deficiency leading to complex 1.

(iv) Poor respiratory chain responsiveness correlated with poor histological assessments of renal morphology and poor long term viability.

CHAPTER 6

THE EFFECT OF IRON CHELATION ON NADH FLUORESCENCE, LIPID PEROXIDATION AND RENAL FUNCTION FOLLOWING 72 H STORAGE

The studies presented in this chapter are based on a proceedings paper published in:
*Biochemical Society Transactions 1995; **23:** 524S,*
and a full paper submitted to Archives of Biochemistry and Biophysics.

6.1 Introduction

In Chapter 5, it was shown that changes in concentration of the respiratory chain components mitochondrial NADH and the oxidised form of cyt aa_3 could be measured non-invasively during *in situ* reperfusion of autografted kidneys using surface fluorescence spectroscopy and NIRS. A good correlation was demonstrated between changes in NADH fluorescence and in the redox state of cyt aa_3 in unstored transplanted kidneys. Hypothermic storage of kidneys for 72 h resulted in abnormal respiratory chain responses to both reperfusion and inhibition of complex I NADH dehydrogenase with sodium pentobarbitone. However, neither the cause nor the exact timing of mitochondrial dysfunction were established.

There is considerable *in vitro* evidence that mitochondrial function, following a period of anoxia, is impaired upon reoxygenation by free radical generation (Malis and Bonventre, 1986; Hardy *et al.*, 1991; Ambrosio *et al.*, 1993; Reinheckel *et al.*, 1995). Complexes I and III of the respiratory chain have been shown to be the major defective sites (Ambrosio *et al.*, 1993). Baker and Kalyanaraman (1989) demonstrated using direct EPR spectroscopy of intact rat hearts that onset and development of ischaemia resulted in progressive reduction of the iron-sulphur centres at these sites of the respiratory chain. Such an alteration in mitochondrial redox state, in association with ischaemic depletion of ADP, can result in the transfer of electrons directly to molecular oxygen upon reoxygenation, generating superoxide radicals ($O_2^{\bullet -}$) and hydrogen peroxide (H_2O_2) (Ambrosio *et al.*, 1993).

Dismutation of $O_2^{\bullet-}$ and decomposition of H_2O_2 to more harmful oxygen intermediates such as hydroxyl radical-like species and singlet oxygen are catalysed by transition metals such as iron via a Fenton type reaction (Kirschner and Fantini, 1994; Wink *et al.*, 1994). During normal cellular metabolism, iron is bound either to ferro-proteins such as the cytochromes or to the iron storage protein ferritin and its degradation product haemosiderin. Little, if any "free" iron is thought to be available to catalyse oxidative free radical reactions (Gower *et al.*, 1989). However, it has previously been shown that a significant early event during renal ischaemia is the delocalization of catalytic low molecular weight iron, which may be a result of reductive mobilization of ferritin iron or degradation of labile cytochrome P-450 (Gower *et al.*, 1989; Goddard *et al.*, 1992; Paller and Jacob, 1994). Although iron release from the haem proteins myoglobin and haemoglobin is another possible source of catalytic iron, this is thought to require an excess of hydrogen peroxide, and may not be feasible under the ischaemia-reperfusion conditions encountered during renal transplantation (Gower *et al.*, 1993). Regardless of its source, it is not known whether delocalized iron contributes to respiratory chain damage *in vivo* in renal ischaemia-reperfusion injury - either directly by complexing to mitochondrial membranes or indirectly by affecting cellular ionic (particularly calcium) homeostasis.

In Chapter 4, the kinetics of haemoglobin oxygenation in stored and unstored autografted rabbit kidneys were determined. It was shown that cortical vascular resistance and haemoglobin oxygenation were very similar in both groups during the first 5 min of reperfusion. If mitochondrial dysfunction in this model were a result of free radical-mediated injury to the respiratory chain, rather than secondary ischaemia, it should therefore be shown to occur within the first 5 min of reperfusion. Moreover, if free radical-mediated injury is indeed iron dependent, it should be possible to reduce indices of damage by chelation of delocalized catalytic iron. Iron chelators such as desferrioxamine (DFX), which cannot enter cells by passive diffusion (Lloyd *et al.*, 1991) are likely to affect only external cell membrane function, or possibly trans-cellular iron equilibria (Paller and Hedlund, 1994), and may not affect respiratory chain function. However, "intracellular" chelators, typically of small size and relatively high oil/water partition coefficients (Collis *et al.*, 1993; Hider *et al.*, 1994) such as the bidentate hydroxypyridinone CP102 (Hider *et al.*, 1994) and the monohydroxyamate N-methyl hexanoylhydroxamic acid (NMHH) (Collis *et al.*, 1993; Green *et al.*, 1993) are able to permeate cell membranes and may therefore have a direct effect on mitochondrial function - for example, by preventing the energy independent accumulation of iron in the mitochondrial membranes (Kukielka *et al.*, 1994).

6.2 Objective

The studies presented in this chapter were designed to:

(i) Determine the effect of 72 h hypothermic renal storage on respiratory chain function, as judged by mitochondrial NADH fluorescence, within the first 5 min of revascularization.

(ii) Assess the relative effect of "intracellular" and "extracellular" iron chelation as means of improving mitochondrial function, cellular integrity and renal viability after 72 h storage and transplantation.

6.3 Methods

6.3.1 Methodology

A total of 50 adult female NZW rabbits (2.5 - 3 kg), in 5 groups of 6 and 4 subgroups of 5 animals (described below) were anaesthetized by an i.m. injection of fentanyl fluanisone and diazepam; oxygen was supplied via an open face mask (see Chapter 2 for full details). Kidneys were flushed with ice-cold (0-2^{0}C) HCA and either autografted immediately, or flushed and then stored in HCA (or HCA containing one of the iron chelators) at 0-2^{0}C for 72 h prior to autografting.

The rates of change in fluorescence intensity of NADH were measured by surface fluorescence spectroscopy in response to two events:

(i) Reperfusion of unstored or 72 h stored transplanted kidneys with oxygenated blood.

(ii) Inhibition of complex I NADH dehydrogenase by sodium pentobarbitone after 4.5 min of reperfusion.

In addition, the effect of the three chelators on the post-ischaemic formation of two markers of lipid peroxidation (TBA-reactive material and Schiff's bases) was investigated in the contra-lateral kidneys, stored for 0 or 72 h, as described in Chapter 2. Renal morphology was evaluated by light and electron microscopy. The effect of the iron chelators on long-term viability was determined by measurement of serum urea and creatinine levels in rabbits allowed to recover after autografting.

6.3.2 Drug Dosage

Drug doses were based on previous DFX dosing regimen used in this laboratory, in which rabbits were dosed at 50 mg/kg DFX. DFX (M_r 560) is a hexadentate iron chelator, whereas CP102 (M_r 183) and NMHH (M_r 145) are bidentate. DFX therefore chelates three times as much iron on a molecular weight basis. Accordingly, CP102 and NMHH were given at three times the dose of DFX on a molar

weight basis (i.e. CP102 dose was 50 mg/kg and NMHH dose was 40 mg/kg). In addition, DFX was added to the HCA solution at a concentration of 100 μM; CP102 and NMHH at concentrations of 300 μM.

6.3.3 Experimental Groups

Group 1: Freshly nephrectomized right kidneys (n=6) were flushed with 40 ml HCA (0-2^{0}C) via the renal artery and autografted immediately into the left renal bursa, prior to measurements of NADH fluorescence. The contra-lateral kidney was removed during the autograft operation, flushed with HCA, homogenized and stored at −20^{0}C as described in Chapter 2 for later analysis of Schiff's bases and TBA-reactive material.

Group 2: Kidneys (n=6) were flushed as in Group 1 and then stored in HCA surrounded by ice to maintain a temperature of 0-2^{0}C for 72 h before autografting, for measurements of NADH fluorescence. Contra-lateral kidneys were stored in HCA for 72 h for measurement of Schiff's bases and TBA-reactive material. An additional 5 animals were allowed to recover for assessment of long term viability.

Group 3: The bidentate iron chelator 1-hydroxyethyl-3-hydroxypyridin-4-one (CP102) was added to the HCA solution at a concentration of 300 μM and kidneys were stored for 72 h, as in Group 2. Upon reperfusion, a 40 mg/kg bolus of CP102 was given i.v. to the recipient. In 6 animals NADH fluorescence was measured; an additional 5 animals were allowed to recover for assessment of long term viability. Contra-lateral kidneys were stored in HCA + CP102 for 72 h for measurement of Schiff's bases and TBA-reactive material.

Group 4: The bidentate monohydroxamate iron chelator N-methyl hexanoylhydroxyamic acid (NMHH) was added to the HCA solution at a concentration of 300 μM and kidneys were stored for 72 h as in Group 2. Upon reperfusion, a 40 mg/kg bolus of NMHH was given i.v. to the recipient. In 6 animals NADH fluorescence was measured; an additional 5 animals were allowed to recover for assessment of long term viability. Contra-lateral kidneys were stored in HCA + NMHH for 72 h for measurement of Schiff's bases and TBA-reactive material.

Group 5: The hexadentate trihydroxamate iron chelator DFX was added to the HCA solution at a concentration of 100 μM and kidneys were stored for 72 h as in Group 2. Upon

reperfusion, a 50 mg/kg bolus of DFX was given *i.v.* to the recipient. In 6 animals NADH fluorescence was measured; an additional 5 animals were allowed to recover for assessment of long term viability. Contra-lateral kidneys were stored in HCA + DFX for 72 h for measurement of Schiff's bases and TBA-reactive material.

6.4 Results

6.4.1 Surface Fluorescence Measurements of Mitochondrial NADH.

In Fig 6.1 are shown emission spectra of NADH from 400-600 nm obtained by excitation at 366 nm before, during and 3.5 min after termination of reperfusion in a Group 1 kidney. The intensity of the reflectance signal measured at 366 nm did not significantly alter in the course of reperfusion and is not shown; nor were there significant differences in reflectance between any groups (1 to 5) at equivalent time points. The relative fluorescence intensity of NADH at 480 nm prior to reperfusion was taken to represent 100% of NADH fluorescence, and percentage changes during and after reperfusion were calculated from this value. There were no significant differences in pre-reperfusion fluorescence intensity at 480 nm between the five groups (n = 6 in each group). In Group 1, pre-reperfusion NADH fluorescence was 3.4 (± 1.3) arbitrary units; in Group 2, the value was 3.9 (± 1.0); Group 3 = 2.9 (± 1.3); Group 4 = 3.8 (± 0.8); Group 5 = 3.5 (± 0.7).

In Fig 6.2 are shown the mean percentage changes (n=6) during reperfusion of Group 1 (unstored) and Group 2 (72 h stored) kidneys. In Group 1, reperfusion resulted in the oxidation of 89.9% (± 4.3%) of NADH within 90 sec, *ie.* scan 2 to scan 5 ($p<0.005$, n=6). Thereafter values oscillated within the range 70% to 100% oxidized. Infusion with sodium pentobarbitone (200 mg/kg) after 4.5 min of reperfusion resulted in rapid formation of NADH to 58.3% (± 6.5%) of pre-reperfusion values within 90 sec (scan 11 to scan 15), a highly significant ($p<0.005$) increase. In Group 2 kidneys there were similarly rapid oxidations of NADH by 83.7% (± 8.5%) within 90 sec of reperfusion ($p<0.005$, n=6). Oscillations thereafter were not as great as those observed in Group 1 kidneys, values ranging from 81% to 100% oxidized. Infusion of sodium pentobarbitone after 4.5 min of reperfusion did not result in significant increases in NADH regeneration though there was a slight increase in oxidation to 22.8% (± 3.7%) of pre-reperfusion values within 90 sec (scan 11 to scan 15).

Reperfusion of Group 3 kidneys resulted in rapid oxidation of 81.6% (± 10.3%) NADH within 90 sec, *ie.* scan 2 to scan 5 ($p<0.005$, n=6, Fig 6.3). In Group 4 kidneys, there was an 83.7% (± 9.9%) oxidation within 90 sec ($p<0.005$). Infusion of sodium pentobarbitone resulted in more rapid increases in NADH fluorescence compared with Group 2 kidneys in both Group 3 and Group 4 kidneys (to 23.9% ± 6.2% and 32.6% ± 6.2% respectively within 90 sec). However these increases in NADH

fluorescence were not significantly greater than those occurring in Group 2 kidneys. NADH fluorescence measurements did not increase further up to 20 min after sodium pentobarbitone infusion; hence the figures do not display data beyond 3.5 min post sodium pentobarbitone infusion.

Addition of the "extracellular" iron chelator DFX (Group 5) did result in significant differences compared with Group 2 kidneys (Fig 6.3). Reperfusion resulted in the rapid oxidation of 100% (± 0.5%) NADH within 90 sec ($p<0.005$, n=6) - a significantly greater oxidation than that occurring in Group 1 kidneys ($p<0.05$). Thereafter there was practically no oscillation in fluorescence intensity at 480 nm. Sodium pentobarbitone infusion resulted in small but significant increases in fluorescence intensity to 18.1% (± 1%) of pre-reperfusion values within 90 sec ($p<0.05$, n=6). Nevertheless, the absolute magnitude of fluorescence intensity was not significantly greater than in Groups 2, 3 and 4.

6.4.2 Determination of Lipid Peroxidation

Storage of kidneys at 0-2°C in HCA solution for 72 h resulted in highly significant ($p<0.005$) increases in oxidative membrane damage compared with unstored controls in both the cortex and medulla as determined by the subsequent *in vitro* formation of TBA-reactive material and Schiff's bases (Figs 6.6 and 6.7). Inclusion of CP102, NMHH and DFX in the HCA flush and storage solution all highly significantly ($p<0.005$) reduced the formation of both markers of lipid peroxidation in the renal cortex compared with Group 2 kidneys; levels of both markers were not significantly different from Group 1 (unstored) kidneys. All three chelators were also highly effective ($p<0.005$ compared with Group 2) at inhibiting Schiff's base formation in the medulla of stored kidneys; again, the reduced levels were not significantly different from those formed in Group 1 kidneys (Fig. 6.7). Although production of TBA-reactive material in the medulla was also highly significantly ($p<0.005$) reduced by all three iron chelators, levels of TBA-reactive material were not reduced to the low levels found in Group 1 kidneys ($p<0.005$ compared with Group 1).

6.4.3 Histology

Histological analysis of kidneys prior to reperfusion using both light and electron microscopy showed no observable morphological or ultrastructural damage in any group (as seen in Chapter 3). After 4.5 min of reperfusion of Group 1 kidneys there was minimal to mild cortical oedema as assessed by light microscopy (Plate 6.1 and Fig 6.8) but no mitochondrial swelling (as judged by electron microscopy). In Group 2 kidneys, 4.5 min reperfusion resulted in mild cortical oedema and some hydropic degeneration (as assessed by light microscopy) but little electron microscopical evidence of mitochondrial swelling (Plates 6.2 and 6.3 and Fig 6.8). Addition of CP102 and NMHH both highly significantly ($p<0.005$) reduced cortical oedema to minimal or absent, as assessed by light microscopy

(Plate 6.4 and Fig 6.8). Oedema was significantly ($p<0.05$) reduced by DFX. There was little microvascular congestion in the cortex of any kidney, but moderate to severe medullary congestion in all stored kidneys, regardless of treatment with iron chelators.

6.4.4 Survival Determination

In Figs 6.9 and 6.10 are shown serum concentrations of creatinine and urea respectively, in Sub-groups 2-5. In Group 2 (72 h stored transplanted) 4 of 5 rabbits had developed uraemia by day 6. Treatment with iron chelators did not significantly affect either the long term viability or the serum levels of urea and creatinine. In cases where renal function was insufficient to support life, either complete infarction had occurred (Plate 6.5), or there was gradual severe necrosis of the whole kidney (Plate 6.6). That necrosis was gradual in these instances was illustrated by the demarcation of successive necrotic zones by acute inflammatory infiltrate and casts (necrotic debris); large calcific deposits were also prominent.

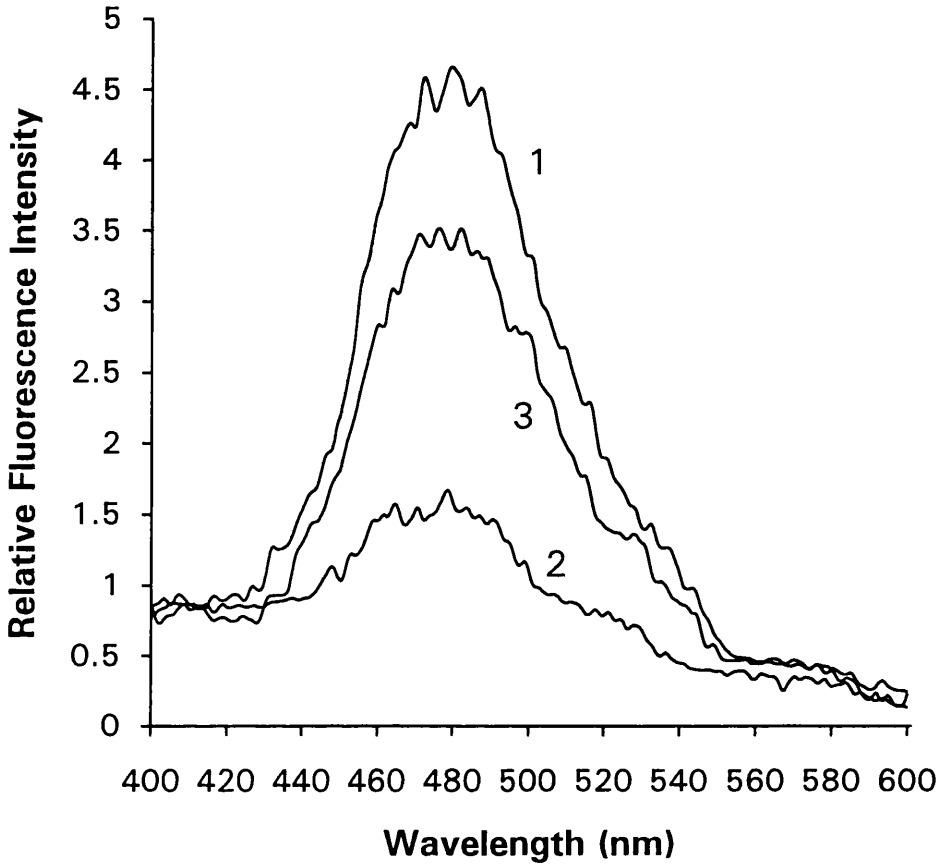

Fig 6.1 Relative fluorescence intensity of NADH from 400-600 nm in a Group 1 kidney obtained by excitation at 366 nm, showing oxidation of NADH upon reperfusion and partial regeneration of NADH after inhibition of complex I. 1: NADH fluorescence after completion of the autograft but prior to removal of the clamps for reperfusion; 2: NADH fluorescence after 90 sec of reperfusion; 3: NADH fluorescence 90 sec after termination of reperfusion by *i.v.* infusion of sodium pentobarbitone.

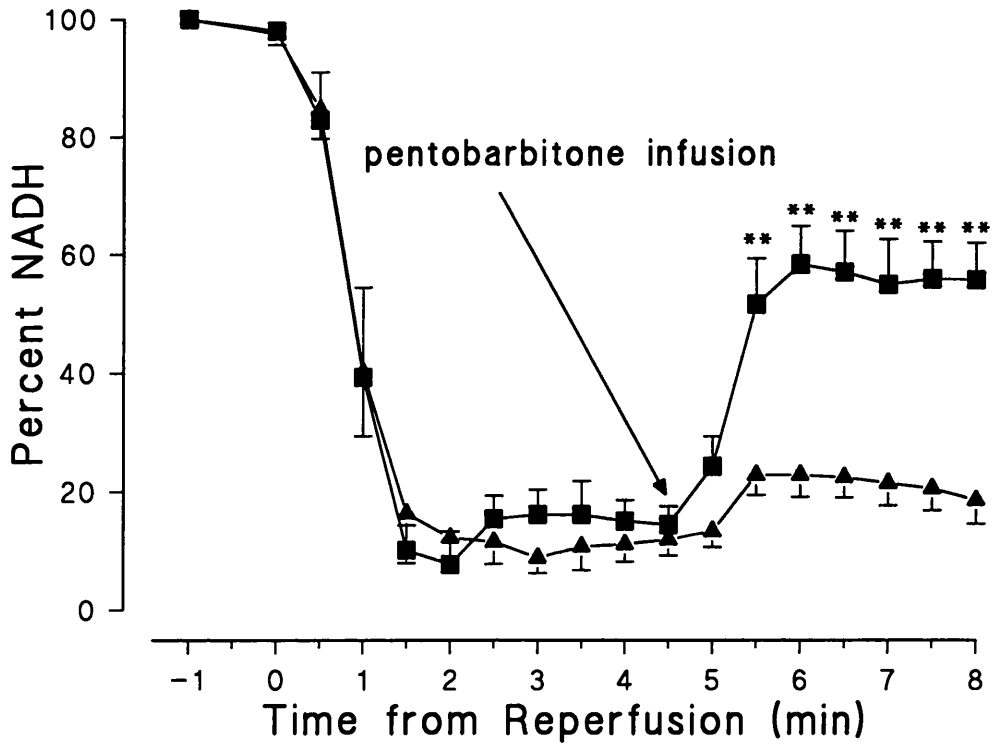

Fig 6.2 Mean and SEM changes (n=6) in relative fluorescence intensity of NADH expressed as percentage changes over time in Group 1 (■, unstored) and Group 2 (▲, 72 h stored) kidneys. Reperfusion of the organ *in situ* took place at 0 min; inhibition of complex 1 by sodium pentobarbitone infusion at 4.5 min. There was a highly significant decrease in NADH fluorescence intensity within 90 sec of reperfusion in both groups ($p<0.005$, stars not shown). $^{**}p<0.005$ refers to highly significant increases in NADH fluorescence intensity following sodium pentobarbitone inhibition of complex I at 4.5 min. The results show that NADH regeneration is impaired in stored transplanted kidneys when the respiratory chain is inhibited at complex I.

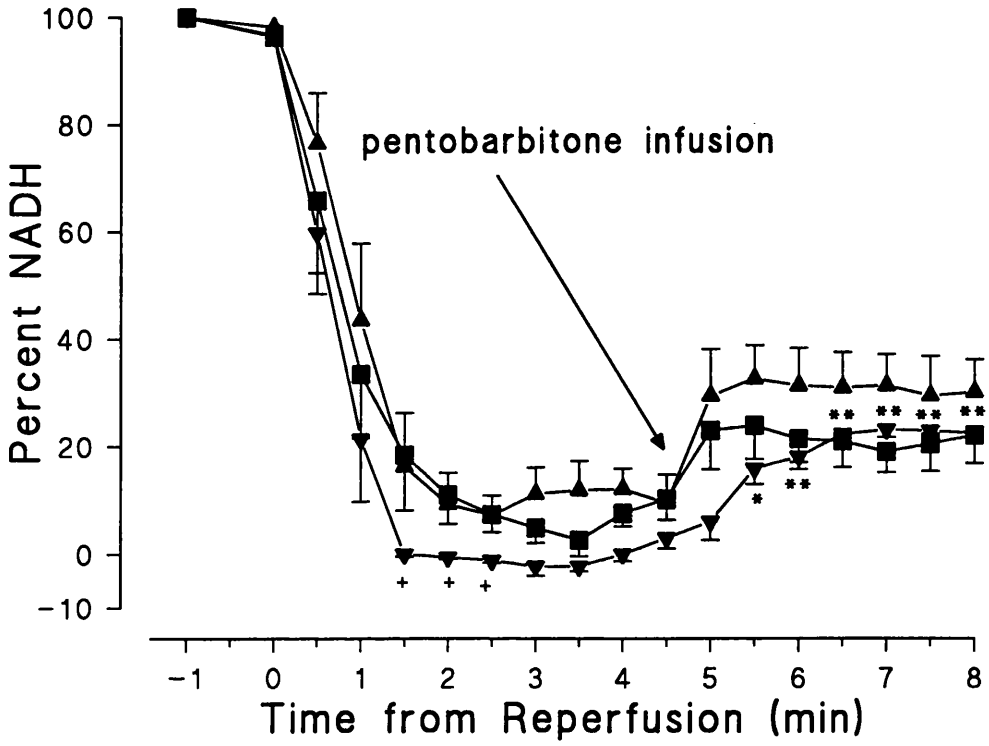

Fig 6.3 Mean and SEM changes (n=6) in relative fluorescence intensity of NADH expressed as percentage changes over time in Groups 3 (■, 72 h stored + CP102), 4 (▲, 72 h stored + NMHH) and 5 (▼, 72 h stored + DFX) kidneys. Reperfusion of the organ *in situ* took place at 0 min; inhibition of complex 1 by sodium pentobarbitone infusion at 4.5 min. There was a highly significant decrease in NADH fluorescence intensity within 90 sec of reperfusion in all three groups ($p<0.005$, stars not shown). $^{**}p<0.005$ refers to highly significant increases in NADH fluorescence intensity following sodium pentobarbitone inhibition of complex 1 at 4.5 min. $^{+}p<0.05$ refers to significant differences in NADH fluorescence intensity in Group 5 compared with Group 2 at equivalent time points. The results show that none of the iron chelators significantly improved NADH regeneration following inhibition of the respiratory chain at complex I compared with Group 2, suggesting that they do not affect respiratory chain function.

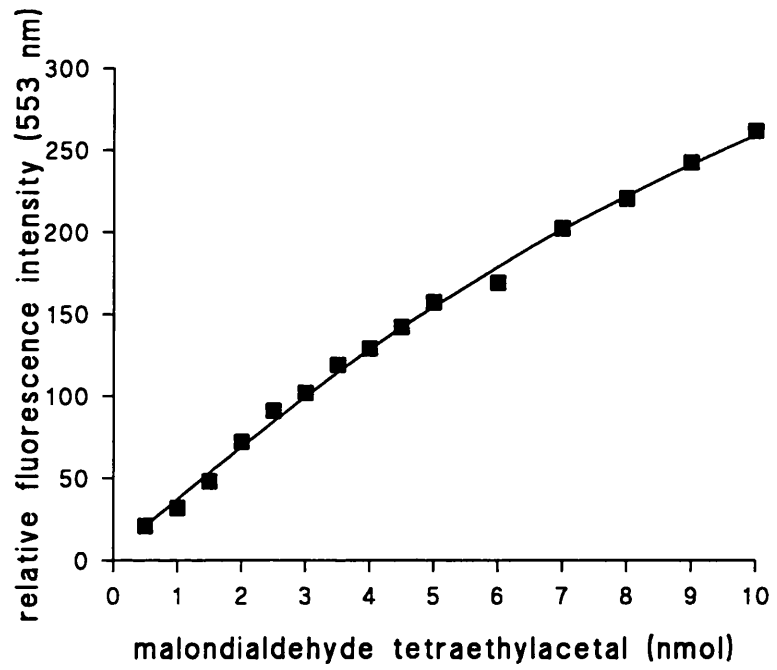

Fig 6.4 Standard curve for malondialdehyde tetraethylacetal (nmol) vs relative fluorescence intensity at 553 nm when excited at 513 nm (values are mean of duplicate determinations).

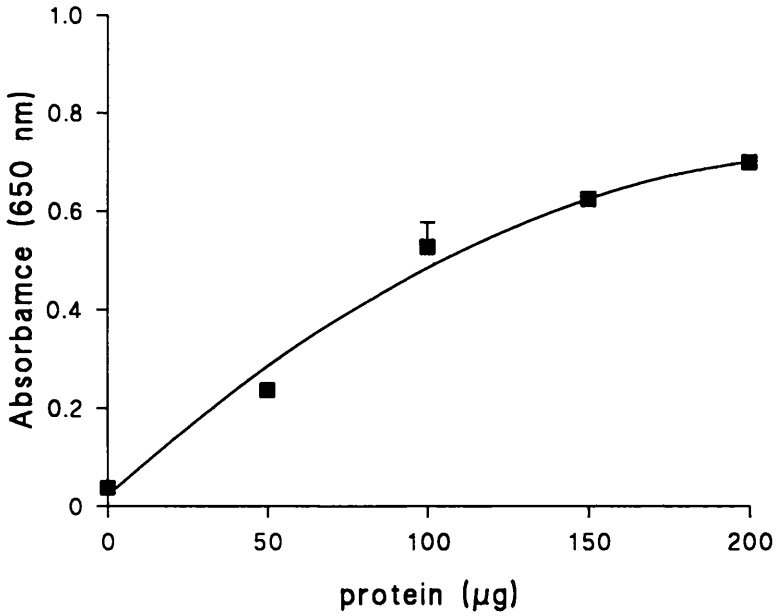

Fig 6.5 Standard curve for bovine serum albumin (μg) vs absorbance at 650 nm. Results are presented as mean ± SEM of triplicate determinations.

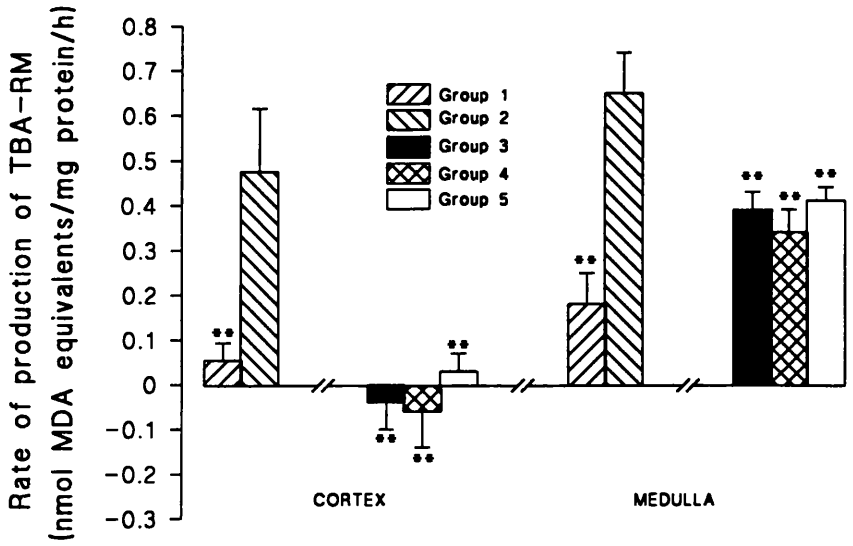

Fig 6.6 Rates of formation of TBA-reactive material in homogenates of renal cortex and medulla, showing highly significant reductions in formation of TBA-reactive material with all three iron chelators compared with untreated stored kidneys. Results are presented as mean and SD (n=6) for Groups: 1 (unstored); 2 (72 h stored); 3 (72 h stored + CP102); 4 (72 h stored + NMHH); and 5 (72 h stored + DFX). $^{**}p<0.005$, all compared with Group 2.

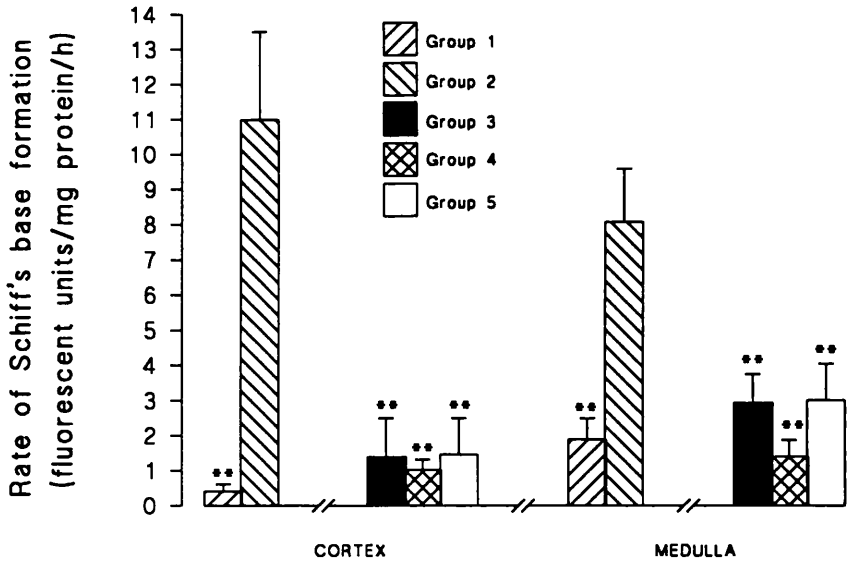

Fig 6.7 Rate of formation of Schiff's bases in homogenates of renal cortex and medulla, showing highly significant reductions in Schiff's base formation with all three iron chelators compared with 72 h stored kidneys. Results are presented as mean and SD (n=6) for Groups: 1 (unstored); 2 (72 h stored); 3 (72 h stored + CP102); 4 (72 h stored + NMHH); and 5 (72 h stored + DFX). $^{**}p<0.005$, all groups compared with Group 2.

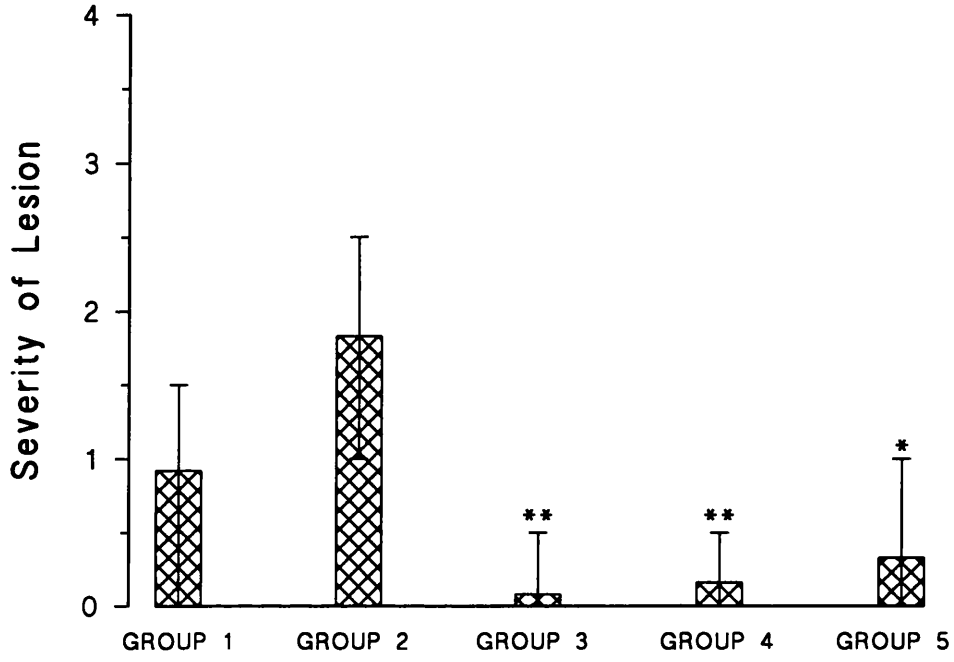

Fig 6.8 Degree of oedema (as assessed by light microscopy) in the renal cortex after 4.5 min of reperfusion, showing significant reductions in oedema by all three iron chelators, compared with untreated 72 h stored transplanted kidneys. Results are presented as mean and range scores (n=6) in Group 1 (unstored), Group 2 (72 h stored), Group 3 (72 h stored + CP102), Group 4 (72 h stored + NMHH) and Group 5 (72 h stored + desferrioxamine). Tissue was scored blind by an independent pathologist on a scale of 0 (absent); 1 (minimal); 2 (mild); 3 (moderate) and 4 (severe). $*p<0.05$, $**p<0.005$, all groups compared with Group 2.

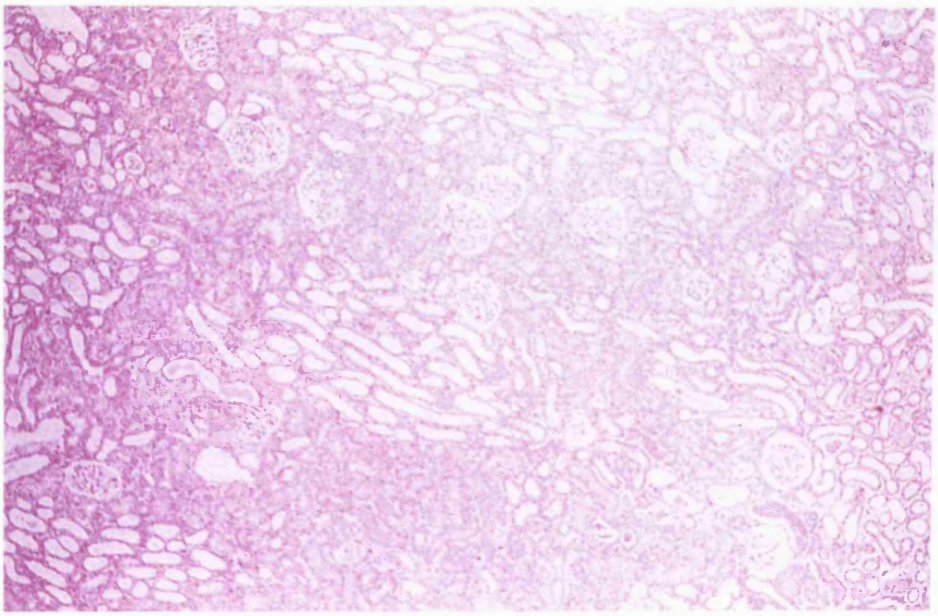

Plate 6.1 **Light micrograph of the renal cortex showing minimal to mild intracellular oedema in a Group 1 (unstored transplanted) kidney (magnification x 40).**

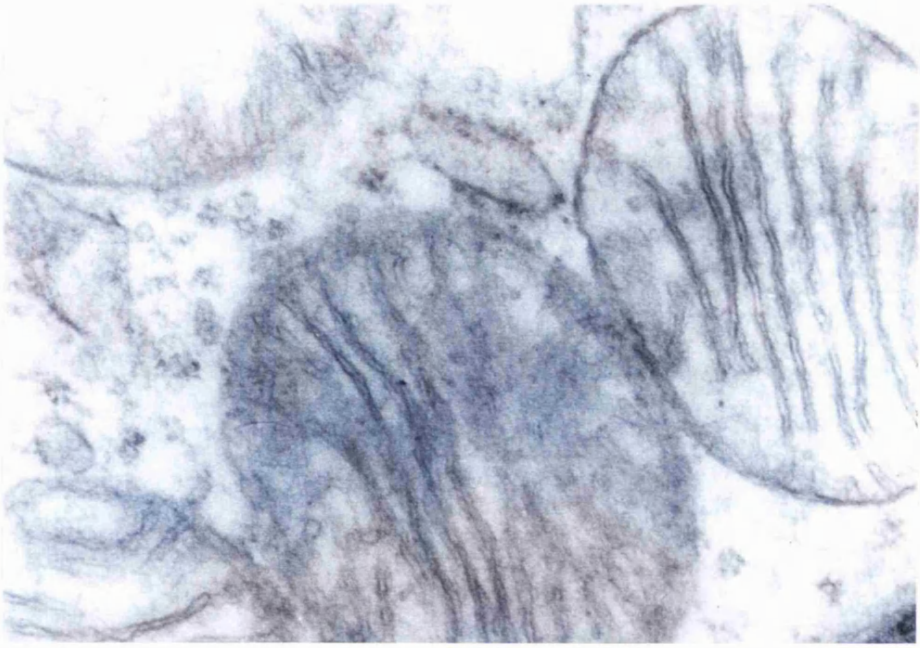

Plate 6.2 **Electron micrograph showing slightly swollen cortical proximal tubular mitochondria in a Group 2 (72 h stored transplanted) kidney (magnification x 25,000).**

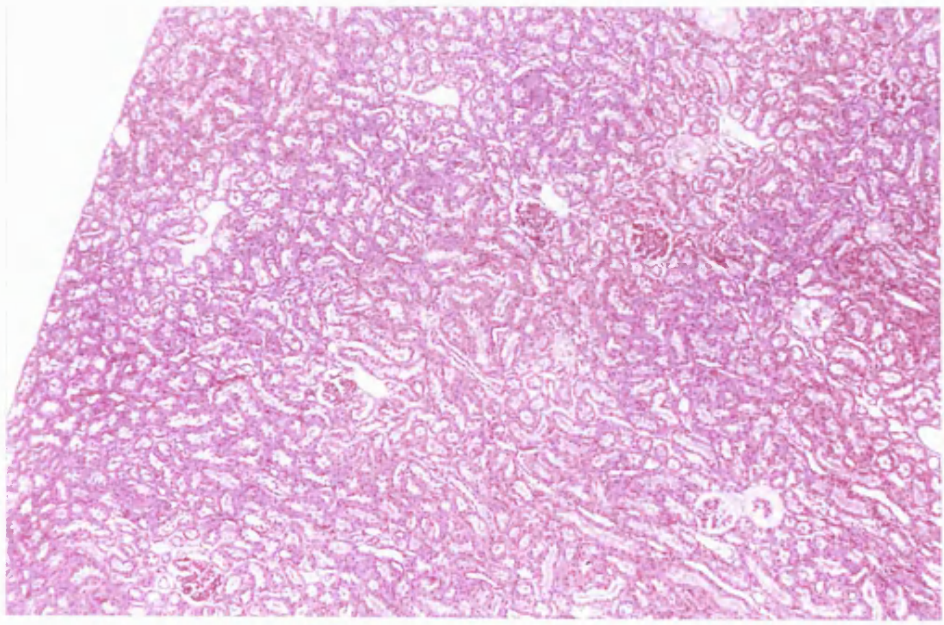

Plate 6.3 **Light micrograph of the renal cotex showing mild to moderate cortical intracellular oedema in a Group 2 (72 h stored transplanted) kidney (magnification x 40).**

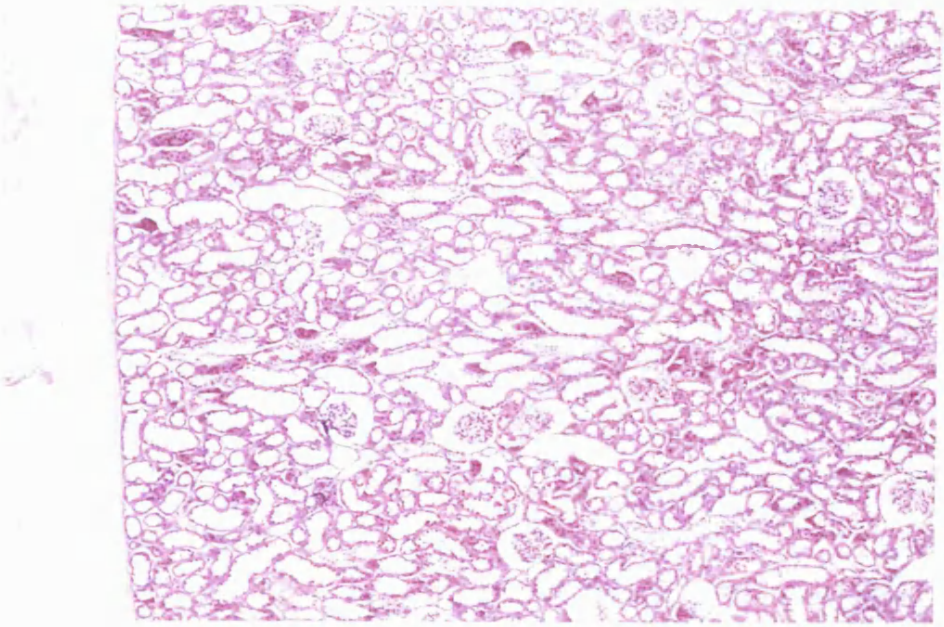

Plate 6.4 **Light micrograph of the renal cotex showing significant reduction in cortical intracellular oedema in a Group 3 (72 h stored + CP 130) transplanted kidney (magnification x 40).**

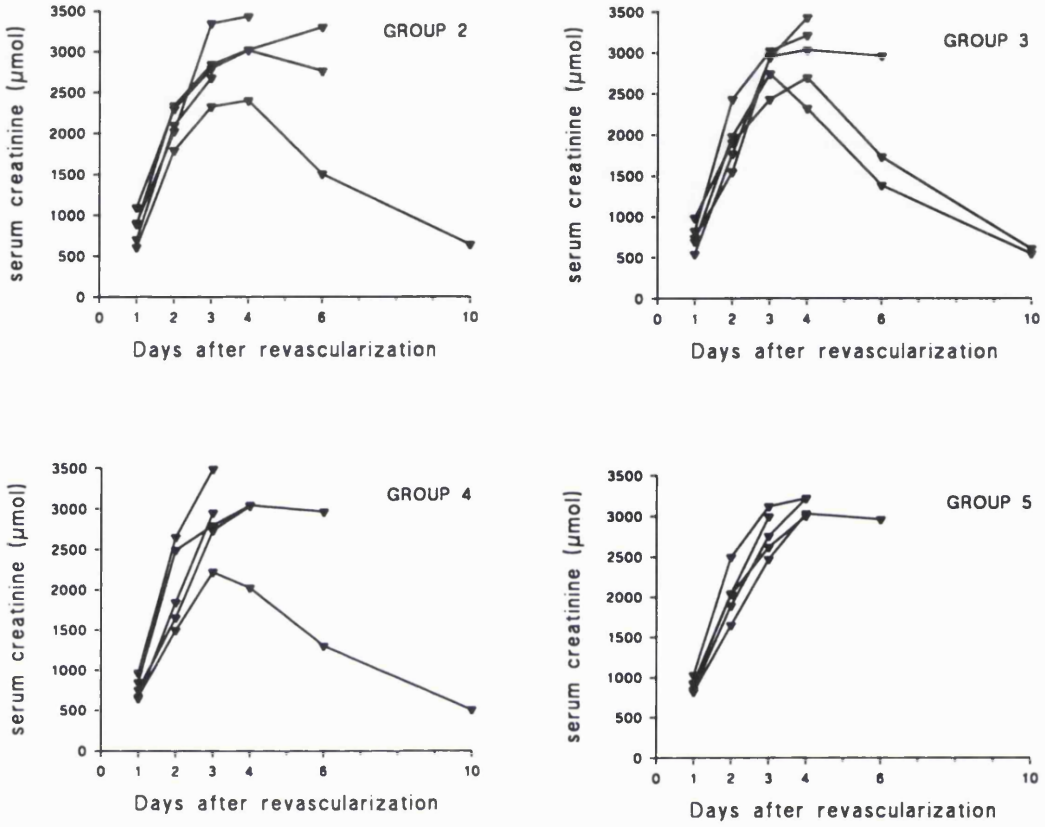

Fig 6.9 Concentration of serum creatinine (µmol) in Groups 2, 3, 4 and 5 for up to 10 days post transplant (▼ denotes individual rabbits).

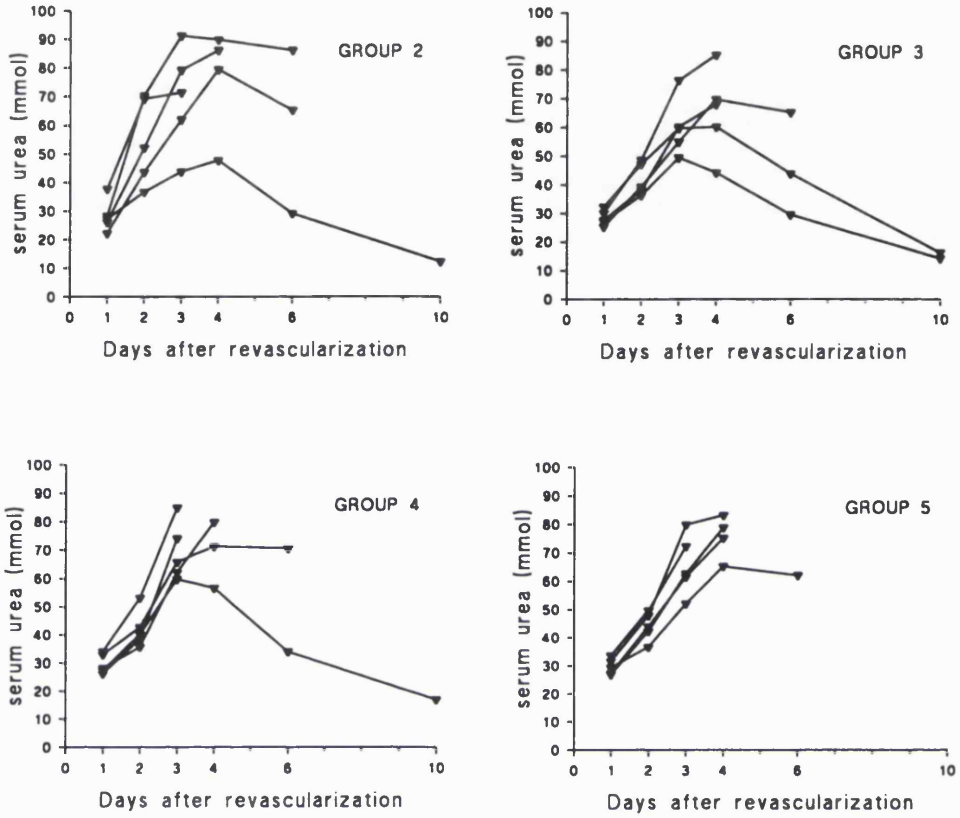

Fig 6.10 Concentration of serum urea (mmol) in Groups 2, 3, 4 and 5 for up to 10 days post transplant (▼ denotes individual rabbits).

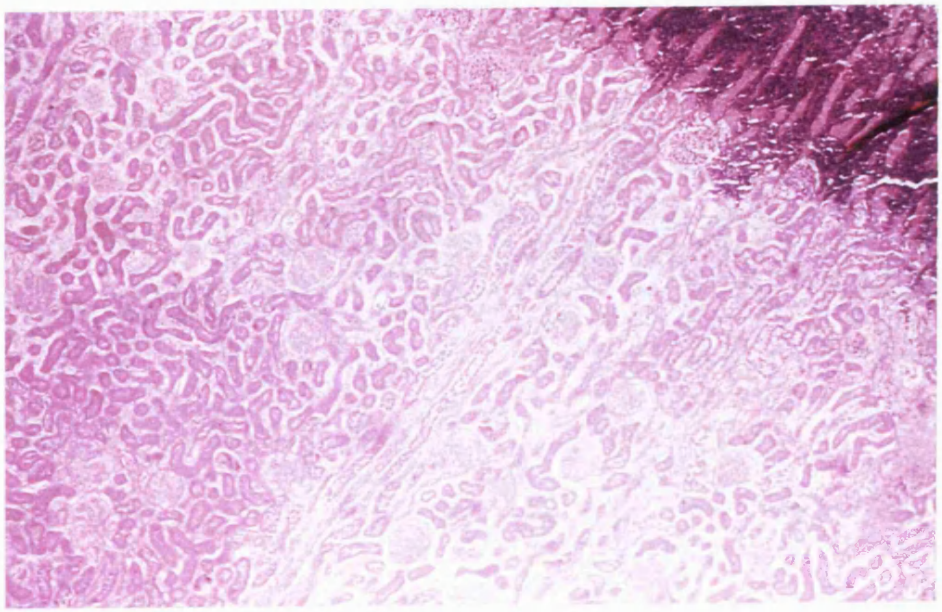

Plate 6.5 **Light micrograph of the renal cortex of a Group 2 infarcted kidney at autopsy 3 days after revascularization (magnification x 40), showing tubular outlines and massive inflammatory infiltrate at the top right.**

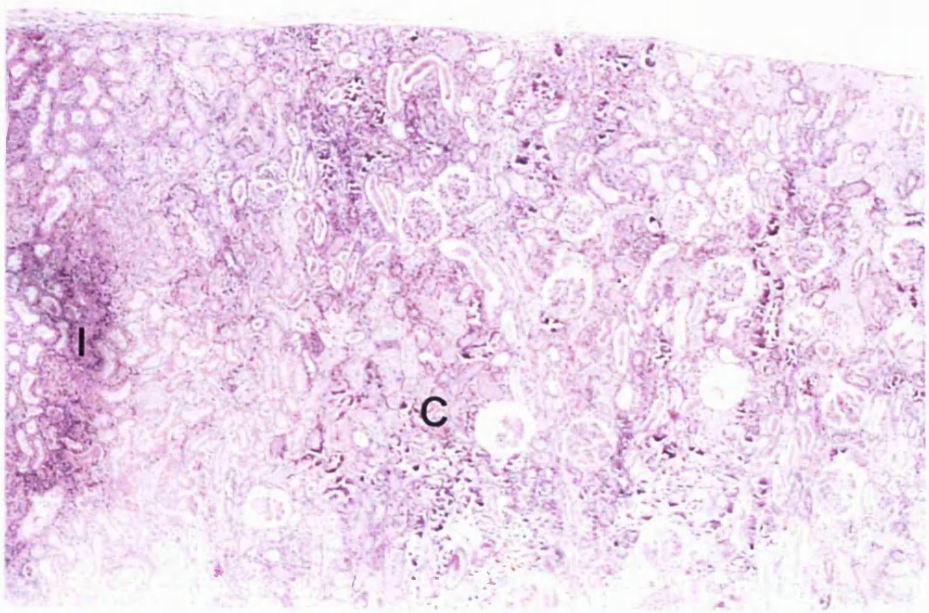

Plate 6.6 **Light micrograph of the renal cortex of a Group 2 kidney which had undergone gradual severe necrosis of the entire kidney at autopsy 6 days after revascularization, showing mild inflammatory infiltrate at the left (I) and calcified necrotic tissue in the centre (C).**

6.5 Discussion

The measured emission spectra in the rabbit kidney cortex were characteristic for NADH fluorescent emission when excited at 366 nm as previously reported (Tokunaga *et al.*, 1987; Thorniley *et al.*, 1994; Thorniley *et al.*, 1995), and as determined in Chapter 5. NADH fluorescence in Group 1 kidneys prior to transplantation (3.4 ± 1.3 arbitrary units; n=6) was not significantly different from fluorescence in Group 2 kidneys after 72 h cold preservation in HCA (3.9 ± 1.0; n=6). It is unlikely that NADH fluorescence was enhanced by the cold during storage (concomitant with a decline in total NADH) as it has previously been shown that perfusion of nephrectomised kidneys with ice cold perfusate reduces renal core temperature to 1-2^{0}C within 2 min and the temperature thereafter remains constant (Lam *et al.*, 1989). Thus, the core temperature of both stored and unstored perfused kidneys should have been equivalent.

Earlier studies of NADH fluorescence in intact porcine and rat livers and in isolated hepatocyte suspensions suggested that extended cold preservation resulted in an irreversible decrease in fluorescence which correlated with decreased total adenine nucleotides, energy charge and cell viability (Ozaki *et al.*, 1989; Obi-Tabot *et al.*, 1993). The fact that this did not occur in 72 h preserved (Group 2) kidneys suggests that mitochondrial integrity (but not necessarily functional capacity) was not significantly compromised prior to reperfusion. This premise is supported by both electron and light microscopical analysis of unreperfused 72 h stored renal tissue, which showed no observable ultrastructural damage in the renal cortex (see Chapter 3). These findings correspond to those of Hardy and co-workers (1991) who demonstrated that cardiac mitochondrial complex I activity is not significantly depressed by hypoxia alone, but is significantly decreased upon reoxygenation.

Reperfusion of both Group 1 and Group 2 autografted kidneys resulted in the rapid disappearance (within 90 sec) of 89.9% (± 4.3%) and 83.7% (± 8.5%) respectively of the NADH peaks measured before reperfusion. It was shown in Chapter 5 that the presence of blood did not affect the maximum measured NADH signal, so it may be surmised that the disappearance of the NADH peak was a result of NADH oxidation, as previously shown in isolated hepatic and renal models of asanguineous perfusion (Franke *et al.*, 1976; Tokunaga *et al.*, 1987). However, from the data presented in this chapter it was not possible to determine whether NADH oxidation occurred via an intact respiratory chain, or whether the rapid oxidation of NADH was a result of early uncoupling of the respiratory chain, perhaps as a consequence of ischaemic depletion of ADP levels (Ambrosio *et al.*, 1993). The fact that in both stored and unstored kidneys the kinetics of NADH oxidation during reperfusion was very similar (Fig 6.2) may indicate that NADH oxidation occurred via the same mechanism in both cases.

Reperfusion was terminated by rapid i.v. infusion of sodium pentobarbitone, which inhibits NADH dehydrogenase at complex I of the respiratory chain. In Chapter 5, it was shown that after 3 h reperfusion of unstored transplanted kidneys sodium pentobarbitone infusion resulted in rapid increases in the relative fluorescence intensity of NADH to pre-reperfusion levels (Thomiley *et al.*, 1994; and Chapter 5). However, infusion of sodium pentobarbitone after only 4.5 min of reperfusion in Group 1 kidneys in the studies presented in this chapter resulted in the regeneration of only 58.3% (± 6.5%) of the original NADH peak (Fig 6.2). These findings suggest that some degree of mitochondrial dysfunction occurred during the early period of reperfusion even in unstored kidneys, which was presumably induced by the warm ischaemic period of the transplantation operation itself. The fact that continuation of reperfusion for 3 h allowed complete regeneration of NADH suggests that this early damage to Group 1 kidneys was reversible.

In contrast, there were no significant changes in NADH fluorescence following sodium pentobarbitone infusion after 4.5 min in Group 2 kidneys. Histological analysis at this time point showed mild cortical oedema (compared with minimal oedema in Group 1 kidneys) but no signs of perturbation of cortical microcirculation. It is therefore unlikely that failure to regenerate NADH was a result of compromised circulation - and indeed, had this been the case (in the absence of mitochondrial damage) one would have expected an increase in NADH fluorescence during reperfusion and this did not occur. Thus, failure to regenerate NADH must presumably have been a result of substrate deficiency leading to complex I, or of damage to complex I, or of hydrolysis of NAD^+ to ADPribose and nicotinamide as a result of oxidant induced mitochondrial Ca^+ release (Richter, 1993). It was shown in Chapter 5 that reperfusion of 72 h stored kidneys for 3 h resulted in the development of severe cortical oedema. Despite these time-dependent differences in the severity of oedema, there were no significant differences in the rate of increase or in the magnitude of NADH fluorescence following sodium pentobarbitone infusion after 4.5 min or 3 h of reperfusion. Such a poor correlation between severity of oedema and changes in NADH fluorescence suggests that cellular integrity is not the sole determinant of mitochondrial function in stored kidneys. This conclusion is in agreement with the work of Boydstun and co-workers (1993) who showed that recovery of renal ATP levels shortly after ischaemia did not correlate with cellular integrity (as measured by release of lactate dehydrogenase).

In vitro evidence of autocatalytic free radical mediated injury to complex I of the respiratory chain has been strengthened by demonstrations that respiratory chain function can be improved by use of free radical scavengers, antioxidants, iron chelators, calcium antagonists or specific inhibitors of respiratory complexes (Paraidathathu *et al.*, 1992; Schulze-Osthoff *et al.*, 1992; Ambrosio *et al.*,

1993). However, it has been shown that inhibition of free radical generation at complex I using sodium pentobarbitone resulted in activation of an NADH oxidase in the outer mitochondrial membrane (Ambrosio *et al.*, 1993). Other investigators have shown that inhibition of mitochondrial lipid peroxidation by means of respiratory chain inhibitors had no effect on lipid peroxidation in other cellular fractions (Turrens *et al.*, 1982; Vandeplassche *et al.*, 1989). Thus, specific prevention of respiratory chain damage *in vivo* could not be expected to prevent global damage to the proximal tubule.

An important early event during ischaemia is the delocalization of low molecular weight chelatable iron (Gower *et al.*, 1989; Kukielka *et al.*, 1994). In kidneys, $O_2^{\bullet-}$ or H_2O_2 generation can occur not only in the respiratory chain complexes but also via mitochondrial NADH oxidase (Ambrosio *et al.*,, 1993), xanthine oxidase (Roy and McCord, 1983; Ratych and Bulkley, 1986), and cytochrome P-450 (Paller and Jacob, 1994) - in addition to neutrophil mediated free radical release (Ratych and Bulkley, 1986). Iron (or copper) is required to catalyse the reduction of hydrogen peroxide to hydroxyl radical-like species via a Fenton type reaction (Kirschner and Fantini 1994; Wink *et al.*, 1994) which mediate not only lipid peroxidation but also highly site-specific inactivation of proteins, including several membrane bound sulphydryl-containing ion pumps such as Ca-ATPase (Bellomo *et al.*, 1983; Holmberg *et al.*, 1991). Effective intracellular chelation of catalytic iron is therefore potentially the most effective means of global protection of the proximal tubule.

Desferrioxamine (DFX) is the most widely used iron chelator (Gower *et al.*, 1989; Lloyd *et al.*, 1991). It has previously been shown that DFX can completely inhibit susceptibility to *in vitro* lipid peroxidation in homogenates of the renal cortex and that it improves long term renal viability if given in conjunction with a cyclo-oxygenase inhibitor such as indomethacin (Gower *et al.*, 1989). Studies of tumour necrosis factor (TNF)-mediated cytotoxicity in mouse fibrosarcoma cells showed that TNF treatment resulted in a free radical mediated uncoupling of the respiratory chain at complex I which was inhibitable by DFX (Schulze-Ostoff *et al.*, 1991). However, DFX cannot rapidly enter cells by passive diffusion (Lloyd *et al.*, 1991), is in any case filtered rapidly through the glomeruli into the urinary space and is not accumulated in measurable quantities in the renal parenchyma (Toffa *et al.*, 1991). Coupling DFX to lipophilic steroids, thereby targetting it to the plasma membrane, has been shown to increase its potency as much as 10 to 100 fold (Braughler *et al.*, 1988). However, such moieties would certainly not enter the cell and could only affect respiratory chain function indirectly through maintainance of cell membrane integrity or by affecting transcellular iron equilibria (Paller and Hedlund, 1994).

The influence of the two bidentate iron chelators, which should rapidly permeate membranes, was therefore compared with DFX in terms of their effect on NADH fluorescence, post-ischaemic lipid peroxidation, renal histology and long term viability. All three iron chelators significantly reduced post-ischaemic susceptibility to lipid peroxidation (Figs 6.6 and 6.7). In the cortex, levels of TBA-reactive material and Schiff's bases were reduced to the very low levels found in Group 1. In contrast, in the medulla TBA reactivity was only partially reduced. Previous experiments in this laboratory have demonstrated that approximately 50% of the TBA-reactive material formed in the medulla following ischaemia is derived from prostaglandin biosynthesis and not lipid peroxidation *per se* (Gower *et al.*, 1989). The extent of the decrease in TBA-reactivity in the medulla, coupled with the more marked lowering of medullary Schiff's base formation is therefore consistent with the three iron chelators being powerful antioxidants but poor inhibitors of cyclooxygenase.

Despite their effectiveness at inhibiting lipid peroxidation, none of the iron chelators had a pronounced effect on NADH fluorescence. There were no significant differences in the magnitude of the NADH peaks prior to reperfusion compared with Group 1 kidneys, nor in the rates of oxidation of NADH at reperfusion. Curiously, however, desferrioxamine treatment resulted in 100% (± 0.5%) oxidation of NADH upon reperfusion, a significantly ($p<0.05$) greater oxidation than occurred in Group 1 kidneys. This may be an indication of complete uncoupling of the respiratory chain, but the mechanism by which desferrioxamine could induce such an event is unclear. It is conceivable that desferrioxamine could reduce extracellular calcium influx by preventing iron mediated inactivation of plasma membrane calcium ionophores, while having no effect on intracellular calcium cycling across the inner mitochondrial membrane. Such cycling has been shown to result in rapid oxidation of mitochondrial NAD(P)H (O'Connor, 1977) and ultimately in the hydrolysis of NAD^+ (Richter, 1993). This scenario is supported by the fact that inhibition of complex I in this group resulted in a small but significant (18.1% ± 1%; $p<0.05$, n=6) increase in NADH fluorescence, suggesting the respiratory chain had become uncoupled rather than there being a complete loss of substrate or denaturation of complex I.

Inhibition of complex I in Groups 3 and 4 (treated with CP102 and NMHH respectively) resulted in larger increases in NADH fluorescence to 23.9% (± 6.2%) and 32.6% (± 6.2%) respectively but these increases did not attain significance. The reasons for this lack of protective effect are not clear, but it is possible that the iron chelators were not present in the mitochondria in sufficient concentration to prevent free radical mediated damage to the RC. However, it is unlikely that the chelators did not penetrate to intracellular sites *per se*. *In vitro* cell culture studies using CP102 showed that doses as low as 30 mM were sufficient to mobilize iron from ferritin - not necessarily beneficial in the context

of ischaemia-reperfusion injury as opposed to iron overload syndrome (Porter *et al.*, 1989) - but indicative that the chelator does reach intracellular sites. The partition coefficients of both CP102 and NMHH (<1), while being sufficiently high to facilitate membrane permeation, are not compatible with their accumulation in cellular membranes (Porter *et al.*, 1989). It is possible then that neither drug was able to inhibit oxidative reactions catalysed by accumulated iron in the mitochondrial membranes (Kukielka *et al.*, 1994). Nevertheless, if this accumulated iron is derived from ferritin (an aqueous protein) or from cytochrome P-450 (Paller and Jacob, 1994) it seems likely that iron chelation in the aqueous phase would reduce mitochondrial membrane accumulation of iron.

A practical problem pertaining to the use of bidentate iron chelators is the formation at low concentrations of uni- and bi-chelator/iron complexes, both of which are capable of catalysing redox reactions. Conversely, if too high a concentration is achieved, chelators with access to intracellular sites may actually mobilize iron from ferritin *in vivo*. The dosing regimen employed in these studies were intended to minimalize these possibilities. It has previously been shown that in the course of 72 h cold ischaemia the concentration of desferrioxamine-chelatable low molecular weight iron increases from a negligible concentration to a mean of 90 μM (Healing *et al.*, 1990). Thus a concentration of 300 μM CP102 or NMHH should chelate, on a 3:1 ratio all available delocalized iron. Similarly, a dose of 50 mg/kg CP102 or 40 mg/kg NMHH given i.v. to the recipient upon reperfusion should produce effective concentrations of 300 μM as the drugs do not concentrate in membranes and are not metabolized in the liver (Porter *et al.*, 1989; Hider *et al.*, 1994). That these doses were indeed therapeutic rather than toxic is suggested by the fact that all three iron chelators not only reduced both markers of lipid peroxidation highly significantly ($p<0.005$) (Figs 6.6 and 6.7) but also improved the morphological appearance of the cortex (Plate 6.4 and Fig 6.8). Despite this, none of the chelators improved the long term viability of single stored autografted kidneys (Figs 6.9 and 6.10).

The ineffectiveness of intracellular iron chelation at improving either mitochondrial function or long term viability may therefore be related to the nature of damage occurring in the respiratory chain complexes. Firstly, it is possible that steric distortions may have rendered catalytic the prosthetic iron of the iron-sulphur centres at complex I (which are likely to be inaccessible to intracellular chelators except at very high concentrations). Secondly, $O_2^{\bullet-}$ or H_2O_2 could be capable of independently inactivating complex I in the absence of iron. Finally, mitochondrial dysfunction may result from ADP depletion or calcium cycling across the inner mitochondrial membranes, leading to NAD^+ hydrolysis (Richter, 1993); irreversible mitochondrial injury being secondary to irreversible loss of cellular integrity in this context. As all three iron chelators studied in this chapter had only minor effects on mitochondrial function, but significantly reduced post ischaemic lipid peroxidation and

improved the morphological appearance of the cortex, their mode of action may have been related to improvements in cellular integrity. Improvements in cellular integrity alone do not therefore necessarily correlate with long term renal function.

6.6 Conclusions

(i) Hypothermic storage of NZW rabbit kidneys for 72 h resulted in severe mitochondrial dysfunction within the first 5 min of reperfusion.

(ii) Neither "extracellular" nor "intracellular" iron chelation improved mitochondrial function despite both types of chelator having highly significant ($p<0.005$) ameliorative effects on susceptibility to lipid peroxidation and cortical intracellular oedema.

(iii) Iron delocalization is unlikely to be a critical determinant of mitochondrial function during reperfusion of hypothermically stored transplanted kidneys, but may contribute to loss of cellular integrity.

(iv) Cellular integrity during early reperfusion and long-term viability do not necessarily correlate.

CHAPTER 7

THE EFFECT OF INHIBITION OF LIPOXYGENASE USING A SPECIFIC IRON CHELATOR

The studies presented in this chapter are based on a paper published in:
*Transplantation 1994; **58:** 1303-1308.*

7.1 Introduction

In Chapter 6, it was shown that iron chelation reduced susceptibility to lipid peroxidation and improved the morphological appearance of the cortex, but did not affect mitochondrial function, medullary congestion or long term viability. Mitochondrial dysfunction was demonstrated within the first 5 min of reperfusion, and did not appear to be causally related to medullary congestion or secondary ischaemia. It was suggested that mitochondrial dysfunction could have been mediated by increased calcium cycling, in line with reports of others (Hardy *et al.*, 1991; McAnulty *et al.*, 1991; Richter, 1993).

Calcium activation of phospholipases during or immediately after long-term preservation may damage mitochondria or other organelles as a result of enzymatic catabolism of cell membranes (McAnulty *et al.*, 1991). Phospholipase A_2 activity results in release of arachidonic acid, which can be metabolised by cyclooxygenase, lipoxygenase or cytochrome P-450 to form a variety of products including hydroperoxides, leukotrienes, prostaglandins and thromboxanes (Lefer, 1985; Frazier and Yorio, 1992; see Chapter 1). Small amounts of lipid hydroperoxide can be amplified by the arachidonate-lipoxygenase combination, generating more lipid peroxide (Lands, 1986). Such feedback amplification may produce a vigorous cellular response to oxygen radicals, mediated by eicosanoids binding to specific cellular receptors. Thus oxy-radicals could stimulate highly selective cellular responses rather than simply random destructive radical degradations (Lands, 1986).

It was shown some years ago that the use of desferrioxamine in conjunction with indomethacin, a potent inhibitor of cyclooxygenase, significantly improves renal function and long-term viability (Gower *et al.*, 1989). More recently it has been reported that inhibition of phosholipase A_2 and cyclooxygenase has a beneficial effect on viability of transplanted dog kidneys following prolonged

storage (Schilling *et al.*, 1993). The role of lipoxygenase in ischaemia-reperfusion injury is more equivocal. It has been suggested that leukotriene B_4, a powerful chemoattractant for neutrophils, plays a central role in post ischaemic renal injury (Linas *et al.*, 1988; Klausner *et al.*, 1989). However, studies using the selective 5-lipoxygenase inhibitor diethylcarbamazine have not precluded the possibility that it acts simply as an antioxidant (Klausner *et al.*, 1989). Nevertheless, it is possible that combined inhibition of lipoxygenase and chelation of catalytic iron, using a novel single agent, could ameliorate ischaemia-reperfusion injury in the NZW rabbit renal autograft model.

Compound BW B70C (E-N-(3-(3-(4-fluorophenoxy) phenyl)-1 (R,S)-methylprop-2-enyl)-N-hydroxyurea) is a potent inhibitor of leukotriene B_4 synthesis *in vitro* and *in vivo*, with an IC_{50} of 0.1 μM (Salmon and Garland, 1991). BW B70C is the hydroxyurea analogue of a key acetohydroxamic acid BW A360C. The hydroxyurea moiety is less readily metabolised to the glucuronide than the acetohydroxamate so plasma levels remain higher and the duration of inhibition of 5-lipoxygenase is longer. In rabbits, an oral dose of 10 mg/kg resulted in complete inhibition of LTB_4 formation in A23187-stimulated whole blood *ex vivo* for 12 h (compared with 8 h for BW A360 C) (Salmon and Garland, 1991). The mode of action of BW B70C is uncertain, but it seems likely that it acts as a site directed peroxyl radical scavenger. In addition, it has been shown to act *in vitro* as an iron chelator and free radical scavenger (Salmon and Garland, 1991).

7.2 Objective

The aims of this chapter were to:

(i) Establish the efficacy of BW B70C in inhibiting 5-lipoxygenase in the NZW rabbit renal autograft model.

(ii) Establish the significance of leukotriene B_4 mediated inflammatory damage *per se* in the transplanted stored kidney.

7.3 Methods

7.3.1 Methodology

A total of 48 adult female NZW rabbits (2.5-3 kg) were anaesthetized by an i.m. injection of fentanyl fluanisone followed by slow injection of diazepam; oxygen (2 L/min) was supplied via an open face mask (see Chapter 2). Kidneys were flushed with ice-cold (0-2^{0}C) HCA and stored in HCA (or HCA containing BW B70C) at 0-2^{0}C for 48 h prior to autografting. The 48 h preservation period was adopted in the studies presented in this chapter in order to maximise the threshold of recovery while nevertheless causing substantial ischaemia-reperfusion injury.

Renal vein serum eicosanoid levels were assayed by ELISA as described in Chapter 2. Leukotriene B_4 mediation of vascular permeability was evaluated by colloidal carbon labelling and of inflammation by histological analysis (light and electron microscopy). Serum levels of thromboxane b_2 (the breakdown product of TxA_2, a potent vasoconstrictor and inflammatory mediator) and 6-keto-prostaglandin $F_{1\alpha}$, a breakdown product of prostacyclin, a vasodilator and physiological mediator of renal blood flow and ion pump function) were also measured to determine whether inhibition of lipoxygenase enhanced cyclooxygenase metabolism. The effect of BW B70C on the long-term function and viability of autografted single stored kidneys was assessed by measurement of serum creatinine and urea levels and monitoring of the long-term survival of the animals (see Chapter 2 for details of all methodologies used).

7.3.2 BW B70C Dosage and Experimental Groups

BW B70C (10 mg/kg in 0.25% w/v carboxy-methylcellulose) was administered orally (via a stomach line) 12 h and 1 h prior to autografting and at a concentration of 15 μM in the flush/preservation solution (Group 2). Controls (Group 1) were treated with vehicle only.

Measurements of renal pathophysiology were made in 4 subgroups of 12 animals (6 in Group 1 and 6 in Group 2):

(i) Measurement of renal vein serum [LTB_4], [6-k-$PGF_{1\alpha}$] and [TxB_2] after 10 and 30 min, 1, 2, 4 and 6 h of reperfusion (see Chapter 2 for details). After 6 h of reperfusion, renal morphology was evaluated using light and electron microscopy

(ii) Measurement of peri-vascular penetration of infused colloidal carbon after 30 min of reperfusion to give an indication of vascular permeability (see Chapter 2)

(iii) Evaluation of inflammatory infiltrate and renal histopathology 3 days after revascularization

(iv) Determination of long-term viability (see Chapter2).

7.4 Results

7.4.1 ELISA Assays of Serum Eicosanoid Concentrations

In Group 1 kidneys (untreated with BW B70C) 48 h hypothermic storage and transplantation of kidneys resulted in a significant elevation in renal vein serum LTB_4 levels from 235 ± 77 pg/ml after 10 min reperfusion to 2092 ± 282 pg/ml after 30 min ($p<0.05$, n=4; Fig 7.4). After 2 h, LTB_4 levels had dropped significantly to a plateau value of 288 ± 22 pg/ml ($p<0.05$, n=4) which remained steady for the following 4 h. In Group 2 kidneys, treatment with BW B70C caused a significant reduction in

LTB_4 serum levels at 30 min and 1 h to 131 ± 13 pg/ml ($p<0.01$, n=4) and 157 ± 17 pg/ml ($p<0.01$, n=4) respectively. Thereafter, serum levels were similar to Group 1.

Serum 6-k-$PGF_{1\alpha}$ concentration increased significantly after 1 h of reperfusion in Group 1 animals from 523 ± 66.5 pg/ml at 1 h to 2092 ± 115 pg/ml after 6 h ($p<0.05$, n=4; Fig 7.5). In Group 2 (BW B70C treated) animals there was a slight but significant delay in the increase in 6-k-$PGF_{1\alpha}$ after 1 h compared with Group 1 animals ($p<0.05$, n=4). In Group 1, 6-k-$PGF_{1\alpha}$ concentration was 1673 ± 326.5 pg/ml (n=4) after 2 h compared with 993 ± 90 pg/ml (n=4) in Group 2 animals. In Group 1, TxB_2 concentrations remained steady at approximately 300 - 400 pg/ml for the 6 h of reperfusion measured (n=4; Fig 7.6). There were no significant differences between controls and BW B70C treated animals.

7.4.2 Histology After 6 h Reperfusion

Control kidneys (Group 1) exhibited moderate to severe (3-4) cortical oedema and mild (2) congestion (6 of 6 kidneys). There was no frank necrosis or haemorrhage. BW B70C treatment had no apparent effect on the severity of cortical oedema at this time point (in 6 of 6 kidneys). Surprisingly, both the degree of congestion and the incidence of haemorrhage were significantly exacerbated by BW B70C treatment ($p<0.05$, n=6 in each group; Fig 7.7). Congestion was moderate to severe (3-4) and there was minimal to mild (1-2) haemorrhage in 6 of 6 of the BW B70C treated kidneys.

7.4.3 Estimation of Vascular Permeability

In Group 1 kidneys, perivascular-trapped carbon was detectable by light microscopy in a narrow but continuous band in the cortico-medullary junction area (n=6; Plate 7.1). In all cases, peri-vascular carbon penetration was mild to moderate (2-3). Elsewhere in the kidney, perivascular carbon retention was minimal or absent (in 6 of 6 kidneys). Treatment with BW B70C had no observable effect on either peri-vascular carbon penetration or intra-renal distribution (in 6 of 6 kidneys).

7.4.4 Estimation of Inflammatory Infiltrate and Renal Histopathology

Group 1 kidneys exhibited mild tubular necrosis and patchy or wide-spread calcification by light microscopy (Fig 7.8; Plate 7.2). Both frank tubular necrosis and calcification were significantly reduced by BW B70C treatment ($p<0.05$, n=6 in each group; Fig 7.8; Plate 7.3). These observations were confirmed by electron microscopical analysis. In Group 1 kidneys, the proximal tubules exhibited severe blebbing, intraluminal vacuolation, nuclear margination and condensation, and degeneration of cellular organelles (Plate 7.4). In Group 2 kidneys, the proximal tubules (particularly

the S3 segments) were well preserved, with intact brush borders, and minimal cellular or mitochondrial swelling. Cristae structures were well defined and regularly spaced (Plate 7.5).

There was very little inflammatory infiltrate in any specimen, so it was not possible to demonstrate a discernable inhibition by BW B70C.

7.4.5 Survival Determination

BW B70C treatment did not improve the long-term viability of transplanted 48 h stored kidneys. In 3 of 6 Group 1 rabbits therewere no symptoms of renal failure after 3 weeks compared with 2 of 6 Group 2 animals (as shown in chapter 3, 48 h hypothermic storage of kidneys results in approximately 50% post-operative survival). There were no obvious beneficial or deleterious effects of BW B70C either in terms of graded physiological function (serum urea and creatinine levels) or in the subsequent histological appearance of the kidneys. In BW B70C treated animals, peak serum creatinine was 2016 ± 286 μM compared with 1785 ± 390 μM in untreated controls (Fig 7.9). Peak serum urea values in BW B70C treated animals were 45.2 ± 15.3 mM, and 37.2 ± 6.3 mM in untreated controls (Fig 7.10). There were no significant differences between these values.

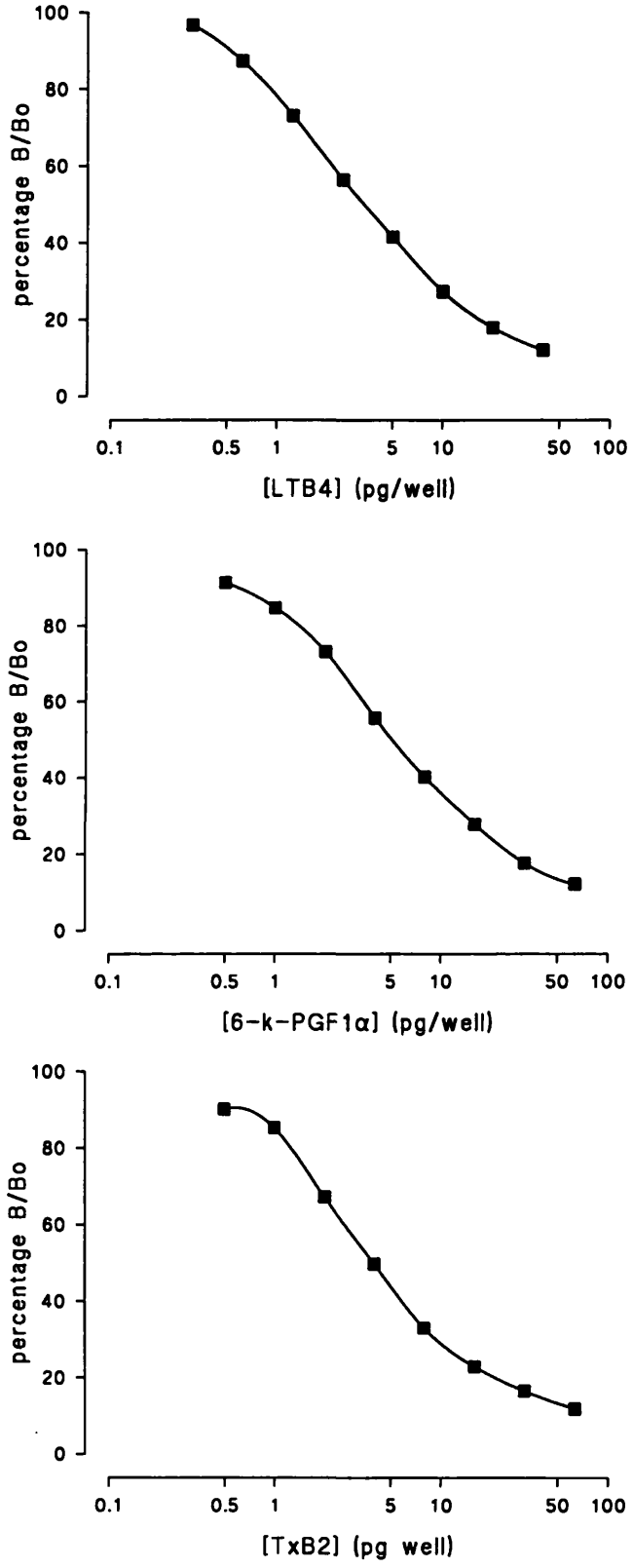

Figs 7.1-3
Standard curves for LTB_4 (top), 6-k-$PGF_{1\alpha}$ (middle) and TxB_2 (bottom): $\%B/B_0$ (percentage of bound ligand for each standard) is plotted as a function of the log eicosanoid concentration per well (pg). Each point is the mean of duplicate determinations.

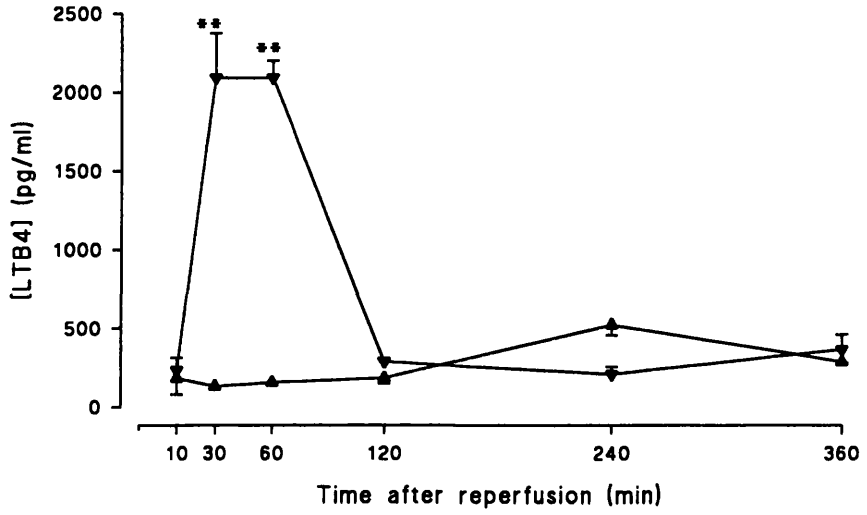

Fig 7.4 LTB_4 concentration in serum samples taken directly from the renal vein at 10, 30, 60, 120, 240 and 360 min after reperfusion. The results show highly significant reductions in serum [LTB_4] by BW B70C over the first 30 to 60 min of reperfusion. ▼ = Group 1 (control); ▲ = Group 2 (BW B70C treated). Results are presented as mean ± SEM (n=4). $^{**}p<0.005$.

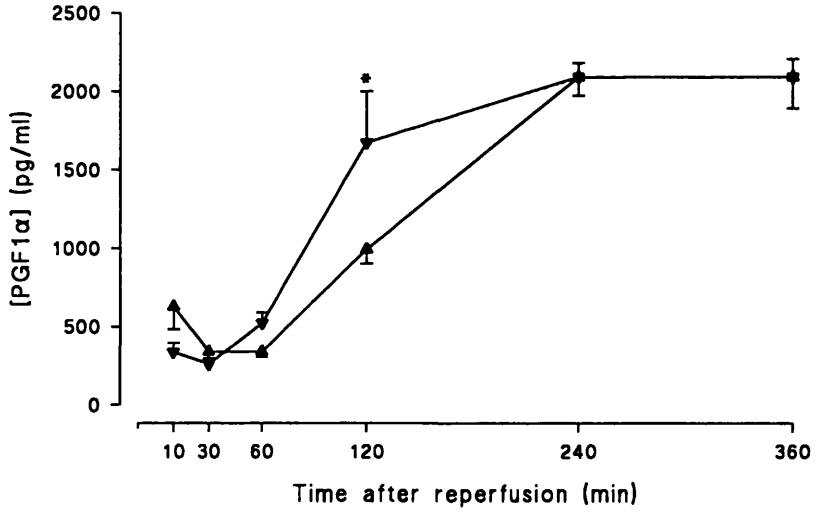

Fig 7.5 6-k-$PGF_{1\alpha}$ concentration in serum samples taken directly from the renal vein at 10, 30, 60, 120, 240 and 360 min after reperfusion. The results show significant increases in serum [6-k-$PGF_{1\alpha}$] in both groups after 60 min of reperfusion but occurring more slowly in animals treated with BW B70C. ▼ = Group 1 (control); ▲ = Group 2 (BW B70C treated). Results are presented as mean ± SEM. $^{*}p<0.05$.

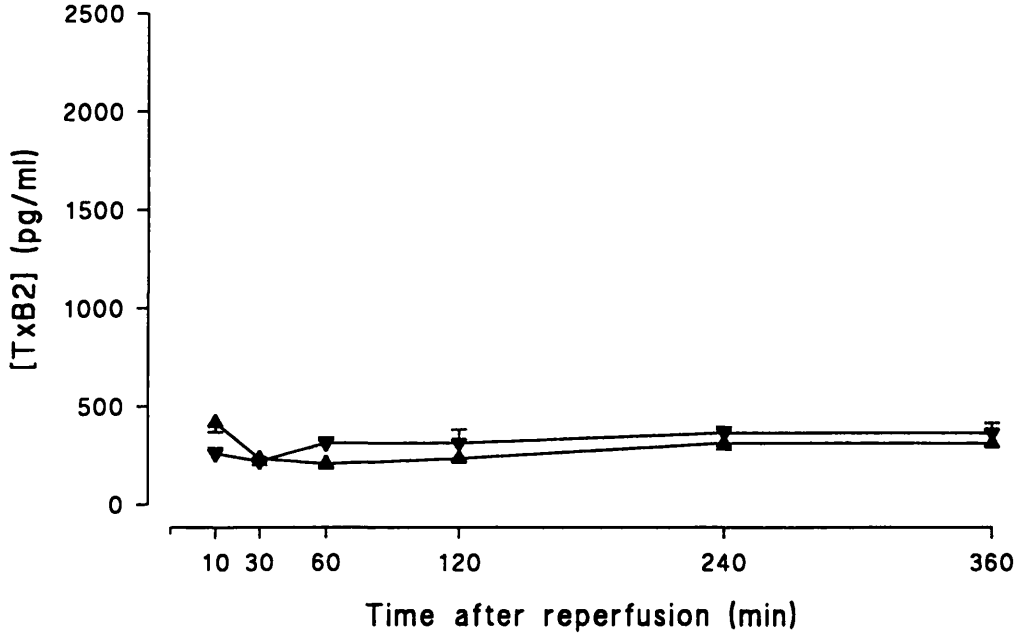

Fig 7.6 TxB_2 concentration in serum samples taken directly from the renal vein at 10, 30, 60, 120, 240 and 360 min after reperfusion. The results show no change in serum [TxB_2] during the 6 h of reperfusion. ▼ = Group 1 (control); ▲ = Group 2 (BW B70C treated). Results are presented as mean ± SEM.

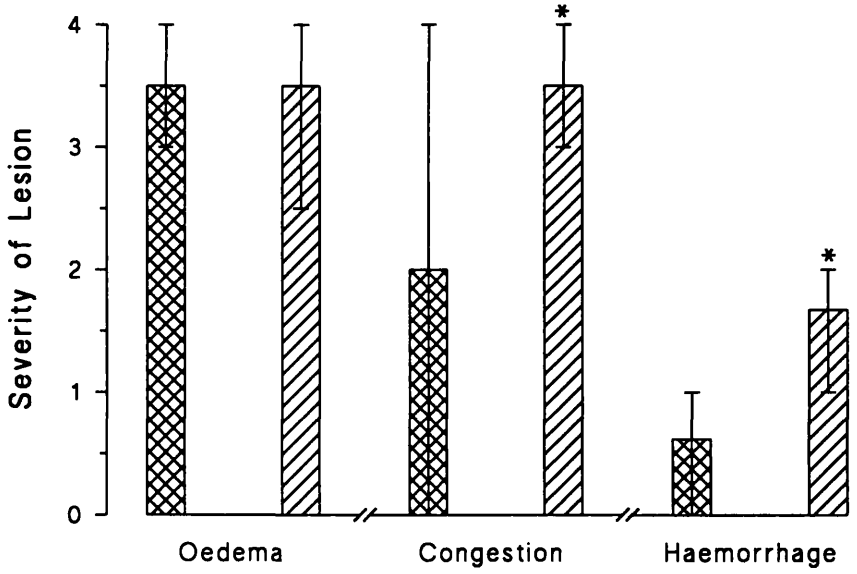

Fig 7.7 Severity of cortical intracellular oedema, congestion and haemorrhage following 48 h of storage and 6 h of reperfusion in Group 1 (control, checked bars) and Group 2 (BW B70C treated, hatched bars) kidneys. The results show that BW B70C significantly exacerbated both medullary congestion and haemorrhage. Results are presented as mean ± range (n=6). *$p<0.05$.

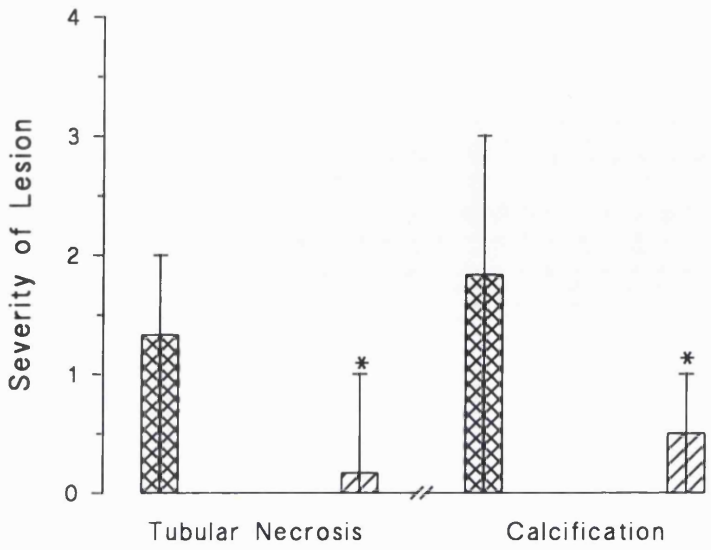

Fig 7.8 **Severity of tubular necrosis and calcification in the renal cortex following 48 h storage and 3 days reperfusion in Group 1 (control, checked bars) and Group 2 (BW B70C treated, hatched bars) kidneys. The results show that BW B70C had a significant protective effect on tubular necrosis and calcification 3 days after revascularization. Results are presented as mean ± range (n=6). *$p<0.05$.**

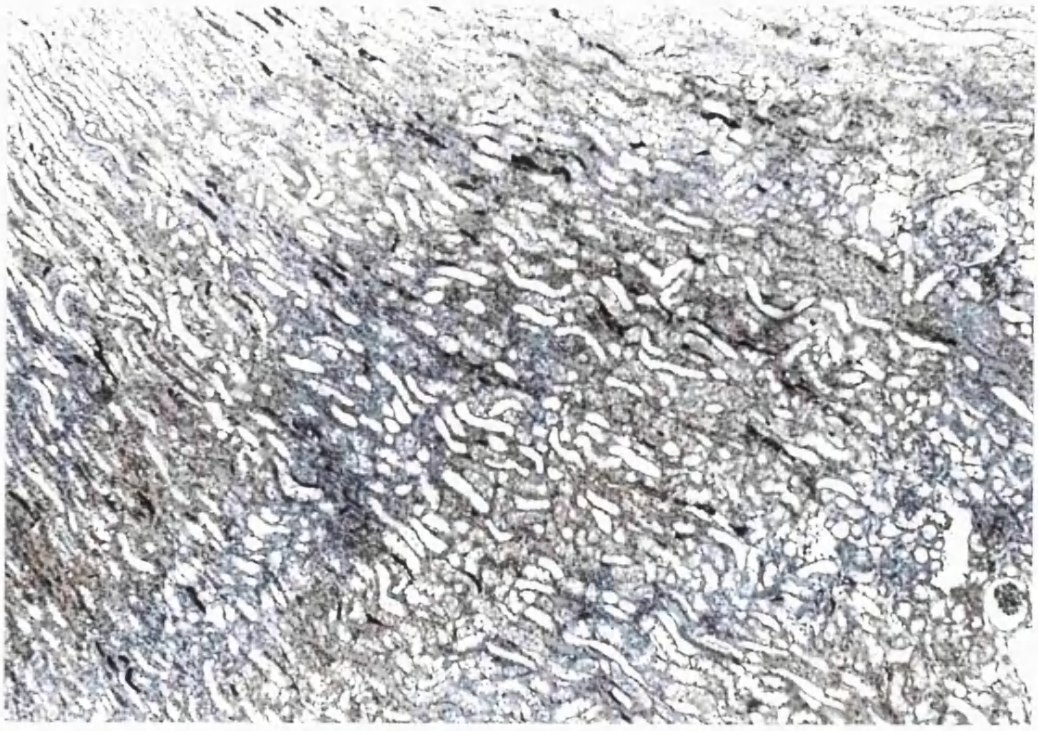

Plate 7.1 **Light micrograph of peri-vascular colloidal carbon penetration in the cortico-medullary junction of a Group 1 (untreated) kidney after 30 min of reperfusion (magnification x 40).**

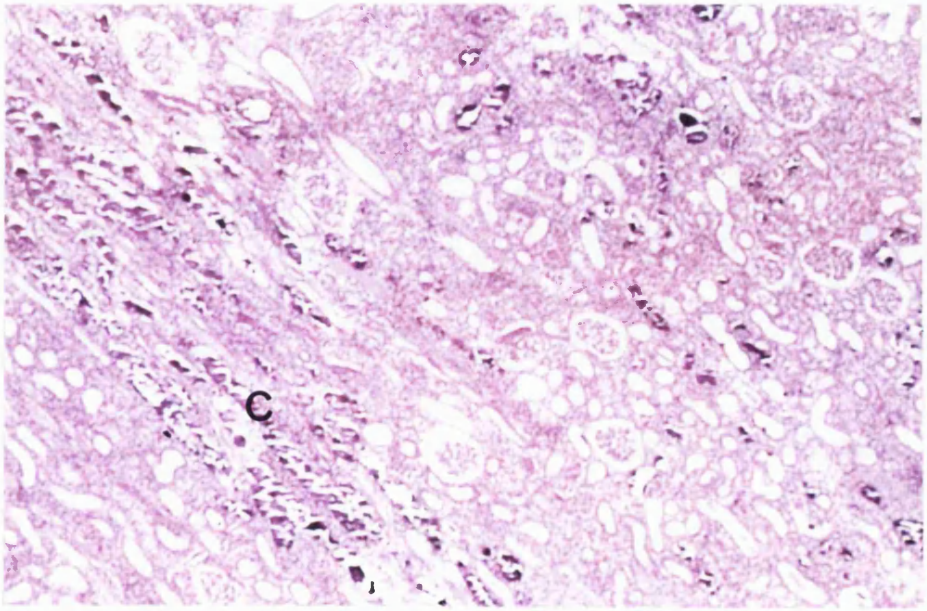

Plate 7.2 Light micrograph of the renal cortex of a Group 1 (untreated) kidney 3 days after revascularization showing widespread cortical calcification (C) (magnification x 60).

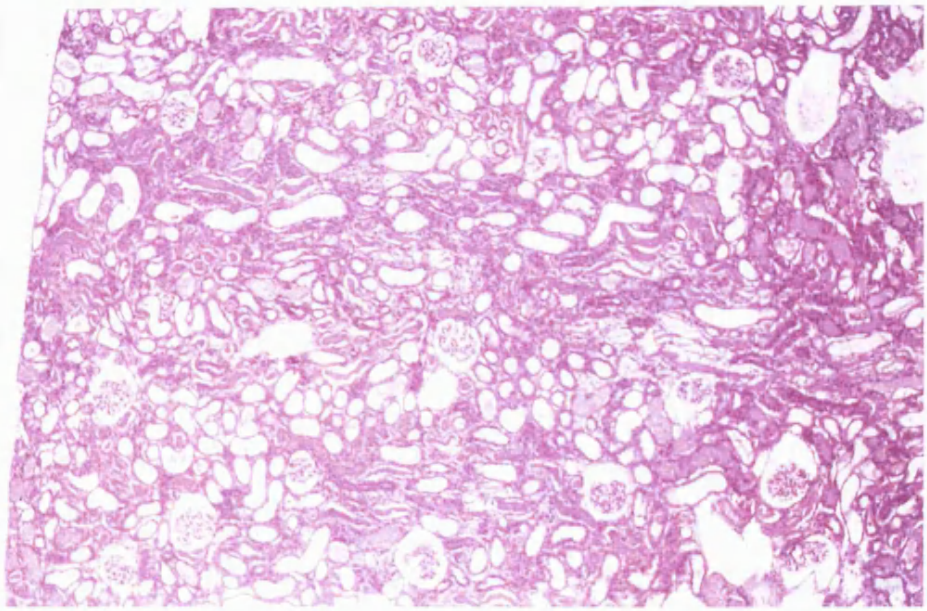

Plate 7.3 Light micrograph of the renal cortex of a Group 2 (BW B70C treated) kidney 3 days after revascularization showing well preserved tubular structure (magnification x 40).

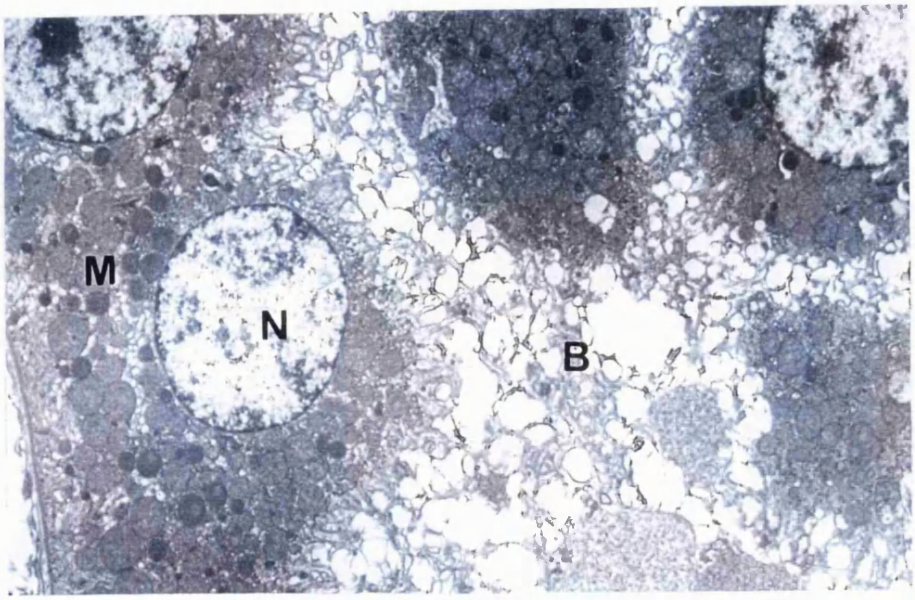

Plate 7.4 **Electron micrograph of cortical proximal tubules in a Group 1 (untreated) kidney 3 days after revascularization (magnification x 5,000), showing loss of nuclear material (N), swollen mitochondria (M) and loss of brush border (B).**

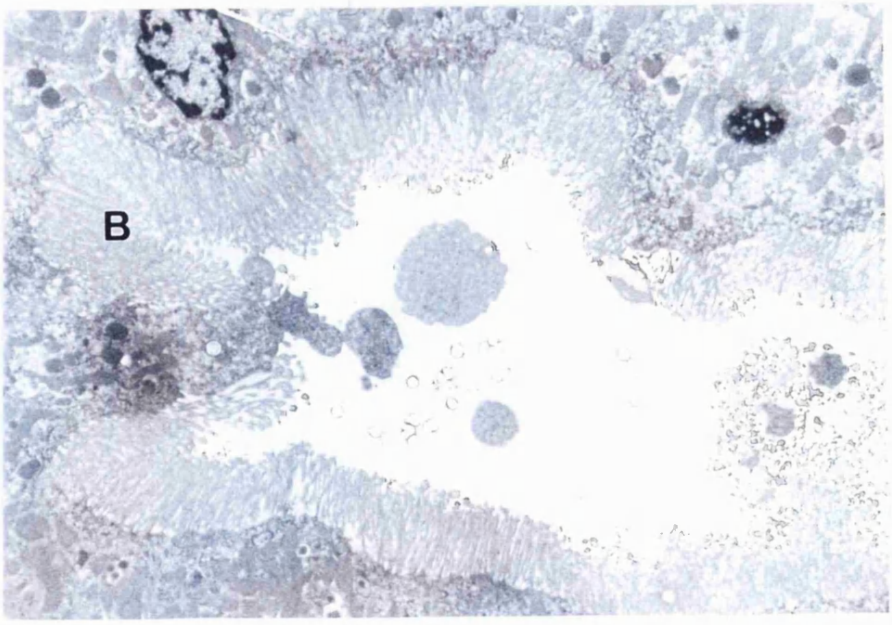

Plate 7.5 **Electron micrograph of cortical proximal tubules in a Group 2 (BW B70C treated) kidney 3 days after revascularization (magnification x 5,000), showing intact brush border (B), normal nuclear appearance (N) and unswollen mitochondria.**

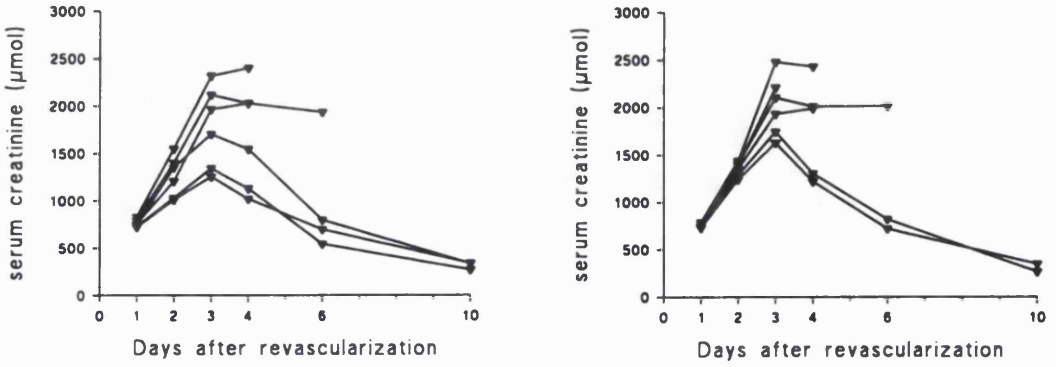

Fig 7.9 Concentration of serum creatinine in Group 1 (left) and Group 2 (right) kidneys. ▼ represents values for a single animal.

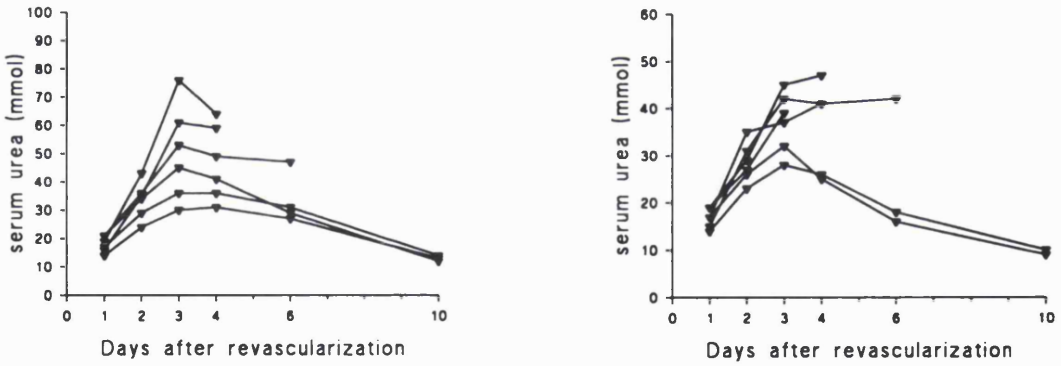

Fig 7.10 Concentration of serum urea in Group 1 (left) and Group 2 (right) kidneys. ▼ represents values for a single animal.

7.5 Discussion

The results presented in this chapter demonstrate that inhibition of LTB_4 synthesis in this model of renal storage and transplantation does not prevent the development of acute renal failure. This conclusion is based on the ELISA data demonstrating a significant elevation in LTB_4 levels 30 min after reperfusion and the inhibition of this rise by BW B70C (Fig 7.4). A similar elevation in LTB_4 levels has been reported previously using radioimmunoassay following renal pedicle occlusion (Klausner *et al.*, 1989). It is possible that the LTB_4 antibody cross-reacted with unknown plasma lipids or proteins but the complete inhibition by BW B70C to near background levels makes this unlikely. A second factor is the delay in increase of LTB_4 levels - there was no change in LTB_4 levels during the first 10 min of reperfusion (Fig 7.4). Although there are reports of 12- and 15-lipoxygenase activity in the renal cortex (Winokur and Morrison, 1981; Lianos *et al.*, 1985; Frazier and Yorio, 1992) there are no reports of 5-lipoxygenase activity (Frazier and Yorio 1992) and subsequent leukotriene production by renal tissue. The source of LTB_4 is therefore likely to have been activated neutrophils and a delay in neutrophil accumulation and activation may account for the delay in serum LTB_4 elevation. As a large influx of neutrophils was not observed using light microscopy, it is possible that release of LTB_4 from neutrophils occurred before neutrophil rolling and adhesion.

Unlike Klausner *et al.* (1989) and Lelcuk *et al.* (1985) a significant increase in TxB_2 levels during reperfusion was not detected (Fig 7.6). One possible explanation for this is that both these studies dealt with kidneys in which ischaemia was induced by clamping of the renal pedicle. The vasculature was therefore congested with erythrocytes and other blood cells throughout the period of warm ischaemia and as discussed in Chapter 3 this scenario is very different from the cold ischaemic/HCA flush model discussed here. It has been argued that TxA_2 is an essential mediator of reperfusion injury (Lelcuck *et al.*, 1985), and Klausner and co-workers (1989) demonstrated that TxA_2 synthesis was neutrophil dependent rather than platelet dependent. This is curious since if the source of LTB_4 in the present study was indeed activated neutrophils, one would expect a concommittant rise in TxB_2 levels. However, this was not observed (Fig 7.6). TxA_2 is a potent vasoconstrictor and platelet aggregator. Despite this, there is little evidence of thrombocyte aggregation or fibrin deposition in post-ischaemic kidneys and heparinization prior to ischaemia does not prevent vascular congestion (Sheehan and Davis, 1959; Ratych and Bulkley, 1986; Mason *et al.*, 1989). These observations must cast doubt on the role of thromboxane A_2 as a mediator of ischaemia-reperfusion injury in kidneys stored for 48 h prior to transplantation.

In contrast, serum 6-k-$PGF_{1\alpha}$ concentration increased significantly after 1 h of reperfusion in both controls and in BW B70C treated animals, albeit more slowly in Group 2 (Fig 7.5). 6-k-$PGF_{1\alpha}$ is a

breakdown product of prostacyclin, a vasodilator. Lelcuk *et al.* (1985) reported that ischaemia and reperfusion resulted in an imbalance of eicosanoid synthesis in favour of vasoconstriction. In this study, the ratio of TxB_2/6-k-$PGF_{1\alpha}$ was much higher (0.60 ± 0.22, n=4) during the first 1 h of reperfusion than after 2 h (0.19 ± 0.11, n=4) or 6 h (0.17 ± 0.13, n=4). These data are therefore in accordance with those of Lelcuk and colleagues. It is interesting that the increase in 6-k-$PGF_{1\alpha}$ concentration after 1 h correlates with improved renal perfusion as medullary congestion clears (Lane *et al.*, 1994 and Chapter 4) It is possible that improved medullary blood flow, which is not a consequence of vasodilation in the medulla but rather of a reduction in medullary oedema (Mason *et al.*, 1989) results in increased prostacyclin synthesis in the medulla and consequently vasodilation of the cortical arterioles. Prostacyclin is also capable of activating cAMP-dependent protein kinase in endothelial cells, thereby stimulating the augmentation of endothelial cytoskeletal fibres and consequently reducing vascular permeability (Killacky *et al.*, 1986; Alexander *et al.*, 1988; Casnocha *et. al.*, 1989) and of inhibiting adenylate cyclase in mTAT cells (see also Chapter 10) thereby reducing active Na^+Cl^- reabsorption (Greger, 1985; Smith, 1987; Frazier and Yorio, 1992). Similar alterations are mediated by the loop diuretic frusemide and are considered in Chapter 9.

BW B70C treatment resulted in significantly worse medullary congestion and haemorrhage after 6 h of reperfusion compared to Group 1 (Fig 7.7). These results were startling on preliminary consideration. However, recently there have been reports that renal epithelial cell K^+, Na^+ and Cl^- ion channels are modulated by lipoxygenase intermediates via a G protein $G_{\alpha i}$ subunit (Cantiello *et al.*, 1990; Scherer and Breitwieser, 1990; Frazier and Yorio, 1992,). Inhibition of 5-lipoxygenase with nordihydroguaiaretic acid (NDGA) resulted in an inhibition of Na^+ channel activity which was restored on addition of LTD_4 or the parental leukotriene substrate 5-HPETE (Cantiello *et al.*, 1990). These studies have been concerned in the main with apical ion channel regulation in polarized epithelial cells. However, patch-clamp experiments involving the inwardly rectifying K^+ current in isolated bullfrog atrial cells have shown similar G protein modulation by arachidonic acid metabolites (Scherer and Breitwieser 1990). Thus, it seems likely that regulation of ion channel activity may be a common mechanism shared by some lipoxygenase products (Frazier and Yorio, 1992 and Chapter 1).

These findings offer a possible explanation for the exacerbation of vascular congestion and haemorrhage by BW B70C reported here. It is established that medullary congestion is a result of oedematous swelling of the medullary thick ascending tubule (mTAT) in the outer band of the outer medulla (Mason *et al.*, 1989 and Chapter 3). It is known moreover that significant Na^+, K^+ and Cl^- reabsorption occurs in the mTAT (Greger, 1985). It is conceivable that inhibition of basolateral but not apical ion pump function in these tubules by BW B70C could prolong their recovery from

intracellular oedema and thereby exacerbate congestion and haemorrhage. This hypothesis is supported by the fact that BW B70C treatment also slightly delayed the rise in 6-k-$PGF_{1\alpha}$ levels after 1 h of reperfusion (Fig 7.5). As noted already, this rise appeared to correlate inversely with the severity of oedema and clearance of medullary congestion (see Chapter 4). However, this rather speculative conclusion assumes that Na^+-pump function is not severely compromised and that mitochondrial function is sufficient to provide for the energy expenditure of the Na^+- pumps as well as other vital cellular functions. This may be true following the relatively short 48 h renal storage prior to autografting in the studies presented in this chapter but must be equivocal following 72 h storage in the light of the results presented in Chapter 6.

These results were unexpected since LTB_4 is known to stimulate vascular permeability. The vascular labelling studies reported here showed no difference in vascular permeability between controls and BW B70C treated kidneys. From this and the fact that mTAT swelling occurs during rather than after ischaemia (Mason *et al.*, 1989 and Chapter 3) it seems likely that damage to the endothelium had occurred during the storage period itself. Oedema remains perhaps the most serious obstacle to prolonged renal storage. The relative success of preservation solutions such as the University of Wisconsin solution may be a consequence of the effectiveness of the impermeants raffinose and lactobionate (Wahlberg *et al.*, 1986). It has been shown that mannitol, the impermeable constituent of HCA is permeable to the renal tubules after severe ischaemia (Ruka *et al.*, 1978) and is in any case more freely permeable than raffinose (Wahlberg *et al.*, 1986). It is possible that inhibition of 5-lipoxygenase would be of greater value if mTAT swelling was prevented by use of a more effective impermeant. The studies presented in Chapter 9 evaluate the possible therapeutic benefits that may be achieved by substitution of impermeant solutes.

After 3 days of reperfusion there was very little inflammatory infiltrate in any of the control or BW B70C treated kidneys. Neutrophils are seldom observed by routine histological methods in ischaemic kidneys, but intra-vital microscopy of neutrophil entrapment and adherence suggests that a few neutrophils may induce significant functional disturbance by obstructing individual capillaries in a stochastic fashion (Schmid-Schonbein 1987). The delayed burst of LTB_4 synthesis during early reperfusion would also tend to support this view. However, the negligible inflammation after 3 days of reperfusion was surprising as by this time there was wide-spread tubular necrosis and calcification in control kidneys (Fig 7.8 and Plate 7.2).

Treatment with BW B70C significantly reduced both tubular necrosis and calcification at this time point (Fig 7.8 and Plate 7.3) but it was not possible to demonstrate an inhibition of inflammation.

These findings suggest that BW B70C may be acting as an intra-cellular iron chelator or free radical scavenger within the proximal tubule, or could have supressed lipoxygenase-mediated amplification of lipid hydroperoxides (which would occur predominantly in the renal cortex; see Chapter 1). If this is the case, it is curious that BW B70C had no effect on oedema of the proximal tubule after 6 h of reperfusion. However, it has previously been demonstrated that a novel hexadentate iron chelator, CP130 reduced cortical oedema following 45 min of warm ischaemia but only after 1 h of reperfusion (Gower *et al.*, 1993). Oedema is a reversible cell injury and progression from oedema to necrosis is dependent upon irreversible damage to membrane integrity, membrane protein function, mitochondrial function, intracellular signalling mechanisms or DNA (Farber *et al.*, 1981). It is possible therefore that BW B70C ameliorated iron- or lipoxygenase-dependent irreversible injury to the proximal tubule. The fact that this did not improve the long-term viability of transplanted 48 h stored kidneys may be a corollary of early reperfusion damage to the medulla, which might possibly have been exacerbated by cyclooxygenase-mediated amplification of lipid hydroperoxides, delayed elevation of serum prostacyclin levels leading to depression of cAMP-dependent cytoskeletal augmentation in the endothelium and stimulation of $Na^{+}Cl^{-}$ reabsorption (Killacky *et al.*, 1986; Alexander *et al.*, 1988; Casnocha *et. al.*, 1989) or failure to improve mitochondrial function.

7.6 Conclusions

(i) BW B70C alone did not improve renal viability following 48 h storage.

(ii) BW B70C treatment resulted in a significant inhibition of LTB_4 synthesis in this model of ischaemia-reperfusion injury.

(iii) Inhibition of LTB_4 synthesis did not influence long term graft viability.

(iv) Inhibition of LTB_4 synthesis did not affect vascular permeability following 48 h cold ischaemia.

(v) BW B70C treatment resulted in significant amelioration of acute tubular necrosis in the renal cortex, which may have been the result of an antioxidant/iron binding effect.

CHAPTER 8

EBSELEN: THE EFFECT OF A NON-IRON CHELATING ANTIOXIDANT ON RENAL PRESERVATION

The studies presented in this chapter are based on a paper published in:
Biochemical Pharmacology 1992; 43: 2341-2348.

8.1 Introduction

In Chapter 7, it was shown that inhibition of lipoxygenase using a novel site-directed peroxyl radical scavenger (BW B70C) did not prevent the development of acute renal failure. However, BW B70C did significantly reduce the severity of both acute tubular necrosis and calcification in the renal cortex 3 days after revascularization. It was suggested that BW B70C could have suppressed lipoxygenase-mediated feedback amplification of lipid peroxides (Lands, 1986). Lipoxygenase activity is associated with glomerular epithelial and mesangial cells in the renal cortex (Jim *et al.*, 1982). In contrast, cyclooxygenase is expressed predominantly in the interstitial cells, thin descending limbs and collecting ducts of the medulla (Frazier and Yorio, 1992). Since BW B70C actually exacerbated ischaemia-reperfusion damage in the medulla a similar feedback amplification system involving cyclooxygenase rather than lipoxygenase, and therefore uninhibited by BW B70C, may have been operating in the renal medulla.

Ebselen (PZ 51, 2-phenyl-1,2-benzisoselenazol-3-(2H) one) is a seleno-organic compound with both antioxidant and anti-inflammatory properties (Sies, 1994). In addition to displaying a glutathione peroxidase-like activity at physiological concentrations of glutathione (Müller *et al.*, 1984) ebselen has been shown to inhibit a range of enzymes involved in the inflammatory response, including:

(i) 5-lipoxygenase in rabbit reticulocytes, rat peritoneal neutrophils and human platelets in the absence of glutathione (Safayhi *et al.*, 1985; Kühl *et al.*, 1986; Schewe *et al.*, 1994)

(ii) Cyclooxygenase in human platelets (Kühl *et al.*, 1986)

(iii) NADPH cytochrome P-450 reductase in rat and mouse liver microsomes (Wendel *et al.*, 1986; Nagi *et al.*, 1989) and other flavin based components of the electron transport chain including NADH-cytochrome b_5 reductase (Nagi *et al.*, 1989)

(iv) Nitric oxide synthase in rabbit aorta rings (Zembowicz *et al.*, 1993).

The potential sites of interaction of ebselen in the oxidative cascades are shown in Figs 8.1 and 8.2.

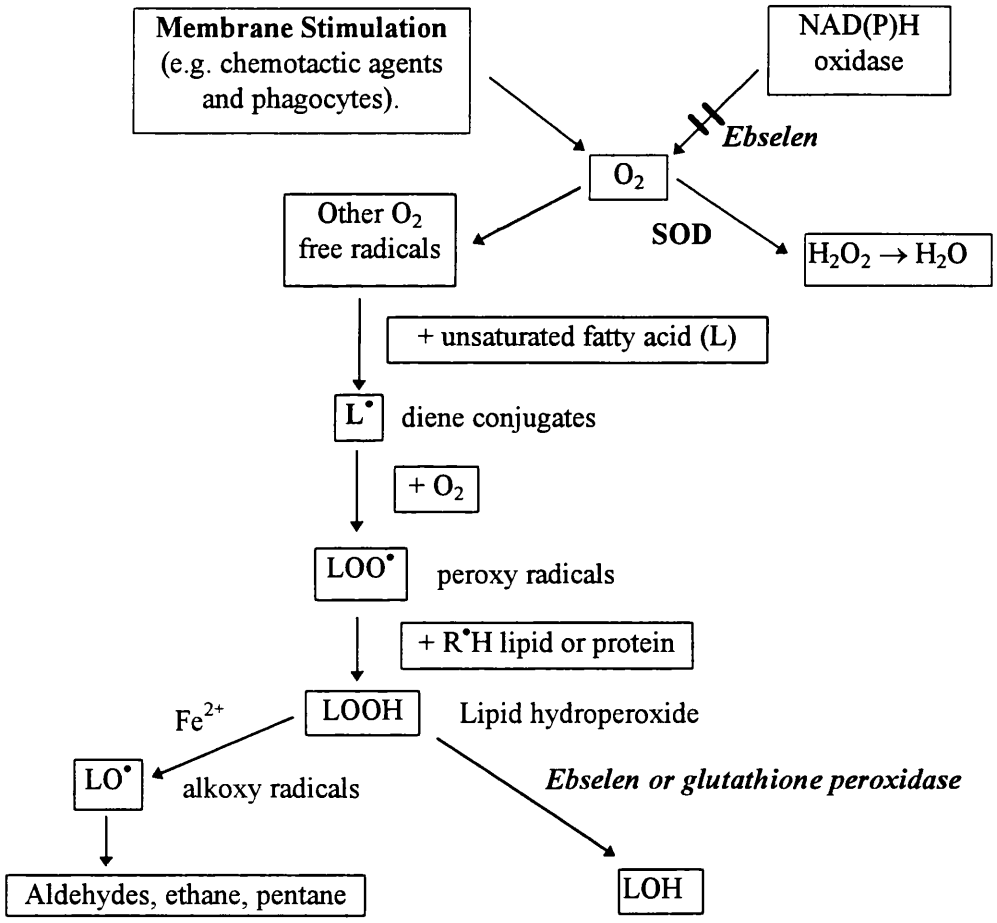

Fig 8.1 Inhibition of lipid peroxidation by ebselen.

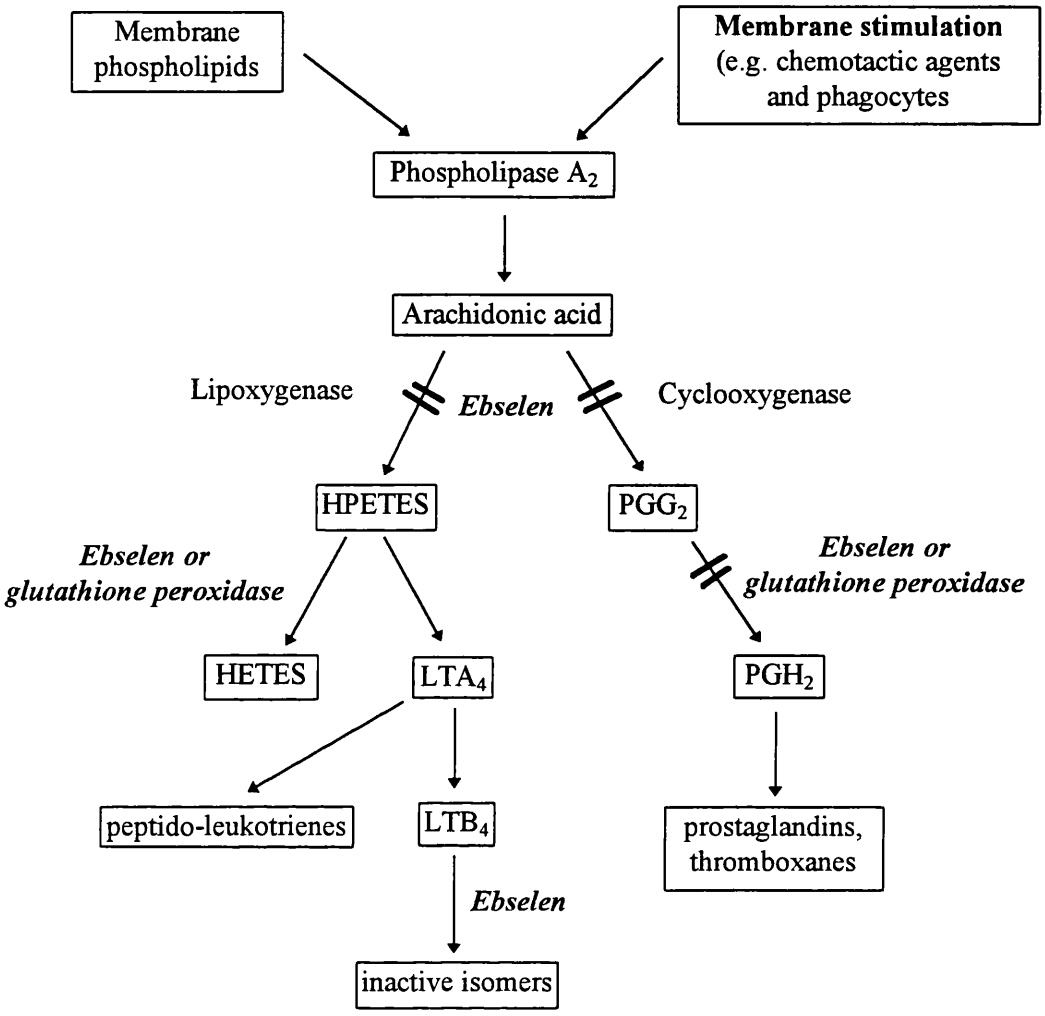

Fig 8.2 Interactions of ebselen in the eicosanoid cascade.

Thus, ebselen could act as a chain breaking anti-oxidant or glutathione peroxidase mimic to inhibit lipid peroxidation, or inhibit hydroperoxide amplification by inhibition of the fatty acid oxygenases. In addition, inhibition of electron transfer from cytochrome P-450 reductase could stabilize the P-450 system, and ameliorate release of haem iron during ischaemia (Paller and Jacob, 1994). There is no direct evidence of ebselen interacting with electron transfer in the mitochondrial respiratory chains, but it has been shown to reduce lipid peroxidation in mitochondrial membranes (Narayanaswami and Sies, 1990).

Unfortunately, ebselen is very rapidly metabolised *in vivo* and two principal products (metabolites I: 2-glucuronylselenobenzanilide and II: 4-hydroxy-2-methylselenobenzanilide) have been identified

(Terlinden *et al.*, 1988). The speed of transformation is so rapid that the parent drug is undetectable by HPLC in human, pig, rat or rabbit plasma following oral or intra-peritoneal administration (Terlinden *et al.*, 1988). The antioxidant capacity of the two principle metabolites is therefore of great practical importance unless a more effective means of presenting the untransformed drug is devised. The antioxidant activities of a range of related seleno-organic compounds have been tested on iron/ADP/ascorbate induced lipid peroxidation in rat liver microsomes and the two principal metabolites were found to be ineffective in this system (Narayanaswami and Sies, 1990). However, the iron/ADP/NADPH system was used in the present study, as the ability of ebselen and its metabolites to inhibit NADPH cytochrome P-450 reductase *in vitro* may be important in the context of renal preservation.

Despite the metabolic limitations of its *in vivo* usage, ebselen has been shown to reduce infarct size in the post-ischaemic myocardium (Hoshida *et al.*, 1994), to ameliorate experimentally induced lung injury and cerebral ischaemia in rats (Cotgreave *et al.*, 1988, Tanaka *et al.*, 1990) and to protect against galactosamine/endotoxin induced hepatitis in mice (Wendel and Tiegs 1986).

8.2 Objectives

The studies presented in this chapter were designed to:

(i) Determine the global antioxidant capacity of the major ebselen metabolites *in vitro*

(ii) Assess the efficacy of ebselen in reducing renal ischaemia-reperfusion injury.

8.3 Methods

8.3.1 Methodology

The antioxidant capacity of ebselen and its two major metabolites was tested *in vitro* in peroxidising rat liver microsomes, in which lipid peroxidation (detected by measurement of TBA-reactive material) was initiated by ferric sulphate/ADP/NADPH (see Chapter 2).

In the renal studies, a total of 22 adult female NZW rabbits (2.5 - 3 kg), in 5 groups (described below) were anaesthetized by an i.m. injection of fentanyl fluanisone and diazepam; oxygen was supplied via an open face mask (see Chapter 2 for full details). Kidneys were flushed with ice-cold (0-2^{0}C) HCA and stored in HCA (or HCA containing ebselen (100 μM in 0.1% ethanol (v/v) final)) at 0-2^{0}C for 48 or 72 h prior to measurement of susceptibility to lipid peroxidation or autografting for assessment of long term viability.

The effect of ebselen on the post-ischaemic formation of TBA-reactive material and Schiff's bases was investigated in kidneys stored for 0 or 72 h. Slices were taken from kidneys prior to homogenization for morphological evaluation using light microscopy. The effect of ebselen on long-term viability was determined by measurement of serum urea and creatinine levels in rabbits allowed to recover after autografting of kidneys stored for 48 h. The 72 h preservation period was chosen to facilitate comparisons of susceptibility to lipid peroxidation with the results of other chapters; the 48 h preservation time for survival studies was adopted as the expected 50% survival of renal grafts gives the clearest indication of any effect of ebselen, whether beneficial or deleterious. (An extra group of 72 h preserved kidneys was transplanted but survival was very poor in both groups (1 and 0 out of 6 respectively) and the results are not presented).

8.3.2 Drug Dosage

(i) *In vitro*. Ebselen (in 10µl DMSO, final concentrations of 1.6, 3.2 and 10µM) was added to the microsomal suspension (see Chapter 2) 5 min prior to initiation of peroxidation. Metabolites I and II were also dissolved in DMSO (10 µl) to produce final concentrations of 3.2, 10 and 50 µM

(ii) *In vivo*. During nephrectomy, ebselen (1 mM) was administered i.v. in 60 ml isotonic saline containing 3% cremophor (w/v) to achieve solubilization, using a Braun Perfusor VI pressure pump. Controls received vehicle only. Kidneys were stored at 0-2^{0}C for 48 or 72 h in HCA containing ebselen (100 µM in 0.1% ethanol (v/v) final). When rabbits were to be recovered in the course of survival studies, ebselen (1mM in 60 ml saline/3% cremophore) was infused i.v. at a rate of 120 ml/h, starting 15 minutes prior to reperfusion.

8.3.3 Experimental Groups

Group 1: Freshly nephrectomized kidneys from bilaterally nephrectomized rabbits (n=6; taken at random from a pool of 18 kidneys from rabbits which had undergone bilateral nephrectomy under terminal anaesthesia) were flushed with 40 ml HCA (0-2^{0}C) and homogenized immediately for measurement of susceptibility to lipid peroxidation.

Group 2: Freshly nephrectomized kidneys from bilaterally nephrectomized rabbits (n=6) were flushed with 40 ml HCA (0-2^{0}C) via the renal artery and stored for 72 h prior to assessment of susceptibility to lipid peroxidation.

Group 3: Freshly nephrectomized kidneys from bilaterally nephrectomized rabbits (n=6) were flushed with 40 ml HCA containing ebselen (0-2^{0}C) via the renal artery and stored

for 72 h in HCA containing ebselen, prior to assessment of susceptibility to lipid peroxidation.

Group 4: Freshly nephrectomized right kidneys (n=6) were flushed with 40 ml HCA (0-2^{0}C) via the renal artery and stored for 48 h prior to autografting for assessment of long term viability.

Group 5: Freshly nephrectomized right kidneys (n=6) were flushed with 40 ml HCA (0-2^{0}C) containing ebselen via the renal artery and stored for 48 h prior to autografting for assessment of long term viability.

8.4 Results

8.4.1 Determination of Microsomal Lipid Peroxidation

NADPH/Fe^{3+}-ADP was found to be a potent stimulator of microsomal lipid peroxidation (Fig 8.3, control). The reaction was essentially complete at 30 min and maximal microsomal lipid peroxidation was found to be between 40-55 nmol MDA equivalents/mg protein.

Ebselen was found to be a very effective inhibitor of lipid peroxidation in this model system. At a concentration of 1.6 μM, peroxidation was very significantly decreased and was completely inhibited by 3.2 μM and 10 μM ebselen over the course of 1 h (Fig 8.3). These results agree well with previously published studies (Müller *et al.*, 1984; Hayashi and Slater, 1986; Noguchi *et al.*, 1992).

The effects of ebselen metabolites I and II on microsomal lipid peroxidation are shown in Figs 8.4 and 8.5 respectively. Metabolite I displayed no antioxidant activity and indeed was found to be slightly pro-oxidative up to a concentration of 50 μM. Metabolite II did inhibit lipid peroxidation but was much less effective than ebselen itself. At 1.6 μM, no effect on the rate of lipid peroxidation was observed; 10 μM metabolite II displayed a faint antioxidant effect, and 50 μM inhibited peroxidation by approximately 40% over 1 h.

8.4.2 Determination of Lipid Peroxidation in Renal Homogenates

Storage of rabbit kidneys at 0-2^{0}C in hypertonic citrate solution for 72 h of cold ischaemia resulted in highly significant ($p<0.005$) increases in oxidative membrane damage in both the cortex and medulla as determined by the subsequent *in vitro* formation of Schiff's bases (Fig 8.8) and TBA-reactive material (Fig 8.9). Inclusion of ebselen (100 μM), in the HCA flush and storage solution very significantly ($p<0.005$) reduced the formation of both markers of lipid peroxidation in the cortex of

kidneys following storage for 72 h when compared with untreated controls stored for the same length of time (Figs 8.8 and 8.9). Indeed, susceptibility to lipid peroxidation in the cortex of kidneys rendered cold ischaemic in the presence of ebselen was reduced to the low levels found in fresh organs. Ebselen was also highly effective ($p<0.005$ compared with stored controls) at inhibiting Schiff's base formation in the medulla of kidneys following cold ischaemia, again the values being reduced to fresh levels (Fig 8.8). The production of TBA-reactive material in the medulla was significantly ($p<0.05$) reduced by ebselen inclusion in the flush and storage solutions to about 50% of the value found in stored untreated organs (Fig. 8.9).

8.4.3 Histology

Both intracellular and interstitial oedema was noted in the medulla of all stored kidneys and was present to a lesser degree in the cortex. Oedema was moderate at worst. Congestion, haemorrhage and necrosis were not present. Oedema was scored on a scale of 0 (absent) to 4 (severe). Ebselen reduced medullary oedema from 2 to 1.33, and cortical oedema from 1 to 0.33. These reductions failed to reach statistical significance (n=6 in each group). The extent of oedema in the medulla correlated well with the rate of lipid peroxidation as determined by the production of TBA-reactive material (correlation coefficient = 0.84, p= 0.0007) and inversely with ebselen treatment (Fig 8.11). However, in the cortex there was no such correlation between lipid peroxidation measured *in vitro* and oedematous change (Fig 8.10; correlation coefficient = 0.48, p= 0.12).

8.4.4 Survival Determination

After 48 h storage, 50% (3 of 6) rabbits in the untreated control group survived indefinitely, but only 17% (1/6) ebselen treated rabbits survived beyond 10 days. However, there was no statistically significant difference between these two groups. Thus, no beneficial or deleterious effect of ebselen was demonstrated. Nor was it possible to show a beneficial or deleterious effect of ebselen in terms of graded physiological function (serum urea and creatinine levels; Figs 8.12 and 13). However, ebselen did have a remarkable beneficial effect on inflammatory infiltrate in the cortex of autopsied kidneys. In 5 of 6 kidneys treated with ebselen there was very little inflammatory infiltrate (Grade 1 -2), whereas control kidneys that were unable to support life (3 of 6) had severe (Grade 4) inflammatory infiltrate (Plates 8.1 and 8.2).

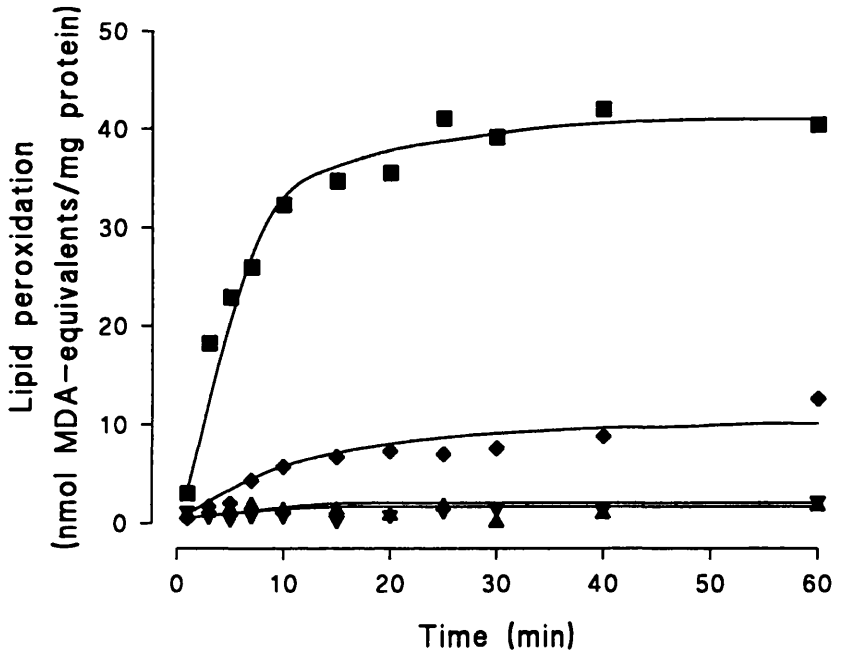

Fig 8.3 **Effect of ebselen on hepatic microsomal lipid peroxidation initiated by NADPH/$Fe_2(SO_4)_3$-ADP. Ebselen completely inhibited microsomal lipid peroxidation at doses of 3.2 μM and above over the 1 h measured. ■ =control; ▼ =10 μM; ▲ =3.2 μM; ◆ =1.6 μM. Values represent the mean of 3 determinations.**

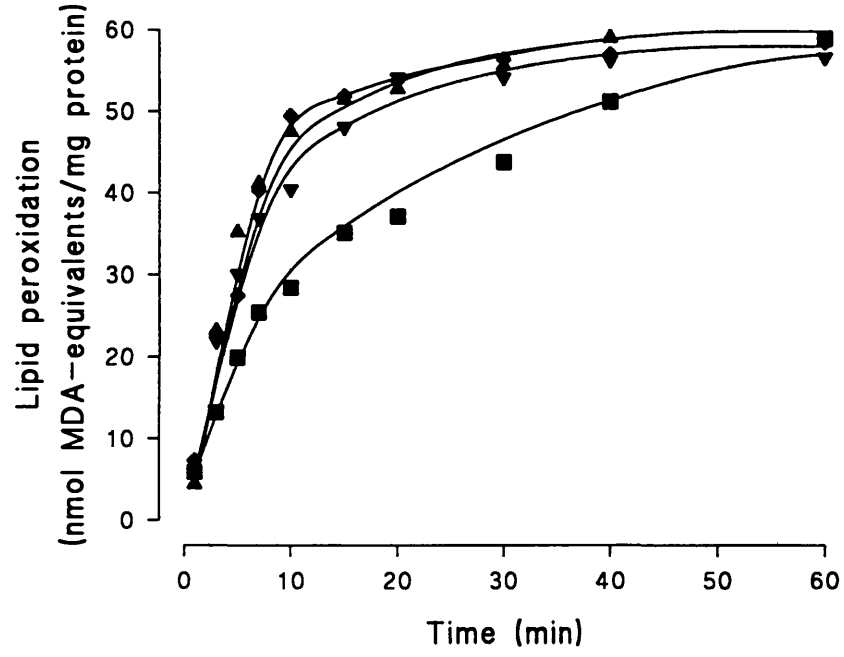

Fig 8.4 **Effect of metabolite I on hepatic microsomal lipid peroxidation initiated by NADPH/$Fe_2(SO_4)_3$-ADP. Metabolite I appeared to have a slightly pro-oxidative effect on microsomal lipid peroxidation. ■ =control; ▲ =50 μM; ▼ =10 μM; ◆ =3.2 μM. Values represent the mean of 3 determinations.**

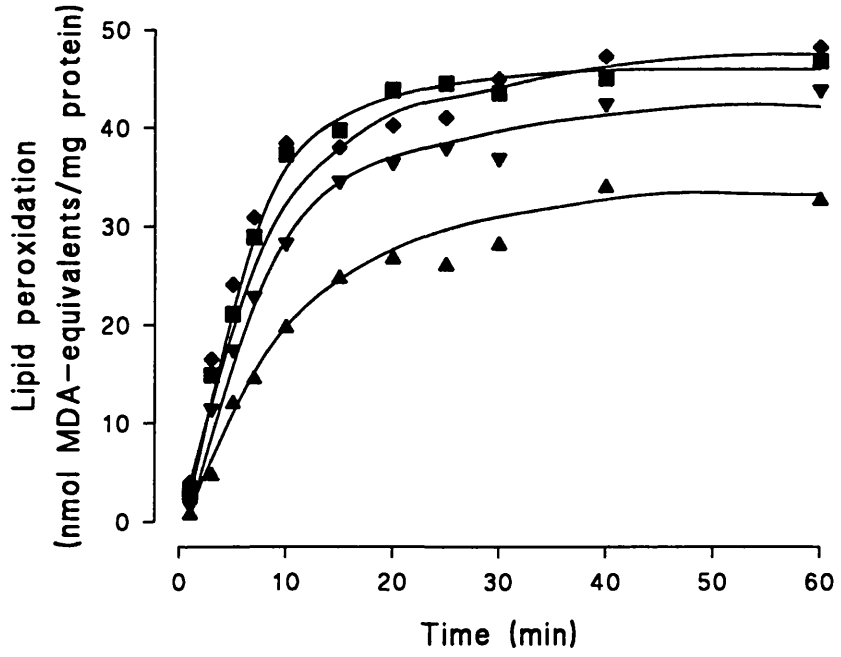

Fig 8.5 Effect of metabolite II on hepatic microsomal lipid peroxidation initiated by NADPH/$Fe_2(SO_4)_3$-ADP. Metabolite II appeared to have a slight antioxidant effect on microsomal lipid peroxidation. ■ =control; ▲ =50 μM; ▼ =10 μM; ◆ =3.2 μM. Values represent the mean of 3 determinations.

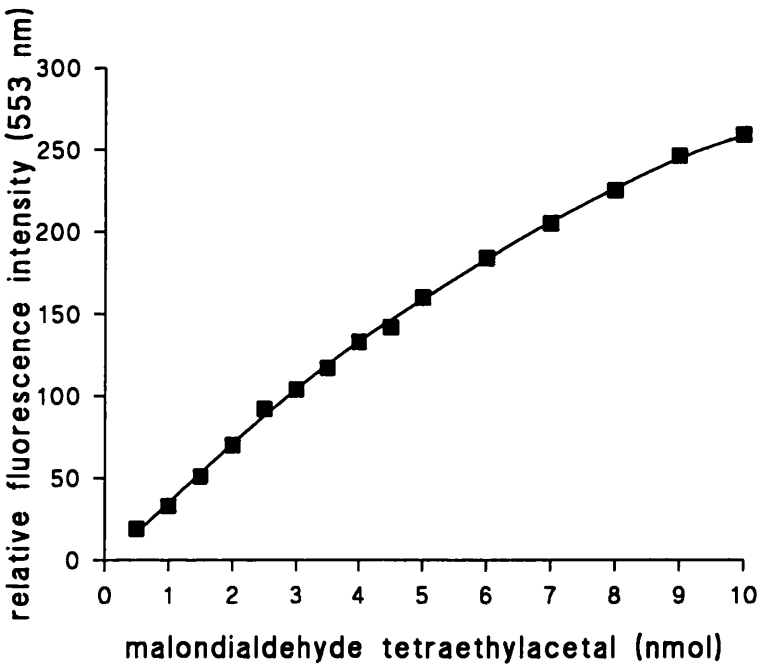

Fig 8.6 Standard curve for malondialdehyde tetraethylacetal (nmol) versus relative fluorescence intensity at 553 nm when excited at 513 nm (values are mean of duplicate determinations).

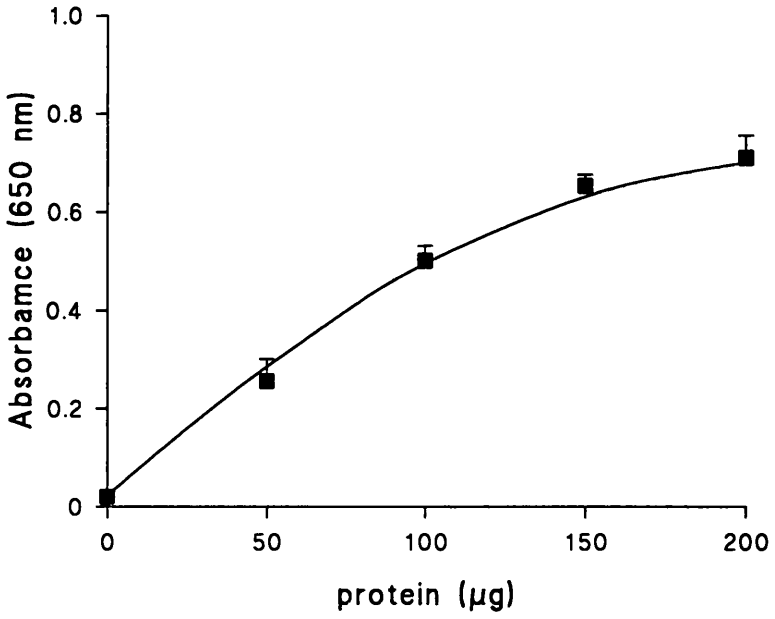

Fig 8.7 Standard curve for bovine serum albumin (μg) vs absorbance at 650 nm. Results are presented as mean ± SEM of triplicate determinations.

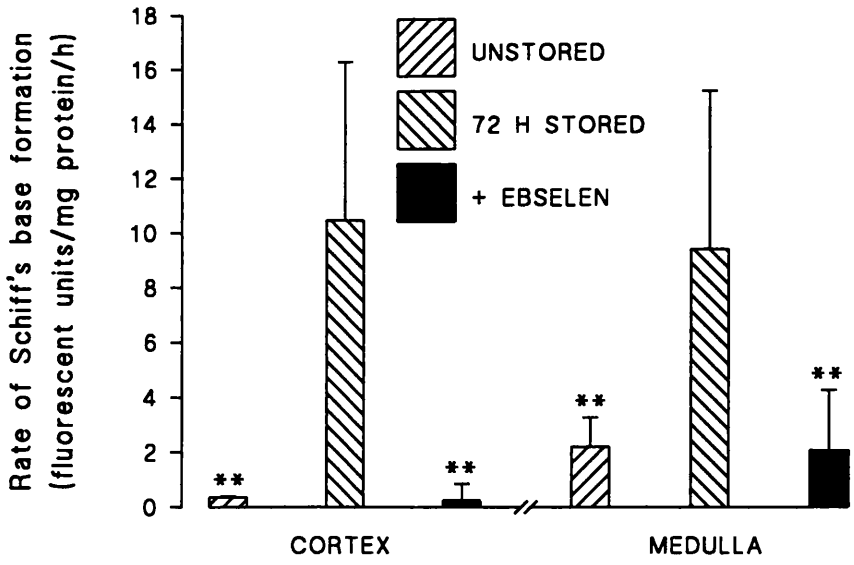

Fig 8.8 Effect of ebselen on formation of Schiff's bases in homogenates prepared from the cortex and medulla of kidneys stored for 0 or 72 h at 0-2^{0}C in HCA ± ebselen (100 μM). Ebselen reduced susceptibility to Schiff's base formation in 72 h stored kidneys to baseline in both cortex and medulla. $^{**}p<0.005$; $^{*}p<0.05$ compared with untreated stored organs. Values represent the mean and S.D. of 6 separate determinations performed in duplicate.

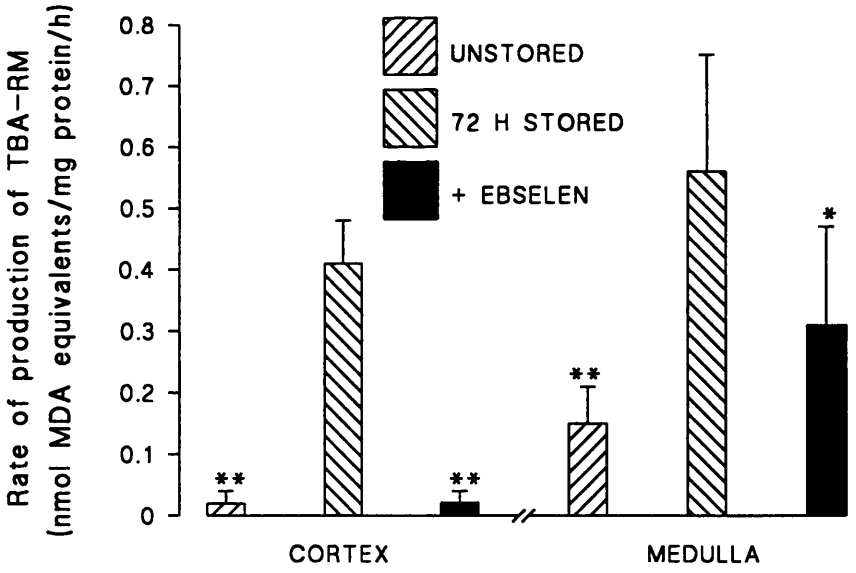

Fig 8.9 Effect of ebselen on formation of TBA-reactive material in homogenates prepared from the cortex and medulla of kidneys stored for 0 or 72 h at 0-2^{0}C in HCA ± ebselen (100 μM). Ebselen reduced susceptibility to formation of TBA-reactive material to baseline in the cortex and by approximately 50% in the medulla. $^{**}p<0.005$; $^{*}p<0.05$ compared with untreated stored organs. Values represent the mean and S.D. of 6 separate determinations performed in duplicate.

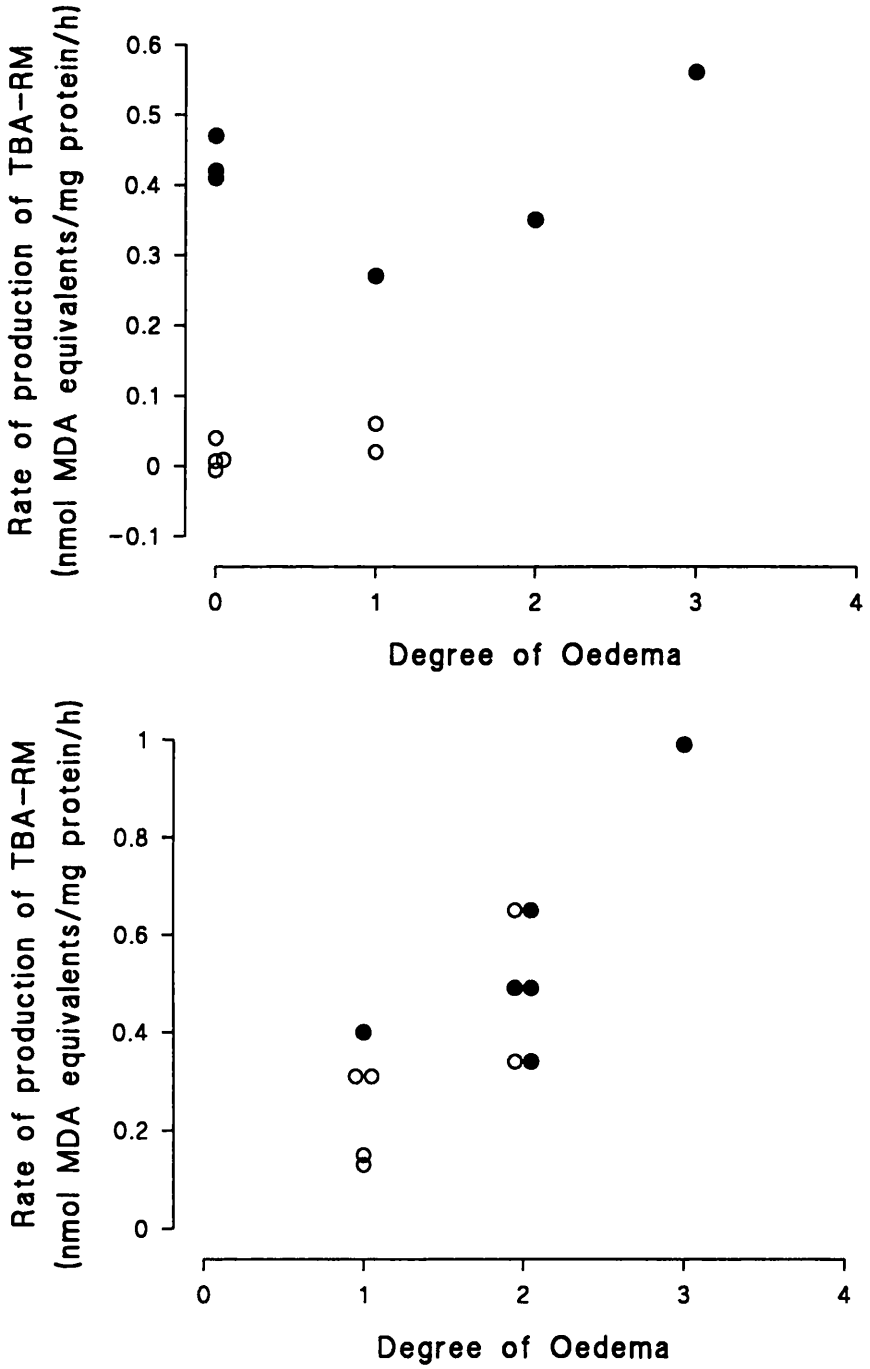

Figs 8.10 and 8.11
Correlation between the rate of lipid peroxidation (TBA-reactive material) and the extent of oedema in the cortex (top) and medulla (bottom) of kidneys stored for 72 h at 0-2^{0}C in HCA +ebselen (100 μM) (O) or without ebselen (●). There is a reasonable correlation between the formation of TBA-reactive material in the medulla during the ischaemic period (correlation coefficient 0.84) but not in the cortex (correletion coefficient 0.48), suggesting that cyclooxygenase may have produced TBA-reactive prostanoids during the ischaemic period, promoting the development of oedema. Ebselen may have attenuated this process to some extent.

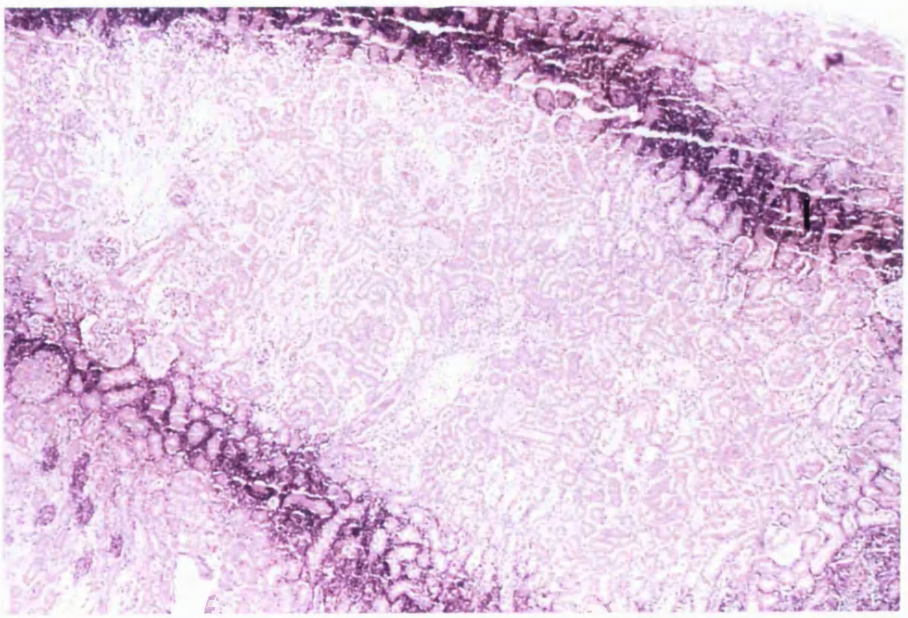

Plate 8.1 **Light micrograph of the renal cortex of a Group 1 (control) kidney at autopsy 6 days after revascularization, showing severe inflammatory cell infiltrate in two bands (I)(magnification x 40).**

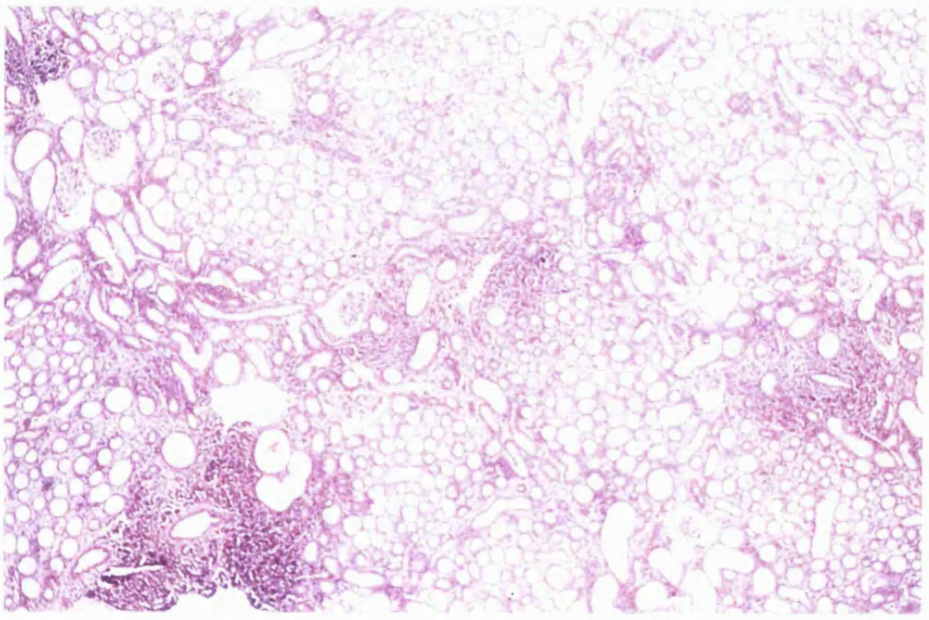

Plate 8.2 **Light micrograph of the renal cortex of a Group 2 (ebselen-treated) kidney at autopsy 6 days after revascularization showing much more limited inflammatory infiltrate and evidence of tubular dilatation and tissue re-modelling**

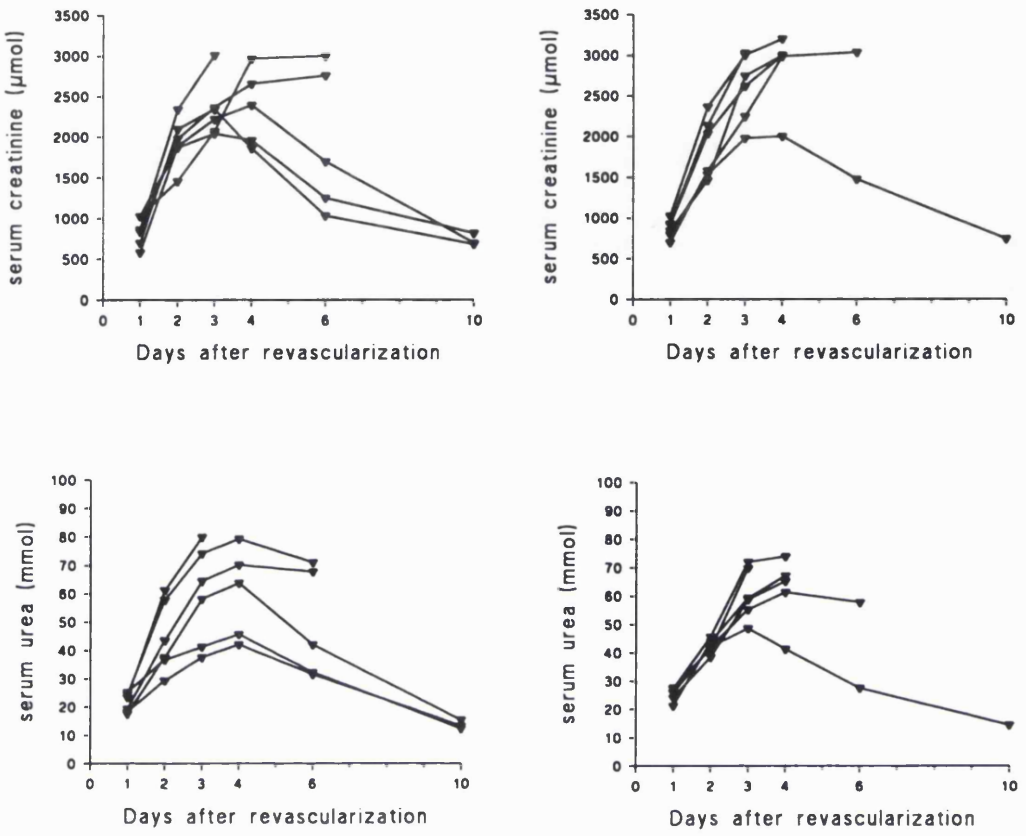

Figs 8.12 and 13
Concentration of serum creatinine (top) and urea (bottom) in untreated recipients of 48 h stored autografted kidneys (left) and ebselen treated rabbits (right). ▼ represents values for single animals.

8.5 Discussion

An important factor in the therapeutic use of ebselen appears to be the speed of its metabolism. Following oral administration, untransformed ebselen is not detectable in plasma but is rapidly transformed into a variety of metabolites, of which two (metabolites I (2-glucuronyl-selenobenzanilide) and II (4-hydroxy-2-methyl-selenobenzanilide)) are prominent (Terlinden *et al.*, 1988; Fischer *et al.*, 1988; Müller *et al.*, 1988). If the antioxidant activity of ebselen plays an important role in its pharmacological effects, then the antioxidant efficacy of the principal metabolites is an important consideration in its clinical utility.

The *in vitro* microsomal studies presented in this chapter demonstrate that the antioxidant efficacy of the two principal metabolites towards lipid peroxidation stimulated by iron/ADP/NADPH is much lower than the untransformed drug and probably too low for any antioxidant effect to occur *in vivo*. However, the powerful inhibitory effect of ebselen itself toward lipid peroxidation, as shown in previous studies (Müller *et al.*, 1984; Hayashi and Slater, 1986; Noguchi *et al.*, 1992) was confirmed.

For the antioxidant activity of ebselen to be of clinical relevance in renal preservation, a system by which untransformed ebselen is presented directly to the kidney is therefore necessary. For this reason, ebselen was administered i.v. despite its low solubility in aqueous solution. In these studies, ebselen was solubilized using ethanol (for the micromolar range) and cremophor EL (for the millimolar range). Electron microscopical investigations of the renal toxicity of these treatment regimens showed no significant histological or ultrastructural damage.

Direct flushing of the kidney with HCA containing 100 μM ebselen led to a highly significant ($p<0.005$) protective effect on the susceptibility of both the renal cortex and medulla to lipid peroxidation following 72 h of cold ischaemia. Except for the production of TBA-reactive material in the medulla, which was reduced by ebselen by about 50%, all other markers of lipid peroxidation were reduced to the very low levels found in fresh controls. As discussed in Chapter 6, TBA-reactive substances are produced as side products during prostaglandin and thromboxane synthesis (Hayashi and Shimizu, 1982). Previous experiments in this laboratory have demonstrated that approximately 50% of the TBA-reactive material produced in the post-ischaemic medulla is formed by this mechanism (Gower *et al.*, 1987). The almost complete inhibition of Schiff's base formation in the medulla in comparison with the partial reduction in TBA-reactive material by ebselen suggests that it acts as a powerful antioxidant but poor inhibitor of cyclooxygenase in this model. This was surprising, as ebselen has been reported to inhibit cyclooxygenase in human platelets with an IC_{50} of around 5 μM (Kühl *et al.*, 1986).

The kidney, and particularly the medulla (Robak and Sobanska, 1976) is capable of synthesizing a range of prostaglandins including the vasoconstrictor thromboxane A_2 and the vasodilators prostacyclin and PGE_2. Hypoxia has been shown to stimulate the production of some of these metabolites in renal mesangial cells (Jelkmann *et al.*, 1985). In whole kidneys subjected to ischaemia an imbalance in eicosanoids in favour of vasoconstriction on reperfusion has been demonstrated (Lelcuk *et al.*, 1985). In addition, some prostaglandins, particularly PGE_2, have been shown to have a direct inhibitory effect on ion transport in the different sections of the nephron, especially the mTAT (Frazier and Yorio 1992). Thus, adverse effects on the metabolism of arachidonic acid via cyclooxygenase as a result of hypothermic storage and the apparent inability of ebselen to inhibit this enzyme under the conditions employed may have been partly responsible for the observed failure of renal function following the autograft of a single stored kidney.

Ebselen has also been reported to inhibit lipoxygenase and speed the breakdown of LTB_4 to inactive isomers (Kühl *et al.*, 1986). Lipoxygenase is known to be present in the renal cortex (Lianos *et al.*, 1985), and it has been postulated that a significant amount of lipid peroxidation occurs via this pathway in the cortex of post-ischaemic rabbit kidneys on the basis that lipid-soluble Schiff's bases were produced even in the presence of indomethacin (a cyclooxygenase inhibitor) and desferrioxamine (Gower *et al.*, 1987). The fact that in the present study ebselen virtually abolished lipid peroxidation in the cortex of cold- stored kidneys suggests that its effect as a lipoxygenase inhibitor may be playing a significant role under these conditions. This hypothesis is supported by the striking reduction in inflammatory infiltrate by ebselen even in kidneys unable to support life. However, as discussed in Chapter 7, inhibition of lipoxygenase alone does not prevent the development of acute renal failure. The limited methodology employed in this chapter (no direct measurements of serum eicosanoid levels) reflects the time at which the work was completed (very early in the programme of research reported in this thesis). However, since ebselen did not improve the long term viability of stored kidneys, it was not considered important to repeat experiments using these more sensitive techniques.

Histological examination of renal slices taken from kidneys subsequently assayed for markers of lipid peroxidation demonstrated that the degree of medullary oedema correlated well with susceptibility to oxidative stress as measured by TBA-reactivity and inversely (but not significantly) with ebselen treatment. It is possible that the oedematous changes associated with ischaemia in the medulla were a consequence of damaging eicosanoid production (eg. thromboxane A_2) during the ischaemic period itself. Although oxygen tension is presumed to be low during ischaemia when intracellular conditions

are reductive, it is noteworthy that the content of TBA-reactive material in the medulla of stored organs is significantly higher immediately following ischaemia than in fresh organs (see Chapter 3); and it is known that free radical reactions can occur at very low pO_2 (<1 μM; Rao *et al.*, 1983). In contrast, cortical TBA-reactive material content did not rise significantly during the storage period and Schiff's base reactivity did not increase in either the cortex or medulla. Furthermore, there was no correlation between the degree of oedema and these parameters of *in vitro* lipid peroxidation, suggesting that they are both free-radical mediated and post-ischaemic events. The non-significant inhibition by ebselen of medullary TBA-reactive material formation therefore implies a partial inhibition of cyclo-oxygenase under these conditions.

The failure of renal function following autografting of kidneys stored for 48 h, despite the intensity of the ebselen regime, both i.v. and in the flush, may have been the result of a combination of factors:

(i) As suggested above, it is likely that ebselen did not inhibit cyclo-oxygenase in this model and did not affect medullary congestion;

(iii) Spectroscopic analyses have shown that ebselen interacts with the thiolate anion in cytochrome P-450 (Kühn-Velten and Sies, 1989; Akerboom *et al.*, 1995) and the reaction can be prevented by sulphydryl compounds such as dithiothreitol (Kühn-Velten and Sies, 1989). The authors suggested that benzisoselenazolones may be able to interact with sulphydryl groups of membrane associated proteins. A similar mechanism has been proposed for the inactivation of nitric oxide synthase (Zembowicz *et al.*, 1993) in which ebselen was shown to "trap" the critical thiol essential for the catalytic activity of nitric oxide synthase in the form of an inactive selenyl sulphide, and the reaction was reversed by addition of glutathione or dithiothreitol. Such interactions could result in the inactivation of crucial sulphydryl containing ion pumps such as the Na-K-ATPase or the Ca-ATPase and this may have reduced the long term viability of kidneys treated with ebselen.

8.6 Conclusions

(i) Ebselen significantly reduced lipid peroxidation in both peroxidising rat liver microsomes and homogenates of renal cortex and medulla.

(ii) The two principal metabolites of ebselen were not effective at reducing lipid peroxidation in rat liver microsomes.

(iii) Ebselen did not appear to inhibit cyclooxygenase in kidneys stored for 72 h.

(iv) Ebselen attenuated cortical inflammation but did not improve the long-term viability of kidneys stored for 48 h before autografting.

CHAPTER 9

THE EFFECT OF MANNITOL AND POLYETHYLENE-GLYCOL ON THE HAEMODYNAMIC AND DIURETIC ACTIONS OF FRUSEMIDE

The studies presented in this chapter are based on a paper to be published in: Transplantation (1996) (in press).

9.1 Introduction

In Chapter 8, it was shown that ebselen significantly reduced susceptibility to lipid peroxidation, ameliorated both cortical and medullary oedema and attenuated inflammation but did not prevent the development of acute renal failure. It was suggested that, contrary to *in vitro* reports, ebselen did not inhibit cyclooxygenase in this model. Suppression of cyclooxygenase has previously been shown to improve renal viability following long-term hypothermic storage (Gower *et al.*, 1989, Schilling *et al.*, 1993). However, in Chapter 7 it was shown that reperfusion of 48 h stored kidneys did not result in significant increases in serum thromboxane B_2 levels, one of the principal vaso-active products of cyclooxygenase. Furthermore, in Chapters 3 and 4, it was shown that medullary congestion was a result of oedematous swelling of the medullary thick ascending tubules (mTAT) rather than vasoconstriction or thrombosis. The damaging effects of cyclooxygenase may therefore be mediated not by vascular changes but by feedback amplification or a direct effect on ion transport in the nephron and particularly the mTAT (Frazier and Yorio 1992).

As was shown in Chapter 3, the mTAT is highly susceptible to ischaemia alone. This susceptibility stems from their high requirement for oxygen to carry out the work of active tubular reabsorption in an environment brinking on hypoxia even under normal conditions (Brezis *et al.*, 1984; Brezis *et al.*, 1984; Heyman *et al.*, 1994). Inhibition of active transport by ouabain (a specific inhibitor of Na-K-ATPase) and frusemide (a specific inhibitor of Na-K-2Cl-cotransporter in the mTAT) has been shown to reduce hypoxic injury to both the mTAT and the *pars recta* in the isolated perfused kidney (Heyman *et al.*, 1994; Kumada *et al.*, 1994).

Inhibition of active tubular reabsorption by frusemide is reflected in changes in the redox state of cyt aa_3 and in renal oxygenation (Epstein *et al.*, 1982). These parameters can be measured *in vivo* using NIRS (Balaban and Sylvia, 1981). NIRS in transmission mode measures concentration changes in HbO_2, Hb and the oxidised form of cyt aa_3 across the entire kidney (see Chapters 2, 4 and 5). It has previously been shown in the isolated perfused kidney that agents altering metabolism or active transport primarily in the renal cortex had little or no effect on the redox state of cyt aa_3 suggesting that the rate of oxygen consumption is not a critical determinant of cyt aa_3 redox status in these sections of the tubule (Epstein *et al.*, 1982). In contrast, inhibition of active reabsorption in the mTAT in the isolated perfused kidney resulted in an increase in oxygen tension and a corresponding increase in the redox state of cyt aa_3 (Epstein *et al.*, 1982). Thus, it should be possible to monitor the effect of frusemide on metabolic activity in the mTAT non-invasively by measurements of changes in the redox state of cyt aa_3, using NIRS in transmission mode.

During hypothermic renal storage, oedematous swelling of the mTAT results in mechanical constriction of the peritubular capillaries and *vasa recta* (Yamamoto *et al.*, 1984; Bayati *et al.*, 1990 and Chapter 3). Upon reperfusion, outflow of blood from the medulla is blocked (Bayati *et al.*, 1990). Medullary haemostasis results in profound haemoglobin desaturation and secondary ischaemia in the surrounding parenchyma (Lane *et al.*, 1996 and Chapter 4). In these circumstances, inhibition of active tubular reabsorption by frusemide may be less effective at reducing cellular injury than in the isolated perfused kidney: firstly, medullary haemostasis may prevent frusemide from reaching the mTAT; secondly, the severity of ischaemia-reperfusion injury during renal transplantation may result in an irreversible loss of mTAT integrity, such that frusemide could have at best a limited effect on cellular metabolism. It is hypothesized that amelioration of cellular swelling during the storage period by use of more effective impermeants could improve cellular integrity during reperfusion, increase medullary blood flow and maximise the potential therapeutic effects of frusemide.

9.2 Objective

The studies presented in this chapter were performed in order to compare the effect of two impermeants (mannitol and polyethylene glycol) incorporated into the preservation solutions on the haemodynamic and diuretic actions of frusemide in autografted kidneys following 72 h hypothermic storage.

9.3 Methods

9.3.1 Methodology

A total of 30 adult female NZW rabbits (2.5 - 3 kg), in 6 groups of 5 animals (described below) were anaesthetized by an i.m. injection of fentanyl fluanisone and i.v.bolus of diazepam; oxygen (2 l/min) was supplied via an open face mask.

The effect of frusemide on the redox state of cyt aa_3 and on renal haemodynamics during 35 min of *in vivo* reperfusion of unstored transplanted kidneys was characterized using NIRS in transmission mode and compared with its effect on kidneys stored for 72 h prior to transplantation in two different preservation solutions (one containing mannitol, the other containing PEG). A reperfusion period of 35 min was chosen as it is commensurate with the acute duration of action of frusemide *in vivo*. Changes in NIRS parameters were correlated with changes in renal morphology, as assessed by light microscopy.

9.3.2 Preservation Solutions

Two solutions were compared:

(i) standard HCA, containing mannitol as an impermeant

(ii) HCA-PEG, in which mannitol was replaced by polyethylene glycol, average molecular weight 600. There were no other differences between the two solutions. PEG was originally included at the same concentration as mannitol but is a non-ideal solute in terms of its colloidal osmotic pressure. The concentration of PEG added was therefore reduced to maintain a final measured osmolarity of 485 mOsm/L, to compare with standard HCA solution (see Table 1).

9.3.3 Experimental Groups

Group 1: Freshly nephrectomized left kidneys were flushed with 40 ml HCA (0-2^{0}C) via the renal artery and autografted immediately into the left renal bursa. Kidneys were monitored continuously *in situ* during reperfusion by NIRS for 35 min. After this time, reperfusion was terminated by lethal infusion of sodium pentobarbitone (200 mg/kg).

Group 2: The experimental protocol was identical to Group 1, except that the recipients received a rapid i.v.. infusion of frusemide (0.6 mg/kg) after 5 min of reperfusion.

Group 3: Kidneys were flushed as in Group 1 and then stored in HCA containing mannitol (see Table 1) surrounded by ice to maintain a temperature of 0-2^{0}C for 72 h prior to autografting. Recipients did not receive frusemide.

Group 4: The protocol was identical to Group 3, except that the recipients received a rapid i.v. infusion of frusemide (0.6 mg/kg) after 5 min of reperfusion.

Group 5: Kidneys were flushed and then stored in HCA-PEG and surrounded by ice to maintain a temperature of 0-2^{0}C for 72 h prior to autografting. Recipients did not receive frusemide.

Group 6: The protocol was identical to Group 5, except that the recipients received a rapid i.v.. infusion of frusemide (0.6 mg/kg) after 5 min of reperfusion.

Table 9.1 Composition of mannitol and polyethylene glycol-based HCA solutions

(mmol/l)	HCA-Mann	HCA-PEG
Sodium	80	80
Potassium	80	80
Magnesium	35	35
Citrate	55	55
Sulphate	35	35
Mannitol (g/litre)	34	–
Polyethylene Glycol (g/litre)	–	60
Osmolarity (mOsmol/litre)	485	485
pH	7.1	7.1

9.4 Results

9.4.1 Near Infrared Spectroscopy

In Figs 9.1 and 9.2 are shown representative time course plots of changes in concentration of HbO_2, Hb and cyt aa_3 in Group 1 (control, Fig 9.1) and Group 2 (unstored frusemide treated, Fig 9.2) autografted kidneys during 35 min of reperfusion. In untreated kidneys, reperfusion resulted in rapid increases in both [HbO_2] and [Hb] and a large reduction in cyt aa_3 within 2 min. In this case, there was a pronounced hyperaemia in the first 2 min, followed by a modest haemoglobin desaturation that persisted throughout the monitoring period. Reperfusion was continued for 30 min in 5 of 5 Group 1 and 5 of 5 Group 2 animals prior to termination by lethal infusion of sodium pentobarbitone. Sodium pentobarbitone infusion resulted in falls in both [HbO_2] and [Hb] and no apparent change in the oxidation state of cyt aa_3. In the Group 2 kidney, frusemide (0.6 mg/kg) was rapidly infused i.v. to the recipient after 5 min of reperfusion, at which point the major haemodynamic changes occurring during initial reperfusion had already taken place and a relatively stable baseline could be monitored. Frusemide infusion resulted in an increase in [HbO_2] and a decrease in [Hb] but no apparent changes in oxidation of cyt aa_3. Lethal infusion of sodium pentobarbitone resulted in a large fall in [HbO_2], a large rise in [Hb] and a large oxidation of cyt aa_3.

In Fig 9.3 is shown the mean and SEM changes in total haemoglobin concentration ([HbT]) and oxygenation index ([HbO_2] - [Hb]) in Groups 1 and 2 that took place from an initial (zeroed) point 2 min prior to frusemide infusion (*i.e.* after 3 min of reperfusion). There were no significant differences in [HbT] between the two groups. In Group 2 kidneys, frusemide infusion resulted in significant increases in oxygenation index by 5 min ($p<0.05$) compared with Group 1 kidneys, which did not receive frusemide. The oxygenation index remained significantly higher in frusemide-treated kidneys for the duration of reperfusion. In kidneys stored in the mannitol-based solution (Groups 3 and 4, Fig 9.4), frusemide infusion resulted in significant increases in the haemoglobin oxygenation index compared with untreated kidneys ($p<0.05$) but this was delayed by 15 min compared with Group 1 (Figs 9.3 and 9.4). As in unstored autografted kidneys, there were no significant differences in [HbT] (Fig 9.4). In Groups 5 and 6 (stored in the PEG-based solution), there were no significant differences in either the oxygenation index or [HbT] between the two groups during the 30 min of reperfusion monitored (Fig 9.5).

Termination of reperfusion by lethal infusion of sodium pentobarbitone (200 mg/kg) resulted in falls in both [HbT] and the oxygenation index in all groups as expected. The fall in oxygenation index was significantly greater ($p<0.005$) in Group 2 than in any other group, indicative of greater haemoglobin saturation in this group immediately before pentobarbitone infusion.

There was a tendency for cyt aa_3 to become reduced during reperfusion in all groups (Figs 9.6-9.8), but only in Groups 2 (unstored, treated with frusemide) and 4 (stored for 72 h in the mannitol based solution, and treated with frusemide) did the changes achieve significance ($p<0.05$). However, although in Group 2 kidneys cyt aa_3 became significantly reduced compared with the degree of oxidation at time 0, it was not significantly different from untreated controls (Group 1) at any time point. It was notable that changes in cyt aa_3 oxidation in unstored kidneys were greater than those occurring in stored kidneys; and changes in the oxidation state of cyt aa_3 in kidneys stored in the PEG-based solution (Groups 5 and 6, Fig 9.8) were negligible. Upon termination of reperfusion by lethal infusion of sodium pentobarbitone there were significant increases in oxidation of cyt aa_3 in Groups 2 and 4 only ($p<0.05$), but a tendency towards oxidation in all groups.

9.4.2 Histology

Minimal to mild medullary congestion was apparent in both unstored groups of kidneys and this was exacerbated with storage regardless of treatment (Fig 9.9). However, there was a tendency for congestion to be more severe in kidneys stored in the PEG-based solution compared with the mannitol based solution. Frusemide infusion significantly reduced cortical oedema in unstored kidneys ($p<0.05$), and had a tendency to do this in stored kidneys; however, the changes here did not achieve significance. There was no inflammatory infiltrate, no frank necrosis, no haemorrhage and very little cortical congestion in any specimen.

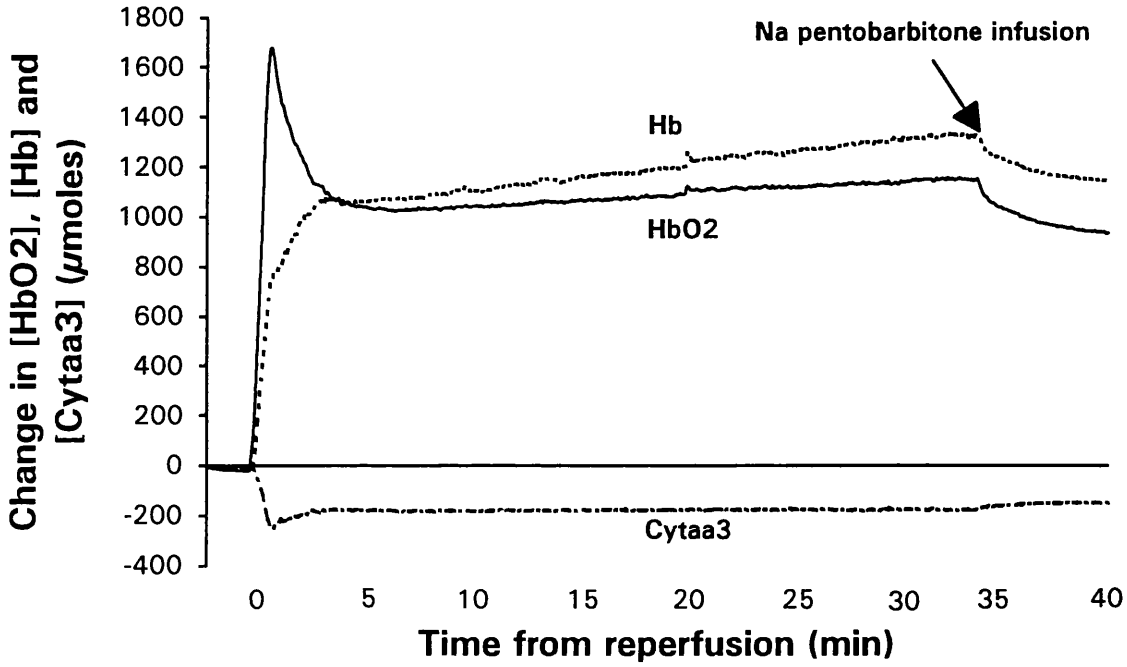

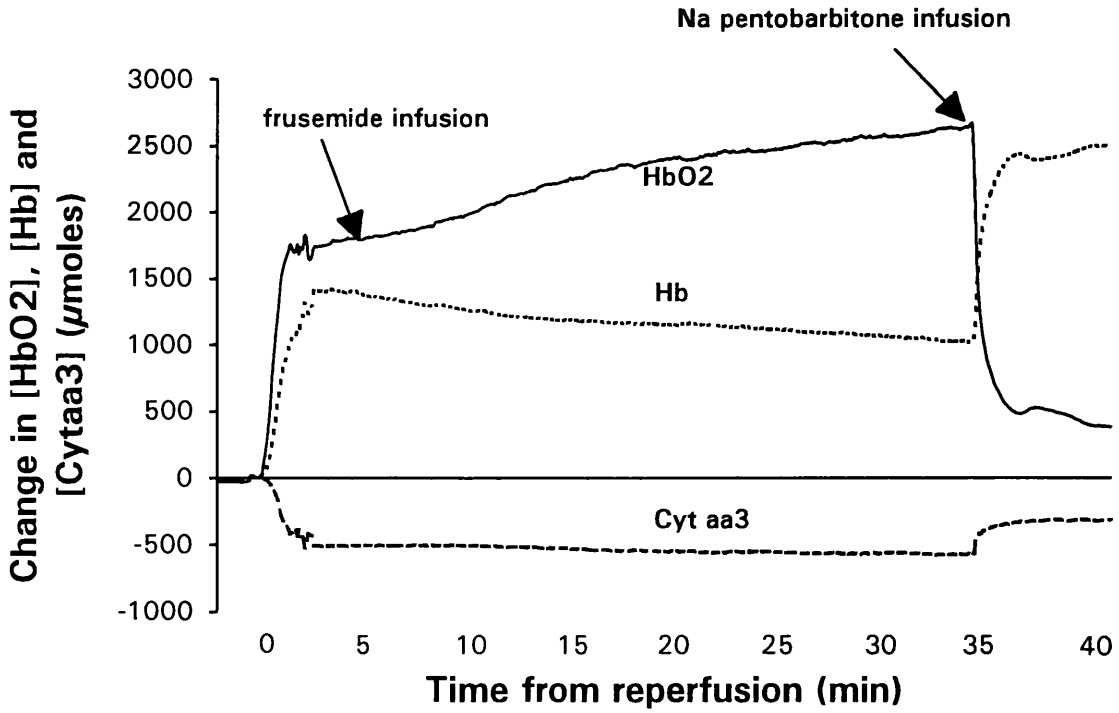

Figs 9.1 and 2

Representative time course plots of changes in HbO_2, Hb and cyt aa_3 in single Group 1 (unstored untreated, top) and Group 2 (unstored + frusemide, bottom) autografted kidneys during 35 min of reperfusion. Reperfusion of the autografted kidney took place at time 0. Reperfusion was terminated after 35 min by lethal sodium pentobarbitone infusion, which inhibits complex I of the respiratory chain. The figures show that frusemide infusion stimulated an increase in trans-renal haemoglobin oxygenation compared with untreated controls.

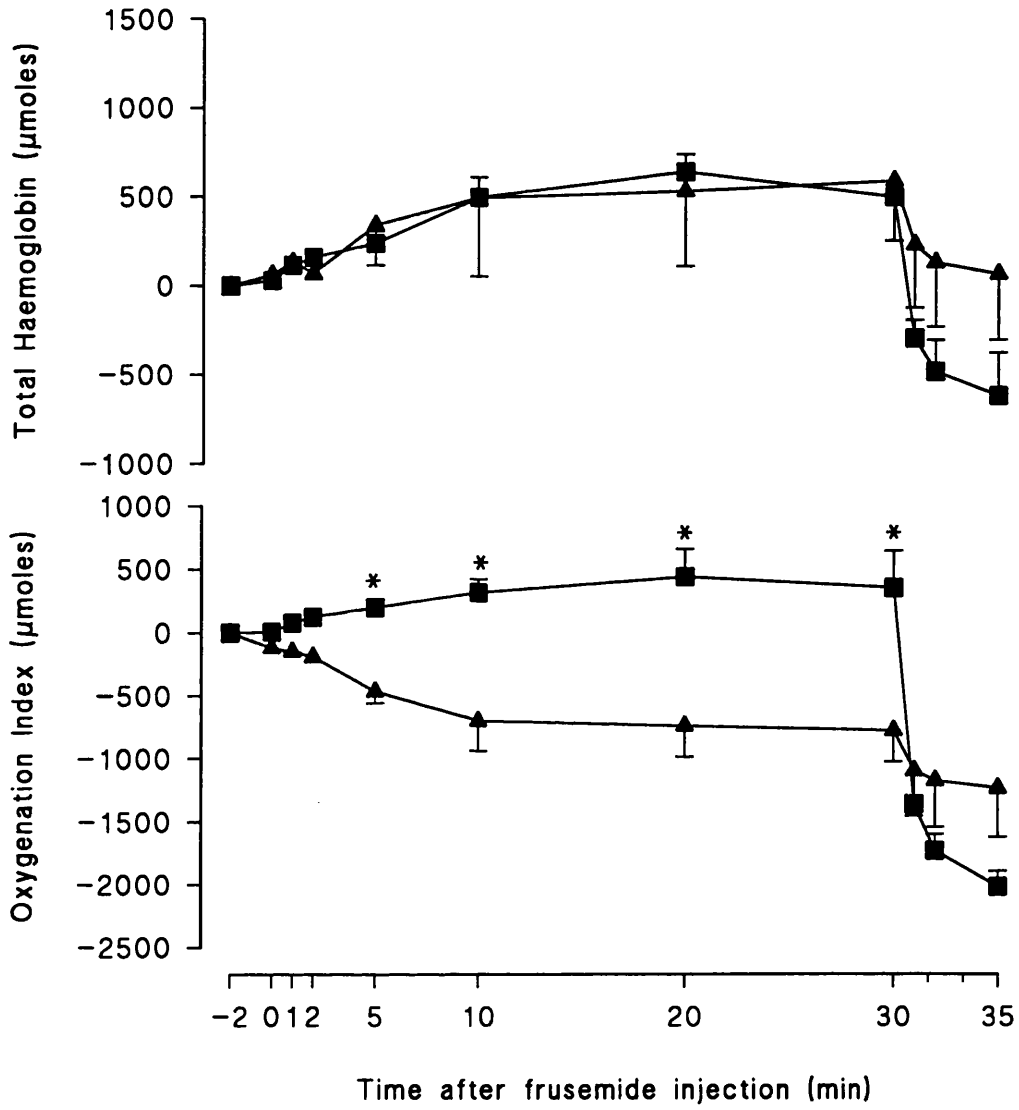

Fig 9.3 Mean and SEM changes (n=5) in [HbT] and the haemoglobin oxygenation index (HbO_2-Hb) upon frusemide infusion after 5 min of reperfusion in Group 1 (▲, unstored, no frusemide) and Group 2 (■, unstored + frusemide). Reperfusion was terminated at 30 min by lethal infusion of sodium pentobarbitone. *$p<0.05$ between groups at equivalent time points. The results show significantly better haemoglobin oxygenation in frusemide-treated kidneys compared with untreated controls. There were no significant differences in [HbT] between the two groups.

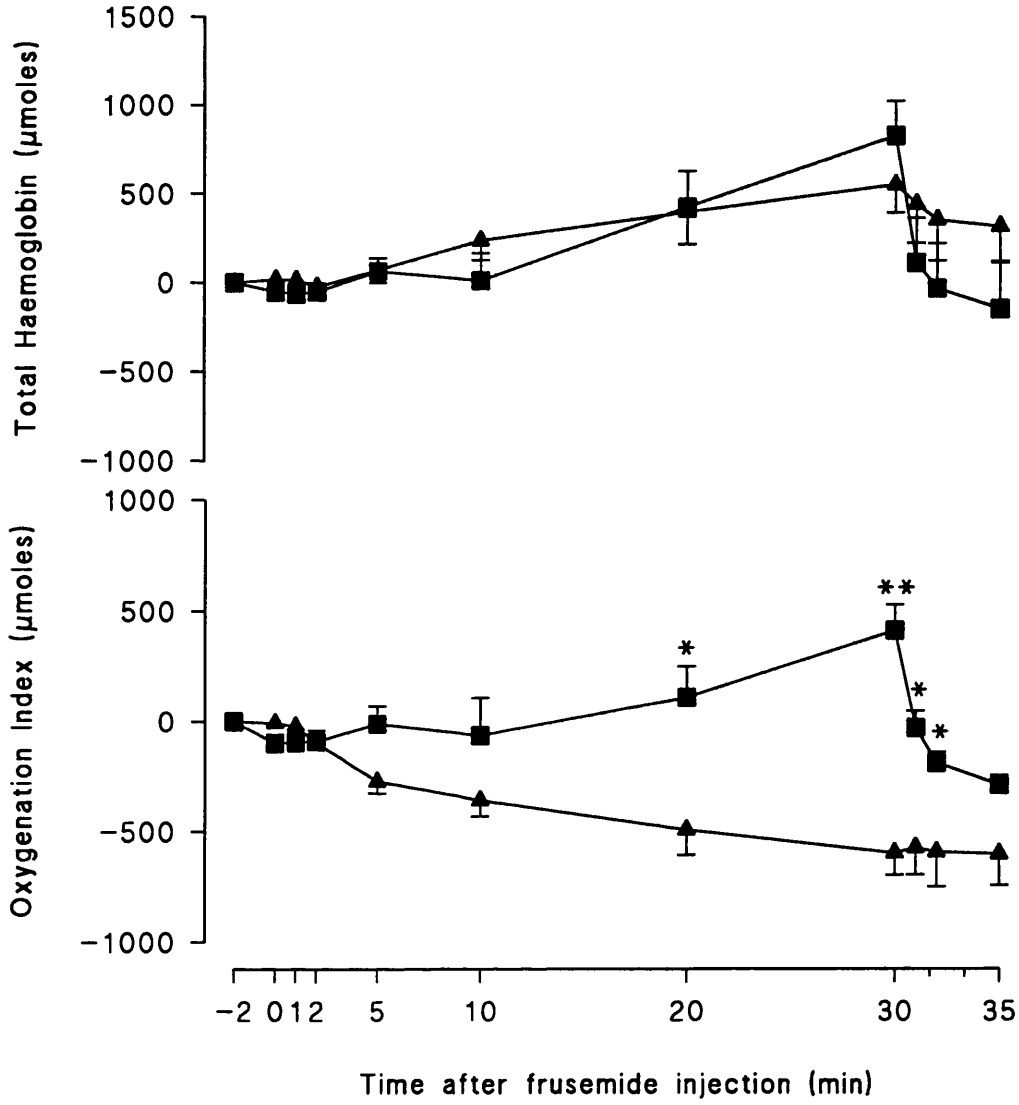

Fig 9.4 Mean and SEM changes (n=5) in [HbT] and the haemoglobin oxygenation index (HbO_2-Hb) upon frusemide infusion after 5 min of reperfusion in Group 3 (▲, 72 h stored in HCA; untreated) and Group 4 (■, 72 h stored in HCA; + frusemide). Reperfusion was terminated at 30 min by lethal infusion of sodium pentobarbitone. $^{**}p<0.005$, $^{*}p<0.05$ between groups at equivalent time points. The results show significantly better haemoglobin oxygenation in frusemide-treated kidneys that had been stored in the mannitol-based solution compared with those stored in the same solution but not receiving frusemide. There were no significant differences in [HbT] between the two groups.

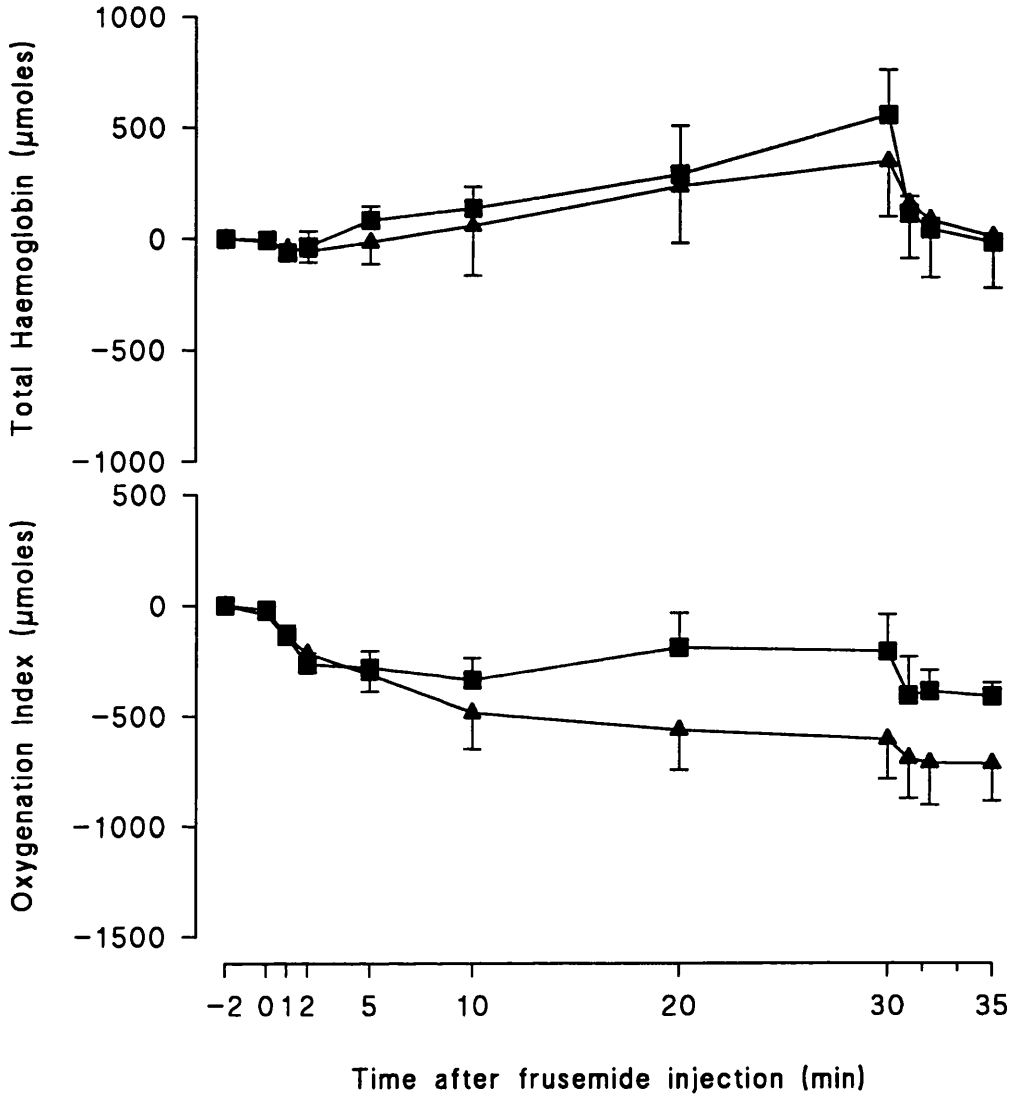

Fig 9.5 Mean and SEM changes (n=5) in [HbT] and the haemoglobin oxygenation index (HbO_2-Hb) upon frusemide infusion after 5 min of reperfusion in Group 5 (▲, 72 h stored in HCA-PEG; untreated) and Group 6 (■, 72 h stored in HCA-PEG; + frusemide). Reperfusion was terminated at 30 min by lethal infusion of sodium pentobarbitone. There were no significant differences in haemoglobin oxygenation between any kidneys stored in HCA-PEG regardless of frusemide treatment. There were no significant differences in [HbT] between the two groups.

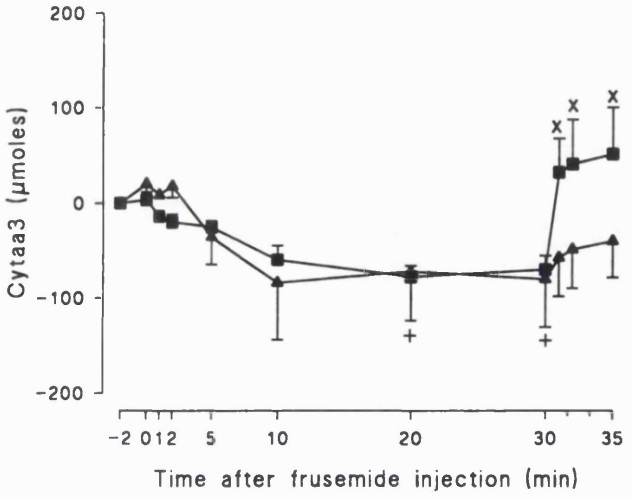

Fig 9.6 Mean and SEM changes (n=5) in cyt aa_3 oxidation upon frusemide infusion after 5 min of reperfusion in Group 1 (▲, unstored, no frusemide) and Group 2 (■, unstored + frusemide). Reperfusion was terminated at 30 min by lethal infusion of sodium pentobarbitone. $^{+}p<0.05$ within Group 2 from time 0 min; $^{x}p<0.05$ within Group 2 from time 30 min. Cyt aa_3 became reduced in both frusemide-treated and untreated kidneys. Inhibition of complex I caused a significant oxidation of cyt aa_3 in fruemide-treated kidneys only.

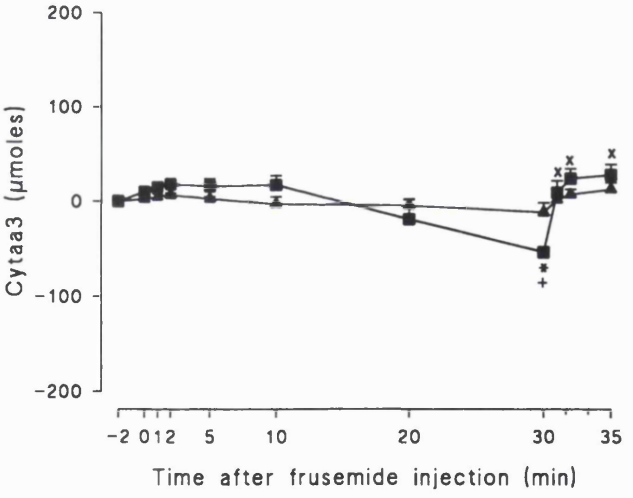

Fig 9.7 Mean and SEM changes (n=5) in cyt aa_3 oxidation upon frusemide infusion after 5 min of reperfusion in Group 3 (▲, 72 h stored in HCA; untreated) and Group 4 (■, 72 h stored in HCA; + frusemide). Reperfusion was terminated at 30 min by lethal infusion of sodium pentobarbitone. $^{*}p<0.05$ between groups at equivalent time points; $^{+}p<0.05$ within Group 4 from time 0 min; $^{x}p<0.05$ within Group 4 from time 30 min. Cyt aa_3 became significantly reduced in frusemide treated kidneys only but this was delayed compared with Group 2 kidneys. Inhibition of complex I resulted in significant oxidation of cyt aa_3 in frusemide-treated kidneys only.

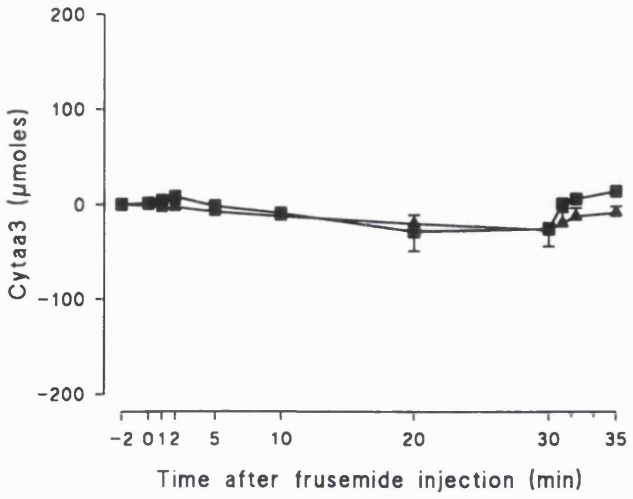

Fig 9.8 Mean and SEM changes (n=5) in cyt aa_3 oxidation upon frusemide infusion after 5 min of reperfusion in Group 5 (▲, 72 h stored in HCA-PEG; untreated) and Group 6 (■, 72 h stored in HCA-PEG; + frusemide). Reperfusion was terminated at 30 min by lethal infusion of sodium pentobarbitone. There were no significant changes in cyt aa_3 oxidation in either group of kidneys that had been stored in HCA-PEG regardless of treatment or stimulus.

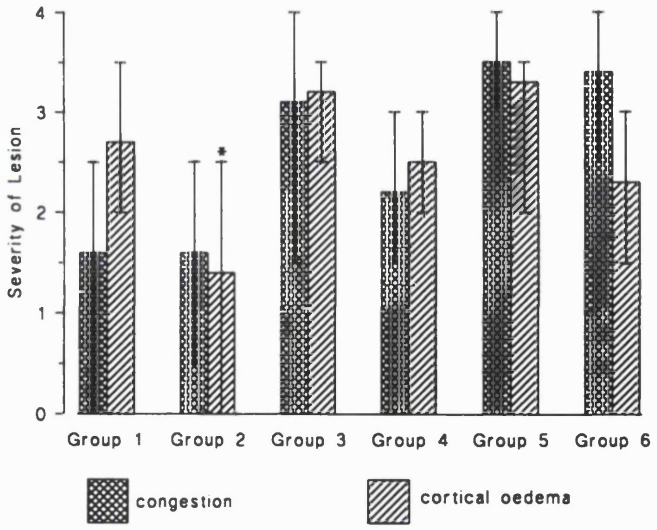

Fig 9.9 Degree of medullary congestion and oedema (as assessed by light microscopy) in the renal cortex after termination of reperfusion. There was a trend towards better preservation in kidneys stored in HCA-mann in terms of both medullary congestion and cortical oedema but this did not achieve significance. Results are presented as mean and range scores (n=5) in Groups: 1 (unstored); 2 (unstored + frusemide); 3 (72 h stored in HCA-mann); 4 (72 h stored in HCA-mann + frusemide); 5 (72 h stored in HCA-PEG); and Group 6 (72 h stored in HCA-PEG + frusemide). Tissue was scored blind by an independent pathologist on a scale of 0 (absent); 1 (minimal); 2 (mild); 3 (moderate) and 4 (severe). *$p<0.05$ Mann Whitney U test.

9.5 Discussion

In the isolated perfused kidney, inhibition of the Na-K-2Cl cotransporter in the mTAT by frusemide causes oxidation of cyt aa_3 which has been detected using dual wavelength white light spectroscopy (Epstein *et al.*, 1982). Inhibition of active reabsorption not only increases viability of the mTAT cells but by increasing oxygen tension in the cortico-medullary junction also has a positive effect on survival of the *pars recta* of the proximal tubule (Heyman *et al.*, 1994). However, when Atkins and Lankford (1991) measured the oxidation of cyt aa_3 *in vivo* they found that, surprisingly, frusemide infusion caused a reduction in cyt aa_3 in the outer medulla. Using laser doppler flowmetry, they demonstrated that the reduction in cyt aa_3 correlated with decreased bloodflow through the outer medulla (Atkins and Lankford, 1991).

Frusemide has several documented properties in addition to its inhibition of active reabsorption in the mTAT. It:

(i) Acts as a vasodilator, probably by increasing the rate of breakdown of arachidonic acid (Wilson *et al.*, 1982; Gerber 1983; Wilson *et al.*, 1993);
(ii) Inhibits tubulo-glomerular feedback (Tucker and Blantz, 1984);
(iii) Increases plasma renin activity (Gerber, 1983);
(iv) Is a weak inhibitor of carbonic anhydrase in the cortical proximal tubules (Radke *et al.*, 1972);
(v) Has a direct inhibitory effect on electron transport in the mitochondrial respiratory chains (Orita *et al.*, 1983).

These various properties of frusemide are likely to have diverse effects on renal physiology, dependent on the timing and dosage of frusemide infusion, and the model studied. In the present study, the effect of frusemide on cyt aa_3 oxidation in unstored transplanted kidneys appeared to be analogous to the study of Atkins and Lankford (1991) (Fig 9.6). However, the reduction in cyt aa_3 upon frusemide infusion was coupled with an increase in haemoglobin oxygenation (Fig 9.3). This seemingly paradoxical effect could be explained by the following mechanisms operating in unison:

(i) Frusemide infusion stimulated cortical vasodilation and a corresponding decrease in medullary bloodflow (Atkins and Lankford, 1991; Brezis *et al.*, 1994).
(ii) The expected increase in cyt aa_3 oxidation as a result of inhibition of the Na-K-2Cl cotransporter in the mTAT by frusemide was overshadowed by the fall in medullary bloodflow, leading to the observed reduction in cyt aa_3.

(iii) Cortical vasodilation, coupled with a reduction in active transport as a consequence of inhibition of active sodium reabsorption in the mTAT and possibly of mitochondrial electron transfer in the cortex (Orita *et al.*, 1983) resulted in diminished cortical oxygen extraction, hence the observed increase in the haemoglobin oxygenation index.

This scenario is complicated further by hypothermic preservation prior to transplantation. The vasoactive effects of frusemide are thought to be mediated by increased prostaglandin synthesis, particularly the vasodilator prostacyclin (Wilson *et al.*, 1982). However, hypoxia has been shown to stimulate the production of some arachidonic acid metabolites in renal mesangial cells (Jelkman *et al.*, 1985). In whole kidneys subjected to ischaemia an imbalance in eicosanoid synthesis in favour of vasoconstriction upon reperfusion has been demonstrated (Lelcuk *et al.*, 1985; Klausner *et al.*, 1989). Even in the absence of ischaemia, inhibition of thromboxane synthase enhances frusemide-induced renal vasodilation and diuresis (Wilson *et al.*, 1982; Pinzani *et al.*, 1988). Thus frusemide infusion could lead to the indiscriminate production of vasoconstrictor eicosanoids such as thromboxane A_2 following ischaemic insult.

Another important consideration is the derivation of vasoactive and ion-flux modulating eicosanoids via the cytochrome P-450 mono-oxygenase system (Escalante *et al.*, 1990; Escalante *et al.*, 1994). It has recently been shown by Paller and Jacob (1994) that a proportion of catalytic iron responsible for the production of hydroxyl radical-type species may be derived from degeneration of labile cytochrome P-450. If this is the case, the capacity of the cytochrome P-450 system for metabolising the precursors of these metabolically active eicosanoids could be seriously compromised during ischaemia. Thus both the vasoactive and diuretic potency of frusemide may depend on successful preservation of cellular and metabolic integrity during the storage period. Preservation of cellular integrity may also play an important role in the tubulo-glomerular feedback suppression mediated by frusemide (Tucker and Blantz, 1984). After severe ischaemia, the GFR has been shown to be reduced by as much as 95% compared with normal values (Ratych and Bulkley, 1986). The mechanism is controversial, but has been attributed to a decrease in the trans-glomerular hydraulic pressure gradient as a result of post-glomerular tubular obstruction or tubular backleak (Ratych and Bulkley, 1986). Not only would this abolish the inhibitory effect of frusemide on tubulo-glomerular feedback but would in addition drastically reduce active reabsorption in the mTAT, rendering loop diuresis superfluous.

A prime factor in the preservation of cellular integrity during organ storage is the selection of osmotically active impermeant solutes in the preservation solution (Kumano *et al.*, 1994). The beneficial effect of the University of Wisconsin (UW) solution may be a consequence of amelioration

of cell swelling and oedema during cold storage by the impermeants raffinose and lactobionate (Kumano *et al.*, 1994). The effectiveness of an impermeant appears to correlate with its molecular weight (Marsh *et al.*, 1989; Kumano *et al.*, 1994). Mannitol has been used in Marshall's hypertonic citrate solution with good clinical results for many years but its efficacy during prolonged hypothermia seems to be limited by its relatively low molecular weight (Marsh *et al.*, 1989). In contrast, impermeant polyethylene glycols (PEGs) of medium to high molecular weight have been shown to be highly effective at reducing cellular swelling via a combination of colloidal osmotic pressure and unexplained interactions with the cell membrane (Marsh *et al.*, 1989).

The effects of frusemide on cellular metabolism in organs stored prior to transplantation have not been previously studied. The studies presented in this chapter have therefore addressed the effects of frusemide infusion on cyt aa_3 oxidation and renal haemodynamics in kidneys stores for 72 h in solutions containing mannitol or PEG prior to transplantation using NIRS. Data obtained may help to explain the relationship between cellular swelling and ion pump and respiratory chain function soon after reperfusion. It was shown in Chapter 6 that respiratory chain function during the first 5 min of reperfusion provides a good indication of long-term renal viability. The responsiveness of the respiratory chain to frusemide infusion over a period commensurate with its physiological duration of action (about 30 min) may therefore be considered to reflect not only early renal function but also, by extrapolation, long-term renal viability.

Infusion of frusemide after 72 h storage in the mannitol-based solution resulted in a significant ($p<0.05$) increase in oxygenation index (Fig 9.4) but this was significantly delayed compared with Group 2 (unstored) kidneys ($p<0.005$; Figs 9.3 and 9.4). The increase in oxygenation index was synchronous with a significant reduction in cyt aa_3 ($p<0.05$; Fig 9.7) suggesting that, as in unstored kidneys, frusemide infusion stimulated cortical vasodilation. The delay in the response of these parameters to frusemide in comparison with unstored transplanted kidneys may be related to the medullary perfusion defect. It was shown in Chapter 4 that medullary congestion begins to clear 30 min to 1 h after reperfusion in the renal autograft model used here and that its clearance is associated with a significant rise in serum levels of 6-keto-$PGF_{1\alpha}$ (Lane *et al.*, 1994 and Chapter 7), a breakdown product of the vasodilator prostacyclin, but not with an increase in oxygenation index (Thorniley *et al.*, 1994; Lane *et al.*, 1996 and Chapter 4). Prostacyclin modulates cAMP levels in both endothelial cells and mTAT cells, leading respectively to decreases in endothelial cell permeability and Na^+ reabsorption (Greger, 1985; Casnocha *et al.*, 1989). This should abate the process of haemoconcentration in the peritubular capillaries and ameliorate swelling of the mTAT.

Thus, it is possible that stimulation of eicosanoid synthesis by frusemide could facilitate clearance of medullary congestion in an energy dependent manner, leading to a reduction in cyt aa_3 despite increased bloodflow. This premise is supported to some extent by histological analysis of the severity of medullary congestion: there was a tendency towards reduced congestion in kidneys stored in mannitol prior to frusemide treatment compared to controls (Groups 3 and 4; Fig 9.9). Although this did not attain significance, the numbers studied were small and clearance of medullary congestion was in any case at an early stage.

In contrast, there was a surprisingly poor response to frusemide infusion in the kidneys stored in the PEG-based solution in terms of both the oxygenation index and cyt aa_3 oxidation and histology (Figs 9.5, 9.8 and 9.9). There are several possible explanations for this.

Firstly, PEG is non-ideal in terms of its colloidal osmotic pressure. Inclusion of PEG in the preservation solution at an equivalent concentration (in mmol/l) to mannitol resulted in a measured osmolarity of 700 mOsmol/l compared with to 485 mOsmol/l with mannitol (unpublished results). Accordingly, the concentration of PEG added to the solution was reduced to produce a final measured osmolarity of 485 mOsmol/l. It is possible that this manoeuvre diminished the efficacy of PEG in ameliorating cell swelling.

Secondly, Belzer and co-workers used high MW PEGs as their effect seemed to derive from an unexplained interaction with cell membranes rather than being simply a function of their colloidal osmotic pressure (Marsh *et al.*, 1989). In the present experiments, relatively low MW PEGs were used (average MW 600) as this is the lowest weight compatible with impermeability (Hider *et al.*, 1994) and should produce the highest colloidal osmotic pressure, allowing comparison with mannitol. It is possible that lower MW PEGs do not interact with cell membranes in the same fashion as more highly polymerized forms.

Thirdly, PEG may actually be toxic to renal cells. Although PEG can be taken up by renal lysosomes (Singhal *et al.*, 1987) and this may eventually be deleterious, the process occurs only slowly and is unlikely to have occurred during the preservation period. However, Kopolovic and colleagues (1989) have shown in the isolated perfused kidney that PEG can cause ultrastructural damage to different sections of the tubule depending on their degree of water permeability. PEG was found to cause particular damage to the mTAT - a pertinent finding in view of the specificity of frusemide for the mTAT.

Finally, the relatively high efficacy of mannitol compared to PEG may be related to other reported properties of mannitol: in addition to acting as an impermeant solute, mannitol can stimulate vasodilation (Goldberg and Lillienfield, 1965) and act as a scavenger of reactive oxygen metabolites (Hansson *et al.*, 1983).

9.6 Conclusions

(i) NIRS in transmission mode is a sensitive means of determining the haemodynamic and metabolic responses to frusemide in rabbit renal autografts.

(ii) Frusemide infusion resulted in significant increases in renal haemoglobin oxygenation in unstored autografted kidneys.

(iii) The expected increase in oxidation of cyt aa_3 did not occur, suggesting that the changes in renal haemodynamics overshadowed the diuretic effect of frusemide.

(iv) Frusemide infusion to kidneys stored in the mannitol based solution resulted in significant increases in haemoglobin oxygenation, but these were delayed by 15 min compared with unstored transplanted kidneys.

(v) The increase in haemoglobin oxygenation in kidneys stored in the mannitol based solution was accompanied by a significant reduction in cyt aa_3, suggesting that frusemide stimulation of cortical vasodilation was accompanied by clearance of medullary congestion.

(vi) Kidneys stored in the PEG-based solution responded poorly to frusemide infusion and presented a poor histological picture.

(vii) The selection of impermeant is therefore important and mannitol was significantly superior to PEG in this model.

CHAPTER 10

THESIS DISCUSSION

10.1 Analysis of Methodology

In the course of clinical transplantation, it is difficult to distinguish the pathology of acute rejection from that of ischaemic acute renal failure, as both processes involve vascular injury, acute inflammation and tubular necrosis. The use of an autograft model in the studies presented in this thesis has eliminated interference from rejection processes, allowing the pathogenesis of ischaemia-reperfusion injury to be studied in isolation. Nevertheless, the model is still considerably more complex than *ex vivo* or *in vitro* preparations, in which the elements of blood do not play a role. Models of warm ischaemia, in which the renal vessels are clamped *in situ* for varying periods of time, are a closer approximation to the conditions encountered during transplantation. However, in these models, degradation of haemoglobin from trapped erythrocytes during the ischaemic period may contribute significantly to vascular or parenchymal necrosis. Furthermore, hypothermia does not play a role in warm ischaemic models, either protective or detrimental; nor is it possible to manipulate the components of a preservation solution.

A renal autograft model therefore offers the best experimental simulation of the ischaemia-reperfusion conditions encountered during clinical renal transplantation. The methodology that must be employed is correspondingly complex, and the results obtained can be difficult to interpret. Nevertheless, if qualified by a combination of simple biochemical techniques, such as assays of susceptibility to lipid peroxidation, and careful histological examination, it is possible to gain an understanding of the underlying molecular and cellular pathology. Moreover, the effect of specific pharmacological intervention is a powerful diagnostic tool even if not ultimately successful in preventing acute renal failure, as it can give an indication of the importance of single toxic mediators (such as delocalized catalytic iron or individual eicosanoids) in the aetiology of ischaemia-reperfusion injury.

The thesis has been structured thematically rather than by methodology. The chapters are not therefore presented in chronological order of completion and the methods used not always consistent. However, the methods used were those available and applicable at the time of the experiment.

The most powerful non-invasive methods for *in vivo* measurements employed in the thesis were NIRS and surface fluorescence spectroscopy and the results of each required careful interpretation. Both techniques give an indication of the changes in concentration, rather than the absolute content, of endogenous chromophores or fluorophores.

10.1.1 Near Infrared Spectroscopy

NIR signals derived from biological tissues can be interpreted only if changes in absorption of each chromophore can be distinguished from simultaneous changes in the absorption of others. The NIR spectra of HbO_2, Hb and cyt aa_3, which are the only oxygen-dependent chromophores in the near infrared region in the kidney, are broad and overlap extensively. As these three overlapping spectra must be deconvoluted, absorption data are needed from at least three NIR wavelengths to measure the contributions of the three molecular species. The Hamamatsu instrument used in these studies employed four wavelength algorithms to provide accurate descriptions of NIR absorptions and scattering by tissues.

These algorithms were based on published absorption spectra which had been obtained using isolated chromophores in non-scattering media. The HbO_2 and Hb absorption spectra were measured in haemolysed human blood (Wray *et al.*, 1988) whereas the cyt aa_3 difference spectrum was obtained using purified cytochrome extracted from mitochondria (Brunori *et al.*, 1981). The relative contribution of each chromophore to the total optical density measured under different conditions at each of the four wavelengths was used to generate the multiplication factors (given in Chapter 2) and the modified Beer-Lambert Law (applicable to a scattering medium) was applied to each wavelength. One indication of the reliability of these algorithms *in vivo* is the independence of changes in the oxidation of cyt aa_3 compared with changes in HbO_2 under specific conditions. For example, cyt aa_3 has been shown to become oxidised in damaged tissues in which the mitochondria were uncoupled or in response to respiratory chain inhibitors even though no change in HbO_2 levels was detected (Pintadosi, 1989).

The results presented in Chapters 5 and 9 confirmed the independence of the cyt aa_3 response following infusion of the respiratory chain inhibitor sodium pentobarbitone. As expected, inhibition of electron transfer by blockade of NADH dehydrogenase at complex I resulted in reproducible oxidations of cyt aa_3. However, the situation upon reperfusion appeared to be more complex. The transition from an asanguinous state to full blood reperfusion that occurs upon revascularization is a factor that could affect the algorithms reliability. The changes in cyt aa_3 oxidation that occurred upon reperfusion in the studies presented in Chapter 5 displayed an independence from haemoglobin

oxygenation that suggested they were not artefactual. Nevertheless, in some instances such as those shown in Figs 9.1 and 9.2 there were very large reductions in cyt aa_3 upon reperfusion that appeared to be mirrored reflections of the increases in Hb concentration. It is possible that these were genuine biological responses. Such reductions could indicate that: (i) cyt aa_3 had become hyperoxidised during ischaemia; (ii) there had been a conformational change at complex IV rendering the Cu_A centre inaccessible to molecular oxygen; or (iii) formation of "pulsed" cyt aa_3 (the active form of cyt aa_3 responsible for the reduction of molecular oxygen) occurred so rapidly upon reperfusion that the large reduction measured was simply a reversion to baseline (Antonini *et al.*, 1977).

It is not inconceivable that cyt aa_3 could have become hyperoxidised as a result of standard flushing procedures with cold hypertonic citrate solution, as the solution was equilibrated with atmospheric oxygen, and rapid induction of intra-renal hypothermia should suppress electron transfer. The high concentration of reduced pyridinine nucleotides measured using surface fluorescence spectroscopy during renal storage tends to counter this possibility, since it suggests that intra-cellular conditions were reductive. However, suppression of electron transfer as a consequence of hypothermia should theoretically also prevent oxidation of NADH even in the presence of oxygen. The second possibility involving conformational change is less likely, as large reductions in cyt aa_3 were observed even in unstored transplanted kidneys and most *in vitro* studies have shown that complex IV activity is relatively unaffected even by extended periods of hypoxia and reoxygenation (Malis and Bonventre, 1986; Hardy *et al.*, 1991; Veitch *et al.*, 1992; Ambrosio *et al.*, 1993). Similarly, although extremely rapid formation of "pulsed" cyt aa_3 has been shown to occur *in vitro* (Antonini *et al.*, 1977) it is unlikely to occur at similar speeds *in vivo* as its formation is dependent upon the speed of reperfusion. The NIRS studies presented in Chapter 4 showed that full renal reperfusion required a minimum of 30 sec even in unstored transplanted kidneys, a time scale comfortably within the limits of NIR detection. Discrimination between artefacts generated by algorithm unreliability and genuine biological responses may be achieved by monitoring changes in cyt aa_3 oxidation during standard flushing procedures using either oxygenated or hypoxic (nitrogenated) HCA solution.

10.1.2 Surface Fluorescence Spectroscopy

Surface fluorescence spectroscopy of mitochondrial NADH is less fraught with methodological difficulties. Three constituents of autografted kidneys potentially interfere with mitochondrial NADH fluorescence: (i) cytosolic NADH; (ii) NADPH; and (iii) Hb. O'Connor (1977) reported that NADH fluorescence signals from cytosolic NADH were negligible compared with those from the mitochondrial pool as a result of quenching of fluorescence by cytosolic glyceraldehyde -3-phosphate dehydrogenase. NADPH, which has similar optical properties to NADH, is not responsive to changes

in arterial oxygen partial pressure (Chance and Williams, 1955). Quenching of fluorescence by Hb has been shown to occur *in* vivo but with a curious delay of up to 5 min after clamping of the vessels before Hb interferes with NADH fluorescence (Kobayashi *et al.*, 1971). The results presented in Chapters 5 and 6 suggest that the presence of blood did not interfere with mitochondrial NADH fluorescence in the NZW rabbit renal autograft model. Thus, abrupt changes in pyridinine nucleotide fluorescence are almost certainly attributable to changes in concentration of mitochondrial NADH.

Evaluation of *in vivo* surface fluorescence spectroscopy and NIRS data must also take into account the discrepancy between measurements of NADH fluorescence (which reflect changes in the superficial renal cortex) and measurements of cyt aa_3 (which reflect absorption across the entire kidney). In fact, Epstein and co-workers (1982) showed that agents capable of altering metabolism or active transport primarily in the cortex of isolated perfused kidneys had little or no effect on the redox state of cyt aa_3, suggesting that the rate of oxygen consumption was not a critical determinant of cyt aa_3 redox status in these sections of the tubule. Thus, the NIRS measurements of changes in the redox state of cyt aa_3 reported in Chapters 5 and 9 may primarily reflect changes in the cortico-medullary junction. However, such discrepancies, if recognized, can be used to distinguish between damage occurring in different regions of the kidney and give a strong indication that mitochondrial dysfunction occurs in the superficial cortex as well as in the poorly perfused cortico-medullary junction.

10.1.3 Biochemical Analysis

The major biochemical analyses used in this thesis were: (i) ELISA assays of serum eicosanoids; and (ii) fluorescence assays of Schiff's bases and TBA-reactive material in renal homogenates.

The ELISA assays were carried out using commercially available kits. The most important experimental constraint was the difficulty in obtaining large serum samples directly from the renal vein. Full blood samples (0.5 ml) were sufficient to allow duplicate assays of leukotriene B_4, thromboxane B_2 and 6-k-$PGF_{1\alpha}$, which involved identical purification procedures. However, the serum samples were too small to permit assays of other prostaglandins requiring separate purification procedures such as PGE_2 of PGF_2. As there are numerous PGE_2 receptors in the mTAT and PGE_2 has been shown to have a direct effect on ion pump function in these tubules, ELISA assays of serum PGE_2 levels following transplantation would be valuable.

Assays of lipid peroxidation have been criticised from many quarters (Fuld *et al.*, 1986; Gamelin and Zager, 1988; Fuller *et al.*, 1988; Halliwell and Gutteridge 1989). Firstly there are various cellular processes in addition to lipid peroxidative chain reactions that generate Schiff's bases or thiobarbituric

acid reactive material, such as the inflammatory enzymes lipoxygenase and cyclooxygenase (Gower *et al.*, 1989). Secondly, the assay (as performed in these studies) is a measure of *susceptibility* to lipid peroxidation rather than the actual amount of peroxide generated by the system: it cannot therefore be considered other than very circumstantial evidence of radical reactions that have actually taken place *in vivo* (Green *et al.*, 1986). Thirdly, it is quite possible that lipid peroxidation does not play a major role in the aetiology of renal ischaemia-reperfusion injury compared with more specific alterations in protein or DNA oxidation (Holmberg *et al.*, 1991; Caraceni *et al.*, 1994). Finally, trapped haemoglobin in warm ischaemic models may falsely raise apparent tissue MDA levels as the OD spectrum of haem overlaps with that of malondialdehyde (Uchiyama and Mihara, 1978; Fuld *et al.*, 1986; Gamelin and Zager, 1988) and release of haemoglobin iron during tissue homogenization could drive the Fenton reaction, stimulating free radical generation (Cross *et al.*, 1987).

Despite these drawbacks, assays of susceptibility to lipid peroxidation in renal homogenates have several advantages. First and foremost, assays of lipid peroxidation are simple and reproducible, unlike other methods of detecting radicals and their byproducts, such as paramagnetic electron spin resonance spectroscopy, chemiluminescence or ethane exhalation. They may therefore be used as an adjunct to more complicated experiments involving surface fluorescence or NIR spectroscopy. Second, the assay gives an indication of the ability of an antioxidant agent to inhibit lipid peroxidation or eicosanoid synthesis in a model system of equivalent biochemical components to those encountered *in vivo* (unlike microsomal models or cell cultures) but without the accompanying pharmacokinetic uncertainties that can confound interpretation of truly *in vivo* determinations. Thus, an agent such as desferrioxamine may successfully inhibit lipid peroxidation in renal homogenates, demonstrating that its iron chelating or antioxidant capacity is effective in this model system, whereas its *in vivo* efficacy may be affected by its low access to intracellular sites. Third, the contribution of inflammatory processes to the total quantity of Schiff's bases or TBA-reactive material measured can be established by the use of specific agents such as indomethacin or desferrioxamine to suppress cyclooxygenase metabolism or iron-mediated lipid peroxidation respectively. Fourth, an assay of *susceptibility* to lipid peroxidation is well within the limits of sensitivity of the technique, whereas direct measurements of limited or localised peroxide generation (which may nonetheless have a significant effect on cellular function) may be on the limits of detection, yielding variable or conflicting results. Further to this, analysis of susceptibility to lipid peroxidation could be argued to provide an indirect measure of susceptibility to other forms of oxidative damage such as oxidation of proteins and DNA, whereas direct measurements of lipid peroxidation must remain just that. Finally, haemoglobin artefacts can be eliminated by *in vitro* incubation of renal homogenates prepared from kidneys flushed clean of blood upon nephrectomy and subsequently stored for the desired period, but

not reperfused with blood. The fact that TBA and Schiff's base assays have previously been shown to correlate well both with long-term renal viability and with the therapeutic efficacy of antioxidant drugs is in itself a justification for their continued usage (Fuller *et al.*, 1988).

10.1.4 Histological Analysis

Histological analysis of renal tissue subjected to ischaemia-reperfusion injury was one of the primary analytical techniques used in this thesis. All biochemical or spectroscopic measurements have been qualified by light or electron microscopical assessment of changes in renal morphology. There are two major criticisms that may be raised concerning hisological analysis: (i) it is difficult to quantify data without risk of subjectivity; and (ii) it is possible that the morphological changes observed, particularly at the electron microscopical level, are artefactual. The problem of quantitation and subjectivity can be partially resolved using morphometric analysis. However, in kidneys it can be difficult to distinguish between different segents of the nephron by diameter or density, particularly when such discrimination is between the S1, S2 or S3 segments of the proximal tubule or between the mTAT and the straight descending limbs. Histological analysis has therefore been restricted to subjective semi-quantitative estimations of renal damage corroborated blindly by an independent pathologist. The problem of artefact at the electron microscopical level is long-standing but should not be applicable to the studies reported in this thesis (as opposed to identification of unknown subcellular structures). Electron microscopical changes have parallelled changes observed by light microscopy throughout the studies presented in this thesis and may reasonably be considered genuine morphological change rather than handling artefact.

10.2 Hypothesis and Aims

It was hypothesized at the close of the Chapter 1 that:

Acute renal failure following prolonged hypothermic storage and transplantation is a consequence of both oxidative reperfusion injury and secondary ischaemia. Therefore, pharmacological strategies aimed at prolonging the 'safe' storage time of transplanted kidneys cannot be successful unless thay effectively combat both causes.

The results presented in this thesis are consistent with the hypothesis but have not wholly proved it. Proof of the hypothesis requires fulfilment of four conditions, which were encompassed within the aims of the thesis, as stated in Chapter 1:

1. *To establish patterns of damage to the renal parenchyma and vascular system resulting from storage and transplantation in the NZW rabbit renal autograft model.*

If cell damage occurs by different mechanisms in the kidney as proposed in the hypothesis, the timing, distribution and severity of injury should vary in different regions of the kidney. It was shown in Chapter 3 that the mTAT became mildy oedematous during prolonged storage, but that other cell types were well preserved. Upon reperfusion, those sections of nephron associated with high work loads, especially the proximal tubules and the mTAT, suffered the greatest histopathological damage, but their vascular environments were significantly different. The peritubular capillaries of the outer medulla which supply the mTAT were severely congested with erythrocytes, while the cortical peritubular capillaries supplying the proximal tubules were not congested. Autopsies of kidneys taken from rabbits suffering acute renal failure suggested that ATN was restricted mostly to the renal cortex and the cortico-medullary junction. Not only was mTAT necrosis less marked but there were no vestiges of erythrocyte congestion at this time. Thus, the first condition of the hypothesis, that different cell types should respond differently to hypothermic storage and transplantation was fulfilled.

2. *To develop non-invasive methods of measuring renal haemoglobin and tissue oxygenation in vivo.*

Free radical-mediated injury is likely to occur immediately upon reperfusion, whereas secondary ischaemic damage is dependent upon poor or patchy perfusion and haemoglobin oxygenation. It was evident by light microscopy that blood penetrated the entire vascular network of the kidney upon reperfusion (see Chapters 3 and 4). Thus, secondary ischaemic damage must depend on subsequent haemoglobin de-oxygenation, the kinetics of which were previously unknown in autografted kidneys. To define haemoglobin oxygenation kinetics *in vivo* the non-invasive technique NIRS was used (see Chapters 2 and Chapter 4). It was shown that NIRS in transmission mode could be used to measure changes in concentration of HbO_2 and Hb across the entire kidney.

Renal haemoglobin oxygenation was comparable in unstored and 72 h stored autografted kidneys during the first 5 min of reperfusion, but there was a profound haemoglobin desaturation in stored kidneys thereafter. This very low haemoglobin saturation must have rendered the medulla, and possibly the cortex, hypoxic throughout the procedure. Nevertheless, both barium sulphate angiography and conventional histology suggested that cortical vascular resistance was relatively unaffected by prolonged ischaemia throughout the period of reperfusion, whereas medullary vascular resistance was very high during at least the first 1 h of reperfusion. However, medullary vascular resistance had fallen significantly after 3 h of reperfusion. Thus, the second condition of the

hypothesis that there should be areas within the kidney potentially susceptible to secondary ischaemic damage as a result of profound haemoglobin desaturation was fulfilled.

3. *To define the relationship between tissue oxygenation and mitochondrial function in vivo.*

The premise that free radical-mediated injury should be detectable immediately upon reperfusion whereas secondary ischaemic damage must develop during periods of haemoglobin desaturation left a window during the first 5 min of reperfusion of stored kidneys when haemoglobin oxygenation was not significantly different from unstored controls. The determinations of lipid peroxidation in renal homogenates presented in Chapter 3 suggested that stored kidneys were indeed susceptible to oxidative injury upon reperfusion but did not prove that this was a cause, rather than a symptom, of tubular necrosis.

To monitor changes in renal metabolic function induced by ischaemia and reperfusion *in vivo*, NIRS was used in conjunction with surface fluorescence spectroscopy to provide an indication of changes in the redox state of the respiratory chain components cyt aa_3 and mitochondrial NADH respectively. The results (Chapter 5) demonstrated that these techniques were sufficiently sensitive to measure mitochondrial responses to:

- Reperfusion;
- Changes in arterial oxygen partial pressure;
- Specific inhibition of the respiratory chain at complex I.

Furthermore, it was shown that:

- The presence of blood (HbO_2 or Hb) did not significantly affect the signals measured;
- There were good correlations between changes in mitochondrial NADH fluorescence, the oxidation state of cyt aa_3 and the severity of oedema in autografted kidneys;
- Both cyt aa_3 and NADH responded abnormally to reperfusion of 72 h stored kidneys compared with unstored kidneys.

Surface fluorescence measurements of mitochondrial NADH were extended in Chapter 6 to give an indication of the kinetics of change of NADH fluorescence within the first 5 min of reperfusion. These measurements reflected mitochondrial function in the superficial cortex, which was shown in Chapter 4 to be well oxygenated during this period in both stored and unstored autografted kidneys. The rate

of oxidation of NADH upon reperfusion was similar in both groups of kidneys but inhibition of complex I after 4.5 min of reperfusion resulted in significant regeneration of NADH in unstored kidneys and very poor regeneration in 72 h stored kidneys. It was concluded that renal ischaemia-reperfusion injury can occur rapidly and directly, with or without medullary congestion and attendent secondary ischaemia. These results fulfil the third condition of the hypothesis that there should be areas in the kidney susceptible to direct ischaemia-reperfusion injury regardless of changes in haemoglobin oxygenation.

4. *To investigate specific therapeutic approaches to mitigating renal ischaemia-reperfusion injury in vivo.*

The final condition of the hypothesis may be subdivided into three propositions: (i) pharmacological strategies specifically directed to reduce free radical mediated injury will reduce indices of damage in those cell types susceptible to oxidative reperfusion injury but will not prevent acute renal failure; (ii) pharmacological strategies directed to reduce secondary ischaemic damage will ameliorate cellular swelling and necrosis in poorly perfused regions of the kidney but will not prevent free radical-mediated injury elsewhere; and (iii) combined therapy involving both suppression of free radical mediated injury and secondary ischaemic injury will improve post-ischaemic renal function and prevent development of acute renal failure.

In Chapter 6, three iron chelators (desferrioxamine, CP102 and NMHH) were used in an attempt to improve respiratory chain function during the first 5 min of reperfusion of autografted 72 h stored kidneys, according to the hypothesis that delocalized iron is necessary to catalyse the formation of hydroxyl radicals from superoxide (generated by electron leakage at complex I). None of the chelators significantly enhanced NADH regeneration following inhibition of complex I compared with untreated controls but all three significantly reduced susceptibility to lipid peroxidation and improved the morphological appearance of the cortex, suggesting that they could have preserved cellular integrity during early reperfusion. These limited effects were not sufficient to improve long-term renal viability, either because the chelators did not improve mitochondrial function or because they had no effect on medullary congestion and secondary ischaemia. These results are nonetheless consistent with the first proposition (above) that amelioration of direct ischaemia-reperfusion injury does not in itself improve long-term viability.

The early susceptibility of the medulla to lipid peroxidation described in Chapter 3 suggested that hydroperoxides were formed in the medulla via the activation of cyclooxygenase and lipoxygenase, and that these vaso-active products could have contributed to medullary congestion. In Chapter 7, it

was proposed that a novel inhibitor of lipoxygenase, BW B70C, could improve long term renal viability by a combination of mechanisms including (i) inhibition of leaukotriene B_4 synthase, thereby attenuating vascular permeability, mTAT swelling and neutrophil activation; (ii) amelioration of lipoxygenase-mediated hydroperoxide amplification, thereby reducing calcium-activated mitochondrial lipid peroxidation; and (iii) chelation of delocalized iron, thereby reducing iron-mediated lipid peroxidation, inactivation of specific membrane pumps and denaturation of DNA.

BW B70C was shown to significantly inhibit leukotriene B_4 synthesis and to limit the volumes of cortical necrosis and calcification three days after revascularization but to have no effect on vascular permeability and to exacerbate medullary congestion and haemorrhage. The reasons for this were obscure. It was postulated that inhibition of lipoxygenase by BW B70C could have inhibited basolateral Na^+, K^+ and Cl^- channels in the mTAT by suppressing the metabolism of lipoxygenase intermediates to metabolites capable of stimulating ion pump activity, while having no effect on apical membrane pumps. Such a scenario could have exacerbated swelling of the mTAT by preventing fluid movement from the mTAT to the interstitium. A similar mechanism involving inhibition of active reabsorption by prostacyclin was suggested in Chapter 9 and is discussed more fully in Section 10.4. Another possibility is that BW B70C, by inhibiting lipoxygenase, could have stimulated arachidonic acid metabolism via cyclooxygenase or cyctochrome P-450. It was shown in Chapter 7 that serum levels of thromboxane B_2, the breakdown product of the most potently damaging eicosanoid TxA_2, and 6-k-$PGF_{1\alpha}$, the breakdown product of prostacyclin, were not significantly from controls. Nevertheless, it is feasible that formation of other prostaglandins, HPETES and HETES (see Chapter 1) was enhanced and that this could have caused hydroperoxide amplification in the mTAT. Thus again, as predicted in the first proposition (above) an agent which significantly reduced cortical tubular necrosis and calcification during the first few days of reperfusion did not ameliorate medullary damage and did not therefore prevent acute renal failure.

The possibility that cyclooxygenase products were partly responsible for vascular and tubular damage in the medulla was explored in experiments using the organo-selenium compound ebselen (Chapter 8), which in addition to various antioxidant properties has been shown to inhibit cyclooxygenase *in vitro* with an IC_{50} of 0.5 mM. However, despite causing significant reductions in susceptibility to iron- and lipoxygenase-mediated lipid peroxidation and in cortical inflammation at autopsy following 48 h of storage and autografting, ebselen treatment did not appear to inhibit cyclooxygenase or to have any effect on medullary congestion, mTAT swelling or long-term renal viability. As was the case with BW B70C, these results are compatible with the first proposition - a disappointment in the light of ebselens broad range of antioxidant properties *in vitro*.

The effect of two impermeant colloids (PEG and mannitol) on ischaemia-reperfusion injury to the mTAT was evaluated in Chapter 9 using NIRS to monitor changes in the redox state of cyt aa_3 following frusemide infusion (which should predominantly effect the mTAT) and histological analysis. Paradoxically, frusemide infusion caused reductions (rather than the expected oxidations) of cyt aa_3 in the presence of both mannitol and PEG despite increases in renal oxygenation. This may have reflected an increase in cortical bloodflow and an associated decrease in medullary bloodflow as described previously (Atkins and Lankford, 1991; Brezis *et al.*, 1994). Although neither mannitol or PEG had a significant effect on tubular swelling, as judged using light microscopy, there were nevertheless consistent and significant differences in responsiveness to frusemide in terms of the redox state of cyt aa_3, suggesting that the impermeant solute included in the preservation solution does indeed have an effect on tubular function and that mannitol was superior to PEG in this model.

As both ebselen and low molecular weight PEG were ineffective at reducing mTAT swelling and medullary congestion in this model, it was not possible to prove the second and third propositions of the final condition of the hypothesis that amelioration of ischaemia-reperfusion injury following prolonged renal storage is dependent on the successful preservation of both medullary and cortical function. Nevertheless, the results obtained were compatible with the hypothesis throughout the thesis, and the importance of reducing mTAT swelling and vascular congestion in the medulla and of improving mitochondrial function and cellular integrity in the cortex has been repeatedly demonstrated.

10.3 Conclusions, Reflections and Future Perspectives

The results of the studies presented in this thesis highlight two major areas of importance in the pathogenesis of acute renal failure following hypothermic storage and transplantation:

- Global mitochondrial dysfunction;
- Swelling and dysfunction of mTAT cells.

In vivo mitochondrial function was abnormal in both the superficial cortex and cortico-medullary junction within the first 5 min of reperfusion. Mitochondrial dysfunction was not causally related to secondary ischaemia (Chapters 4 and 6) and may or may not have been a consequence of free radical generation. Abnormal (or absent) changes in cyt aa_3 oxidation immediately upon reperfusion (Chapter 5) suggest that the defect could have occurred during the cold ischaemic period but this does not necessarily rule out free radical-mediated injury (see below). Mitochondrial dysfunction was apparent

even after inhibition of complex I with sodium pentobarbitone, suggesting that the primary lesion may be localized to complex I or result from substrate deficiency leading to complex I (Chapter 6). This conclusion is supported by the rapid oxidation of mitochondrial NADH upon reperfusion of stored kidneys, despite no change in the oxidation of cyt aa_3 response in the same kidneys (Chapter 5). 'Intracellular' iron chelators, while reducing susceptibility to lipid peroxidation and improving the histological apearance of the cortex did not affect the deficit in mitochondrial function (Chapter 6). Therefore, it seems unlikely that delocalized iron is responsible for catalysing the inactivation of complex I via the Fenton reaction. Free radical-mediated injury may nevertheless be implicated either via direct $O_2^{\bullet-}$ toxicity or as a result of specific auto-inactivation involving disrupted iron-sulphur centres or cytochromes. The apparent localization of damage to complex I suggests that direct $O_2^{\bullet-}$-mediated toxicity may not be the most important mechanism, as its relatively low reactivity would tend to induce more diffuse damage to the respiratory chain.

The causes and consequences of mTAT swelling also appear to be complex. The colloidal carbon perfusion studies presented in Chapter 7 suggest that endothelial permeability may become selectively enhanced in the outer band of the outer medulla during the ischaemic period itself. Increased endothelial permeability, when coupled with the inactivation of mTAT Na^+-K^+-ATPase and the consequent depolarization and increased basolateral permeability of these cells (see below) may stimulate tubular swelling and compression of the *vasa recta* and peritubular capillaries. The studies presented in Chapter 9 show that this process can be modulated but not prevented by substitution of impermeant solutes. However, a carefully controlled study comparing a larger number of solutes, including rafinose, lactobionate and high molecular weight PEG on mTAT function would be valuable.

The pathophysiological implications of mTAT swelling and dysfunction are also complex. It is clear from the studies presented in Chapters 3, 4, 7 and 9 that medullary congestion, and therefore presumably mTAT dysfunction, are reversible over several hours. Eicosanoids certainly play a role in modulating both mTAT and global renal function during reperfusion, but whether this is achieved principally through their vaso-activity, via diverse effects on active ion transport, particulary Na^+-K^+-ATPase, or a combination of the two, is unclear. Increases in plasma prostacyclin levels do appear to be associated with improvements in renal blood flow (Chapter 7) and may also be associated with an energy-dependent restitution of cellular homeostasis (see below). This hypothesis is supported by the consistently observed steady-state reductions in cyt aa_3 during the clearance of medullary congestion, which were associated with improved histological appearance and possibly long-term viability (Chapter 9). However, the therapeutic implications of the studies presented in Chapters 6 to 9 are

uncertain. All the agents tested - iron chelators, antioxidants, specific inhibitors of eicosanoid synthesis, impermeant solutes and diuretics - had some positive effects on renal pathophysiology, but none had a significant impact on the long-term viability of stored autografted kidneys. In this respect, the studies presented in this thesis serve to emphasize the complexity of the problem *in vivo*.

Therapeutic enhancement of mitochondrial function *in vivo* is likely to founder mostly on the pharmacology of the antioxidant agents used. Many *in vitro* studies have shown that complex I is particulary susceptible to hypoxia and reoxygenation (Malis and Bonventre, 1986; Hardy *et al.*, 1991; Veitch *et al.*, 1992; Ambrosio *et al.*, 1993; Sammut *et al.*, 1995; Reinheckel *et al.*, 1995) and a range of agents from calcium and iron chelators to potassium cyanide have proved effective at protecting respiratory chain activity *in vitro* (Turrens *et al.*, 1982; Ferrari *et al.*, 1982; Vandeplassche *et al.*, 1989; Schultze-Osthoff *et al.*, 1992; Paraidathathu *et al.*, 1992; Ambrosio *et al.*, 1993; Richter, 1993). Most approaches to protecting respiratory chain activity *in vitro* have fallen into two categories: (i) suppression of mitochondrial inner membrane lipid peroxidation, especially oxidation of cardiolipin and auto-oxidation of complex I (Fry and Green, 1981) using a combination of iron chelation and calcium blockade (Schultze-Ostoff *et al.*, 1992); and (ii) direct inhibition of electron transfer at different points in the respiratory chain, for example using sodium pentobarbitone to block complex I, or potassium cyanide to block complex IV (Ambrosio *et al.*, 1993).

As seen in Chapter 6, the use of intracellular iron chelation *in vivo* had much less effect on respiratory chain function than predicted from *in vitro* results. With the exception of the studies presented in this thesis, no published data are available evaluating the effect of iron chelation on *in vivo* mitochondrial function. The value of calcium channel blockers such as verapamil is counterbalanced *in vivo* by the inclusion of calcium chelators such as citrate in the preservation solution (Green *et al.*, 1993). Ruthenium red, which inhibits mitochondrial calcium uptake, has been shown to enhance mitochondrial function both *in vitro* and *in vivo* (Ferrari *et al.*, 1982), but to cause significant increases in cellular lipid peroxidation, and to be detrimental to long-term viability (Green *et al.*, 1993). Thus, the effectiveness of iron or calcium chelation as an approach to mitigating renal ischaemia-reperfusion injury is highly dependent on the pharmacology of individual agents, and the specificity of action *in vivo*. In contrast, the use of respiratory chain inhibitors *in vivo* requires a delicate balance to be achieved between maintainance of respiratory chain integrity by suppression of electron transfer and the energetic demands of the cell, or indeed the recipient. It is possible that this approach may prove beneficial *in vivo* if the drug is: (i) a reversible inhibitor, such as sodium pentobarbitone; (ii) administered in the preservation solution only; and (iii) combined with a Na-K-ATPase inhibitor, such

as ouabain, during early reperfusion, to reduce the work-load of the kidney (Heyman *et al.*, 1994; Kumada *et al.*, 1994).

Glycine is another cyto-protectant that has been shown to dramatically reduce mitochondrial membrane degeneration and ATP depletion in renal tubule cells and hepatocytes by as yet unexplained mechanisms (Weinberg *et al.*, 1991; den-Butter *et al.*, 1993; Marsh *et al.*, 1993). Protection by glycine takes place entirely during hypoxia or metabolic inhibition (Weinberg *et al.*, 1987), and may be related to: (i) inhibition of calcium-dependent polyphosphoinositide hydrolysis, which does not require energy and can occur during ischaemia (Garza-Quintero *et al.*, 1993); (ii) conjugation of glycine with acyl-CoA compounds, which damage membranes because of their detergent properties (Weinberg *et al.*, 1991); or (iii) binding of acetaldehyde, which has been proposed to regulate the respiratory chain by changing the structural-functional state of ubiquinone (Korneev and Komissarova, 1994). However, Wetzels and colleagues (1993) were unable to demonstrate any protective effect of glycine in a warm ischaemic model of acute renal failure, while Heyman and colleagues (1993) showed that glycine infusion actually increased necrosis of the thick ascending tubules in the renal medulla following ischaemia.

A less hazardous approach has been suggested by Veitch and co-workers (1992), who demonstrated that anoxic perfusion of Langendorff-perfused rat hearts prior to global ischaemia resulted in significant protection of complex I activity during reperfusion, compared with hearts that had not been subject to anoxic pre-perfusion. These authors suggested that anoxic pre-perfusion could have prevented oxygen derived free radical formation during ischaemia itself, as free radical activity has been demonstrated at very low oxygen partial pressures (≤1 mmHg; Rao *et al.*, 1983). The results presented in Chapter 8, showing a correlation between medullary oedema prior to reperfusion and susceptibility to lipid peroxidation, suggested that free-radical mediated events, such as those mediated by cyclo-oxygenase activation, could indeed occur during the storage period prior to transplantation (Gower *et al.*, 1992). Removal of residual oxygen by anoxic flushing may therefore prove beneficial during renal storage prior to transplantation.

Anoxic pre-perfusion can be regarded as conferring a kind of acquired resistance to acute oxidative stress. The period of time between anoxia and ischaemia in the experiments of Veitch and colleagues was too short to allow increased expression of stress proteins. However, pre-conditioning of organs by induction of stress or "heat shock" proteins several hours before ischaemia has led to exciting new possibilities in organ preservation. The heat shock response was first discovered over 30 years ago, and it has since become clear that many types of metabolic insult, including exposure to metabolic

poisons, such as endotoxin, or to ischaemia and reperfusion, can elicit increased expression of stress proteins (Minowada and Welch, 1995).

Recently, it has been shown that prior administration of endotoxin conferred resistance to glycerol mediated acute renal failure by induction of increased haem oxygenase and ferritin synthesis (Vogt *et al.*, 1995). Haem oxygenase is a microsomal enzyme that catalyses the rate limiting step in the degradation of haem. Although degradation of haemoglobin may not play an important role in renal ischaemia-reperfusion injury, at least in the early stages (Gower *et al.*, 1993), it has been shown by Paller and associates that degradation of labile cytochrome P-450 is a major source of catalytic iron during renal ischaemia-reperfusion injury (Paller and Jacob, 1994). Not only would increased haem oxygenase activity allow degradation of any haem released from endogenous oxidatively denatured haem proteins, but increased tissue ferritin should bind iron released from haem (Vogt *et al.*, 1995). Furthermore, increased haem oxygenase activity leads to increases in bilirubin and biliverdin, which are efficient free-radical scavengers, and carbon monoxide (CO), which has been shown to activate guanylate cyclase in vascular smooth muscle in a manner analogous to nitic oxide, thereby stimulating vasodilation (Utz and Ullrich, 1991; Maines, 1993).

Another family of stress proteins of potentially great importance in renal ischaemia-reperfusion injury is the HSP-70 family. It has been shown that renal ischaemia causes redistribution of proximal tubule or mTAT Na-K-ATPase from a restricted baso-lateral expression to the apical membrane (Molitoris *et al.*, 1992; Van Why *et al.*, 1994). Restitution of baso-lateral localization of Na-K-ATPase occurs during reperfusion at speeds related to the severity of injury (Van Why *et al.*, 1994). It is not known whether loss of mTAT or proximal tubule polarity affects the development of oedema or modulation of the pump (by agents such as ouabain or 12(R)-HETE, a cytochrome P-450 arachidonate metabolite), but Na-K-ATPase found in apical membranes after ischaemia does bind ouabain (Molitoris *et al.*, 1988).

It has been proposed that members of the HSP-70 heat shock protein family assist cell repair by interacting with aberrant proteins after stress (Pelham 1986), and translocating them across intracellular membranes (Chirico *et al.*, 1988; Deshais *et al.*, 1988; Van Why *et al.*, 1994). HSP-70 proteins and mRNA are rapidly induced after renal ischaemia, and the pattern of HSP-72 distribution during the recovery period parallels the changes in Na-K-ATPase localization (Van Why *et al.*, 1992). Inducible HSP-70 mRNA progresses from negligible levels to peak induction within 2 h of reflow (Van Why *et al.*, 1992), which also reflects the timing of clearance of medullary congestion in the NZW rabbit renal autograft model (Chapter 4). Thus it is possible that prior induction of an HSP-70

response by ischaemic pre-conditioning or endotoxin treatment could potentiate recovery of mTAT polarity following hypothermic storage, ameliorate oedematous swelling in the cortico-medullary junction, and thereby reduce erythrocyte congestion and secondary ischaemia.

Ischaemic swelling of the mTAT may be partly a consequence of loss of cellular polarity and membrane integrity, but is also likely to be related to increases in vascular permeability during ischaemia and reperfusion. It was shown in Chapter 7 that there were significant increases in vascular permeability, as indicated by perivascular trapping of infused colloidal carbon, in a narrow band in the outer stripe of the outer medulla. Loss of baso-lateral Na-K-ATPase activity, either by ischaemic inactivation, oxidation of sulphydryl groups upon reperfusion, or redistribution to the apical membrane, results in baso-lateral membrane depolarization and susceptibility to cellular swelling (Greger, 1985). Ischaemic redistribution of Na-K-ATPase seems to be due to a loss of attachment to the cytoskeleton and disruption of intercellular tight junctions (Molitoris, 1991). Similarly, increases in vascular permeability during ischaemia and reperfusion appear to be dependent upon disruption of cytoskeletal F-actin filaments of endothelial cells, resulting in cell rounding formation of inter-cellular gaps (Wong and Gotlieb, 1990; Hidalgo *et al.*, 1995).

Endothelial monolayer permeability appears to be modulated by agents capable of stimulating intra-cellular cyclic AMP (cAMP) levels (Casnocha *et al.*, 1989). The mechanism is controversial, but evidence suggests that a cAMP-dependent protein kinase could mediate cytoskeletal alterations leading to increased numbers of stress fibres and augmentation of intercellular junctions (Killacky *et al.*, 1986; Alexander *et al.*, 1988; Casnocha *et al.*, 1989). A number of agents are capable of stimulating adenylate cyclase *in vitro*, including forskolin, isobutyl-methylxanthine (IBMX) and prostacyclin (Casnocha *et al.*, 1989). It was shown in Chapter 7 that serum levels of prostacyclin increased significantly after 30 to 60 min of reperfusion of 48 h stored kidneys and it is perhaps not co-incidental that the rise was associated with clearance of medullary erythrocyte congestion. It is possible that prostacyclin mediated a reduction of endothelial permeability by activation of adenylate cyclase, thereby ameliorating oedematous swelling of the mTAT and reducing haemoconcentration in the peritubular capillaries.

Curiously, prostacyclin and PGE_2 appear to inhibit cAMP generation in the mTAT at high concentrations through coupling to G_i proteins, but stimulate adenylate cyclase at low concentrations via G_s proteins (Smith *et al.*, 1987; Frazier and Yorio, 1992). Agents which stimulate cAMP generation in the mTAT, such as antidiuretic hormone (ADH), increase active sodium chloride reabsorption by means of elevating trans-epithelial conductance and potential difference, and

depolarizing the baso-lateral membrane, thereby increasing its conductance (Greger, 1985). Inhibition of these changes by prostacyclin or PGE_2 should therefore reduce sodium chloride absorption, prevent fluid movement from the peritubular capillaries into the tubule, and enhance recovery of the mTAT following ischaemic insult. Although indiscriminate use of cAMP stimulators *in vivo* would not necessarily be beneficial, infusion with stable prostacyclin analogues, such as iloprost, may help to reduce medullary congestion following prolonged ischaemia before endogenous synthesis is stimulated.

A combination of these factors may significantly enhance renal preservation. It is possible that an endotoxic shock to the donor, some three to six hours prior to nephrectomy, could stimulate expression of stress proteins, including haem oxygenase, ferritin and HSP-70, thereby rendering the kidney less susceptible to ischaemia-reperfusion injury after subsequent storage. In addition, it may prove beneficial to render the preservation solution anoxic (by previous gassing with nitrogen), and to store kidneys in sealed containers, to prevent free radical-mediated injury occurring during the preservation period itself. The preservation solution could reasonably be based on hypertonic citrate solution, since this is a very simple and cheap formulation, and might include additionally (i) glycine, or ruthenium red, to protect specifically against mitochondrial damage; (ii) an iron chelator, such as CP102, to reduce free radical mediated injury, particularly in the renal cortex; (iii) a cyclic AMP activator, preferably iloprost, to reduce endothelial permeability; and (iv) an impermeant colloid such as raffinose, or a high molecular weight polyethylene glycol (in place of mannitol), to reduce mTAT swelling. It may also be beneficial to continuously infuse iloprost, CP102 and frusemide (to inhibit active reabsorption) during reperfusion, for a period of approximately 45 min, to ameliorate the acute phase of medullary congestion.

LIST OF PUBLICATIONS

Full Papers

Lane NJ, Thorniley MS, Manek S, Fuller BJ, Green CJ. The effect of mannitol and polyethylene glycol on the action of frusemide during renal storage and transplantation. *Transplantation* (in press, June 1996).

Thorniley MS, Lane NJ, Simpkin S, Fuller BJ, Jenabzadeh MZ, Green CJ. Monitoring of mitochondrial NADH levels by surface fluorometry as an indication of ischaemia during hepatic and renal transplantation. In *Oxygen Transport to Tissue* Vol XVII (Eds Ince C, Kesecioglu J, Trelci I, Apkir K); Plenum Press (in press, June 1996).

Lane NJ, Thorniley MS, Manek S, Fuller BJ, Green CJ. Hemoglobin oxygenation kinetics and secondary ischemia in renal transplantation. *Transplantation* 1996; **61:** 689-696

Lane NJ. Radical problems in renal transplantation. *Biologist* 1996; **43:** 110-113.

Lane NJ, Thorniley MS, Manek S, Fuller BJ, Green CJ. Inhibition of leukotriene B_4 synthesis does not prevent development of acute renal failure following storage and transplantation. *Transplantation* 1994; **58:** 1303-1308.

Thorniley MS, Lane NJ, Manek S, Green CJ. Non-invasive measurement of respiratory chain dysfunction following hypothermic renal storage and transplantation. *Kid Int* 1994; **45:** 1489-1496.

Gower JD, Lane NJ, Goddard JG, Manek S, Ambrose IJ, Green CJ. Ebselen: Antioxidant capacity in renal preservation. *Biochem Pharmacol* 1992; **43:** 2341-2348.

Submitted

Lane NJ, Thorniley MS, Manek S, Collis CS, Rice-Evans C, Hider RC, Fuller BJ, Green CJ. Iron chelation and respiratory chain function in renal ischaemia-reperfusion injury. Submitted to *Arch Biochem Biophys* (June 1996).

Proceedings Papers

Lane NJ, Thorniley MS, Manek S, Fuller BJ, Green CJ. Iron chelation, respiratory chain function and tubular necrosis in renal transplantation. *Biochem Soc Trans* 1995; **23:** 524S.

Thorniley MS, Lane NJ, Manek S, Green CJ. *In vivo* monitoring of respiratory chain dysfunction following renal storage and transplantation. *Biochem Soc Trans* 1993; **21:** 500S.

Thorniley MS, Lane NJ, Manek S, Green CJ. Non-invasive monitoring of renal haemoglobin oxygenation kinetics following hypothermic storage and transplantation. *Biochem Soc Trans* 1993; **21:** 501S.

Published Abstracts

Lane NJ, Thomiley MS, Manek S, Fuller BJ, Green CJ. Iron chelation and respiratory chain function *in vivo* in renal ischaemia-reperfusion injury. *Clin Sci* 1995; **89:** 31P.

Lane NJ, Thomiley MS, Manek S, Green CJ. Vascular congestion does not correlate with mitochondrial dysfunction following renal transplantation. *J Pathol* 1994; **172 (suppl):** 138A.

Thomiley MS, Lane NJ, Green CJ. Non-invasive monitoring of renal tissue oxygen sufficiency for transplantation. *Clin Sci* 1993; **85:** 22P.

Toffa SEK, Fuller BJ, Gower JD, Lane NJ, Green CJ. Oxygen-free reperfusion of ischaemic kidneys. *Int J Rad Biol* 1992; **62:** 116.

REFERENCES

Acquatella H, Gonzales MP, Morales JH, Wittembury G. Ionic and histologic changes in the kidney after perfusion and storage for transplantation. *Transplantation* 1972; **14:** 480-489.

Akerboom TP, Sies H, Ziegler DM. The oxidation of ebselen metabolites to thiol oxidants catalyzed by liver microsomes and perfused rat liver. *Arch Biochem Biophys* 1995; **316:** 220-226.

Alexander JS, Hechtman HB, Shepro D. Phalloidin enhances endothelial barrier function and reduces inflammatory permeability *in vitro*. *Microvasc Res* 1988; **35:** 308-315.

Ambrosio G, Zweier JL, Duilio C, Kuppusamy P, Santoro G, Elia PP, Tritto I, Cirillo P, Condorelli M, Chiariello M, Flaherty JT. Evidence that mitochondrial respiration is a source of potentially toxic oxygen free radicals in intact rabbit hearts subjected to ischemia and reflow. *J Biol Chem* 1993; **268:** 18532-18541.

Andersson G, Jennische E. Lack of causal relationship between medullary blood congestion and tubular necrosis in postischaemic kidney damage. *Acta Physiol Scand* 1987; **130:** 429- 432.

Antonini E, Brunori M, Colosimo A, Greenwood C, Wilson MT. Oxygen "pulsed" cytochrome c oxidase: functional properties and catalytic relevance. *Proc Natl Acad Sci USA* 1977; **74:** 3128-3132.

Atkins JL, Lankford SP. Changes in cytochrome oxidation in outer and inner stripes of outer medulla. *Am J Physiol* 1991; **261:** F849-F857.

Avramovic A. Le transplantation du rein. *Lyon Chir* 1924; **21:** 734-756.

Baker JE, Kalyanaraman B. Ischaemia-induced changes in myocardial paramagnetic metabolites: implications for intracellular oxy-radical generation. *FEBS Lett* 1989; **244:** 311-314.

Balaban RS, Sylvia AL. Spectrophotometric monitoring of O_2 delivery to the exposed rat kidney. *Am J Physiol* 1981; **241:** F257-F262.

Bartels H, Bohmer M. Micro-determination of creatinine. *Clin Chim Acta* 1971; **32:** 81-85.

Baud L, Ardaillou R. Involvement of reactive oxygen species in kidney damage. *Br Med Bull* 1993; **49:** 621-629.

Bayati A Christofferson R, Kallskog O, Wollgast M. Mechanism of erythrocyte trapping in ischaemic acute renal failure. *Acta Physiol Scand* 1990; **138:** 13-23.

Beinert H, Shaw RW, Hansen RE, Hartzell CR. Studies on the origin of the near-infrared (800-900 nm) absorption of cytochrome c oxidase. *Biochim Biophys Acta* 1980; **591:** 458-470.

Bellomo G, Mirabelli F, Richelmi P, Orrenius S. Critical role of sulfhydryl groups in ATP-dependent Ca sequestration by plasma membrane fraction from rat liver. *FEBS Lett* 1983; **163:** 136-139.

Belzer FO, Southard JH. Principles of solid organ preservation by cold storage. *Transplantation* 1988; **45:** 673-676.

Bidlack WR, Tappel AL. Fluorescent products of phospholipids during lipid peroxidation. *Lipids* 1973; **8:** 203-207.

Borel JF, Feurer C, Gubler HU, Stahelin H. Biological effects of cyclosporin A: a new anti-lymphocytic agent. *Agents Actions* 1976; **6:** 468-475.

Boydstun II, Thulin G, Zhu XH, Avison MJ, Gaudio KM, Siegel NJ. Disassociation of post-ischemic recovery of renal adenosine triphosphate and cellular integrity. *Ped Res* 1993; **33:** 595-597.

Braughler JM, Burton PS, Chase RL, Pregenzer JF, Jacobsen EJ, VanDoornik FJ, Tustin JM, Ayer DE, Bundy GL. Novel membrane localized iron chelators as inhibitors of iron dependent lipid peroxidation. *Biochem Pharmacol* 1988; **37:** 3853-3860.

Brazy JE. Near infra-red spectroscopy. *Clinics in Perinatology* 1991; **18:** 519-534.

Brazy JE, Lewis DV, Mitnick MJ, Jobsis-Vandervliet FF. Non-invasive monitoring of cerebral oxygenation in preterm infants: Preliminary observations. *Pediatrics* 1985; **75:** 217-225.

Brazy JE, Lewis DV. Changes in cerebral volume and cytochrome aa_3 hypertensive peaks in preterm infants. *J Pediatr* 1986; **108:** 983-987.

Brenner BM, Zatz R, Ichikawa I. The renal circulations. In *The Kidney* (Eds Brenner BM, Rector FC); WB Saunders Company, Philadelphia, 1986; pp 93-123.

Brezis M, Heyman SN, Epstein FH. Determinants of intrarenal oxygenation II. Hemodynamic effects. *Am J Physiol* 1994; **267:** F1059-F1068.

Brezis M, Rosen S, Silva P, Epstein FH. Selective vulnerability of the medullary thick ascending tubule limb to anoxia in the isolated perfused rat kidney. *J Clin Invest* 1984; **73:** 182-190.

Brezis M, Rosen S, Spokes K, Silva P, Epstein FH. Transport-dependent anoxic cell injury in the isolated perfused rat kidney. *Am J Pathol* 1984; **116:** 327-341.

Brezis M, Seymour R, Silva P, Epstein FH. Renal ischemia: A new perspective. *Kidney Int* 1984; **26:** 375-383.

Brunori M, Giacometti GM. Photochemistry of hemoproteins. *Methods Enzymol* 1981; **76:** 582-595

Cadenas E, Boveris A, Ragan CI, Stoppani OK. Production of superoxide radicals and H_20_2 by NADH ubiquinone reductase and ubiquinone cyt-c reductase from beef heart mitochondria. *Arch Biochem Biophys* 1977; **180:** 248-257.

Calman KC, Quinn RO, Bell PR. Metabolic aspects of organ storage and the prediction of viability. In *Organ Preservation* (Ed Pegg DE); Churchill Press, London 1973: pp 225-240.

Calne RY. The rejection of renal homografts. Inhibition in dogs by 6-mercaptopurine. *Lancet* 1960; **i:** 417-418.

Calne RY, Pegg DE, Pryse-Davies J. Renal preservation by ice cooling: An experimental study relating to kidney transplantation from cadavers. *BMJ* 1963; **5358:** 651-655.

Calne RY, White DJ, Thiru S, Evans DB, McMaster P, Dunn DC, Craddock GN, Pentlow BD, Rolles K. Cyclosporin A in patients receiving renal allografts from cadaver donors. *Lancet* 1978; **2:** 1323-1327.

Cantiello HF, Patenaude CR, Codina J, Birnbaumer L, Ausiello DA. $G_{\alpha i\text{-}3}$ regulates epithelial Na^+ channels by activation of phospholipase A_2 and lipoxygenase pathways. *J Biol Chem* 1990; **265:** 21624-21628.

Carrel A, Guthrie CC. The transplantation of veins and organs. *Am Med* 1905; **10:** 1011.

Casnocha SA, Eskin SG, Hall ER, McIntire LV. Permeability of human EC monolayers: Effect of vasoactive agonist on cAMP. *J Appl Physiol* 1989; **67:** 1997-2005.

Chan A, Chittinandana A, Shapiro JI, Shanley PF, Schrier RW. Effect of an endothelin-receptor antagonist on ischemic acute renal failure. *Am J Physiol* 1994; **266:** F135-F138.

Chance B, Williams GR. Respiratory enzymes and oxidative phosphorylation. I. Kinetics of oxygen utilisation. *J Biol Chem* 1955; **217:** 383-393.

Chien KR, Abrams J, Pfau RG, Farber JL. Prevention by chlorpromazine of ischemic liver death. *Am J Pathol* 1977; **88:** 539-558.

Chirico WJ, Waters MJ, Blobel G. 70 k heat shock related proteins stimulate protein translocation into microsomes. *Nature Lond* 1988; **332:** 800-805.

Collins GM, Bravo-Shugarman M, Terasaki PI. Kidney preservation for transplantation. *Lancet* 1969; **6:** 1219-1222.

Collis CS, Davies MJ, Rice-Evans C. The effects of N-methyl butyrohydroxamic acid and other monohydroxamates on reperfusion-induced damage to contractile function in the isolated rat heart. *Free Rad Res Comms* 1993; **18:** 269-277.

Conney AH. Induction of microsomal enzymes by foreign chemicals and carcinogenesis by polycyclic aromatic hydrocarbons: G. H. A. Clowes Memorial Lecture. *Cancer Res* 1982; **42:** 4875-4917.

Connor HD, Gao W, Nukina S, Lemaster JJ, Mason RP, Thurman RG. Evidence that free radicals are involved in graft failure following orthotopic liver transplantation in the rat - an electron paramagnetic resonance spin trapping study. *Transplantation* 1992; **54:** 199-204.

Cope M. PhD thesis 1992 (University of London).

Cope M, Delpy DT. A system for long-term measurement of cerebral blood and tissue oxygenation in newborn infants by near-infrared transillumination. *Med Biol Eng Comput* 1988; **26:** 289-294.

Cope M, Delpy D, Reynold EOR, Wray S, Wyatt JS, Van Der Zee P. Methods of quantifying cerebral near infra-red spectroscopy data. *Adv Exp Med Biol* 1988; **222:** 183-189.

Cotgreave IA, Johansson U, Westergren G, Moldeus PW, Brattsand R. The anti-inflammatory activity of ebselen but not thiols in experimental alveolitis and bronchiolitis. *Agents Actions* 1988; **24:** 313-319.

Cotterill LA, Gower JD, Fuller BJ, Green CJ. Evidence that calcium mediates free radical damage through activation of phospholipase A_2 during cold storage of the rabbit kidney. *Adv Exp Med Biol* 1990; **264:** 397-400.

Crane MM. Observations on the function of the frog's kidney. *Am J Physiol* 1927; **81:** 232.

Cronin RE. Drug therapy in the management of acute renal failure. *Am J Med Sci* 1986; **292:** 112-119.

Cross CE, Halliwell B, Boush ET, Pryor WA, Amos BN, Saul RC, McCord JM, Harman D. Oxygen radicals and human disease. *Ann Intern Med* 1987; **107:** 526-545.

Dahle LK, Hill EG, Holmes RT. The thiobarbituric reaction and the autooxidation of polyunsaturated fatty acid methyl esters. *Arch Biochem Biophys* 1962; **98:** 253-261.

Davies KJA. Protein damage and degradation by oxygen radicals. I. General aspects. *J Biol Chem* 1987; **262:** 9895-9901.

Davies KJA, Delsignore ME, Lin SW. Protein damage and degradation by oxygen radicals. II. Modification of amino acids. *J Biol Chem* 1987; **262:** 9902-9907.

Davies KJA, Delsignore ME. Protein damage and degradation by oxygen radicals. III. Modification of secondary and tertiary structure. *J Biol Chem* 1987; **262:** 9908-9913.

Davies KJA, Lin SW, Pacifici RE. Protein damage and degradation by oxygen radicals. IV. Degradation of denatured protein. *J Biol Chem* 1987; **262:** 9914-9920.

Deetjen P, Boylan JW, Kramer K. *Physiology of the kidney and water balance*. Springer-Verlag, New York, 1975.

Delpy DT, Cope M, Van Der Zee P, Arridge S, Wray S, Wyatt J. Estimation of optical pathlength through tissue from direct time of flight measurement. *Phys Med Biol* 1988; **33:** 1433-1442.

Dempster WJ. Kidney homotransplantation. *Br J Surg* 1953; **40:** 447-465.

Den-Butter G, Schilling MK, Lindell SL, Gandolf D, Southard JH, Belzer FO. Effect of glutathione and glycine in kidney preservation. *Transplant Proc* 1993; **25:** 1633-1634.

Deshais RJ, Koch BD, Werner-Washburn M, Craig EA, Schekman R. A subfamily of stress proteins facilitates translocation of secretory and mitochondrial precursor polypeptides. *Nature Lond* 1988; **332:** 800-805.

Eke A, Hutiray G, Kovach AGB. Induced hemodilution detected by reflectometry for measuring microregional blood flow and blood volume in cat brain cortex. *Am J Physiol* 1979; **236:** 759-768.

Epstein FH, Balaban RS, Ross BD. Redox state of cytochrome aa_3 in isolated perfused rat kidney. *Am J Physiol* 1982; **243:** F356-F363.

Escalante B, Erlij D, Falck JR, McGiff JC. Cytochrome P-450 arachidonate metabolites effect ion fluxes in rabbit medullary thick ascending limb. *Am J Physiol* 1994; **266:** C1775-C1782.

Escalante B, Erlij D, Falck JR, McGiff JC. Ion transport inhibition in the medullary thick ascending limb of Henle's loop by cytochrome P-450-arachidonic acid metabolites. *Adv Prostaglandin Thrombox Leuk Res* 1990; **21:** 209-212.

Farber JL, Chien KR, Mittnacht S. The pathogenesis of irreversible cell injury in ischaemia. *Am J Pathol* 1981; **102:** 271-281.

Farrari R, Ceconi C, Curello S, Cargnoni A, Medici D. Oxygen free radicals and reperfusion injury: The effect of ischaemia and reperfusion on cellular ability to neutralise oxygen toxicity. *J Mol Cell Cardiol* 1986; **18 (suppl 4):** 67-69.

Fawcett JK, Scott JE. A rapid and precise method for the determination of urea. *J Clin Pathol* 1960; **13:** 156-159.

Ferrari R, di-Lisa F, Raddino R, Visioli O. The effects of ruthenium red on mitochondrial function during post-ischaemic reperfusion. *J Mol Cell Cardiol* 1982; **14:** 737-740.

Fischer H, Terlinden R, Löhr JP, Römer A. A novel biologically active selenoorganic compound VIII. Biotransformation of ebselen. *Xenobiotica* 1988; **18:** 1347-59.

Franke CH, Barlow CH, Chance B. Oxygen delivery in perfused rat kidney: NADH fluorescence and renal functional state. *Am J Physiol* 1976; **231:** 1082-1089.

Frazier LW, Yorio T. Eicosanoids: their function in renal epithelia ion transport. *Proc Soc Exp Biol Med* 1992; **201:** 229-243.

Fridovich I. Superoxide dismutase: An adaptation to a paramagnetic gas. *J Biol Chem* 1989; **264:** 7761-7764.

Fry M, Green DE. Cardiolipin requirement for electron transfer in complexes I and III of the mitochondrial respiratory chain. *J Biol Chem* 1980; **256:** 1874-1880.

Fuld R, Spar B, Urbaitis BK. Measurement of malondialdehyde in kidney following ischemia and reflow. *Kidney Int* 1986; **29:** 301A.

Fuller BJ, Pegg DE. The assessment of renal preservation by normothermic bloodless perfusion. *Cryobiology* 1976; **13:** 177-184.

Fuller BJ. Storage of cells and tissues at hypothermia for clinical use. *Symp Soc Exp Biol* 1987; **41:** 341-362.

Fuller BJ, Gower JD, Green CJ. Free radical damage and organ preservation, fact or fiction? *Cryobiology* 1988; **25:** 377-393.

Garza-Quintero R, Weinberg JM, Ortega-Lopez J, Davis JA, Venkatachalam MA. Conservation of structure in ATP-depleted proximal tubules: role of calcium, polyphosphoinositides, and glycine. *Am J Physiol* 1993; **265:** F605-F623.

Gabriel R. *A patients guide to dialysis and transplantation,* 3rd edition. MTP Press Ltd, Lancaster, 1990.

Gabriel R. *Postgraduate nephrology*, third edition. Butterworths, London, 1985.

Gamelin LM, Zager RA. Evidence against oxidant injury as a critical mediator of postischemic acute renal failure. *Am J Physiol* 1988; **255:** F450-F460.

Gerber JG. Role of prostaglandins in the hemodynamic and tubular effects of furosemide. *Fed Proc* 1983; **42:** 1707-1710.

Goddard JG, Gower JD, Green CJ. A chelator is required for microsomal lipid peroxidation following reductive ferritin-iron mobilization. *Free Rad Res Comms* 1992; **17:** 177-185.

Goldberg AH, Lillienfield LS. Effects of hyperoncotic mannitol on renal vascular resistance. *Proc Soc Exp Biol Med* 1965; **119:** 635-642.

Gottschalk CW. Osmotic concentration and dilution of the urine. *Am J Med* 1964; **36:** 670.

Gowans JL, McGregor DD, Cowen DM. Initiation of immune responses by small lymphocytes. *Nature* 1962; **196:** 651-655.

Gower JD, Ambrose IJ, Manek S, Bright J, Dobbin PS, Hider RC, Goddard JG, Thorniley MS, Green CJ. The effect of a synthetic hexadentate iron chelator (CP130) and desferrioxamine on rabbit kidneys exposed to cold and warm ischaemia. *Agents Actions* 1993; **40:** 96- 105.

Gower JD, Baldock RJ, Sullivan AM, Dore CJ, Coid CR, Green CJ. Protection against endotoxin-induced foetal resorption in mice by desferrioxamine and ebselen. *Int J Exp Pathol* 1990; **71:** 433-440.

Gower JD, Fuller BJ, Green CJ. Lipid peroxidation in the cortex and medulla of rabbit kidneys subjected to cold ischaemia and the value of protective agents. *Free Rad Res Comms* 1987; **3:** 107-115.

Gower JD, Healing G, Fuller B, Simpkin S and Green CJ. Protection against oxidative damage in cold-stored rabbit kidneys by desferrioxamine and indomethacin. *Cryobiology* 1989; **26:** 309-317.

Gower JD, Healing G, Green CJ. Measurement by HPLC of desferrioxamine-available iron in rabbit kidneys to assess the effect of ischaemia on the distribution of iron within the total pool. *Free Rad Res Comms* 1989; **5:** 291-299.

Gower JD, Lane NJ, Goddard JG, Manek S, Ambrose IJ, Green CJ. Ebselen: Antioxidant capacity in renal preservation. *Biochem Pharmacol* 1992; **43:** 2341- 2348.

Granger DN, Benoit JN, Suzuki M, Grisham MB. Leucocyte adherence to venular endothelium during ischemia-reperfusion. *Am J Physiol* 1989; **257:** G683-G688.

Green CJ. Renal transplantation and ischaemia-reperfusion injury. In *Immunopharmacology of free radical species* (Eds Blake D, Winyard PG); Academic Press Ltd, London, 1995: pp 85-96.

Green CJ. *Recent progress in organ transplantation.* The Medicine Group (UK) Ltd, Oxford, 1988.

Green CJ, Cotterill L, Gower JD. Renal ischaemia. In *Cellular Membrane: A key to disease processes* (Eds Ohnishi ST, Ohnishi T); CRC Press, London, 1993; pp285-310.

Green CJ, Healing G, Lunec J, Fuller BJ, Simpkin S. Evidence of free radical-induced damage in rabbit kidneys after simple hypothermic preservation and autotransplantation. *Transplantation* 1986; **41:** 161-165.

Green CJ, Brosnan JT, Fuller BJ, Lowry M, Stubbs M, Ross BD. Effect of hibernation on liver and kidney metabolism in 13-lined ground squirrels. *Comp Biochem Physiol B* 1984; **79:** 167-171.

Green ESR, Evans H, Rice-Evans P, Davies MJ, Salah N, Rice-Evans C. The efficacy of monohydroxamates as free radical scavenging agents compared with di- and trihydroxamates. *Biochem Pharmacol* 1993; **45:** 357-366.

Greger R. Ion transport mechanisms in the thick ascending limb of Henle's loop of mammalian nephron. *Physiol Rev* 1985; **65:** 760-797.

Guder WG, Ross BD. Enzyme distribution along the nephron. *Kidney Int* 1984; **26:** 101-111.

Gunning ME, Ingelfinger JR, King AJ, Brenner BM. In *The kidney*, Vol I 3rd edition (Ed Brenner BM); WB Saunders & Company, USA, 1996: pp 627-712.

Gutteridge JMC. Iron promoters of the Fenton reaction and lipid peroxidation can be released from haemoglobin by peroxides. *FEBS Lett* 1986; **201:** 291-295.

Halliwell B, Gutteridge JMC. Lipid peroxidation, oxygen radicals, cell damage and antioxidant therapy. *Lancet* 1984; **1:** 1396-1398.

Halliwell B, Gutteridge JMC (Eds). *Free radicals in biology and medicine*. Oxford University Press, Oxford, 1985.

Halushka PB, Lefer AM. Thromboxane in health and disease. *Fed Proc* 1987; **46:** 131-132.

Hamilton PA, Hope PI, Cady EB, Delpy DT, Wyatt JS, Reynolds EOR. Impaired energy metabolism in brains of newborn infants with increased cerebral echodensities. *Lancet* 1986; **i:** 1242-1246.

Hampson NB, Piantadosi CA. Skeletal muscle cytochrome aa_3 oxidation level varies as a function of systemic oxygen consumption during controlled hemorrhage in cats. *Am Rev Respir Dis* 1986; **133:** A37.

Hanley MJ, Davidson K. Prior mannitol and furosemide infusion in a model of ischemic acute renal failure. *Am J Physiol* 1981; **241:** F556-F564.

Hansson R, Jonsson O, Lundstam S, Pettersson S, Schersten T, Waldenstrom J. Effects of free radical scavengers on renal circulation after ischaemia in the rabbit. *Clin Sci* 1983; **65:** 605-610.

Hardy L, Clark JB, Darley-Usmar VM, Smith DR, Stone D. Reoxygenation-dependent decrease in mitochondrial NADH:CoQ reductase (complex I) activity in the hypoxic/reoxygenated rat heart. *Biochem J* 1991; **274:** 133-137.

Harris DNF, Bailey SM. Near infrared spectroscopy in adults. *Anaesthesia* 1993; **48:** 694-696.

Hayaishi O, Shimizu T. Metabolic and functional significance of prostaglandins in lipid peroxide research. In *Lipid peroxides in biology and medicine* (Ed Yagi K); Academic Press, Tokyo, 1982: pp 41-53.

Hayashi M, Slater TF. Inhibitory effects of ebselen on lipid peroxidation in rat liver microsomes. *Free Rad Res Comms* 1986; **2:** 179-85.

Hazeki O, Tamura M. Near infrared quadruple wavelength spectrophotometry of the rat head. *Adv Exp Med Biol* 1989; **248:** 63-70.

Healing G, Gower J, Fuller B, Green C. Intracellular iron redistribution. An important determinant of reperfusion damage to rabbit kidneys. *Biochem Pharmacol* 1990; **39:** 1239-45.

Hellberg PAO, Kallskog O, Wolgast M. Red cell trapping and postischemic renal bloodflow. Differences between the cortex, outer and inner medulla. *Kidney Int* 1991; **40:** 625-631 .

Hellberg PAO, Nygren A, Hansell P, Fasching A. Post-ischaemic administration of hyperosmolar mannitol enhances erythrocyte trapping in outer medulla vasculature in the rat kidney. *Renal Physiol Biochem* 1990; **13:** 328-332.

Heyman SN, Brezis M, Epstein FH, Spokes K, Rosen S. Effect of glycine and hypertrophy on renal outer medullary hypoxic injury in ischemia reflow and contrast nephropathy. *Am J Kidney Dis* 1992; **19:** 578-586.

Heyman SN, Rosen S, Epstein FH, Spokes K, Brezis ML. Loop diuretics reduce hypoxic damage to proximal tubules of the isolated perfused kidney. *Kidney Int* 1994; **45:** 981-985.

Hidalgo MA, Mann DJ, Fuller BJ, Green CJ. Effects of depolarising or non-depolarising preservation solutions on human endothelial cells during cold hypoxia. *Clin Sci* 1995; **90:** 135-141.

Hider RC, Porter JB, Singh S. The design of therapeutically useful iron chelators. In *The development of iron chelators for clinical use* (Eds Bergeron RJ, Brittenham GM); CRC Press, London, 1994: pp 353-371.

Hollenberg NK, Epstein M, Rosen SM, Basch RI, Oken DE, Merrill JP. Acute oliguric renal failure in man: Evidence for preferential renal cortical ischemia. *Medicine* 1968; **47:** 455-474.

Holmberg SRM, Cumming DVE, Kusama Y, Hearse DJ, Poole-Wilson PA, Shattock MJ, Williams AJ. Reactive oxygen species modify the structure and function of the cardiac sarcoplasmic reticulum calcium-release channel. *Cardioscience* 1991; **2:** 19-25.

Hoshida S, Kuzuya T, Nishida M, Yamashita N, Hori M, Kamada T, Tada M. Ebselen protects against ischemia-reperfusion injury in a canine model of myocardial infarction. *Am J Physiol* 1994; **267:** H2342-H2347.

Hume DM, Merrill JP, Miller BF, Thorn GW. Experiences with renal homotransplantation in humans: report of 9 cases. *J Clin Invest* 1955; **34:** 327-382.

Hume DM, Jackson BT, Zukoski. The homotransplantation of kidneys and of fetal liver and spleen after total body irradiation. *Ann Surg* 1960; **152:** 354-373.

Ianotti F, Crockard A, Ladds G, Symon L. Are prostaglandins involved in experimental ischaemic oedema in gerbils? *Stroke* 1981; **12:** 301-306.

Jacobsson J, Odlind B, Tufveson, Wahlberg J. Effects of cold ischaemia and reperfusion on trapping of erythrocytes in the rat kidney. *Transplant Int* 1988; **1:** 75-79.

Jamison RL, Bennett CM, Berliner RW. Countercurrent multiplication by the thin loops of Henle. *Am J Physiol* 1967; **212:** 357-66.

Jelkman W, Kurtz A, Fostermann U, Pfeilschifter J, Bauer C. Hypoxia enhances prostacyclin synthesis in renal mesangial cell cultures. *Prostaglandins* 1985; **30:** 109-118.

Jim K, Hassid A, Sun F, Dunn MJ. Lipoxygenase activity in rat kidney glomeruli, glomerular epithelial cells, and cortical tubules. *J Biol Chem* 1982; **257:** 10294-10299.

Jobsis FF. Non-invasive infra-red monitoring of cerebral and mycardial oxygen sufficiency and circulatory parameters. *Science* 1977; **198:** 1264-1267.

Jobsis-Vandervliet FF, Fox E, Sugioka K. Monitoring of cerebral oxygenation and cytochrome aa_3 redox state. *Int Anesth Clin* 1987; **25:** 209-230.

Jobsis FF, Lamanna, JC. Kinetic aspects of intracellular redox reactions. In *Extrapulmonary manifestations of respiratory disease* (Ed Robin ED); Marcel Dekker, New York, 1978; pp 63-108.

Joris I, Cuenoud HF, Doern GV, Underwood JM, Majno G. Capillary leakage in inflamation: A study by vascular labelling. *Am J Pathol* 1990; **137:** 1353-1363.

Karow A, Pegg D (Eds). *Organ preservation for transplantation.* Decker, New York, 1981.

Killacky JJF, Johnston MG, Movat HZ. Increased permeability of microcarrier-cultured endothelial monolayers in response to histamine and thrombin. *Am J Pathol* 1986; **122:** 50-61.

Kirschner RE, Fantini GA. Role of iron and oxygen derived free radicals in ischemia-reperfusion injury. *J Am Coll Surg* 1994; **179:** 103-117.

Klausner JM, Paterson IS, Goldman G, Kobzik L, Rodzen C, Lawrence R, Valeri CR, Shepro D, Hechtman HB. Postischemic renal injury is mediated by neutrophils and leukotrienes. *Am J Physiol* 1989; **256:** F794-F802.

Kobayashi S, Kaede K, Nishiki K, Ogata E. Microfluorometry of oxidation-reduction state of the rat kidney *in situ*. *J Appl Physiol* 1971; **31:** 693-696.

Kopolovic J, Brezis M, Spokes K, Rosen S. Polyethylene glycol effect on the oxygenated and hypoxic isolated perfused rat kidney. *Virchows Arch Pathol Anat Histopathol* 1989; **414:** 429-437.

Korneev AA, Komissarova AA. [The molecular-cellular regulation of the mitochondrial respiratory chain]. *Izv Akad Nauk Ser Biol* 1994; **3:** 363-374.

Kühl P, Borbe HD, Romer A, Fischer H, Parnham MJ. Selective inhibition of LTB_4 formation by ebselen: A novel approach to anti-inflammatory therapy. *Agents Actions* 1986; **17**: 366-367.

Kuhn W, Ryffel K. Herstellung konzentrierter lösungen aus verdünnten durch blosse Membranwirkung. Ein modellversuch zur funktion der niere. *Hoppe-Seyler's Physiol Chem* 1942; **276:** 145.

Kühn-Velten N, Sies H. Optical spectral studies of ebselen interaction with cytochrome P-450 of rat liver microsomes. *Biochem Pharmacol* 1989; **38:** 619-625.

Kukielka E, Cederbaum AI. Ferritin stimulation of hydroxyl radical production by rat liver nuclei. *Arch Biochem Biophys* 1994; **308:** 70-77.

Kukielka E, Dicker E, Cederbaum AI. Increased production of reactive oxygen species by rat liver mitochondria after chronic ethanol treatment. *Arch Biochem Biophys* 1994; **309:** 377-386.

Kumada N, Kim T, Ohyama A, Tujino T, Iwai Y, Itoh T, Sugimura K, Nakatani T, Yamamoto K, Kisimoto T. Ouabain-containing Euro-Collins solution prevents acute tubular necrosis following kidney preservation. *Transplant Proc* 1994; **26:** 935.

Kumano K, Wang W, Masaki Y, Endo T. Roles of solution impermeants during kidney storage. *Transplant Proc* 1994; **26:** 2410-2412.

Lam FT, Mavor AID, Potts DJ, Giles GR: Improved 72 hr renal preservation with phosphate buffered sucrose. *Transplantation* 1989; **47:** 767-771.

Lands WEM. Interactions of lipid hydroperoxides with eicosanoid biosynthesis. *J Free Rad Biol Med* 1985; **1:** 97-101.

Lands WEM. Amplification of oxyradicals by eicosanoid synthesis. *Agents Actions* 1986; **18 (suppl):** 89-93.

Lane NJ, Thorniley MS, Manek S, Fuller BJ, Green CJ. Inhibition of leukotriene B_4 synthesis does not prevent development of acute renal failure following storage and transplantation. *Transplantation* 1994; **58:** 1303-1308.

Lane NJ, Thorniley MS, Manek S, Fuller BJ, Green CJ. Iron chelation, respiratory chain function and tubular necrosis in renal transplantation. *Biochem Soc Trans* 1995; **23:** 524S.

Lane NJ, Thorniley MS, Manek S, Green CJ. Vascular congestion does not correlate with mitochondrial dysfunction following renal transplantation. *J Pathol* 1994; **172 (suppl):** 138A.

Lane NJ, Thorniley MS, Manek S, Fuller BJ, Green CJ. Hemoglobin oxygenation kinetics and secondary ischemia in renal transplantation. *Transplantation* 1996; **61:** 689-696.

Lash A, Saleem A. Iron metabolism and its regulation. A review. *Ann Clin Lab Sci* 1995; **25:** 20-30.

Laurindo FRM, Da Luz PL, Uint L. Evidence for superoxide-dependent coronary vasospasm after angioplasty in intact dogs. *Circulation* 1991; **83:** 1705-1715.

Lefer AM. Eicosanoids as mediators of ischaemia and shock. *Fed Proc* 1985; **44:** 275-280.

Lefer AM, Ma XL. Endothelial dysfunction in the splanchnic circulation following ischaemia and reperfusion. *J Cardiovasc Pharmacol* 1991; **17 (suppl 3):** S186-S190.

Levy MN. Oxygen consumption and blood flow in the hypothermic perfused kidney. *Am J Physiol* 1959; **197:** 1111-1114.

Leichtweiss HP, Lubbers DW, Weiss C, Baumgarth H, Reschke W. The oxygen supply of the rat kidney: Measurements of intrarenal $P0_2$ *Pfluegers Arch* 1969; **309:** 328-349.

Lelcuk S, Alexander F, Kobzik L, Valeri CR, Shepro D, Hechtman HB. Prostacyclin and thromboxane A_2 moderate postischemic renal failure. *Surgery* 1985; **98:** 207-212.

Lianos EA, Rahman MA, Dunn MJ. Glomerular arachidonate lipoxygenation in rat nephrotoxic serum nephritis. *J Clin Invest* 1985; **76:** 1355-1359.

Linas SL, Shanley PF, Whittenburg D, Berger E, Repine JE. Neutrophils accentuate ischaemia-reperfusion injury in isolated perfused rat kidneys. *Am J Physiol* 1988; **255:** F728-F735.

Livera LN, Spencer SA, Thorniley MS, Wickramasinghe YABD, Rolfe P. Abnormalities of the cerebral circulation in premature infants during hyoxaemia and bradycardia detected by near infra-red spectroscopy. *Arch Dis Child* 1991; **66:** 376-380.

Lloyd JB, Cable H, Rice-Evans C. Evidence that desferrioxamine cannot enter cells by passive diffusion. *Biochem Pharmacol* 1991; **41:** 1361-1363.

Lowry OM, Rosebrough NJ, Farr AL, Randall RJ. Protein measurement with the folin phenol reagent. *J Biol Chem* 1951; **193:** 265-75.

Maines MD. Carbon monoxide: An emerging regulator of cGMP in the brain. *Mol Cell Neurosci* 1993; **4:** 389-397.

Malis CD, Bonventre JV. Mechanism of calcium potentiation of oxygen free radical injury to renal mitochondria. *J Biol Chem* 1986; **261:** 14201-14208.

Malmstrom BG. Cytochrome oxidase: Some unsolved problems and controversial issues. *Arch Biochem Biophys* 1990; **280:** 233-241.

Maridonneau I, Braquet P, Garay RP. Na^+ and K^+ transport damage induced by oxygen free radicals in human red cell membranes. *J Biol Chem* 1983; **258:** 3107-3113.

Marsh DC, Lindell SL, Fox LE, Belzer FO, Southard JH. Hypothermic preservation of hepatocytes. I. Role of cell swelling. *Cryobiology* 1989; **26:** 524-534.

Marsh DC, Belzer FO, Southard JH. Hypothermic preservation of hepatocytes. II. Importance of Ca^{2+} and amino acids. *Cryobiology* 1990; **27:** 1-8.

Marsh DC, Vreugdenhil PK, Mack VE, Belzer FO, Southard JH. Glycine protects hepatocytes from injury caused by anoxia, cold ischemia and mitochondrial inhibitors, but not injury caused by calcium ionophores or oxidative stress. *Hepatology* 1993; **17:** 91-98.

Marshall VC, Jablonski P, Biguzas M, Howden BO, Walls K. University of Wisconsin solution for kidney preservation: The impermeant components. *Transplant Proc* 1991; **23:** 651-652.

Mason J, Joeris B, Welsch J, Kriz W. Vascular congestion in ischemic renal failure: The role of cell swelling. *Miner Electrolyte Metab* 1989; **15:** 114-24.

Mason J, Welsch J, Takabatake T. Disparity between surface and deep nephron function early after renal ischaemia. *Kidney Int* 1983; **24:** 27-36.

Mason J. The cause and consequences of the perfusion defect that follows renal ischaemia. In *Nephrology* Vol II (Ed Davidson AM); Cambridge University Press, 1988: p 955.

Matsuno T, Nakagawa K, Sasaki H, Ishine N, Inagati M, Yagi T, Haisa M, Tanaka N, Sakagami K, Orita K. Apoptosis in acute tubular necrosis and acute allograft rejection. *Transplant Proc* 1994; **26:** 2170-2173.

Matsuno N, Sakurai E, Tamaki I, Furuhashi K, Saito A, Zhang S, Kozaki K, Shimada A, Miyamoto K, Kozaki M. Effectiveness of machine perfusion preservation as a viability determination method for kidneys procured from non-heart beating donors. *Kidney Int* 1994; **26:** 2421-2422.

Maxwell MP, Marston C, Hadley MR, Salmon JA, Garland LG. Selective 5-lipoxygenase inhibitor BW A4C does not influence progression of tissue injury in a canine model of regional myocardial ischaemia and reperfusion. *J Cardiovasc Pharmacol* 1991; **17:** 539-545.

Mayevesky A. Brain NADH redox state monitored *in vivo* by fibre optic surface fluorometry. *Brain Res Reviews* 1984; **7:** 49-68.

Mayevsky A, Franke KH, Nioka S, Kessler M, Chance B. Oxygen supply and brain function *in vivo*: A multiparametric monitoring approach in the Mongolian gerbil. In *Oxygen Transport to Tissue* Vol XII (Eds Piiper OJ, Goldstick, T.K. and Meyer, M.); Plenum Press, New York, 1990: pp. 303-313.

Mayevsky A, Zarchin N, Kaplan H, Harveri J, Haselgroove H, Chance B. Brain metabolic responses to ischemia in the Mongolian gerbil: *in vivo* and freeze trapped redox scanning. *Brain Res* 1983; **276:** 95-97.

McAnulty JF, Vreugdenhil PK, Southard JH, Belzer FO. Improved survival of kidneys preserved for seven days with a phospholipase inhibitor. *Transplant Proc* 1991; **23:** 691-692.

McCord JM, Oxygen-derived free radicals in post-ischaemic tissue injury. *New Engl J Med* 1985; **312:** 159-163.

McCormick PW, Stewart MC, Lewis GD, Zabramski JM. Measurement of human hypothermic cerebral oxygen metabolism by transmission spectroscopy. *Adv Exp Med Biol* 1993; **333:** 33-42.

McKeown CMB, Edwards V, Phillips MJ, Harvey PRC, Petrunka CN, Strasberg SM. Sinusoidal lining cell damage: The critical injury in cold preservation of liver allografts in the rat. *Transplantation* 1988; **46:** 178-191.

Medawar PB. Behaviour and fate of skin autografts and skin homografts in rabbits. *J Anat* 1944; **78:** 176-199.

Michon L, Hamburger J, Oeconomos N. Une tentative de transplantation rénale chez l'homme; aspects médicaux et biologiques. *Presse Méd* 1953; **61:** 1419-1423.

Mills E, Jobsis FF. Mitochondrial respiratory chain of carotid body and chemoreceptor response to changes in oxygen tension. *J Neurophysiol* 1972; **35:** 405-428.

Minowada G, Welch WJ. Clinical implications of the stress response. *J Clin Invest* 1995; **95:** 3-12.

Mitchison NA. Passive transfer of transplantation immunity. *Nature* 1953; **171:** 267-268.

Moe O, Tejedor A, Campbell WB, Alpern RJ, Henrich WL. Effects of endothelin on *in vitro* renin secretion. *Am J Physiol* 1991; **260**: E521-E525.

Moen J, Claeson K, Pienaar H, Lindell S, Ploeg RJ, McAnulty JF, Vreugdenhil P, Southard JH, Belzer FO. Preservation of dog liver, kidney and pancreas using the Belzer-UW solution with high-sodium and low-potassium content. *Transplantation* 1989; **47:** 940-945.

Molitoris BA, Hoilien CA, Dahl RH, Ahnen DJ, Wilson PD, Kim J. Characterization of ischemia-induced loss of epithelial polarity. *J Membr Biol* 1988; **106:** 233-242.

Mollitoris BA. Ischemia-induced loss of epithelial polarity: Potential role of the actin cytoskeleton. *Am J Physiol* 1991; **260:** F769-F778.

Molitoris BA, Dahl R, Geerdes A. Cytoskeletal disruption and apical redistribution of proximal tubule Na^+-K^+-ATPase during ischaemia. *Am J Physiol* 1992; **263:** F488-F495.

Moncada S, Palmer RM, Higgs EA. Biosynthesis of nitric oxide from L-arginine. A pathway for the regulation of cell function and communication. *Biochem Pharmacol* 1989; **38:** 1709-1715.

Moncada S, Palmer RM, Higgs EA. Nitric oxide: Physiology, pathophysiology, and pharmacology. *Pharmacol Rev* 1991; **43:** 109-142.

Müller A, Cadenas E, Graf P, Sies H. A novel biologically active seleno-organic compound (I). Glutathione peroxidase-like activity in vitro and antioxidant capacity of PZ51 (ebselen). *Biochem Pharmacol* 1984; **33**: 3235-3239.

Müller A, Gabriel H, Sies H, Terlinden R, Fischer H, Römer A. A novel biologically active selenoorganic compound VII. Biotransformation of ebselen in perfused rat liver. *Biochem Pharmacol* 1988; **37:** 1103-1109.

Murray JE, Merrill JP, Harrison JH. Renal homotransplantation in identical twins. *Surg Forum* 1955; **6:** 432-436.

Nagi MN, Laguna JC, Cook L, Cinti DL. Disruption of rat hepatic microsomal electron transport chains by the selenium-containing anti-inflammatory agent ebselen. *Arch Biochem Biophys* 1989; **269:** 264-271.

Narayanaswami V, Siess H. Antioxidant activity of ebselen and related selenoorganic compounds in microsomal lipid peroxidation. *Free Rad Res Comms* 1990; **10**: 237-244.

Noguchi N, Yoshida Y, Kaneda H, Yamamoto Y, Niki E. Action of ebselen as an antioxidant against lipid peroxidation. *Biochem Pharmacol* 1992; **44:** 39-44.

O'Connor MJ. Origin of labile NADH tissue fluorescence. In *Oxygen and Physiological Function* (Ed Jobsis FF); Professional Information Library, Dallas, 1977: pp. 90-99.

Obi-Tabot ET, Hanrahan LM, Cachecho R, Beer ER, Hopkins SR, Chan JCK, Shapiro JM, LaMorte WW. Changes in hepatocyte NADH fluorescence during prolonged hypoxia. *J Surg Res* 1993; **55:** 575-580.

O'Dell R, Schmidt-Nielsen B. Concentrating ability and kidney structure. *Fed Proc* 1960; **19:** 366.

Okamura R, Tanaka A, Ozawa K. Low-temperature fluorometric technique for evaluating the viability of rat liver grafts after simple cold storage. *Transplant Int* 1992; **5:** 165-169.

Opie LH. Proposed role of calcium in reperfusion injury. *Int J Cardiol* 1989; **23:** 159-164.

Orita Y, Fukuhara Y, Yanase M, Ando A, Okada N, Abe H. Effect of furosemide on mitochondrial electron transport system and oxidative phosphorylation. *Drug Res* 1983; **33:** 1446-1450.

Ozaki N, Tokunaga Y, Ikai I, Zaima M, Saku Y, Shimahara Y, Kamiyama Y, Yamaoka Y, Ozawa K, Nakase Y. Pyridine nucleotide fluorometry in preserved porcine liver with fluorocarbon emulsion. *Transplantation* 1989; **48:** 198-201.

Paller MS, Greene EL. Role of calcium in reperfusion injury of the kidney. *Ann N Y Acad Sci* 1994; **723:** 59-70.

Paller MS, Hedlund BE. Extracellular iron chelators protect kidney cells from hypoxia/re-oxygenation. *Free Rad Biol Med* 1994; **17:** 597-603.

Paller MS, Jacob HS. Cytochrome P-450 mediates tissue-damaging hydroxyl radical formation during reoxygenation of the kidney. *Proc Natl Acad Sci USA* 1994; **91:** 7002-7006.

Paller MS, Neumann TV. Reactive oxygen secies and rat renal epithelial cells during hypoxia and reoxygenation. *Kidney Int* 1991; **40:** 1041-1049.

Paraidathathu T, de Groot H, Kehrer JP. Production of reactive oxygen by mitochondria from normoxic and hypoxic rat heart tissue. *Free Rad Biol Med* 1992; **13:** 289-297.

Parving HH, Osterby R, Anderson PW, Hsueh WA. Diabetic nephropathy. In *The kidney*, Vol II 3rd edition (Ed Brenner BM); WB Saunders & Company, USA, 1996: pp 1864-1892.

Pegg DE. An approach to hypothermic renal preservation. *Cryobiology* 1978; **15:** 1-17.

Pelham HRB. Speculations on the functions of the major heat shock and glucose-regulated proteins. *Cell* 1986; **46:** 959-961.

Pelikan PCD, Niemann JT, Xia G, Jagels G, Criley JM. Enhancement of mitochondial oxidative phosphorylation capability by hypoperfusion in isolated perfused rat heart. *Circ Res* 1987; **61:** 880-888.

Pentlow BD, Kostakis AJ,Wall AJ, Baker PG, Smith DP, Calne RY. Preservation of ischaemically injured canine kidneys with HCA - importance of mannitol. *Transplantation* 1979; **27:** 99-101.

Piantadosi CA. Near infrared spectroscopy: Principles and applications to non-invasive assessment of tissue oxygenation. *J Crit Care* 1989; **4:** 308-318.

Piantadosi CA, Griebel JA, Hampson NB. Intramitochondrial oxygenation decreases in forearm muscle during venous congestion. *Clin Res* 1988; **36:** 373A.

Piantadosi CA, Hemstreet TM, Jobsis-Vandervliet FF. Near infrared spectrophotometric monitoring of oxygen distribution to intact brain and skeletal muscle tissues. *Crit Care Med* 1986; **14:** 698-706.

Piantadosi CA. Behavior of the copper band of cytochrome c oxidase in rat brain during FC-43-full-blood substitution. In *Oxygen Transport to Tissue* Vol XI (Eds Rakusan K, Biro GP, Goldstick TK); Plenum Press, New York, 1989: pp 81-90.

Pincemail J, Defraigne JO, Franssen C, Bonnet P, Deby-Dupont G, Pirenne J, Deby C, Lamy M, Limet M, Meurisse M. Evidence for free radical formation during human kidney transplantation. *Free Rad Biol Med* 1993; **15:** 343-348.

Pinzani M, Laffi G, Meacci E, La Villa G, Cominelli F, Gentilini P. Intrarenal thromboxane A_2 generation reduces furosemide-induced sodium and water diuresis in cirrhosis with ascites. *Gastroenterology* 1988; **95:** 1081-1087.

Piper PJ, Stanton AWB, Mcleod LJ. The action of leukotrienes C_4 and D_4 on the porcine renal vascular bed. *Prostaglandins* 1985; **29**: 61-73.

Porter JB, Huehns ER, Hider RC. The development of iron chelating drugs. *Baillier's Clin Haem* 1989; **2:** 257-292.

Proctor HJ, Sylvia AL, Jobsis FF. Failure of brain cytochrome a,a_3 redox recovery after hypoxic hypotension as determined by *in vivo* reflectance spectrophotometry. *Stroke* 1982; **13:** 89-92.

Radke HW, Rumrich G, Kinne-Saffran E, Ullrich KJ. Dual action of acetazolamide and furosemide on proximal volume absorption in the rat kidney. *Kid Int* 1972; **1:** 100-105.

Ramos EL, Ravenscraft MD. Acute renal failure in renal transplantation. In *Acute Renal Failure* (Eds Lazarus JM, Brenner BM); Churchill Livingston, New York, 1993: p441.

Rao PS, Cohen MV, Mueller HS. Production of free radicals and lipid peroxides in early experimental myocardial ischemia. *J Mol Cell Cardiol* 1983; **15:** 713-716.

Ratych RE, Bulkley GB. Free-radical-mediated postischemic reperfusion injury in the kidney. *J Free Rad Biol Med* 1986; **2:** 311-319.

Reinheckel T, Wiswedel I, Noack H, Augustin W. Electrophoretic evidence for the impairment of complexes of the respiratory chain during iron/ascorbate-induced peroxidation in isolated rat liver mitochondria. *Biochim Biophys Acta* 1995; **1239:** 45-50.

Renault G, Muffat-Joly M, Polianski J, Hardy RI, Boutineau JL, Duvent JL, Pocidalo JJ. NADH *in situ* laser flourimetry: Effect of pentobarbital on continuously monitored myocardial redox state. *Lasers Surg Med* 1987; **7:** 339-346.

Rice-Evans CA, Diplock AT. Current status of antioxidant therapy. *Free Rad Biol Med* 1993; **15:** 77-96.

Rich PR. A strategy for location of the site of proton pumping in cytochrome c oxidase. Initial results. *Ann N Y Acad Sci* 1988; **550:** 254-259.

Richter C. Pro-oxidants and mitochondrial Ca^{+}: Their relationship to apoptosis and oncogenesis. *FEBS Lett* 1993; **325:** 104-107.

Robak J, & Sobanska B. Relationship between lipid peroxidation and prostaglandin generation in rabbit tissues. *Biochem Pharmacol* 1976; **25**: 2235-2236.

Rosenthal JT, Danovitch GM, Wilkinson A, Ettenger RB. The high cost of delayed graft function in cadaveric renal transplantation. *Transplantation* 1991; **51:** 1115-1118.

Rosenthal M, Lamanna JC, Jobsis JE, Levasseur JE, Kontos, HA, Patterson JL. Effects of respiratory gases on cytochrome *a* in intact cerebral cortex: Is there a critical $P0_2$? *Brain Res* 1978; **108:** 143-154.

Ross H, Marshall VC, Escott ML. 72-hr canine kidney preservation without continuous perfusion. *Transplantation* 1976; **21:** 498-501.

Roy RS, McCord JM. Superoxide and ischemia: Conversion of xanthine dehydrogenase to xanthine oxidase, in *Oxyradicals and their scavenging systems*, Vol 2 (Eds Greenwald R, Cohen G); Elsevier, New York, 1983: pp 145-153.

Rubin RH, Cotran RS, Tolkoff-Rubin AE. Urinary tract infection, pyelonephritis and reflux nephropathy. In *The kidney*, Vol II 3rd edition (Ed Brenner BM); WB Saunders & Company, USA, 1996: pp 1597-1654.

Ruka MP, Olszenski WL. Lack of protective effect of hypertonic mannitol on ischaemic kidney in dog. *Acta Med Pol* 1978; **19:** 53-57.

Safayhi H, Tiegs G, Wendel A. Inhibition by ebselen (PZ51) of rat peritoneal neutrophil lipoxygenase. *Biochem Pharmacol* 1985; **34:** 2691-2694.

Salmon JA, Garland LG. Leukotriene antagonists and inhibitors of leukotriene biosynthesis as potential therapeutic agents. *Prog Drug Res* 1991; **37:** 9-90.

Sammut IA, Thorniley MS, Simpkin S, Bates TE, Green CJ. Changes in hepatic mitochondrial metabolic parameters following transplantation. *Biochem Soc Trans* 1995; **23:** 527S.

Saran M, Michel C, Bors W. Reactions of NO with $O_2^{\bullet-}$: Implications for the action of endothelium-derived relaxing factor. *Free Rad Res Comm* 1989; **10:** 221-226.

Sasaki K, Ueno A, Kawamura M, Katori M, Shigehiro S, Kikawada R. Reduction of myocardial infarct size in rats by a selective 5-lipoxygenase inhibitor (AA-861). In *Advances in prostaglandin, thromboxane and leukotriene research* (Eds Samuelsson B, Paoletti R, Ramwell PW); Raven Press, New York 1987: p 381.

Scherer RW, Breitwieser GE. Arachidonic acid metabolites alter G protein-mediated signal transduction in heart. *J Gen Physiol* 1990; **96:** 735-755.

Schewe C, Schewe T, Wendel A. Strong inhibition of mammalian lipoxygenases by the anti-inflammatory seleno-organic compound ebselen in the absence of glutathione. *Biochem Pharmacol* 1994; **48:** 65-74.

Schilling M, Saunder A, Southard JH, Belzer FO. Long term renal preservation and prevention of acute tubular necrosis by inhibition of arachidonate metabolism. *Translant Proc* 1993; **25:** 2534-2535.

Schmid-Schonbein GW. Capillary plugging by granulocytes and the no-reflow phenomenon in the microcirculation. *Fed Proc* 1987; **46:** 2397-2401.

Scholz R, Thurman RG, Williamson JR, Chance B, Bücher T. Flavin and pyridine nucleotide oxidation-reduction changes in perfused rat liver. I. Anoxia and subcellular localization of fluorescent flavoproteins. *J Biol Chem* 1969; **244:** 2317-2324.

Schulze-Osthoff K, Bakker AC, Vanhaesebroeck B, Beyaert R, Jacob WA, Fiers W. Cytotoxic activity of tumour necrosis factor is mediated by early damage of mitochondrial functions. *J Biol Chem* 1992; **267:** 5317-5323.

Schwartz M, Dameschek W. Drug induced immunological tolerance. *Nature* 1959; **183:** 1682-1683.

Schwartzman ML, Abraham NG, Carroll MA, Levere RD, McGiff JC. Regulation of arachidonic acid metabolism by cytochrome P-450 in rabbit kidney. *Biochem J* 1986; **238:** 283-290.

Segoloni GP, Messina M, Triolo G, Cogno C, Amoroso A, Vercellone A. Impact of donor age in kidney transplantation. *Transplant Proc* 1991; **23:** 2620-2621.

Sehr PA Bore PJ, Papatheofanis J, Radda GK. Non-destructive measurement of metabolites and tissue pH in the kidney by ^{31}P nuclear magnetic resonance. *Brit J Exp Pathol* 1979; **60:** 632-641.

Shanley PF, Rosen MD, Brezis M, Silva P, Epstein FH, Rosen S. Topography of focal proximal tubular necrosis after ischemia with reflow in the rat kidney. *Am J Pathol* 1986; **122:** 462-468.

Sheehan HL, Davis JC. Renal ischaemia with failed reflow. *J Pathol Bacteriol* 1959; **78:** 105-120.

Sies H. Ebselen: A glutathione peroxidase mimic. *Methods Enzymol* 1994; **234:** 476-482.

Simonsen M, Buemann J, Gammeltoft A, Jensen F, Jørgensen K. Biological incompatability in kidney transplantation in dogs. 1. Experimental and morphological investigations. *Acta Path Microbiol Scand* 1953; **32:** 1-35.

Simonson MS, Dunn MJ. Endothelins: a family of regulatory peptides. State-of-the-art lecture. *Hypertension* 1991; **17:** 856-63.

Singhal PC, Ding GH, DeCandido S, Franki N, Hays RM, Schlondorff D. Endocytosis by cultured mesangial cells and associated changes in prostaglandin E_2 synthesis. *Am J Physiol* 1987; **252:** F627-F634.

Sled VD, Rudnitzky NI, Hatefi Y, Ohnishi T. Thermodynamic analysis of flavin in mitochondrial NADH: ubiquinone oxidoreductase (complex I). *Biochem* 1994; **33:** 10069-10075.

Sled VD, Vinogradov AD. Reductive inactivation of the mitochondrial three subunit NADH dehydrogenase. *Biochim Biophys Acta* 1993; **1143:** 199-203.

Smith WL, Watanabe T, Umegaki K, Sonnenburg WK. General biochemical mechanism for prostanoid receptors to guanine nucleotide regulatory proteins. *Adv Prost Thrombox Leuk Res* 1987; **17:** 463-466.

Starzl TE, Marchioro TL, Waddell WR. The reversal of rejection in human renal homografts with subsequent development of homograft tolerance. *Surg Gynecol Obstet* 1963; **117:** 385-395.

Suematsu T, Abe H. Liver and serum lipid peroxide levels in patients with liver diseases. In *Lipid Peroxides in Biology and Medicine* (Ed Yagi K); Academic Press, Tokyo, 1982: pp 285-93.

Sumimoto R, Jamieson NV, Wake K, Kamada N. 24-hour rat liver preservation using UW solution and some simplified varients. *Transplantation* 1989; **48:** 1-5.

Summers WK, Jamison RL. The no reflow phenomenon in renal ischemia. *Lab Invest* 1971 **25:** 635-643.

Sun Y. Free radicals, antioxidant enzymes and carcinogens. *Free Rad Biol Med* 1990; **8:** 583-599.

Sylvia AL, Piantadosi CA, Jobsis FF. Energy metabolism and *in vivo* cytochrome c oxidase redox relationships in hypoxic rat brain. *Neurol Res* 1985; **7:** 81-88.

Sylvia AL, Piantadosi CA, Jobsis-Vandervliet FF. Cerebral bioenergetics and *in vivo* cytochrome c oxidase redox relationship. *Adv Exp Med Biol* 1986; **191:** 815-821.

Taegtmeyer H, Roberts AFC, Raine AEG. Energy metabolism in reperfused heart muscle: Metabolic correlates to return of function. *J Am Coll Cardiol* 1985; **6:** 864-870.

Tanaka J, Matui T, Asano T, Joshita H, Kametani T. Protective effect of ebselen (PZ-51) on cerebral ischemia. *Free Rad Biol Med* 1990; **9 (suppl 1)**: 157.

Terlinden R, Feige M, Römer A. Determination of the two major metabolites of ebselen in human plasma by high performance liquid chromatography. *J Chromatogr* 1988; **430**: 438-442.

Tesi RJ, Elkhammas EA, Davies EA, Henry ML, Ferguson RM. Pulsatile kidney perfusion for preservation and evaluation: Use of high-risk kidney donors to expand the donor pool. *Transplant Proc* 1993; **25:** 3099-3100.

Thomas CE, Reed DJ. Radical-induced inactivation of the kidney Na^+-K^+-ATPase: Sensitivity to membrane lipid peroxidation and the protective effect of vitamin E. *Arch Biochem Biophys* 1990; **281:** 96-105.

Thorniley M, Wickramasinghe Y, Rolfe P. Near infra-red spectroscopy: A new technique for the non-invasive monitoring of tissue and blood oxygenation *in vivo*. *Biochem Soc Trans* 1988; **16:** 978-982.

Thorniley MS, Lane NJ, Manek S, Green CJ. Non-invasive monitoring of renal haemoglobin oxygenation kinetics following hypothermic storage and transplantation. *Biochem Soc Trans* 1993; **21:** 501S.

Thorniley MS, Lane NJ, Manek S, Green CJ. Non-invasive measurement of respiratory chain dysfunction following hypothermic renal storage and transplantation. *Kidney Int* 1994; **45:** 1489-1496.

Thorniley MS, Simpkin S, Jenabdazeh MZ, Fuller BJ, Green CJ. Monitoring of surface fluorescence NADH levels as an indication of ischaemia during liver isograft transplantation. *Hepatology* 1995; **21:** 1602-1609.

Toffa S, Cheetham K, Fuller BJ, Gower JD, Green CJ. A study of the distribution of desferrioxamine in the isolated perfused rabbit kidney. *Biochem Soc Trans* 1991; **19:** 217S.

Togashi H, Shinzawa H, Yong H, Takahashi T, Noda H, Oikawa K, Kamada H. Ascorbic acid radical, superoxide and hydroxyl radical are detected in reperfusion injury of rat liver using electron spin resonance spectroscopy. *Arch Biochem Biophys* 1994; **48:** 1-7.

Toki Y, Hieda N, Torii T, Hashimoto H, Ito T, Ogawa K, Satake T. The effects of lipoxygenase inhibitor and peptidoleukotriene antagonist on myocardial injury in a canine coronary occlusion-reperfusion model. *Prostaglandins* 198; **35:** 555-571.

Tokunaga Y, Ozaki N, Wakashiro S, Ikai I, Morimoto T, Shimahara Y, Kamiyama Y, Yamaoka Y, Ozawa K, Nakase Y. Fluorometric study for the non-invasive determination of cellular viability in perfused rat liver. *Transplantation* 1987; **44:** 701-706.

Trümper L, Hoffman B, Wiswedel I, Augustin W. Impairment of the respiratory chain in the b-c_1 region as an early functional event during Fe^{2+}/ascorbate induced peroxidation in rat liver mitochondria. *Biomed Biochim Acta* 1988; **47:** 933-939.

Tucker BJ, Blantz RC. Effect of furosemide administration on glomerular and tubular dynamics in the rat. *Kidney Int* 1984; **26:** 112-121.

Turrens JF, Freeman BA, Crapo JD. Hyperoxia increases H_2O_2 release by lung mitochondria and microsomes. *Arch Biochem Biophys* 1982; **217:** 411-421.

Tortora GJ, Grabowski SR. *Principles of anatomy and physiology,* 8th edition. HarperCollins Inc, New York, 1996.

Uchiyama M, Mihara M. Determination of malondialdehyde precursor in tissues by the thiobarbituric acid test. *Anal Biochem* 1978; **86:** 271-278.

Utz J, Ullrich V. Carbon monoxide relaxes ileal smooth muscle through activation of guanylate cyclase. *Biochem Pharmacol* 1991; **41:** 1195-1201.

Vandeplassche G, Hermans C, Thone F, Borgers M. Mitochondrial hydrogen peroxide generation by NADH oxidase activity following regional myocardial ischemia in the dog. *J Mol Cell Cardiol* 1989; **21:** 383-392.

Van Why SK, Hildebrandt F, Ardito T, Mann AS, Siegel NJ, Kashgarian M. Induction and intracellular localization of HSP-72 after renal ischemia. *Am J Physiol* 1992; **263:** F769-F775.

Van Why SK, Mann AS, Ardito T, Siegel NJ, Kashgarian M. Expression and molecular recognition of Na^+-K^+-ATPase after renal ischaemia. *Am J Physiol* 1994; **267:** F75-F85.

Vaughan DL, Wickramsinghe YABD, Russell GI, Thorniley MS, Houston RF, Ruban E, Rolfe P. Is allopurinol beneficial in the prevention of renal ischaemia-reperfusion injury in the rat? Evaluation by near-infrared spectroscopy. *Clin Sci* 1995; **88:** 359-364.

Veitch K, Hombroeck A, Caucheteux D, Pouleur H, Hue L. Global ischaemia induces a biphasic response of the mitochondrial respiratory chain. *Biochem J* 1992; **281:** 709-715.

Vetterlein F, Pethö A, Schmidt G. Distribution of capillary blood flow in rat kidney during postischemic renal failure. *Am J Physiol* 1986; **251:** H510-H519.

Vetterlein F, Bludau J, Penthö-Schramm A, Schmidt G. Reconstruction of blood flow distribution in the rat kidney during postischemic renal failure. *Nephron* 1994; **66:** 208-214.

Vile G, Winterbourn C. Thiol oxidation and inhibition of Ca-ATPase by adramycin in rabbit heart microsomes. *Biochem Pharmacol* 1989; **39:** 769-764.

Vogt BA, Alam J, Croatt AJ, Vercellotti GM, Nath KA. Acquired resistance to acute oxidative stress. Possible role of heme oxygenase and ferritin. *Lab Invest* 1995; **72:** 474-483.

Voronoy I. Sobre el bloqueo del aparato réticulo-endotelial del hombre en algunas formas de intoxicación por el sublimado y sombre la transplantación del riñón cadavérico como método de tratamiento de la anuria consecutiva a aquella intoxicación. *Siglo Méd* 1936; **97:** 296-298.

Wahlberg J, Southard JH, Belzer FO. Development of a cold storage solution for pancreas preservation. *Cryobiology* 1986; **23:** 477-482.

Wahlberg J, Jacobsson J, Tufveson G. Relevance of additive components of University of Wisconsin cold-storage solution. An experimental study in the rat. *Transplantation* 1989; **48:** 400-403.

Watts JA, Koch CD, LaNoue KF. Effects of Ca^{2+} antagonism on energy metabolism: Ca^{2+} and heart function after ischemia. *Am J Physiol* 1980; **238:** F720-F733.

Wearn JT, Richards AN. Observations on the composition of glomerular urine, with particular reference to the problem of reabsorption in the renal tubules. *Am J Physiol* 1924-5; **71:** 209.

Weinberg JM, Davis JA, Abarzua M, Rajan T. Cryoprotective effects of glycine and glutathione against hypoxic injury to renal tubules. *J Clin Invest* 1987; **80:** 1446-1454.

Weinberg JM, Buchanen DN, Davis JA, Abarzua M. Metabolic aspects of protection by glycine against hypoxic injury to isolated proximal tubules. *J Am Soc Nephrol* 1991; **1:** 949-958.

Welling LW, Grantham JJ. Cystic and developmental disease of the kidney. In *The kidney*, Vol II 3rd edition (Ed Brenner BM); WB Saunders & Company, USA, 1996: pp 1828-1863.

Wendel A, Otter R, Tiegs G. Inhibition by ebselen of microsomal NADPH cytochrome-P450 reductase *in vitro* but not *in vivo*. *Biochem Pharmacol* 1986; **35:** 2995-2997.

Wendel A, Tiegs G. A novel biologically active seleno-organic compound. VI. Protection by ebselen (PZ 51) against galactosamine/endotoxin-induced hepatitis in mice. *Biochem Pharmacol* 1986; **35:** 2115-2118.

Wetzels JF, Yu L, Shanley PF, Burke TJ, Schrier RW. Infusion of glycine does not attenuate *in vivo* ischaemic acute renal failure in the rat. *J Lab Clin Med* 1993; **121:** 263-267.

Wiernsperger N, Sylvia AL, Jobsis FF. Incomplete transient ischemia: A non-destructive evaluation of *in vivo* cerebral metabolism and hemodyanics in rat brain. *Stroke* 1981; **12:** 864-868.

Wilson TW, Badahman AH, Kaushal RD. Thromboxane synthase inhibition enhances furosemide-induced renal vasodilation. *Clin Invest Med* 1993; **16:** 372-378.

Wilson TW, Loadholt CB, Privitera PJ, Halushka PV. Furosemide increases urine 6-keto prostaglandin $F_{1\alpha}$. *Hypertension* 1982; **4:** 634-641.

Wink DA, Nims RW, Saavedra JE, Utermahlen WE, Ford PC. The Fenton oxidation mechanism: Reactivities of biologically relevant substrates with two oxidising intermediates differ from those predicted for the hydroxyl radical. *Proc Natl Acad Sci USA* 1994; **91:** 6604-6608.

Winokur TS, Morrison AR. Regional synthesis of monohydroxy eicosanoids by the kidney. *J Biol Chem* 1981; **256:** 10221-10223.

Wirz H, Hargitay B, Kuhn W. Lokalisation des konzentrierungsprozesses in der niere durch direkte kryoskopie. *Helv Physiol Pharmacol Acta*, 1951; **9:** 196.

Wong MKK, Gottlieb AI. Endothelial monolayer integrity: Perturbation of F-actin filaments and the dense peripheral band-vinculin network. *Arteriosclerosis* 1990; **10:** 76-84.

Wray S, Cope M, Delpy DT, Wyatt JS, Reynolds EOR. Characterization of the near infra-red absorption spectra of cytochrome aa_3 and haemoglobin for the non-invasive monitoring of cerebral oxygenation. *Biochim Biophys Acta* 1988; **933:** 184-192.

Wyat JS, Cope M, Delpy DT, Richardson CE, Edwards AD, Wray S, Reynolds EOR. Quantification of cerebral blood volume in human infants by near infra-red spectroscopy. *J Appl Physiol* 1990; **68:** 1086-1091.

Wyatt JS, Cope M, Delpy DT. Quantification of cerebral oxygenation and haemodynamics in sick newborn infants by near infrared spectrophotometry. *Lancet* 1986; **ii:** 1063-1066.

Wyatt JS, Edwards AD, Azzopardi D, Reynolds EOR. Magnetic resonance and near infra red spectroscopy for investigation of perinatal hypoxic-ischaemic brain injury. *Arch Dis Child* 1989; **64:** 953-963.

Yagi K. Assay for serum lipid peroxide level and its clinical significance. In *Lipid peroxides in biology and medicine* (Ed Yagi K); Academic Press, New York, 1982: pp 223-242.

Yamamoto K, Wilson DR, Baumal R. Outer medullary circulatory defect in ischemic acute renal failure. *Am J Pathol* 1984; **116:** 253-261.

Yanagisawa M, Kurihara H, Kimura S, Tomobe Y, Kobayashi M, Mitsui Y, Yazaki Y, Goto K, Masaki T. A novel potent vasoconstrictor peptide produced by vascular endothelial cells. *Nature* 1988; **332:** 411-415.

Younkin D, Medoff-Cooper B, Guillet R, Sinwell T, Chance B, Delivoria-Papadopoulous M. *In vivo* ^{31}P nuclear magnetic resonance of chronic changes in cerebral metabolites following neonatal intraventricular haemorrhage. *Pediatrics* 1988; **83:** 331-336.

Zeidel ML, Brady HR, Kone BC, Gullans SR, Brenner BM. Endothelin, a peptide inhibitor of Na^+-K^+-ATPase in intact renal tubular epithelial cells. *Am J Physiol* 1989; **257:** C1101-C1107.

Zembowicz A, Hatchet RJ, Radziszewski W, Gryglewski RJ. Inhibition of endothelial nitric oxide synthase by ebselen. Prevention by thiols suggests the inactivation by ebselen of a critical thiol essential for the catalytic activity of nitric oxide synthase. *J Pharmacol Exp Ther* 1993; **267:** 1112-1118.

Zimmerhackl BL, Robertson CR, Jamison RL. The medullary microcirculation. *Kidney Int* 1987; **31:** 641-647.

MEDICAL LIBRARY
ROYAL FREE HOSPITAL
HAMPSTEAD